AIX-MARSEILLE UNIVERSITE

ECOLE DOCTORALE : Sciences de la Vie et de la Santé
Unité de recherche : MEPHI-E3-Immunobiologie des relations hôtes-pathogène

Thèse présentée pour obtenir le grade universitaire de docteur

Discipline : Biologie-Santé
Spécialité : Maladies infectieuses

Aurélie DAUMAS

Exploration de la réponse de l'hôte au travers de différentes approches globales

Soutenue le 16 Décembre 2019 devant le jury :

Professeur Florence PINET	Rapporteur
Professeur Alain CARIOU	Rapporteur
Professeur Patrick VILLANI	Examinateur
Professeur Karim ASEHNOUNE	Examinateur
Professeur Brigitte GRANEL	Présidente
Professeur Jean-Louis MEGE	Directeur

Résumé

Introduction : Le sepsis constitue une des principales causes de mortalité tant en médecine ambulatoire qu'en milieu hospitalier notamment dans la population gériatrique. Un diagnostic précoce ainsi que l'identification de la gravité du tableau sont les 2 principaux éléments nécessaires pour une prise en charge rapide, optimale, synonyme d'amélioration du pronostic. La réalité clinique est qu'il est souvent difficile d'affirmer le caractère infectieux de la réaction inflammatoire systémique observée et que malgré l'amélioration des techniques microbiologiques, jusqu'à 40% des infections ne sont pas documentées.

Patients et méthodes : Nous avons utilisé la spectrométrie de masse MALDI-TOF, outil de routine pour l'identification des micro-organismes pour identifier un profil de réponse spécifique des PBMCs à une agression infectieuse. Cette approche pourrait ainsi apporter une aide au clinicien pour orienter la prise en charge du patient avant même l'identification microbiologique. Nous nous sommes également intéressés à la formation *in vitro* de granulomes, structures organisées de la réponse immunitaire, comme moyen d'exploration de l'immunodépression du patient en sepsis sévère et de la personne âgée infectée, à risque d'infections nosocomiales.

Résultats : Nous avons identifié des signatures spécifiques chez les cellules mononucléées stimulées *in vitro* par des agonistes M1, des cytokines M2 ou différentes bactéries. La comparaison de spectres de patients en sepsis sévère avec ou sans documentation microbiologique avec les spectres des PBMCs stimulés *in vitro* a ensuite mis en évidence chez tous les patients une signature spectrale de type Interleukine IL-10 et Interféron IFN-γ ainsi qu'une signature spectrale oligodésoxynucléotides CPG (CpG ODN) suggérant une étiologie bactérienne. L'évaluation *in vitro* de la formation de granulomes a permis de mettre en évidence un défaut de formation de granulomes chez les patients septiques quel que soient leur âge. Pour expliquer ce défaut, les patients en sepsis sévère ne formant pas de granulome présentaient des numérations de monocytes et de lymphocytes diminuées. Chez la personne âgée, une dénutrition était retrouvée chez les patients ne formant pas de granulome. Un déficit en TNF sans augmentation de l'IL-10 associé à un défaut de différenciation des macrophages en cellules épithélioides et en cellules géantes multinucléées sont retrouvés en cas de défaut de formation de granulomes.

Discussion

La spectrométrie de masse MALDI-TOF par son approche de caractérisation cellulaire par « profiling » à partir de l'analyse directe des cellules entières présente de nombreux avantages car elle requiert très peu de préparation des échantillons cellulaires et aucune extraction ou séparation préalable des biomolécules. Elle est extrêmement sensible et reproductible. Malgré les limites de nos travaux, la spectrométrie de masse pourrait permettre de distinguer un SIRS en lien avec une pathologie inflammatoire ou infectieuse ou encore d'aider le clinicien dans un contexte de SIRS non infectieux à dépister l'apparition d'une complication infectieuse avant même la clinique et l'identification d'un micro-organisme sur des prélèvements. La mesure de la formation *in vitro* de granulomes pourrait quant à elle permettre d'évaluer le degré d'immunosuppression et servir à monitorer la réponse immune en réponse à un traitement. D'autres études sont nécessaires pour comprendre les différents mécanismes impliqués dans le défaut de formation des cellules géantes multinucléées.

Conclusion : La réponse de l'hôte à l'infection est complexe. Son exploration nécessite des approches combinées afin de permettre une personnalisation des thérapeutiques dans le cadre du suivi des patients.

Summary

Introduction: Sepsis is a major cause of mortality in both outpatient medicine and hospitals, especially in the geriatric population. Early diagnosis and identification of the severity of the picture are crucial to ensuring swift and optimal management, which is synonymous with a better prognosis. However, the clinical reality is that it is often hard to confirm the infectious nature of the systemic inflammatory response syndrome observed and that, despite advances in microbiological techniques, up to 40% of infections are not documented.

Patients and methods: We used MALDI-TOF mass spectrometry, a routine method for the identification of microorganisms, to identify a specific response profile of PBMCs to infectious aggression. This approach could be used to help clinicians determine patient treatment even before microbiological identification. We also investigated the *in vitro* formation of granulomas–organized structures formed as an immune response–to explore immunodepression in patients with severe sepsis and infected elderly subjects susceptible to nosocomial infections.

Results: We identified specific signatures in monocytes stimulated *in vitro* by M1 agonists, M2 cytokines or various bacteria. The comparison of the spectra of patients with severe sepsis (with or without microbiological evaluation) with the spectra of PBMCs stimulated *in vitro* highlighted an Interleukin IL-10 and Interferon IFN-γ-type spectral signature in all the patients as well as a CpG oligodeoxyribonucleotide (CpG-ODN) spectral signature, thus indicating a bacterial etiology. The assessment of granuloma formation *in vitro* highlighted the absence of granuloma formation in patients with sepsis regardless of their age. The lower monocyte and leukocyte counts in patients with severe sepsis not forming granulomas could explain this defect. In elderly subjects, malnutrition was observed in patients not forming granulomas. A TNF deficiency without an increase in IL-10 associated with defective differentiation of macrophages into epithelioid cells and multinuclear giant cells was observed in cases of defective granuloma formation.

Discussion

The direct analysis of whole cells using MALDI-TOF mass spectrometry profiling offers numerous advantages as it requires very little sample preparation and no prior extraction or separation of the biomolecules. Furthermore, this technique is extremely sensitive and reproducible. Despite the limitations of our research, mass spectrometry could help distinguish SIRS associated with an inflammatory or infectious condition or even help the clinician in cases of non-infectious SIRS to detect the onset of an infectious complication even before the appearance of any clinical signs or the identification of the microorganism. The assessment of granuloma formation *in vitro* could be used to determine the degree of immunosuppression and to monitor the immune response to therapy. Further studies are necessary to understand the different mechanisms involved in the defective formation of multinuclear giant cells.

Conclusion: The host response to infection is complex and its exploration requires the use of combined methods to personalize therapy within the context of patient follow-up.

Remerciements

A Madame le Professeur Florence PINET

Vous avez été dans le jury de thèse de Richard Ouedraogo et c'est ainsi un grand honneur que vous me faites d'avoir accepté de rapporter ce travail. Veuillez recevoir mes sincères remerciements et mon profond respect.

A Monsieur le Professeur Alain CARIOU

Vous suivez mon parcours depuis maintenant quelques années. En tant que rapporteur de mon dossier au CNU, j'avais été très touchée par votre bienveillance et vos conseils pour recentrer mes activités. J'espère depuis ne pas vous décevoir et vous remercie infiniment pour votre soutien et votre disponibilité. Je vous remercie d'avoir accepté de participer au jury de ma thèse dont la finalisation a tardé et surtout d'être à nouveau rapporteur. Veuillez trouver ici le témoignage de ma plus grande considération.

A Monsieur le Professeur Karim ASEHNOUNE

Vous avez accepté sans aucune hésitation de participer à ce jury. Votre travail sur la formation des granulomes chez les patients traumatisés crâniens nous a grandement inspiré. Vous me faites l'honneur d'apporter vos compétences à la critique de mon travail. Veuillez recevoir mes sincères remerciements et mon profond respect

A Monsieur le Professeur Patrick VILLANI

Pour la confiance que vous m'accordez, pour votre aide et votre soutien depuis maintenant 7 ans, je vous remercie sincèrement. Vous m'avez laissé prolonger cette thèse afin de concilier avec bonheur une activité clinique importante à laquelle je suis très attachée, un investissement pédagogique et une implication dans les essais cliniques dans la sclérodermie. Veuillez trouver ici le témoignage de ma reconnaissance et de mon respect le plus sincère.

A Monsieur le Professeur Jean-Louis MEGE

J'imagine que vous deviez penser que je ne l'écrirai plus cette thèse après une maternité puis une mobilité. Je vous remercie pour votre patience, votre indulgence, votre disponibilité et vos encouragements. Vos conseils ont été précieux et votre relecture rassurante. J'espère être à la hauteur de votre confiance.

A Madame le Professeur Brigitte GRANEL

Brigitte, c'était une évidence que tu sois dans ce jury et je te remercie d'avoir accepté. J'avais dit lors de ma thèse d'exercice que je ne comptais pas m'arrêter de travailler avec toi et bien les années le prouvent et ma mobilité actuelle également. La recherche sur la sclérodermie à tes côtés a participé au fait que je ne me suis pas concentrée qu'à cette thèse mais merci pour toutes les opportunités qui m'ont été offertes dans la recherche clinique grâce à la fraction vasculaire stromale ! Je te remercie pour ta disponibilité, ton écoute et la confiance que tu me témoignes. De tout cela, je te suis profondément reconnaissante et redevable.

Je ne peux pas dire qu'il a été plus facile d'écrire cette thèse que les lignes qui vont suivre mais en fait si je suis la personne que je suis aujourd'hui c'est grâce à vous....

A mes parents, *des exemples pour moi, pour votre soutien réconfortant apporté en toutes circonstances et pour votre amour. Je n'en serais pas là aujourd'hui sans vous. Merci pour avoir « adopté » Romain et pour être un papou et une mamou extraordinaires pour Lucas. Je vous aime.*

A ma sœur *que j'aime très fort. J'espère que tu es fière de moi comme je le suis de toi. Je suis une tatie comblée avec Léo et Emma. Fabien merci de prendre soin d'eux.*

A Romain *sans qui je n'en serai pas là aujourd'hui. Je te remercie de m'aimer autant et de comprendre l'importance de mon travail. Tu m'as permis d'avoir le plus grand bonheur de ma vie, Lucas et grâce à toi je peux concilier vie de famille et vie professionnelle. Sans toi à mes côtés, je n'aurai pu gérer ma mobilité et cette thèse. Je vais pouvoir abandonner mon ordinateur plus souvent à la maison maintenant. Je te dois tant…JTM*

A mon loulou *et au bonheur que tu nous apportes au quotidien, tu as changé notre vie et nous t'aimons si fort.*

A ma grand-mère, *tu as contribué à faire de moi la personne et le médecin que je suis devenue. J'espère que tu seras toujours là pour veiller sur nous et pour me faire signe de là-haut si je fais fausse route.*

A mon grand-père, *tu as toujours été là pour moi avec grand-mère, votre maison était mon refuge. Je n'oublierai jamais tout ce que vous avez fait pour moi et tu ne peux pas savoir comme je suis heureuse de te voir si fier avec Lucas.*

A mes grands-parents *partis trop tôt pour tous les souvenirs qu'on se remémore en famille.*

A ma belle-maman *pour votre fils et pour Lucas qui a de la chance d'avoir une Nanny aussi top. Merci pour votre aide et le soutien que vous apportez à Romain quand je ne suis pas là, sans jugement.*

Au reste de la famille, aux souvenirs et à votre soutien.

A Sandie, Olivia et Elodie, *le temps passe si vite... Merci pour notre amitié et pour vos encouragements dans ce parcours pas si reposant. J'ai déteint sur toi ma Sandie pour cette thèse, il fallait la passer !!*

A tous nos amis *que je n'énumèrerai pas de peur d'en oublier un ! pour tous les bons moments que l'on passe ensemble et pour votre présence dès que l'on a besoin. A ma laeti pour être présente le jour J, merci.*

A tous ceux qui m'ont aidé pour réaliser *cette thèse notamment à Christian Capo pour vos conseils et le temps que vous avez passé à m'aider pour la rédaction des articles, Julien Textoris parti trop tôt du laboratoire, Richard pour m'avoir tout appris sur le MALDI, Catherine, Céline, Amira pour votre aide pour les granulomes, Julie pour cette année en commun au laboratoire à compter nos granulomes, Delphine et Mignane pour m'avoir permis d'aborder d'autres aspects de la recherche menée au laboratoire.*

Merci à **mes collègues** *dans le service qui m'ont permis de pouvoir me libérer pour mener à bien les expérimentations nécessaires à cette thèse.*

Merci aux patients qui motivent notre recherche chaque jour et sans qui la recherche ne pourrait parfois pas avancer.

« Dans la vie, rien n'est à craindre, tout est à comprendre. »

Marie Curie (1867 - 1934)

Table des matières

AVANT-PROPOS

Cette thèse est née d'une préoccupation de la clinicienne que je suis, à pouvoir distinguer une réponse inflammatoire systémique d'origine infectieuse ou sepsis, d'un syndrome inflammatoire généralisé (« SIRS » pour « *Systemic Inflammatory Response Syndrome* ») d'une origine non infectieuse pour une prise en charge efficace du patient ; et de la rencontre avec le Professeur JL. MEGE et son équipe qui utilisent différentes approches pour évaluer la réponse de l'hôte à une infection.

Nos hypothèses de travail ont été : - tout d'abord que la spectrométrie de masse MALDI-TOF (pour *Matrix-Assisted Laser Desorption/Ionisation - Time-Of-Flight*) utilisée en routine pour l'identification des micro-organismes par analyse de leurs protéines totales pourrait avoir un intérêt dans l'identification d'un profil de réponse des cellules de l'immunité à une agression et ainsi apporter une aide au clinicien pour orienter la prise en charge du patient avant même d'obtenir une éventuelle identification microbiologique; - puis, nous nous sommes intéressés à la formation *in vitro* de granulomes, structures organisées de la réponse immunitaire, comme moyen d'exploration de l'immunodépression du patient en sepsis sévère et de la personne âgée infectée, à risque d'infections nosocomiales et de décès.

Par souci de clarté, nous rappelons que les recommandations internationales de 2012 (Surviving Sepsis Campaign [1]) distinguaient : 1) le sepsis comme étant un état inflammatoire selon les critères SIRS en relation avec une cause infectieuse, 2) le sepsis sévère correspondant à un sepsis avec apparition d'une défaillance d'organe et 3) le choc septique, défini comme un sepsis sévère avec une altération hémodynamique persistante après remplissage vasculaire. Nous utiliserons ces termes dans ce manuscrit bien que de nouvelles définitions soient utilisées depuis 2016 [2] dans l'idée d'identifier plus précocement les états infectieux susceptibles d'évolution défavorable en l'absence d'un traitement efficace, rapide. Le sepsis à l'heure actuelle est défini comme « un dysfonctionnement d'organe engageant le pronostic vital, provoqué par une réponse inappropriée de l'hôte envers une infection ». Sur le plan clinique, la dysfonction d'organe est représentée par un score SOFA (*Sequential [Sepsis-related] Organ Failure Assessment*) ≥ 2 ou augmenté d'au moins 2 points en cas de dysfonction d'organe présente avant l'infection.

Le sepsis constitue une des principales causes de mortalité tant en médecine ambulatoire qu'en milieu hospitalier notamment dans la population gériatrique. En effet, les infections sont en constante augmentation en raison du vieillissement de la population, de la meilleure prise en charge des pathologies qui les favorisent (diabète, cancers…) mais aussi de l'emploi croissant de thérapies immunosuppressives. Le diagnostic précoce d'une infection ainsi que l'identification de la gravité du tableau sont les 2 principaux éléments nécessaires pour une prise en charge rapide, optimale, synonyme d'amélioration du pronostic [3]. L'association entre le retard thérapeutique et la mortalité est en effet largement démontrée [4]. Cependant, l'utilisation abusive, inadaptée de traitements anti-infectieux à large spectre n'est pas du tout recommandée en raison de l'augmentation du risque de développement de germes résistants.

Les principales limites à une prise en charge rapide et efficace sont d'une part, la capacité à déterminer le caractère infectieux de la réaction inflammatoire systémique observée et, d'autre part, la possibilité d'identifier précocement l'agent pathogène responsable de la pathologie infectieuse éventuelle. En effet, il existe une difficulté diagnostique liée à une symptomatologie infectieuse souvent fruste et peu spécifique (asthénie, absence de fièvre, tachypnée, tachycardie, taux de leucocytes normal…) parfois masquée par une polymédication (anti-inflammatoires, corticoïdes, β-bloquants). De plus, il existe souvent de nombreux facteurs confondants que constituent les comorbidités notamment chez la personne âgée : insuffisance cardiaque, respiratoire, troubles cognitifs, etc.. qui peuvent conduire à un retard de prise en charge, l'étiologie infectieuse n'étant pas rapidement identifiée comme cause de la symptomatologie du patient et de la dégradation de ses fonctions vitales [5,6]. Enfin, malgré l'amélioration des techniques microbiologiques, jusqu'à 40% des infections ne sont pas documentées [7].

D'un point de vue physiopathologique, le sepsis est un phénomène dynamique, complexe où l'infection déclenche une réponse systémique de l'organisme pouvant devenir inappropriée. La réponse immunitaire met en jeu l'immunité innée et adaptative avec une importante capacité d'échange d'informations entre les différents acteurs et une forte régulation pour préserver l'équilibre du système immunitaire. Pour expliciter cette physiopathologie complexe, schématiquement, la réponse immunitaire au cours du sepsis doit être considérée comme un processus biphasique (**figure 1**) [8]. La mise en jeu normale des défenses de l'organisme contre l'agent infectieux déclenche une réponse inflammatoire initiale. Toutefois, chez certains patients, cette réponse peut devenir disproportionnée induisant une défaillance d'organe(s). En réponse, des mécanismes immunorégulateurs se mettent en place pour contrôler la réponse

inflammatoire pouvant aller jusqu'à induire un véritable état d'immunosuppression délétère. En effet, cette immunodépression peut être responsable de la persistance du foyer infectieux initial, favoriser la survenue d'infections nosocomiales et augmente le risque de décès [9,10].

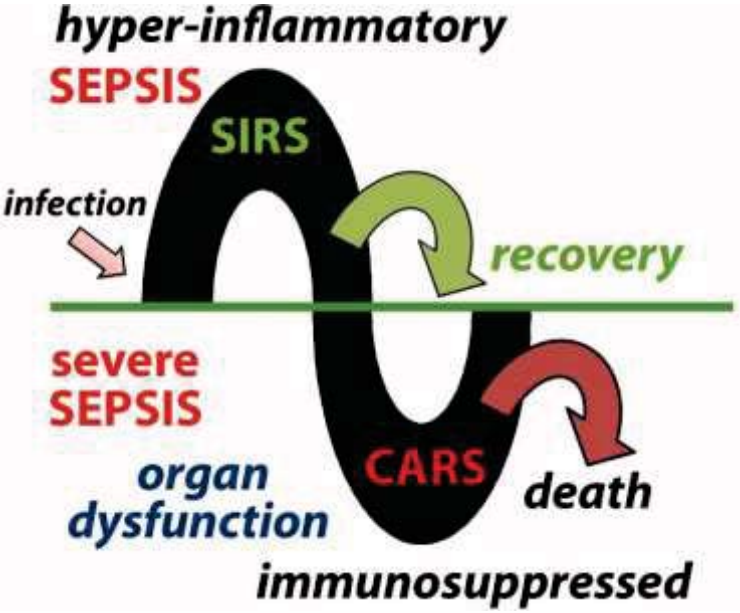

Figure 1 : D'après Faix [8]. Le sepsis peut être divisé en deux phases. Après l'infection, une phase hyper-inflammatoire (SIRS) qui peut évoluer favorablement ou s'emballer et devenir disproportionnée avec l'apparition d'une défaillance d'organe(s). En réponse, une réponse immunorégulatrice apparait (CARS pour « *compensatory anti-inflammatory response syndrome* ») pouvant permettre un rétablissement de l'homéostasie ou conduire à des complications infectieuses voire à la mort.

Chez le sujet âgé, la fréquence du sepsis est élevée et le pronostic généralement plus sévère. A la baisse des défenses immunitaires liées à l'âge s'ajoutent bien souvent le retard diagnostique, de nombreuses comorbidités associées, une polymédication ainsi que le manque de réserves physiologiques à l'origine de la dégradation rapide des fonctions vitales. En effet, le système immunitaire n'échappe pas aux effets du vieillissement, on assiste à une immunosénescence touchant aussi bien l'immunité innée qu'adaptative [11, 12]. Concernant l'immunité innée, le nombre de monocytes pro-inflammatoires et non conventionnels augmente. On observe une diminution de leur capacité d'adhésion mais une augmentation de leur production de TNF-α

[13]. Les neutrophiles sont également impactés par le vieillissement avec des capacités de phagocytose, de chimiotactisme et de production de résidu du stress oxydatif diminuées [14]. Le vieillissement du compartiment lymphocytaire T est caractérisé principalement par : - une diminution du nombre de lymphocytes T naïfs ; - un appauvrissement du répertoire T qui conduit à une diminution de sa capacité à reconnaître de nouveaux antigènes ; - une augmentation de la proportion de lymphocytes T mémoires impliqués dans le contrôle d'infections virales persistantes et - un raccourcissement des télomères [15]. Concernant les lymphocytes B, la production de nouveaux lymphocytes B naïfs est réduite et, par conséquent, les cellules mémoires sont majoritaires. Cependant les lymphocytes B mémoires ont une production d'anticorps altérés participant ainsi au déclin de la qualité de la réponse humorale avec le vieillissement [16]. Le vieillissement s'accompagne aussi d'une production accrue de cytokines pro-inflammatoires, on parle « *inflamm-aging* » dont l'origine semble multifactorielle. Cet état est associé à la fragilité et une augmentation de la morbi-mortalité. A l'inverse, les patients âgés présentant des taux de cytokines anti-inflammatoires élevés semblent mieux vieillir [17].

La situation est donc complexe pour le clinicien face à un malade compte tenu du polymorphisme possible de présentation du sepsis et encore nous n'avons pas évoqué l'impact de la nature du micro-organisme ni du site de l'infection. Il y a donc un espoir important mis dans la recherche de biomarqueurs, facilement et rapidement disponibles pour faire la distinction entre un sepsis et une réaction inflammatoire systémique d'origine non infectieuse. L'intérêt porté à la recherche de biomarqueurs pour le diagnostic du sepsis est croissant notamment avec le développement des nouvelles technologies de biologie moléculaire [8,18]. Cependant, l'étude d'un biomarqueur nécessite de démontrer que les propriétés du biomarqueur augmentent la capacité du médecin à prendre la bonne décision. Or pour cela, des outils basés sur la reclassification des patients sont nécessaires. La reclassification consiste, dans un premier temps, à classer les patients dans des catégories de diagnostic prédéfinies à l'aide d'un modèle de prédiction clinique puis, dans un second temps, à examiner les changements de catégories des patients induits par l'ajout du biomarqueur. A l'heure d'aujourd'hui, aucun biomarqueur ne permet d'affirmer le diagnostic de sepsis avec certitude et compte tenu de la complexité du sepsis, il apparait que ce diagnostic ne pourra être affirmé qu'en combinant différents marqueurs, représentatifs de plusieurs voies fonctionnelles impliquées dans la réponse de l'hôte à une infection ou grâce à une approche globale permettant de mettre en évidence un profil d'expression des cellules en réponse à une infection [19].

Dans le but d'appréhender la réponse de l'hôte à une infection, nous nous sommes intéressés tout d'abord à la spectrométrie de masse MALDI-TOF. Utilisée dans de nombreux laboratoires de microbiologie, cette méthode permet l'obtention d'un spectre caractéristique ou « empreinte spectrale » du micro-organisme à identifier, spectre qui est ensuite comparé aux empreintes spectrales de référence d'une base de données permettant ainsi une identification précise du micro-organisme. L'équipe du Professeur JL. MEGE a étendu en 2010 cette approche à l'identification de cellules eucaryotes avec succès après la construction d'une banque de spectres de référence [20].

Nous avons étudié dans un premier temps la capacité de cette méthode à différencier des profils d'activation de macrophages stimulés par des différents agonistes ainsi que des bactéries inactivées. Nos résultats confirment la sensibilité de la méthode permettant de distinguer différents états d'activation des macrophages (**article 1**). Le protocole expérimental d'analyse des cellules eucaryotes et d'exploration de l'activation des macrophages en spectrométrie de masse MALDI-TOF a été publié dans Methods in Molecular Biology (**article 2**) ainsi que filmé pour la revue JoVE (*Journal of Visualized Experiments*) (**article 3**). Dans l'idée d'une utilisation en routine pour guider le clinicien pour la prise en charge des patients, l'étude des macrophages n'est pas envisageable ni même d'un unique type cellulaire dont l'obtention nécessite un tri, une sélection. Nous nous sommes alors demandé si les cellules mononuclées du sang (PBMCs pour *Peripheral Blood Mononuclear Cells*) avaient une empreinte spectrale reproductible et différente en réponse à différents stimuli. Les PBMCs sont en effet facilement récupérés à partir du sang total par gradient de Ficoll. Nous avons montré que la spectrométrie de masse MALDI-TOF pouvait permettre l'étude des PBMCs. Des signatures spécifiques ont été obtenues suite à la stimulation *in vitro* des PBMCs par différents agonistes. La comparaison de spectres de patients en sepsis sévère avec ou sans documentation microbiologique avec les spectres des PBMCs stimulés *in vitro* a ensuite mis en évidence chez tous les patients une signature spectrale de type Interleukine IL-10 et Interferon IFN-γ en accord avec les 2 réponses inflammatoires et anti-inflammatoires observées dans le sepsis. Une signature spectrale oligodésoxynucléotides CPG (CpG ODN) a également été identifiée suggérant une étiologie bactérienne. Ces données viennent ainsi conforter le diagnostic de sepsis chez les patients sans documentation microbiologique (**article 4**).

Dans un second temps, nous avons voulu explorer la réponse à l'infection, dans 2 populations de patients différentes, des patients en sepsis sévère et des patients âgés. Le granulome résultant d'une coopération étroite entre les cellules de la réponse innée et adaptative dans le but d'éliminer un agent pathogène rebelle, l'évaluation *in vitro* de sa formation nous a paru intéressante. Cette approche était bien établie dans le laboratoire. A. Delaby avait mis au point l'évaluation de la formation des granulomes avec des billes de sépharose recouvertes d'extraits de *Coxiella burnetti.* Elle avait aussi montré que les monocytes étaient les premières cellules à venir recouvrir les billes suivis des lymphocytes et que le défaut de granulomes dans la fièvre Q chronique pouvait être lié à un défaut de migration des monocytes [21,22].

D. Faugaret s'est intéressée quant à elle à l'analyse des modulations du transcriptome lors de la formation des granulomes dirigés contre *Coxiella burnetti* et *Mycobacterium bovis* (BCG). Dans l'article auquel j'ai participé (**article 5**), le premier résultat est qu'environ 60% des gènes modulés sont communs aux cellules des 2 types de granulomes. Parmi ces gènes, on retrouve une signature transcriptionnelle M1 en faveur d'un profil inflammatoire et microbicide des cellules des granulomes ainsi qu'une modulation de gènes impliqués dans le chimiotactisme et par conséquent la formation du granulome. La comparaison des transcriptomes a également mis en évidence des modulations spécifiques. Ainsi, les cellules des granulomes induits par *Coxiella burnetti* présentent une activation des gènes associés à la réponse interféron type I.

Chez les patients en sepsis sévère (**article 6**), l'étude de la formation des granulomes a montré un défaut de formation pour presque 70% d'entre eux alors que les PBMCs de sujets sains et de patients guéris de la fièvre Q formaient des granulomes. Aucune différence significative n'a été retrouvé entre les patients septiques formant des granulomes et ceux n'y arrivant pas. Pour expliquer le défaut de formation de granulomes, les patients septiques ne formant pas de granulome présentaient des taux de monocytes significativement plus faibles et/ou une lymphopénie. Le rôle du TNF dans la formation des granulomes a aussi été suggéré du fait de taux faibles en cas de défaut de formation. Cependant, alors que l'on connait la susceptibilité des patients sous anti-TNF aux infections nécessitant une réponse granulomateuse, l'ajout de TNF ou d'un anticorps monoclonal anti-TNF n'a eu aucun impact sur les résultats obtenus préalablement. Cette méthode permet ainsi de mettre en évidence l'état d'immunodéfaillance de la plupart des patients septiques et confirme le rôle central des monocytes dans la formation du granulome.

Plus récemment, nous avons étudié la capacité de sujets âgés en bonne santé et infectés à former des granulomes en réponse à des extraits de *Coxiella burnetii* et de BCG (**article 7**). Nous avons montré que plus de la moitié des sujets infectés étaient incapables de former des granulomes contre seulement 8% des sujets sains que ce soit en réponse à *Coxiella burnetii* ou BCG. Sur le plan clinique, une dénutrition étaient significativement retrouvée chez les patients ne formant pas de granulome. Contrairement à l'étude chez les patients en sepsis, les sujets âgés incapables de former des granulomes ne présentaient pas de monocytopénie et/ou de lymphopénie. Ce défaut de formation était associé à un défaut de différenciation des macrophages en cellules épithélioides et en cellules géantes multinucléés. En outre, la production de TNF était diminuée sans lien avec une surexpression d'IL-10. Au niveau du transcriptome, tous les gènes décrits et étudiés dans la formation des granulomes [**article 5**], à l'exception d'un gène impliqué dans la polarisation M1 des macrophages, étaient sous-exprimés chez les patients ne formant pas de granulome par rapport aux patients en formant. Ainsi, cette méthode semble être un excellent outil d'évaluation de la capacité du système immunitaire dans son ensemble à répondre à une agression. En objectivant dès J3, l'incapacité des PBMCs d'un patient à former des granulomes, cela pourrait amener à adapter la prise en charge du patient mais reste à démontrer que le pronostic de ces patients est différent de celui des patients qui forment et plus grave. Ce travail est soumis à publication.

Enfin, ces différentes études s'intéressant à l'activation des cellules myéloïdes aussi bien *in vitro* que *in vivo* au cours de maladies infectieuses, m'ont amenée à être co-auteur d'une revue de la littérature remettant en question la distinction simpliste macrophages M1 ou M2 à travers différents exemples (**article 8**). La modulation des phénotypes M1/M2 pourrait ainsi être une stratégie thérapeutique à explorer.

INTRODUCTION

1. Les réponses immunitaires

Le système immunitaire de l'Homme est un système biologique vivant complexe composé d'organes lymphoïdes, de tissus, de cellules, de facteurs humoraux et de cytokines. Sa fonction est d'assurer le maintien de l'intégrité de l'organisme dans un équilibre dynamique. Ce rôle essentiel est illustré au mieux par les maladies qui résultent de son dysfonctionnement : - infections graves, tumeurs, maladies lymphoprolifératives dans les déficits immunitaires congénitaux et acquis, notamment d'origine virale (SIDA) ; - maladies allergiques en cas de réponse excessive ou encore - maladies auto-immunes quand l'organisme déclenche une réaction immunitaire contre lui-même [23].

Il est habituel de distinguer, de manière un peu dogmatique, l'immunité « innée » de l'immunité « adaptative ». À l'évidence, de plus en plus de données montrent que cette distinction ne correspond pas à la réalité. En 1999, Charles Janeway proposait une théorie intégrative suggérant une liaison étroite entre les deux types de réponses [24]. Il existe en effet des « ponts » majeurs entre ces deux réponses immunes, dont on commence seulement à comprendre l'importance aussi bien dans la physiologie du système immunitaire que dans la physiopathologie de l'allergie ou des maladies auto-immunes [25, 26].

Schématiquement, on peut identifier deux systèmes de défense interdépendants contre les agents pathogènes [23, 27]. Par souci de clarté, nous allons aborder l'immunité anti-infectieuse et nous n'aborderons pas les différences qui existent en fonction de la nature du pathogène notamment de son développement intra-cellulaire ou extracellulaire.

Pour protéger l'hôte contre les infections, la réponse immunitaire innée constitue la première ligne de défense. Elle associe des mécanismes physiques, humoraux et cellulaires qui se conjuguent entrainant la réponse inflammatoire. L'immunité innée est une réponse immédiate qui survient en l'absence d'immunisation préalable, non spécifique de l'agent infectieux. Elle fait intervenir des barrières physiques comme la peau et les muqueuses, une composante cellulaire (polynucléaires, monocytes/macrophages, cellules dendritiques, mastocytes,

lymphocytes NK « *natural killer* ») et une composante humorale (système du complément, cytokines, protéines de l'inflammation, peptides antimicrobiens). Récemment, un nouveau groupe de cellules lymphoïdes innées (les ILC « *helper like* ») a été défini avec 3 sous-groupes selon les cytokines produites, les ILC1, IL2 et ILC3 [28, 29]. Ses différents acteurs sont naturellement présents et opérationnels pour défendre l'hôte contre l'agent infectieux mais ne sont pas doués de mémoire.

Les épithéliums constituent des barrières physiques et chimiques contre les infections. Quand ces barrières sont franchies, les tissus lésés et l'agent infectieux vont déclencher la réaction inflammatoire via des signaux de danger avec l'activation des cellules résidentes notamment les mastocytes, cellules dendritiques et macrophages, du système du complément et la synthèse des protéines de l'inflammation. Ce processus va permettre le recrutement des cellules circulantes depuis le sang vers les tissus (diapédèse). Les cellules de l'immunité innée reconnaissent leur cible grâce à des récepteurs de reconnaissance de motifs, les PRRs pour *« Pattern Recognition Receptors »*, qui se lient à des motifs moléculaires conservés au cours de l'évolution des micro-organismes les MAMPs « *Microbe Associated Molecular Patterns »*. Les PRRs reconnaissent aussi des molécules libérées par les cellules endommagées ou signaux de danger (*Danger Associated Molecular Patterns* ou DAMPS). Trois familles de PRRs sont décrites : les PRR solubles et deux types de récepteurs cellulaires, les récepteurs d'endocytose et les récepteurs de signalisation. Les PRR solubles se fixent aux micro-organismes et facilitent leur élimination par les cellules phagocytaires. Il s'agit notamment des facteurs du complément et des protéines de la phase aigüe de l'inflammation [30,31]. Les récepteurs d'endocytose, membranaires, sont exprimés essentiellement par les monocytes et les macrophages. Il s'agit notamment des *scavenger receptors* et des lectines de type C [32,33]. Enfin, les récepteurs de signalisation sont impliqués dans l'activation des cellules. Ils appartiennent à la famille des molécules TLR (*Toll-like receptors)*, NOD (*nuclear oligomerization domain)* et des hélicases. Ces molécules sont soit d'expression membranaire, à la surface des cellules (TLR1, 2, 4, 6) ou dans les endosomes/lysosomes (TLR3, 7, 8, 9), soit d'expression cytosolique (NOD, hélicases) [34-36].

Les PRRs reconnaissent des motifs différents selon leur type. Par exemple, le lipopolysaccharide (LPS), composant majeur des parois des bactéries Gram négatif, se lie au TLR4. En ce qui concerne TLR2, il reconnait entre autres le peptidoglycane et l'acide lipoteïchoïque des bactéries Gram positif, le lipo-arabinomanne des mycobactéries mais aussi la molécule OmpA de la paroi des bactéries à Gram négatif. TLR1/TLR2 détecte les lipopeptides tricylés et TRL6/TRL2 les lipopeptides diacylés. Les ADN bactériens sont

caractérisés par des motifs hypométhylés (motifs CpG) reconnus par TLR9. Les molécules TLR7 et TLR8 reconnaissent les ARN simple brin viraux. TLR3 reconnaît quant à lui les ARN double brins viraux, ainsi que l'homologue structural synthétique (poly[I:C]) [37,38].
L'engagement des PRRs amplifie la réponse inflammatoire, stimule la destruction de l'agent infectieux mais aussi régule le recrutement des cellules et l'apoptose. La phagocytose est le mécanisme majeur de destruction des pathogènes [39]. Elle est facilitée par leur opsonisation. En plus de la phagocytose, les polynucléaires neutrophiles possèdent de nombreuses fonctions microbicides et cytotoxiques : la dégranulation d'enzymes protéolytiques, la production de formes réactives de l'oxygène et la libération de *Neutrophil Extracellular Traps*. Les monocytes/macrophages vont également produire de grandes quantités de cytokines pro ou anti-inflammatoires selon l'environnement et des chimiokines. L'activation des cellules lymphoïdes innées induit la production de peptides antimicrobiens, de cytokines comme l'interferon gamma (IFN-γ) et potentialise leurs activités cytotoxiques [40]. Les cibles des cytokines de l'immunité innée sont les cellules de l'immunité innée elles-mêmes (régulation de la réponse), mais aussi des organes comme le foie (synthèse de protéines comme la CRP), l'hypothalamus (induction de la fièvre) ou les cellules endothéliales pour faciliter le recrutement des cellules au niveau de la zone infectée.

En plus de son action microbicide, la réponse innée va déclencher **la réponse adaptative** et les processus de réparation tissulaire/cicatrisation. La réponse adaptative est spécifique de l'antigène, limitée dans le temps à l'éradication de l'agent infectieux dont elle garde par contre la mémoire. Les cellules dendritiques se situent à l'interface entre immunité innée et immunité adaptative [41]. Elles sont les principales cellules présentatrices d'antigène capables d'activer les lymphocytes T naïfs. Dans les tissus, les cellules dendritiques sont sous forme immature et jouent un rôle de sentinelles spécialisées dans la capture d'antigènes. Les cellules dendritiques ayant capturé des antigènes deviennent matures et migrent vers les ganglions périphériques, pour les présenter aux lymphocytes T naïfs. L'activation complète conduisant à l'expansion clonale des lymphocytes T nécessite une interaction prolongée entre le lymphocyte T et la cellule dendritique. Cette interaction lymphocyte T- cellule dendritique fait intervenir la reconnaissance du peptide par le récepteur T (TCR) associé au complexe CD3, les molécules du CMH de classe II, des molécules de costimulation et d'adhésion. Les cellules dendritiques interviennent aussi en orientant la polarisation fonctionnelle des lymphocytes T afin d'induire vers la réponse la plus adaptée à l'agression. Le signal de différentiation dépend majoritairement des cytokines présentes dans le micro-environnement (IL-12 et IFN-γ pour les Th1, IL-4 pour

les Th2, *Transforming growth factor* TGF-β et diverses cytokines pro-inflammatoires telles que l'IL-6 pour les Th17 ou encore TGF-β et IL-2 pour les T régulateurs induits (iTreg)). La liaison des cytokines à leurs récepteurs induit également l'activation des protéines de la famille STAT (*Signaling Transducer and Activator of Transcription*). Ces protéines induisent une augmentation de l'expression des facteurs de transcription de différents gènes, y compris ceux des cytokines elles-mêmes, ayant comme conséquence la production des « signatures » cytokiniques. Chaque type fonctionnel de lymphocyte T possède ainsi un facteur de transcription majeur et spécifique qui, dans une action conjointe et complexe avec des protéines STAT spécifiques, inhibe le développement des autres profils et polarise la cellule [42]. Les lymphocytes T CD4+ de type Th1 produisent majoritairement de l'IFN-γ, du *Tumor necrosis factor* TNF-α et de l'IL-2 et ainsi sont de puissants inducteurs de la réponse à médiation cellulaire, notamment avec l'activation des macrophages et des lymphocytes T CD8+. Les lymphocytes T CD4+ de type Th2 produisent de l'IL-4, de l'IL-5, de l'IL-10 et de l'IL-13. Ils induisent la production d'IgE et stimulent l'action des éosinophiles, favorisant l'élimination des parasites extra-cellulaires. Les cellules Th17 produisent de l'IL-17, de l'IL-22. Ces cellules sont importantes pour le contrôle des infections bactériennes extra-cellulaires et fongiques. Les iTreg quant à eux régulent l'intensité et la durée des réponses immunitaires [43]. Les lymphocytes T CD8 + naïfs doivent être activés pour se différencier en lymphocytes T CD8 + cytotoxiques capables de détruire les cellules qui hébergent un hôte intra-cellulaire. Cette activation dépend de signaux reçus en provenance des cellules dendritiques et des lymphocytes T CD4 + Th1 [44]. Le principal mécanisme de lyse des lymphocytes T CD8 + cytotoxiques est la dégranulation avec relargage de granzyme et de perforine. L'activation des lymphocytes B s'effectue quant à elle par reconnaissance de l'antigène par un récepteur membranaire spécifique appelé BCR et des signaux de co-stimulation solubles et membranaires apportés par les lymphocytes T folliculaires. Les lymphocytes B activés prolifèrent ensuite et se différencient en plasmocytes sécréteurs d'immunoglobulines. Les anticorps ont ensuite plusieurs fonctions à savoir neutraliser des toxines bactériennes, opsoniser une bactérie ou un virus et ainsi favoriser la phagocytose, inhiber l'adhérence bactérienne ou encore activer le système du complément et entrainer la lyse des cellules infectées.

Après élimination de l'agent infectieux, la réponse inflammatoire s'autolimite afin de réduire les dommages tissulaires. Ceci implique la suppression des gradients de molécules chimioattractantes et la production de médiateurs antiinflammatoires. Les macrophages jouent un rôle majeur dans le retour à l'homéostasie par l'élimination des débris cellulaires.

L'efférocytose va entraîner un changement de polarisation des macrophages qui vont passer d'un phénotype pro-inflammatoire (M1) à un phénotype anti-inflammatoire (M2) [45]. Les polynucléaires neutrophiles participent également à la résolution de l'inflammation avec la production de médiateurs anti-inflammatoires. Les cellules de l'immunité innée ne sont donc pas uniquement des cellules tueuses mais jouent également un rôle dans la régulation des réponses immunitaires et le remodelage tissulaire.

Toute primo-infection va induire une mémoire immunitaire. Lors d'un premier contact antigénique, l'organisme développe une réponse primaire mais aussi des cellules mémoires qui seront capables d'agir plus rapidement et plus efficacement lors d'un nouveau contact avec l'antigène correspondant. Une fois l'infection maitrisée, différents mécanismes interviennent pour éliminer la majorité des cellules T effectrices « contraction clonale » tout en permettant la constitution d'un pool hétérogène de cellules T mémoires [46]. L'activation des cellules B naïves spécifiques de l'antigène aboutit également à la production de cellules B mémoires [44]. Les cellules B mémoires, permettent en cas de nouveau contact avec l'antigène une différentiation très rapide en plasmocytes et la production d'une grande quantité d'anticorps de forte affinité. Le principe des vaccins repose sur cette mémoire.

En conclusion, comme le décrit le Professeur J. SIBILIA : « *Le système immunitaire est un véritable orchestre et ses réponses de véritables symphonies. Les "chefs d'orchestre" sont ceux qui mettent en musique en donnant une note personnelle à ce système. Ces sont les organes lymphoïdes centraux dans lesquels s'effectue l'éducation élémentaire des cellules de l'immunité (lymphocytes T et B) et les organes lymphoïdes secondaires dans lesquels s'effectueront les "cours de rattrapage". Les "musiciens" sont les cellules de l'immunité innée et adaptative. Seules les cellules de l'immunité adaptative ont besoin d'une éducation, alors que celles de l'immunité innée ont leurs fonctions préprogrammées. Enfin, les "instruments" sont toutes les substances produites qui permettent la communication entre les cellules.* »

2. Les biomarqueurs pour aider au diagnostic du sepsis

La reconnaissance précoce d'un sepsis est nécessaire pour une prise en charge rapide avec la mise en œuvre d'un traitement anti-infectieux dont le pronostic dépend fortement [4]. Toutefois le diagnostic peut s'avérer difficile dans l'attente ou en l'absence de documentation microbiologique, en raison de signes cliniques et/ou biologiques souvent non spécifiques retrouvés aussi bien dans les pathologies infectieuses que inflammatoires non infectieuses. L'exemple le plus évident est la fièvre qui n'est absolument pas synonyme d'infection et que l'on peut observer dans différentes situations cliniques non infectieuses allant du cancer à l'hyperthyroïdie en passant par les maladies inflammatoires et auto-immunes. Pourtant l'urgence devant un patient fébrile, c'est de poser le diagnostic d'infection qui justifie d'un traitement sans délai. D'autres situations sont également quotidiennes : les tableaux d'altération de l'état général sans point d'appel chez des patients âgés ou encore la dyspnée aiguë chez un patient insuffisant respiratoire chronique. La certitude du diagnostic repose souvent sur l'identification du micro-organisme mais en dehors de la positivité de l'examen direct d'un liquide biologique (liquide céphalo-rachidien, liquide d'ascite, liquide pleural, liquide articulaire), cette confirmation ne peut pas être attendue pour décider de débuter un traitement tout en sachant qu'une documentation microbiologique n'est pas systématique en plus. Cette difficulté à identifier les patients septiques conduit à l'évidence à la sur prescription d'antibiotiques notamment. Ainsi, il existe une demande importante des cliniciens pour des biomarqueurs pour les aider à distinguer les patients nécessitant un traitement anti-infectieux, c'est-à-dire permettant la distinction entre SIRS et sepsis.

Les biomarqueurs connaissent actuellement un développement sans précédent. Plus de 5000 articles sur biomarqueurs et sepsis ont été publiés ces 10 dernières années [18]. Cependant, aucun ne permet de diagnostiquer aujourd'hui un sepsis avec certitude. Ainsi dans les dernières recommandations de la Surviving Sepsis Campaign, il est rappelé que la décision de débuter, modifier ou arrêter un traitement anti-infectieux ne doit jamais être uniquement basé sur un biomarqueur même la procalcitonine (PCT) [47].

La protéine C réactive (CRP) est sans doute le biomarqueur le mieux connu et le plus utilisé au quotidien mais il s'agit d'un biomarqueur d'inflammation, pas d'infection. Synthétisée par les hépatocytes, en réponse à une stimulation par des cytokines, son taux augmente dans les six heures suivant le début du processus inflammatoire pour atteindre un pic entre 24 et 48 heures.

Que l'on regarde la valeur absolue de CRP ou la cinétique d'évolution des taux, les capacités de la CRP à distinguer un sepsis d'un SIRS non infectieux sont très faibles [48,49].

La procalcitonine est le biomarqueur le plus étudié à l'heure d'aujourd'hui. Prohormone de la calcitonine, lors d'un stimulus inflammatoire, la protéolyse de la PCT en calcitonine ne se produit pas, et la PCT intacte est libérée dans la circulation sanguine. La concentration plasmatique de PCT augmente rapidement dès la troisième heure, avec un pic à 24 heures. Initialement considérée comme spécifique des infections, la PCT augmente en fait dans de nombreuses autres situations cliniques (polytraumatisme, brûlures, cancers, etc…). Il existe aussi des faux négatifs (pneumopathies à germes atypiques, tuberculose, etc..). Toutefois, une récente méta-analyse [50] a montré une sensibilité de 0,77 (IC 95% 0,72-0,81) et une spécificité de 0,79 (IC 95% 0,74-0,84) de la PCT pour distinguer un sepsis d'un SIRS d'origine non infectieuse faisant de ce biomarqueur le meilleur par rapport à la CRP [51], le *lipopolysaccharide-binding protein* (LBP) [52], l'IL-6 [52], le *soluble triggering receptor expressed on myeloid cells-1* (sTREM-1) [53] et le *soluble urokinase plasminogen activator receptor* (suPAR) [54]. Mais qui dit meilleur ne dit pas idéal. En plus des biomarqueurs précédemment cités, de nombreux autres ont été proposés pour tenter d'améliorer le diagnostic du sepsis. Force est de constater qu'aucun n'est idéal et qu'il est peu probable qu'un seul biomarqueur puisse diagnostiquer toutes les formes de sepsis. Il n'y a pas une réponse à l'infection mais plutôt une réponse à chaque infection. L'enjeu est donc probablement de trouver les points communs entre la plupart de ces réponses.

Des approches combinant plusieurs biomarqueurs ont ainsi été testées. A titre d'exemple, le « bioscore » développé pour le diagnostic des infections en réanimation, est une combinaison de 3 biomarqueurs : la PCT, le sTREM-1 et l'expression de CD64 sur les neutrophiles, marqueur d'activation leucocytaire au cours de la réponse immunitaire innée. Avec une aire sous la courbe ROC (AUC) à 0,95, supérieure à celle de chaque biomarqueur pris individuellement, l'utilisation de ce « bioscore » à l'admission en réanimation puis à 24 heures permet d'identifier correctement les patients septiques dans la plupart des cas [55]. De même, le panel de six biomarqueurs (suPAR, sTREM-1, MIF [macrophage migration inhibitory factor], CRP, PCT et leucocytes) possède une capacité supérieure en comparaison de chaque marqueur évalué isolément, pour distinguer SIRS/sepsis chez des patients aux urgences ou hospitalisés en maladies infectieuses [56]. Cependant, ces marqueurs restent pour la plupart du domaine de la recherche.

Jusqu'à récemment, les biomarqueurs étudiés étaient tous issus de l'étude des voies fonctionnelles impliquées dans le sepsis. Avec l'avènement des techniques « omiques », une analyse globale sans a priori à l'échelle du transcriptome, du protéome ou encore du métabolome est maintenant possible permettant d'appréhender autrement la réponse de l'hôte. On est ainsi passé d'une approche « réductionniste » se focalisant sur les cellules et molécules individuellement à une approche « systémique » permettant de rendre compte de la manière dont les éléments interagissent entre eux et d'explorer la variabilité des réponses intra et inter-individuelles pour une même agression. Ainsi si on reprend la comparaison du Professeur J. SIBILIA, si on écoute séparément les instruments d'un orchestre, on réalise rapidement qu'il nous est impossible d'apprécier la symphonie.

L'intérêt du transcriptome est maintenant bien connu. Contrairement à l'ADN, dont la séquence est presque identique entre les cellules d'un même organisme, le contenu en ARN est hautement variable selon la cellule ou le tissu étudié(e) et le contexte physiopathologique. On compare souvent le transcriptome à une photographie à un instant précis de l'expression du génome. Grâce aux puces transcriptomiques, il est maintenant possible de savoir, à l'échelle du génome, dans un compartiment cellulaire donné, quels gènes sont actifs, et dans quelle proportion ils sont transcrits. Plusieurs études ont montré que l'analyse transcriptomique permettait d'obtenir une réponse spécifique des patients septiques par rapport aux patients inflammatoires. Ainsi à titre d'exemple, en comparant les profils transcriptomiques des leucocytes de patients atteints de pneumopathie à ceux de patients admis en réanimation avec une présentation clinique semblable mais sans infection, Scicluna et al. [57] ont retrouvé une signature de 78 gènes spécifiques du diagnostic de pneumopathie et ont identifié le ratio d'expression génique FAIM3/PLAC8 comme biomarqueur avec une AUC à 0,845, une valeur prédictive positive (VPP, probabilité d'avoir une pneumopathie en cas de ratio faible) de 83% et une valeur prédictive négative (VPN, probabilité que le diagnostic de pneumopathie soit faux si le ratio est élevé) de 81%. De même, Miller et al. [58] ont mis au point un test SeptiCyte^{TM} LAB qui mesure simultanément le niveau d'expression des gènes CAECAM4, LAMP1, PLA2G7 et PLAC8 permettant de distinguer les patients admis en réanimation pour un sepsis des patients admis pour un syndrome de réponse inflammatoire systémique d'origine non infectieuse avec une AUC à 0,82, une VPP de 69% et une VPN de 91%. Ce test est autorisé par la FDA pour une utilisation en routine en réanimation depuis 2017.

L'analyse du transcriptome permet également de mettre en évidence des différences selon le micro-organisme en cause. Ephraim et al. [59] ont également montré la capacité du

transcriptome à distinguer chez des patients présentant une infection respiratoire haute, une origine virale, d'une origine bactérienne ou non infectieuse. Comparée à la PCT, l'analyse transcriptomique était meilleure pour discriminer les infections bactériennes des tableaux non infectieux [105/124 versus 79/124 (AUC 0,72) ; p<0,001] et pour discriminer les infections bactériennes des tableaux d'autres causes (infections virales et autres) [215/238 versus 186/238 (AUC 0,82) ; p=0,02]. De même, chez des patients présentant une infection respiratoire basse, Suarez et al. [60] ont identifié une signature de 10 gènes permettant de discriminer les infections bactériennes et virales avec une sensibilité de 95%, une spécificité de 92% versus 38% et 91% respectivement pour la PCT. D'autres études confirment l'intérêt du transcriptome pour distinguer l'infection en fonction de la nature de l'agent microbien, par contre il n'est pas mis en évidence de différence en fonction des bactéries ou virus en cause [61,62]. Deux études conduites sur des patients hospitalisés en réanimation n'ont pas montré la capacité de cette technique à discriminer une infection par une bactérie a Gram positif ou négatif [63,64].

Bien que moins connus l'étude du métabolome et du protéome grâce au développement des techniques de spectrométrie de masse est tout aussi intéressante dans le sepsis [65]. A titre d'exemple, Schmerler et al. [66] ont étudié le plasma de 74 patients présentant un SIRS et de 69 patients en sepsis et trouvé 2 lipides (C10:1 et phosphatidylcholine 32:0) significativement élevés chez les patients septiques. Grâce à ces 2 marqueurs, 80% des patients septiques étaient reconnus comme tels et 70% des patients non septiques étaient classés comme non infectés. Overd et al. [67] ont quant à eux étudié 600 protéines chez 765 patients, 319 présentant une infection bactérienne, 334 une infection virale et 112 non infectés. Les concentrations plasmatiques de 3 protéines (TRAIL, IL-10 et CRP) ont permis de distinguer les patients infectés des non-infectés avec une AUC à 0,89.
Ces nouvelles techniques sont ainsi très intéressantes, relativement sensibles et spécifiques. En pleine expansion, elles restent cependant difficiles à envisager en routine pour l'instant. La spectrométrie de masse MALDI-TOF est cependant aujourd'hui utilisée en routine clinique pour l'identification et le typage des micro-organismes [68].

3. La spectrométrie de masse MALDI-TOF

Largement utilisée dans le domaine de la métabolomique et de la protéomique, la spectrométrie de masse est maintenant d'utilisation en routine en microbiologie [69-72]. Elle permet en effet à ce jour dans de nombreux laboratoires l'identification de nombreux micro-organismes entiers sans étape d'extraction protéique dont on obtient un spectre caractéristique par la comparaison du spectre entier avec des bases de données d'empreintes spectrales de référence [68,73,74].

La spectrométrie de masse est une technique d'analyse qui permet de détecter et d'identifier des molécules d'intérêt par mesure de leur masse. Son principe réside dans la séparation en phase gazeuse de molécules chargées en fonction de leur rapport masse/charge (*m/z*).

Un spectromètre de masse comprend toujours un système d'introduction de l'échantillon à analyser, une source d'ionisation permettant le passage en phase gazeuse de l'échantillon et l'ionisation des molécules, un analyseur qui sépare les ions produits selon leur rapport *m/z puis* un détecteur qui fournit un signal électrique proportionnel au nombre d'ions détectés et enfin un système de traitement informatique du signal pour obtenir le spectre de masse représentant les rapports *m/z*, où m représente la masse et z la valence des ions détectés selon l'axe des abscisses et l'abondance relative de ces ions selon l'axe de ordonnées [75].

La méthode MALDI (*Matrix-Assisted Laser Desorption Ionization*) permettant l'analyse de macromolécules en empêchant leur fragmentation, consiste à ajouter à l'échantillon déposé sur un support, une solution organique appelée matrice, qui vont cristalliser ensemble sous l'effet de l'évaporation. Ce mélange est ensuite irradié par un faisceau laser ce qui entraine la désorption (passage en phase gazeuse) puis l'ionisation des molécules (**figure 2**). La technique TOF (*Time of Flight*) qui est associée consiste à mesurer le temps que met un ion, accéléré préalablement par une tension, à parcourir une distance donnée. L'analyseur de temps de vol se compose d'une zone d'accélération où est appliquée une tension accélératrice, et d'une zone appelée tube de vol, libre de champ électrique, dans lequel les ions accélérés volent jusqu'au détecteur (**figure 2**). La séparation des ions va donc dépendre de la vitesse acquise lors de la phase d'accélération. Ainsi les ions ayant une masse élevée parviendront au détecteur plus lentement que les ions de rapport *m/z* plus petit. Le détecteur envoie ensuite les informations enregistrées à l'analyseur qui va traiter les données et les présenter sous forme de spectre.

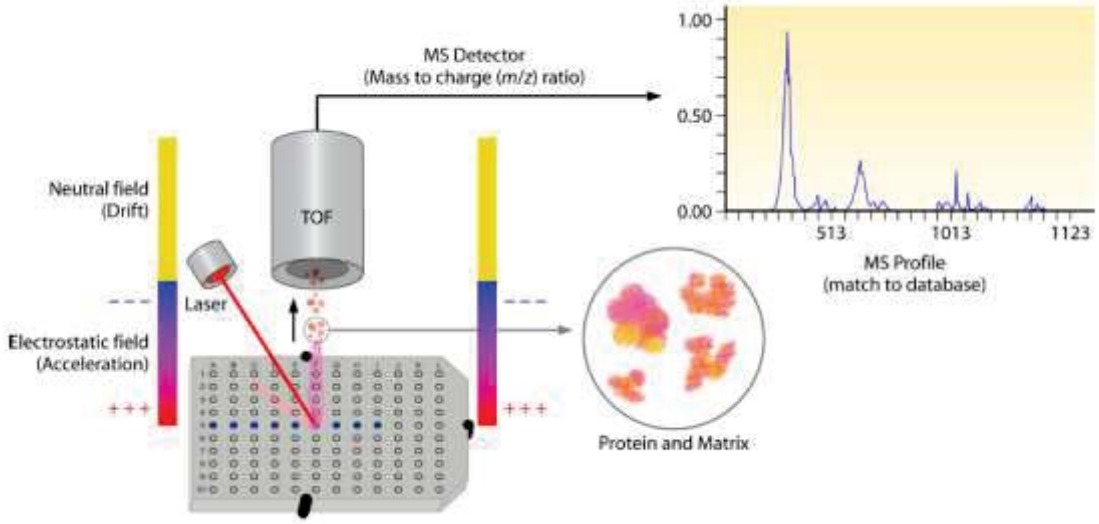

Figure 2 : D'après Clark et al. [72]. Technique MALDI-TOF. Le mélange échantillon à analyser/matrice est irradié par un faisceau laser entrainant le passage en phase gazeuse et l'ionisation des molécules qui sont ensuite accélérées par une impulsion électrique puis passent dans le tube de vol et arrivent jusqu'au détecteur plus ou moins rapidement en fonction de leur vitesse qui dépend de leur masse. Les ions sont séparés selon leur temps de vol, ceux de masse faible atteignant les premiers le détecteur. Le temps de vol pour atteindre le détecteur est ainsi utilisé pour calculer la masse. La somme des ions analysés va former un spectre caractéristique de l'échantillon. Classiquement, l'axe des abscisses correspond au rapport masse sur charge (m/z) et l'axe des ordonnées à l'intensité relative du signal.

L'identification d'un spectre inconnu est réalisée à l'aide d'un algorithme de reconnaissance des pics du spectre inconnu par comparaison avec tous les spectres typiques qui sont enregistrés dans une banque de données. Un score d'appariement précise la ou les identification(s) par ordre de vraisemblance. En microbiologie, les spectres de référence sont créés à partir de pics communs et reproductibles des souches de référence. Un algorithme est utilisé pour comparer le spectre de masse du micro-organisme à identifier aux signatures spectrales de référence ainsi que pour tenir compte de la variabilité entre les réplicats. Le « matching score », fondé sur les masses identifiées et la corrélation de leurs intensités, est généré et utilisé pour classer les résultats. Cette méthode est rapide et simple expliquant son utilisation en routine. Une autre approche consiste en la comparaison de certaines masses du spectre aux masses moléculaires de protéines contenues dans une base de données protéiques. Cette méthode vient de la déduction que la majorité des macromolécules observées sur le spectre ayant des masses

supérieures à 4000 m/z sont des protéines et que la moitié des pics des spectres bactériens correspondent à des protéines ribosomales [60,76,77]. Cependant cette approche nécessite la connaissance des protéomes de tous les micro-organismes d'intérêt clinique ce qui n'est pas le cas pour l'instant.

Chaque instrument est associé à une bibliothèque ou banque de données qui peut être incrémentée, à un algorithme et à des critères d'interprétation différents rendant leur comparaison difficile. Avec le système de Bruker daltonics (appareil Microflex®, logiciel Biotyper®) que nous avons utilisé, un score de correspondance basé sur les masses identifiées et leur corrélation d'intensité est généré et utilisé pour l'identification des microorganismes. Un score entre 2,33 et 3 permet de conclure à une très probable identification d'espèce, entre 2 et 2, 32 à une bonne identification de genre et une probable identification d'espèce, entre 1,7 et 1,999 à une probable identification de genre nécessitant d'autres tests et les scores inférieurs à 1,699 ne permettent pas d'identification.

Seng et al. ont [78] été les premiers à montrer l'intérêt de cette technique avec le système de Bruker daltonics dans l'identification de bactéries à partir de colonies. Depuis le nombre de publications est exponentiel vantant les performances de cette technique également pour l'identification des mycobactéries, levures et champignons [72, 79-82]. L'analyse directe des bactéries à partir d'échantillons de bouillons d'hémocultures positives est maintenant également possible grâce à la commercialisation de kits comme SepsiTyper® pour Bruker daltonics [83]. Cette identification possible à partir des hémocultures permet l'instauration précoce d'un traitement ciblé sur l'espèce identifiée limitant l'utilisation des thérapies à large spectre et réduisant ainsi le risque potentiel de résistances. Clerc et al. [84] ont démontré sur l'étude de 202 cas de bactériémies à bacilles Gram négatif, que les résultats du MALDI-TOF sur le bouillon d'hémocultures conduisaient à une modification de l'antibiothérapie probabiliste initialement débutée dans 35,1% des cas versus dans 20,8% des cas seulement pour les résultats du Gram. Dans 43,7% des cas, les résultats du MALDI-TOF ont conduit à un élargissement du spectre de l'antibiothérapie en raison notamment de la mise en évidence d'un *enterobacter cloacae*. Concernant l'utilisation de la technique sur les urines, différents traitements pré-analytiques des urines ont été proposés avec des résultats très encourageants à condition d'avoir un inoculum bactérien supérieur à 10^5 CFU/mL [85,86]. Le champ d'investigation reste important avec la comparaison des souches, au sein d'une même espèce, l'identification de facteurs de virulence ou encore l'étude de la résistance aux antibiotiques. L'enjeu de la détection de la résistance aux antibiotiques est important car à l'exception de quelques bactéries

pour lesquelles des tests rapides de recherche de résistances existent (ex : la recherche de résistance à la méticilline des staphylocoques), le délai de rendu des antibiogrammes est souvent long. Or si l'identification rapide des bactéries permet d'améliorer l'antibiothérapie probabiliste avec la prise en compte du profil de résistance de l'espèce et de l'écologie de l'environnement, ce sont les résultats de la sensibilité aux antibiotiques qui conditionnent l'antibiothérapie optimale pour le patient. Certaines équipes arrivent à détecter la résistance aux béta-lactamines des entérobactéries et bacilles Gram négatifs non-fermentants ou encore la résistance des entérocoques à la vancomycine grâce à la mise en évidence de pics spécifiques [87-91]. Cependant, aucune de ces méthodes n'est actuellement utilisée en routine.

Lors de l'essor de l'ICM-MS (*Intact Cell MALDI-TOF Mass Spectrometry*), terme retrouvé dans la littérature, l'équipe s'est intéressée à l'application de la méthode MALDI-TOF pour identifier des cellules eucaryotes entières compte tenu des contraintes et limites des techniques existantes. C'est ainsi que Ouedraogo et al. [20] pour la première fois ont réussi à mettre en évidence des signatures spectrales reproductibles de 18 types cellulaires de mammifères et de 4 types d'amibes. Ainsi entre autres, les polynucléaires neutrophiles, les monocytes, les lymphocytes T, les globules rouges, les cellules dendritiques obtenues après culture de monocytes et les macrophages dérivés de monocytes sont identifiables en spectrométrie de masse MALDI-TOF grâce à des pics spécifiques formant une signature spectrale unique. Organisés sous la forme d'un dendogramme, à l'exception des globules rouges, tous les spectres des cellules de mammifères sont regroupés dans un même cluster alors que ceux des cellules des amibes sont dans un autre cluster. Ouedraogo et al. [20] ont également montré que les spectres des cellules immunitaires circulantes avaient de nombreux pics en commun. Dans l'objectif de pouvoir utiliser la technique pour identifier les cellules, pour chaque type cellulaire, un spectre de référence a été créé alimentant ainsi une banque cellulaire. Le test a été ensuite fait en se servant de l'algorithme de l'appareil pour comparer le spectre de monocytes puis d'un mélange de monocytes et lymphocytes T puis de PBMCs (cellules mononuclées du sang obtenues par Ficoll) avec les spectres de la banque. Une identification des cellules a été faite dans les 3 situations. L'équipe a donc transposé avec succès l'utilisation de la spectrométrie de masse MALDI-TOF à la caractérisation et l'identification de cellules.

Cette approche de caractérisation cellulaire par « profiling » à partir de l'analyse directe de cellules eucaryotes entières par spectrométrie de masse MALDI-TOF présente de nombreux avantages car elle requiert très peu de préparation d'échantillons cellulaires et aucune extraction

ou séparation préalable des biomolécules. Elle est extrêmement sensible et reproductible comme le confirme d'autres études avec la mise en évidence des profils spectraux spécifiques de cellules uniques variées chez l'homme comme chez l'animal [92-97] jusqu'à des spectres de groupes de cellules (frottis) [98,99]. Maurer et al. [98] ont en effet créé une base de données de spectres correspondant à des frottis de carcinomes épidermoïdes buccaux et de muqueuses saines de 26 patients. En aveugle, 26 nouveaux prélèvements (de carcinomes, de muqueuses saines et de lésions buccales bénignes) ont ensuite été analysés avec la reconnaissance parfaite des lésions cancéreuses et un seul faux positif. Cette technique a également montré sa capacité pour différencier des lignées cellulaires proches (ex : cellules gliales [94]), évaluer la réponse cellulaire à différentes conditions physiologiques (étapes de maturation, viabilité..) [96,97] et pathologiques [98-100], identifier des réponses à l'exposition à de produits toxiques [101,102] ou à des médicaments [103], ainsi que dépister des performances de lignées cellulaires comme la production d'anticorps [104,105].

A la lecture de ces différentes approches et pouvant assimiler les spectres obtenus par la spectrométrie de masse MALDI-TOF a de véritables « empreintes digitales », nous avons souhaité explorer la polarisation fonctionnelle des macrophages puis l'activation des cellules issues de patients dans l'idée de trouver des signatures ou biomarqueurs potentiels représentatifs de situations pathologiques (infection/inflammation). L'objectif ultime espéré serait de pouvoir rapidement avant même l'identification d'un éventuel micro-organisme soit conforter le clinicien dans son choix de débuter précocement un traitement antimicrobien probabiliste afin de réduire la morbidité et la mortalité, soit à l'inverse lui éviter d'exposer le patient à un traitement large spectre qui risque de faire émerger des résistances.

Au-delà de l'étude de l'activation des cellules de l'immunité en réponse à une agression, nous avons souhaité explorer la variabilité des réponses à l'infection observée en clinique grâce à au modèle *in vitro* de formation de granulomes afin d'appréhender plus finement la réponse de l'hôte et de mieux comprendre les susceptibilités individuelles dans des contextes cliniques particuliers.

4. **<u>Le granulome inflammatoire</u>**

La définition du granulome est anatomopathologique. Il s'agit d'une lésion inflammatoire spatialement limitée, organisée, constituée essentiellement de cellules mononucléées (lymphocytes, monocytes/macrophages, cellules dendritiques) plus ou moins associées en nombre variable à des macrophages spumeux (*foamy*), des cellules épithélioïdes, des cellules géantes multinucléées mais aussi des polynucléaires neutrophiles et éosinophiles et avec la participation de fibroblastes en fonction de la cause de l'inflammation (**figure 3**) [106].

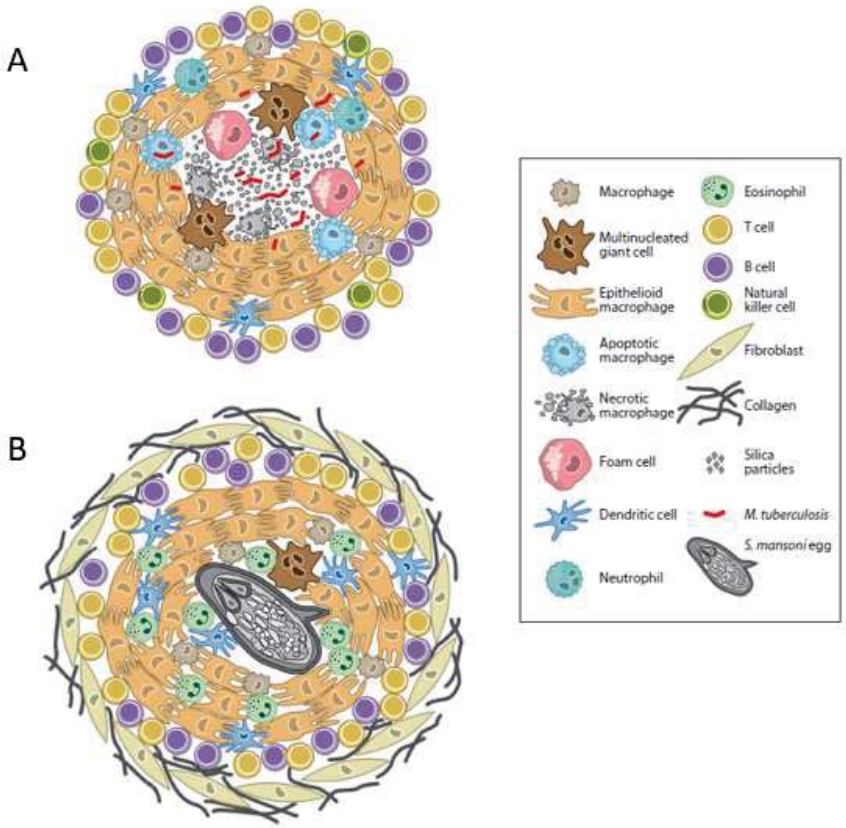

<u>Figure 3</u> : D'après Pagán et al. [106]. Exemples de granulomes. A: Granulome tuberculoïde avec nécrose centrale dans le cadre d'une infection à *Mycobacterium tuberculosis.*; B: Granulome dans le cadre d'une infection à *Schistosoma mansoni*

Le granulome traduit habituellement une réaction inflammatoire chronique en réponse à la persistance d'un agent pathogène (agent infectieux, corps étranger..). Le granulome représente alors un exemple de réaction d'hypersensibilité retardée. Toutefois, dans certains cas comme dans la sarcoïdose ou la maladie de Crohn, l'antigéne responsable n'est pas connu posant un véritable problème diagnostique.

On retrouve dans la composition du granulome les cellules de l'immunité innée mais aussi des cellules spécifiques. Les macrophages spumeux (*foamy*), les cellules épithélioïdes et les cellules géantes multinucléées sont issues de la différentiation des macrophages activés. Les macrophages spumeux sont surtout observés dans les granulomes à mycobactéries. Leur nom vient du fait qu'ils contiennent de nombreuses gouttelettes lipidiques qui serviraient de réserve nutritive pour le pathogène ; lequel pourrait ainsi rester en état de dormance [107]. Les cellules épithélioïdes et les cellules géantes multinucléées sont retrouvées quant à elles dans tout granulome correspondant respectivement à la différentiation des macrophages soumis à une stimulation antigénique prolongée puis à leur fusion. Il semblerait que les cellules épithélioïdes n'aient pas de rôle dans la phagocytose mais plutôt un rôle sécrétoire [108]. En ce qui concerne les cellules géantes multinucléées, la raison de leur formation et leur rôle questionnent toujours. In vitro, la formation de cellules géantes multinucléées peut être induite par différents stimuli entre autres par l'IL-4, l'IL-13, le facteur de croissance GM-CFS (*Granulocyte Macrophage Colony Stimulating Factor*) avec de l'IL-4, de l'IFN-γ plus IL-3 ou encore des lipides mycobactériens [109,110]. Quant à leur rôle, leur capacité de phagocytose serait faible mais en tant que cellules présentatrices de l'antigène, elles participeraient à l'induction de la réponse adaptive [111]. Selon Midle et al. [112], les cellules géantes multinucléées seraient spécialisées dans la phagocytose des cibles de grande taille médiée par le système du complément.

De façon retardée, après reconnaissance de l'antigène et activation, les lymphocytes viennent s'accumuler en couronne à la périphérie du granulome. Le rôle des lymphocytes B est peu étudié. Les lymphocytes T CD8+ ne semblent pas indispensables à la formation des granulomes bien qu'ils soient retrouvés notamment dans les granulomes tuberculeux et induits par *Schistosoma mansoni* [113,114]. Connus pour leurs propriétés cytolytiques notamment par le relargage de granzymes et perforine, dans l'inflammation granulomateuse, ils agiraient aussi par la sécrétion de chimiokines et cytokines notamment IFN-γ. Les lymphocytes T CD4+ jouent par contre un rôle essentiel dans la réponse anti-infectieuse des granulomes. En effet, chez l'homme l'infection par le VIH se traduit par une susceptibilité aux infections entrainant une réponse inflammatoire granulomateuse [115]. De même chez les souris déficientes infectées par *Mycobacterium tuberculosis*, on note un échappement du contrôle de l'infection au bout de quelques jours aboutissant au décès systématique [116].

En fonction de l'ambiance cytokinique liée au pathogène, les lymphocytes T CD4+ vont se différencier notamment en Th1, Th2. Les lymphocytes Th1 sécrétant majoritairement de l'IFN-γ, du TNF-α et de l'IL-2 induisent les réponses immunes cellulaires les plus efficaces contre les virus et bactéries. Les lymphocytes Th2 par la sécrétion d'IL-4, IL-5, IL-10 et IL-13, induisent la production d'IgE et stimulent l'action des éosinophiles, favorisant l'élimination des parasites extra-cellulaires comme les helminthes. Typiquement, on trouve des granulomes « Th1 » dans les infections à mycobactéries, salmonelles ou leishmanies et « Th2 » dans les infections à helminthes comme *Schistosoma mansoni* [117,118]. Les lymphocytes Th17 produisent de l'IL-17, de l'IL-22 et de l'IL-21. Ces cellules sont importantes pour le contrôle des infections bactériennes extra-cellulaires et fongiques. En effet, elles facilitent le recrutement et l'activation des cellules phagocytaires, en particulier les polynucléaires neutrophiles [119].

Le modèle de la tuberculose est l'archétype de cette réponse granulomateuse. Dans la mesure où les bactéries intra-cellulaires survivent au sein des cellules phagocytaires, l'immunité innée est peu efficace. Les cellules NK jouent néanmoins un rôle important car activées par l'IL-12 produite par les macrophages, elles produisent de l'IFN-γ qui renforce l'activation des macrophages infectés et participent au contrôle initial de l'infection. L'immunité humorale est également peu efficace bien que des anticorps dirigés contre les mycobactéries soient présents au cours des infections à mycobactéries ; le principal mécanisme de défense repose donc sur l'immunité adaptative à médiation cellulaire. La réaction d'hypersensibilité retardée dépend de l'activation de lymphocytes T CD4 + Th1 et de la production de cytokines (IFN-γ et TNF-α) qui favorisent le recrutement des leucocytes au niveau du site de l'inflammation et augmentent

la microbicidie des macrophages. Les granulomes limitent le plus souvent la dissémination des bactéries et favorise leur élimination mais parfois, les réponses immunes mises en place contiennent le pathogène sans l'éradiquer (infection latente) avec un risque de réactivation de 5 à 15 % des cas en fonction de l'immuno-compétence du sujet [120]. En cas d'immunodépression, il y a un risque élevé de réactivation avec la survenue d'une tuberculose maladie. Celle-ci dépend de la charge mycobactérienne, en général corrélée au degré d'immuno-compétence. Dans le cas de l'infection par le VIH, les patients ayant une immunodépression profonde présentent souvent des tuberculoses disséminées gravissimes. C'est le cas également des patients porteurs de déficits congénitaux en IL-12 et/ou IFN-γ ou leurs récepteurs [121].

L'étude in situ des granulomes chez l'homme exige des pièces anatomiques provenant de biopsies. Pour pallier cela, une méthode de formation *in vitro* de granulomes a été mise au point en incubant in vitro des cellules mononucléées du sang périphérique (PBMCs) avec des billes de sépharose couplées à des extraits de *Mycobacterium bovis* [110] ou, plus récemment, de *Coxiella burnetii* [21]. Cette méthode simple a permis d'avancer dans la compréhension des mécanismes de formation des granulomes. Il a ainsi été montré dans l'équipe par Delaby et al. [21] que la formation des granulomes résulte de la fixation initiale des monocytes sur les billes puis du recrutement des lymphocytes T et qu'en l'absence de monocytes, il n'y a pas de formation de granulomes. Appliquée dans la fièvre Q chronique, cette méthode a permis de mettre en évidence que le défaut de formation de granulomes constaté résulte d'un défaut de migration des monocytes [22].

Comme nous l'avons vu la réponse immunitaire granulomateuse engage l'ensemble des acteurs du système immunitaire et suit les mêmes étapes que la réponse non granulomateuse. Ainsi l'étude de la formation *in vitro* du granulome représente un moyen d'évaluer de façon globale *ex vivo* la réponse immune de patients. C'est ce que Deknuydt et al. [122] ont fait chez des patients traumatisés crâniens qui dans plus de 40% des cas développent une pneumopathie nosocomiale. Ils ont montré une diminution significative de la formation de granulomes chez les traumatisés crâniens par rapport à des sujets sains et parmi les traumatisés crâniens, ceux développant une pneumopathie nosocomiale en formaient significativement moins que ceux non infectés. Pour expliquer ce défaut de formation, ils ont mis en évidence une diminution significative au niveau des granulomes des cellules géantes multinucléés et des lymphocytes NK chez les traumatisés crâniens.

Il nous a donc semblé opportun d'étudier la réponse immunitaire granulomateuse chez des patients en sepsis sévère et des patients âgés afin d'explorer les mécanismes physiopathologiques qui favorisent les infections dans ces 2 populations.

EXPOSE DES TRAVAUX

Whole-cell MALDI-TOF MS: a new tool to assess the multifaceted activation of macrophages

Ouedraogo R, **Daumas A**, Ghigo E, Capo C, Mege JL, Textoris J.

J Proteomics. 2012 Oct 22;75(18):5523-32.

doi: 10.1016/j.jprot.2012.07.046.

L'utilisation de la spectrométrie de masse MALDI-TOF MS permet à l'heure d'aujourd'hui une identification des germes à partir de cultures et même de certains fluides biologiques infectés. La rapidité et la fiabilité du diagnostic microbien par cette méthode ne sont plus à démontrer. Les micro-organismes inconnus sont identifiés en comparant leurs pics individuels à la banque de données. Le « matching score », fondé sur les masses identifiées et la corrélation de leurs intensités, est généré et utilisé pour classer les résultats.
En utilisant la même approche, Ouedraogo et al. [20] ont montré qu'il était possible de distinguer 22 types cellulaires différents intacts. Après création d'une banque de spectres de référence, la spectrométrie de masse MALDI-TOF a permis d'identifier parmi les cellules mononuclées du sang (PBMCs), les « empreintes » des monocytes et des lymphocytes.

Il est bien connu que les propriétés fonctionnelles des macrophages varient selon leur distribution tissulaire et leur état d'activation. Une classification M1/M2 des macrophages a été proposée sur le modèle de la polarisation lymphocytaire Th1/Th2 [123]. Alors que les macrophages M1 sont inflammatoires et microbicides, les macrophages M2 modulent la réponse immune et sont faiblement microbicides. En réalité, cette notion de polarisation M1/M2 des macrophages recouvre un continuum d'états fonctionnels. Les macrophages peuvent être, initialement inflammatoires avant de participer au remodelage tissulaire et retour à l'homéostasie, ce qui suggère que les changements fonctionnels des macrophages résultent de modifications de leur microenvironnement. L'étude de ces profils bénéficie des approches récentes de biologie systémique qui permettent de mettre en évidence différents types de signatures. Cependant, toutes ces techniques sont longues, plus ou moins sophistiquées et surtout onéreuses.

Ainsi, nous nous sommes demandé si la spectrométrie de masse MALDI-TOF permettrait de détecter différents profils d'activation des macrophages. Aux côtés de Richard Ouedraogo, j'ai pu me familiariser à l'utilisation du spectromètre de masse et à l'analyse des données obtenues. Pour cette étude, les monocytes ont été isolés à partir de PBMCs puis différenciés en macrophages qui ont ensuite été activés par des agonistes M1 (IFN-γ, TNF-α, LPS d'*Escherichia coli*), des agonistes M2 (IL-4, IL-10 et TGF-β) et des bactéries extracellulaires (*Streptococcus agalactiae et Staphylococcus aureus*) et intracellulaires (*Mycobacterium bovis* que l'on retrouve dans le vaccin contre la tuberculose*, Coxiella burnetii* agent de la fièvre Q *et Orientia tsutsugamushi* responsable du typhus des broussailles en Asie) inactivées.
Les cellules activées ont été ensuite déposées sur la plaque du spectromètre et une matrice HCCA (acide a-cyano-4- hydroxycinnamique) a été ajoutée. Les différents mélanges ont ensuite été irradiés. Afin de nous affranchir des outils d'analyse imposés par l'industriel, grâce à Julien Textoris, les données ont été analysées à l'aide du Logiciel gratuit R. Un script d'analyse a ainsi été créé afin de normaliser, aligner et analyser les spectres ainsi obtenus.

Nous avons obtenu après au moins 18h de stimulation par IFN-γ ou IL-4, 2 signatures spectrales très différentes et distinctes de celle des macrophages non activés. Fort de ce premier résultat, nous avons comparé les spectres des macrophages activés par les différents agonistes M1 (IFN-γ, TNF-α, LPS d'*Escherichia coli*) puis ceux des macrophages activés par les différents agonistes M2 (IL-4, IL-10 et TGF-β). On note que les spectres des macrophages activés se regroupent dans un même cluster distinct du cluster avec les spectres des macrophages non activés. On retrouve également une signature spécifique à chaque source d'activation. Il est ainsi possible de distinguer différents profils d'activation des macrophages avec des différences évidentes entre un macrophage M1 et M2.
Nous avons ensuite étudié les spectres des macrophages activés par les bactéries extra-cellulaires et intra-cellulaires. Les signatures induites par les bactéries extracellulaires *Streptococcus agalactiae et Staphylococcus aureus* sont spécifiques de chaque type bactérien et plus proches d'une signature M2 que d'une signature M1. En ce qui concerne les bactéries intracellulaires, les profils d'activation sont distincts les uns des autres à nouveau. Mais alors que les spectres des macrophages activés par *Mycobacterium bovis* clustérisent avec ceux des macrophages activés par L'IL-4 (profil plutôt M2), les spectres des macrophages activés par *Coxiella burnetii et Orientia tsutsugamushi* se regroupent avec ceux des macrophages inactivés.

Il ressort donc de cette étude que la spectrométrie de masse MALDI-TOF est une méthode assez sensible pour détecter rapidement différents états d'activation des macrophages qu'ils soient induits par des agonistes M1, des cytokines M2 ou différentes bactéries. Notre étude met également en évidence la plasticité des macrophages en réponse aux stimuli environnementaux. Cette approche de caractérisation cellulaire par « profiling » à partir de l'analyse directe des cellules entières présente de nombreux avantages car elle requière très peu de préparation des échantillons cellulaires et aucune extraction ou séparation préalable des biomolécules. Elle est extrêmement sensible et reproductible.

JOURNAL OF PROTEOMICS 75 (2012) 5523–5532

Available online at www.sciencedirect.com

SciVerse ScienceDirect

www.elsevier.com/locate/jprot

Whole-cell MALDI-TOF MS: A new tool to assess the multifaceted activation of macrophages

*Richard Ouedraogo, Aurélie Daumas, Eric Ghigo, Christian Capo, Jean-Louis Mege, Julien Textoris**

Unité de Recherche sur les Maladies Infectieuses Tropicales et Emergentes, Aix Marseille Université, CNRS UMR 7278, INSERM U1095, Marseille, France

ARTICLE INFO

Article history:
Received 10 June 2012
Accepted 31 July 2012

Keywords:
Macrophage polarisation
Immune response
Whole-cell MALDI-TOF MS

ABSTRACT

Whole-cell MALDI-TOF MS is routinely used to identify bacterial species in clinical samples. This technique has also proven to allow identification of intact mammalian cells, including macrophages. Here, we wondered whether this approach enabled the assessment human macrophages plasticity. The whole-cell MALDI-TOF spectra of macrophages stimulated with IFN-γ and IL-4, two inducers of M1 and M2 macrophage polarisation, consisted of peaks ranging from 2 to 12 kDa. The spectra of unstimulated and stimulated macrophages were clearly different. The fingerprints induced by the M1 agonists, IFN-γ, TNF, LPS and LPS+IFN-γ, and the M2 agonists, IL-4, TGF-β1 and IL-10, were specific and readily identifiable. Thus, whole-cell MALDI-TOF MS was able to characterise M1 and M2 macrophage subtypes. In addition, the fingerprints induced by extracellular (group B *Streptococcus*, *Staphylococcus aureus*) or intracellular (BCG, *Orientia tsutsugamushi*, *Coxiella burnetii*) bacteria were bacterium-specific. The whole-cell MALDI-TOF MS fingerprints therefore revealed the multifaceted activation of human macrophages. This approach opened a new avenue of studies to assess the immune response in the clinical setting, by monitoring the various activation patterns of immune cells in pathological conditions.

1. Introduction

MALDI-TOF is a MS technique that combines a soft, matrix-assisted, ionization process and a TOF analyzer to separate the generated ions. In MALDI-MS, the mixture of a biological sample with an energy-absorbing matrix allows the genesis of mostly intact-single-charged biomolecules. This property has promoted the technique as one of the most popular in biology and medicine to explore various proteomes.

MALDI-TOF has been extensively used in biology to search biomarkers and to monitor post-translational modifications [1–3]. These approaches usually require large amounts of material, and several steps of fractionation or separation, which are not compatible in the daily monitoring of clinical samples. Another successful application of MALDI-TOF is the identification of microorganisms in clinical samples [4], which is now used in routine in the clinical setting. The spectrum is used as a fingerprint of the bacterial species, without peak identification. Recently, it has been shown that MALDI-TOF MS may also be used to identify whole eukaryotic cells. Buchanan et al. showed that cultured pancreatic islet alpha and beta cells are easily discriminated by MALDI-TOF MS based on the fingerprint

Abbreviations: BCG, Bacille Calmette-Guérin; IFN-γ, Interferon-gamma; IL, Interleukin; LPS, Lipopolysaccharide; M-CSF, Macrophage Colony Stimulating Factor; TGF-β1, Tumor Growth Factor beta 1; TNF, Tumor Necrosis Factor

* *Corresponding author at: URMITE, Faculté de Médecine, 27 Bld.* Jean Moulin, 13385 Marseille Cedex 05, France. Tel.: +33 4 91 32 49 71; fax: +33 4 91 38 77 72.
E-mail address: julien.textoris@ap-hm.fr (J. Textoris).

1874-3919/$ – see front matter © 2012 Elsevier B.V. All rights reserved.
http://dx.doi.org/10.1016/j.jprot.2012.07.046

derived from the different hormone peptides produced by the cells [5]. MALDI-TOF MS has been employed to identify intact mammalian cells including lymphocytes, monocytes, polymorphonuclear cells and erythrocytes. In a similar way, different types of macrophages such as monocyte-derived-macrophages or macrophage cell-lines from different species were easily distinguished [6].

Tissue macrophages play a pivotal role in mounting an immune response to microbial pathogens. They sense infectious agents through receptors that bind conserved and ubiquitous microbial motifs, such as LPS and peptidoglycan and they produce microbicidal compounds [7]. Macrophages present microbial antigens to T cells, thus contributing to the development of adaptive immune response. T cells release cytokines that in turn activate macrophages and either reinforce or regulate their microbicidal activity. Such responses have been classified into M1 and M2 macrophage responses that are analogous to the model of Th1/Th2 lymphocyte polarisation [8–10]. Macrophages activated by the classical pathway (type I cytokines such as IFN-γ and TNF, or bacterial products, such as LPS) are considered M1 macrophages, which are inflammatory, microbicidal and tumouricidal [9,11–14]. Macrophages activated by alternative pathways (IL-4, IL-10, TGF-β1) are considered M2 macrophages, which are poorly microbicidal and tumouricidal and regulate inflammatory and immune responses [10,15,16]. Whole proteome studies have been made using gel-based separation systems and such approach have allowed the identification of a large number of proteins in the proteome, the secretome and in membranes from activated macrophages [17]. Brown et al. showed that 80% of proteins represent the core macrophage proteome, and 20% of proteins define the response-specific proteome. Among the latter proteins, it is possible to identify two unique M1-related signatures induced by either IFN-γ or LPS [18]. Using pulse stable isotope labeling of amino acids in cell culture, Kraft-Terry et al. identified a bioprofile in M-CSF-differentiated monocytes that is consistent with an M2 profile [19].

Due to their high degree of plasticity in response to their micro-environment, macrophages constitute a model of choice to assess the accuracy of whole-cell MALDI-TOF MS to detect subtle modifications. In the current study, we demonstrated that MALDI-TOF MS accuracy is sufficient to study the multifaceted activation of macrophages. When various M1 agonists (IFN-γ, TNF, LPS, LPS+IFN-γ) and M2 agonists (IL-4, TGF-β1, IL-10) were used to stimulate human macrophages, MALDI-TOF MS fingerprints revealed the M1 and M2 subtypes. When macrophages were activated by extracellular bacteria, specific signatures were obtained that were similar to those induced by IL-4. In contrast, intracellular bacteria induced signatures that did not fit with either of the M1 or M2 polarization profiles.

2. Materials and methods

2.1. Bacterial species

Staphylococcus aureus (CIP strain 7625) and group B *Streptococcus* (CIP strain 103227) were obtained from the Laboratory of Microbiology of the Hospital La Timone (Marseille). Briefly, *S. aureus* and group B *Streptococcus* were grown on sheep blood Colombia agar for 2 days, and the purity of the cultures was assessed as previously described [20]. The *Mycobacterium bovis* Bacille Calmette-Guerin (BCG) strain was provided by the Institute Pasteur (CIP strain 105050), and the bacteria were subcultured on Middlebrook 7H10 agar (Becton Dickinson, le Pont de Claix, France) for 2–3 weeks as previously described [21]. *Orientia tsutsugamushi*, strain Kato (CSUR R163), and *Coxiella burnetii*, strain Nine Mile (RSA 493), were cultured on mouse L929 cells in MEM containing 5% FCS and 2 mM L-glutamine as previously described [22]. The L929 cells were infected for approximately 7 days. Infected cells were sonicated and centrifuged at 300 ×*g* for 10 min to discard cellular debris. The supernatants were then centrifuged at higher speed and bacteria were collected. The collected bacteria were washed in PBS (pH 7.2) and stored at −80 °C. Bacterial concentrations were determined by indirect immunofluorescence and/or quantitative PCR using specific primers. The bacterial viability was assessed using the LIVE/DEAD BacLight bacterial viability kit (Molecular Probes, Life Technologies, Saint Aubin, France). Heat-killed bacteria were obtained by incubating the bacteria at 95 °C for 1 h.

2.2. Activation of macrophages

Peripheral blood mononuclear cells were isolated from five buffy coats (Etablissement Français du Sang, Marseille) and three healthy blood donors by Ficoll density gradient as previously described [23]. Monocytes were obtained from mononuclear cells using magnetic beads coated with anti-CD14 Abs (Miltenyi Biotech, Paris, France) according to the manufacturer's instructions. This procedure resulted in more than 95% monocyte purity as assessed by flow cytometry, and monocyte viability was greater than 98% as determined by trypan blue exclusion. Monocytes (10^6 cells in 6-well plates) were incubated in 3 mL of RPMI 1640 containing 20 mM HEPES, 10% human serum AB^+, 2 mM L-glutamine, 100 IU/mL penicillin and 100 μg/mL streptomycin (Life Technologies) for 4 days, and FCS replaced human serum for an additional 3 days. The obtained cell population was identified as macrophages (more than 95% pure) by flow cytometry using CD68 expression as a positive marker of macrophages. Macrophages were stimulated with 20 ng/mL human recombinant IFN-γ (PeproTech, Neuilly-sur-Seine, France), IL-4 (AbCys, Paris, France), IL-10, TGF-β1 (R&D Systems, Lille, France) and TNF (Euromedex, Mundolsheim, France) for different periods of time. Macrophages were also stimulated with 1 μg/mL LPS from *Escherichia coli* (Sigma–Aldrich, Saint Quentin Fallavier, France) or heat-killed bacteria (50 bacteria per cell).

2.3. MALDI-TOF MS

Stimulated macrophages (10^6 cells) were centrifuged for 5 min at 300 ×*g*. The cell pellets were suspended in 10 μL of sterile PBS and frozen at −80 °C for 2 to 3 days. After thawing, 1 μL of the cell suspension was added to 1 μL of α-cyano-4-hydroxy-cynnamique acid matrix and the mixture was deposited onto the MALDI target using an AutoFlexII spectrometer and FlexControl software (Bruker Daltonics, Wissembourg, France) as previously described [6]. The ions that resulted from a 170 ns pulse ion extraction of the laser emitting at 337 nm were subjected to an electric field of 20 kV

and analysed in linear mode with time of flight. The resulting accuracy and resolution was 200 ppm. The generated spectra were a result of the sum of the positive ions that were obtained after 525 laser shots in different locations of the spot. We performed control acquisition with matrix only, with cytokines only or with heat-killed bacteria alone. The peaks identified in these control acquisitions were neither observed nor selected in macrophage acquisitions.

2.4. *Spectrum analysis*

All analyses and graphical outputs were performed using R (version 2.13). Raw data were loaded in R using the *readBrukerFlexData* library. The spectra were analysed using the *MALDIquant* library and specific algorithms. Briefly, the square root of the intensities was used to enhance the graphical visualisation of the spectra. The background was corrected using a statistic-sensitive non-linear peak-clipping algorithm for baseline estimation [24]. Peaks were detected using a signal-to-noise ratio of 6. The detected peaks were considered similar across spectra when the *m/z* values were within a 2000 ppm window. The x-axis of spectra represented the *m/z* ratio of ionised molecules, and the y-axis indicated the relative proportion of these molecules (in relative intensities). The gel view representation indicates the reproducibility of the spectra obtained from different samples that were arranged in a pseudo-gel format. A hierarchical clustering with a ward algorithm for agglomeration and a dissimilarity matrix based on the Jaccard distance were used to classify the spectra. The Jaccard index measures the similarity between Boolean sample sets. The Jaccard distance, which measures dissimilarity between sample sets, is complementary to the Jaccard index and is obtained by subtracting the Jaccard coefficient from 1 or by dividing the difference of the sizes of the union and the intersection of two sets by the size of the union. To obtain reference spectra, we first computed a distance matrix for the class and then obtained the mean distance of each spectrum versus all other spectra of the same class. The reference spectra for each class were defined as the spectra with the minimal mean distance to the class. The implementation of the analysis presented in this manuscript is provided online (Material S1).

3. Results

3.1. *MALDI-TOF MS analysis of macrophages stimulated with IFN-γ and IL-4*

Human monocyte-derived macrophages were stimulated with IFN-γ and IL-4 for 18 h; these treatments are known to polarise macrophages towards M1 and M2 profiles, respectively [9]. Whole cells were then analysed using MALDI-TOF MS, and the representative spectra are shown (Fig. 1A). The spectrum of unstimulated macrophages was composed of numerous peaks concentrated in the range of 2–6 kDa with a major peak at a mass/charge (*m/z*)=4965. The spectral representation of macrophages stimulated with IFN-γ and IL-4 showed dramatic differences between the treatments (Fig. 1A).

The reproducibility of the MALDI-TOF MS data obtained from different macrophage samples was assessed using a virtual gel view representation and hierarchical clustering based on common and specific peaks of spectra. All samples were grouped into three major clusters that were representative of unstimulated macrophages, IL-4-stimulated macrophages and IFN-γ-stimulated macrophages (Fig. 1B). Weak variations in *m/z* values and/or peak intensities were observed among the samples within the same cluster. These variations led us to define reference spectra. To this end, the spectra of the various samples were analysed by comparing the presence or absence of the peaks and by integrating the variability of the intensities of shared peaks. This approach allowed for the identification of specific fingerprints of IFN-γ- and IL-4-stimulated macrophages. When IFN-γ stimulated macrophages were compared with unstimulated macrophages, 20 peaks specifically appeared (see also Table 1) and 13 peaks that were present in the unstimulated macrophages were absent in the IFN-γ-stimulated samples (Fig. 1C). Furthermore, the intensity of the major peak at *m/z*=4965 in the unstimulated macrophages was clearly reduced in the IFN-γ-stimulated samples. When macrophages stimulated with IL-4 were compared with unstimulated macrophages, we found that 22 peaks appeared (see also Table 1) and 13 peaks that were present in the unstimulated macrophages disappeared in the IL-4-stimulated samples (Fig. 1C). The spectra obtained in response to IFN-γ and IL-4 were clearly different (Fig. 1C), demonstrating that the M1 and M2 agonists altered the MALDI-TOF MS fingerprints.

As macrophages are known to be versatile cells, we analysed the time course of their MALDI-TOF MS responses to IFN-γ and IL-4. Differences in time and stimulation were assessed by hierarchical clustering. After 9 h of stimulation, the spectra of macrophages stimulated with IFN-γ or IL-4 were similar and resembled those of unstimulated macrophages. In contrast, macrophages stimulated with IFN-γ or IL-4 for 18, 36 and 48 h clustered according to the agonist (Fig. S1). These results suggest that macrophages exhibited distinct patterns of activation only after 18 h of stimulation. All subsequent analyses were therefore conducted after 18 h of stimulation. Taken together, these results demonstrated that the whole-cell MALDI-TOF MS approach is useful for analysing the activation status of human macrophages.

3.2. *MALDI-TOF MS analysis of macrophages stimulated with M1- and M2-related agonists*

It is commonly accepted that IFN-γ, TNF and LPS induce an inflammatory (M1-type) response in macrophages whereas IL-4, TGF-β1 and IL-10 induce an immunoregulatory (M2-type) response [25]. We therefore sought to determine whether whole-cell MALDI-TOF MS could detect the M1 and M2 subtypes. We found that the spectra from the macrophages stimulated with M1 agonists clustered together and were separate from the unstimulated macrophages. In addition, we detected differences between the M1 agonists; the response to TNF was close to that of IFN-γ, and the response to the combination of IFN-γ and LPS was closer to that induced by LPS than to the response induced by IFN-γ (Fig. 2A). Second, the spectra of macrophages stimulated with M2 agonists were

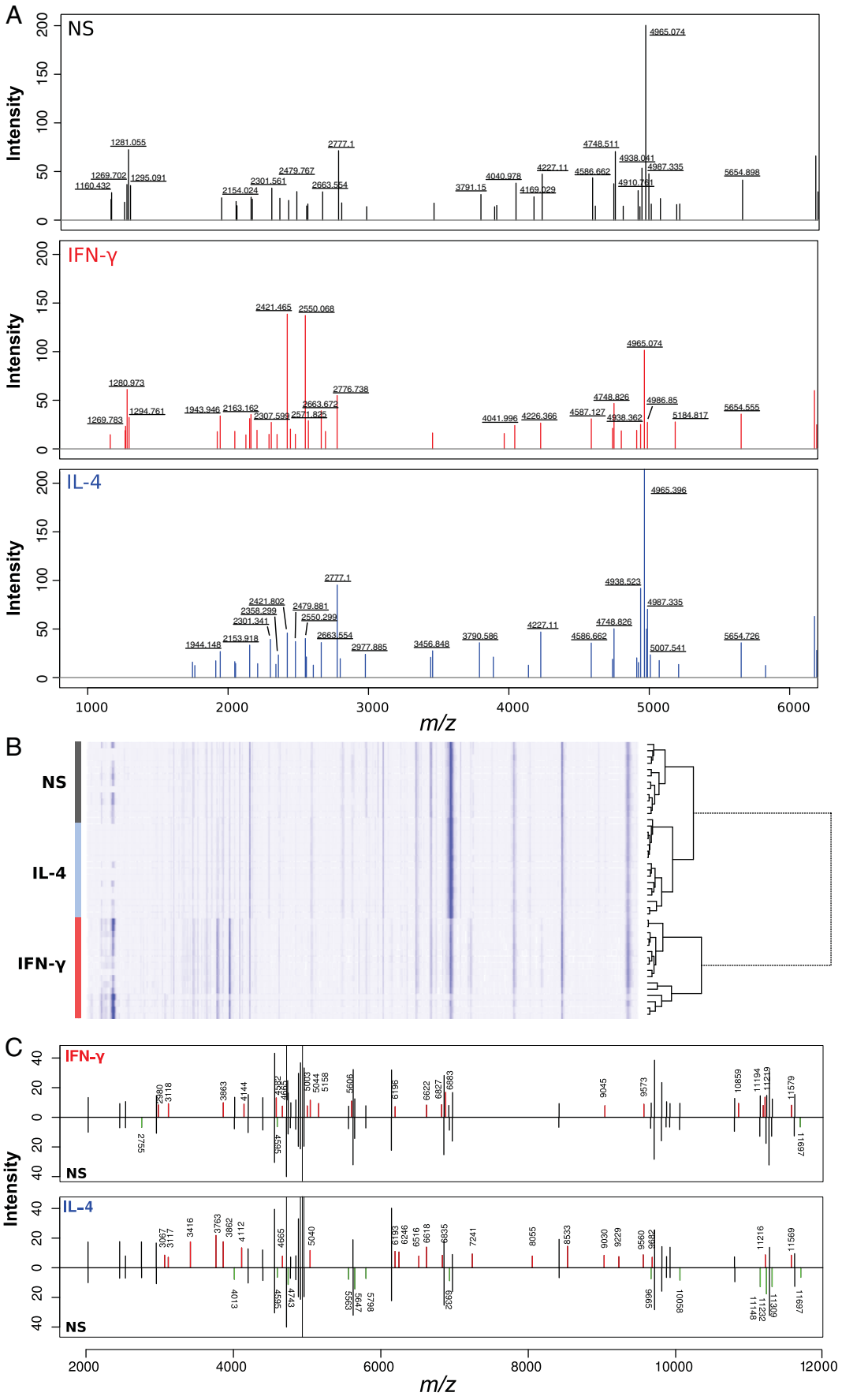
A
NS
IFN-γ
IL-4
Intensity
m/z
B
NS
IL-4
IFN-γ
C
IFN-γ
IL-4
NS
Intensity
m/z

Table 1 – Characteristic peaks of macrophages stimulated with cytokines.
The *m/z* ratio of specific peaks that resulted from the comparison of the reference spectra between stimulated and unstimulated macrophages is shown. Each row corresponds to peaks with different *m/z* values, and peaks that were considered identical are presented in the same row. The peaks that were specific for each experimental condition are underlined. *, M1-related peaks. **, M2-related peaks.

IFN-γ	TNF	IL-4	IL-10
2980	2978	–	2977
–	–	3067	–
3118	3116	3117	–
–	3417	3416	–
–	–	3763	–
3863	3863	3862	–
–	–	–	3962
–	–	4112	–
4144	–	–	4141
4582	–	–	–
4665	4662	4665	–
–	–	–	4978
5003	–	–	–
5044	–	5040	–
5158	–	–	–
–	5387	–	5387
5606	5601	–	–
–	–	–	6052
–	–	–	6080
–	6107	–	–
6196	–	6193	–
–	–	6246	–
–	–	6516	–
–	–	–	6545
6622	6618	6618	–
6827*	6826*	–	–
–	–	6835**	6833**
–	–	–	–
6883	–	–	–
–	–	–	6912
–	6920	–	–
–	7234	7241	7237
–	–	8055	–
–	–	8533	–
–	–	9030	–
–	9039	–	–
9045	–	–	–
–	–	9229	–
–	–	9560**	9561**
–	9565	–	–
9573	–	–	–
–	–	9682	–
10589	–	–	–
–	11187	–	–
11194	–	–	–
–	–	–	11206
11219	–	11216	–
-	11565	11569	–
11579	–	–	11579

Fig. 1 – MALDI-TOF MS spectra of macrophages. A, Monocytes from one healthy blood donor were differentiated into macrophages. Macrophages were stimulated with IFN-γ or IL-4 for 18 h. Macrophages were then collected in 10 μL of PBS, and 1 μL was deposited onto the MALDI target. Representative MALDI-TOF MS spectra are shown. B–C, Macrophages from different blood donors were stimulated with IFN-γ and IL-4 for 18 h. The spectra were arranged in a pseudo-gel format using a gel view representation (B). Spectrum classification resulted in reference spectra. The reference spectra from stimulated macrophages were plotted against the reference spectra from unstimulated macrophages (C). The peaks that were detected when macrophages were stimulated are in red, and the peaks that were present in unstimulated macrophages but not in stimulated macrophages are in green. NS: non-stimulated macrophages. (For interpretation of the references to color in this figure legend, the reader is referred to the web version of this article.)

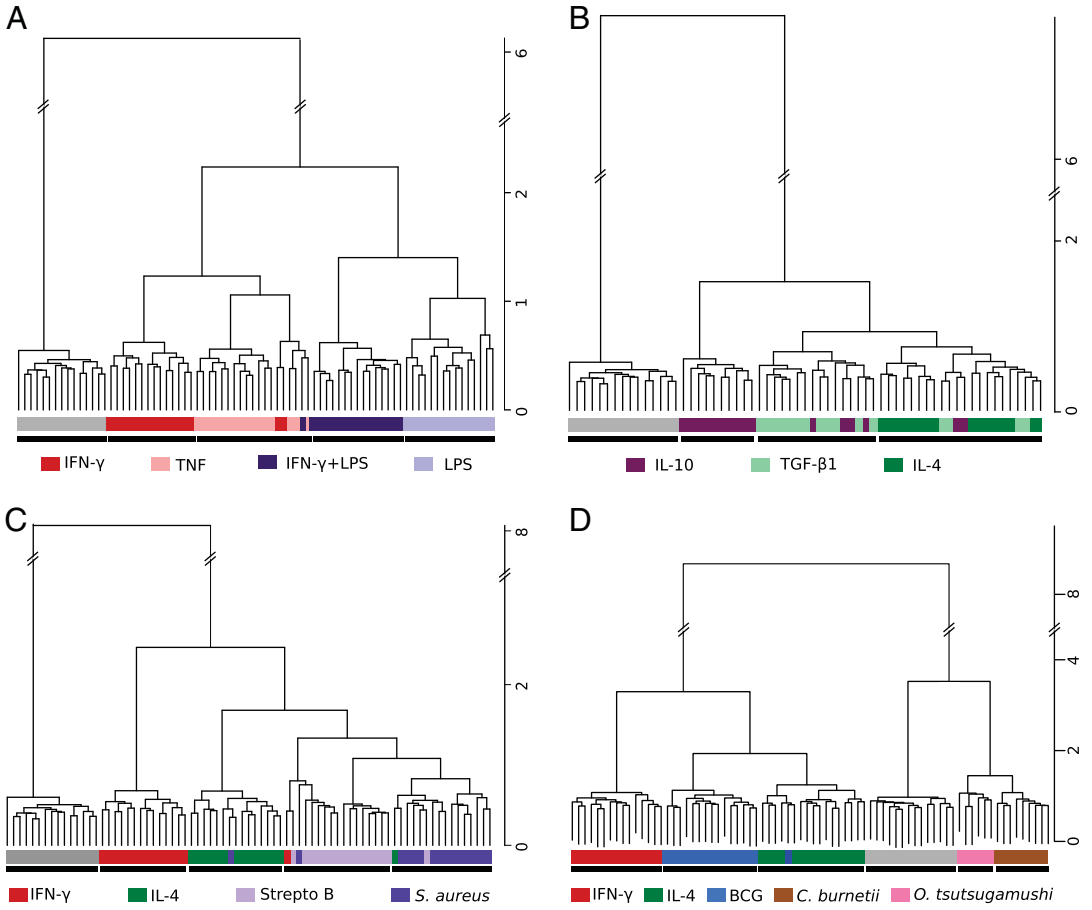

Fig. 2 – Hierarchical clustering of activated macrophages. Macrophages were stimulated with different agonists for 18 h. The results are shown as hierarchical clustering of the data. Macrophages were activated with M1-related agonists (A), M2-related agonists (B), extracellular bacteria (C) and intracellular bacteria (D). Unstimulated macrophages are presented in grey. Strepto B: group B *Streptococcus*.

distinct from those of unstimulated macrophages, and distinct responses to IL-4, TGF-β1 and IL-10 were identified (Fig. 2B), suggesting that MALDI-TOF MS discriminated M2 subtypes. When reference spectra were used to characterise common M1 and M2 peaks, we found that only one peak (m/z=6,826) was common to the spectra induced by IFN-γ and TNF and was absent in the spectra induced by IL-4 and IL-10 (Table 1). Similarly, two peaks (m/z=6835 and 9560) were common to the macrophages stimulated with IL-4 and IL-10 but were absent in the macrophages stimulated with IFN-γ and TNF. In contrast, 8 specific peaks characterised the response of macrophages to IFN-γ when compared with the responses to TNF, IL-4 and IL-10. The responses to TNF, IL-4 and IL-10 included 4, 10 and 7 specific peaks, respectively, compared with the other agonists. The list and the m/z values of these peaks are shown in Table 1. Taken together, these results show that whole-cell MALDI-TOF MS analysis can discriminate macrophages according to their subtypes.

3.3. *MALDI-TOF MS analysis of macrophages stimulated with bacterial pathogens*

To assess the ability of whole-cell MALDI-TOF MS to detect pathogen-associated fingerprints, we investigated the responses of macrophages to representative extra- and intracellular bacteria. The signatures induced by extracellular bacteria including group B *Streptococcus* and *S. aureus*, were highly reproducible and were specific to each type of bacteria. Analysis of the reference spectra showed that 5 and 6 peaks were specifically associated with the responses to *S. aureus* and group B *Streptococcus*, respectively, as compared with the unstimulated macrophages (Table 2). The responses to bacterial organisms were closer to those induced by IL-4 than to those induced by IFN-γ (Fig. 2C), suggesting that the responses were M2-related. Next, the responses of macrophages to intracellular bacteria, such as BCG, *O. tsutsugamushi* and *C. burnetii*, were investigated. Again, these bacteria induced specific responses. Analysis of the reference spectra obtained in response to intracellular bacteria showed that 6, 4 and 8 peaks were specifically associated with the responses to BCG, *O. tsutsugamushi* and *C. burnetii*, respectively (Table 3). The BCG-stimulated macrophages clustered with the IL-4-stimulated samples, suggesting that BCG induced an M2-type response. In contrast, the *O. tsutsugamushi* and *C. burnetii* spectra clustered together and were closer to the unstimulated macrophages than to the IFN-γ- or IL-4-stimulated macrophages (Fig. 2D). These data suggest that M1/M2 polarisation does not completely describe the multifaceted activation of macrophages. They also

Table 2 – Characteristic peaks of macrophages stimulated with extracellular bacteria.
The *m/z* ratio of specific peaks that resulted from the comparison of the reference spectra between stimulated and unstimulated macrophages is shown. Each row corresponds to peaks with different *m/z* values, and peaks that were considered identical are presented in the same row. The peaks that were specific for each experimental condition are underlined.

IFN-γ	IL-4	*S. aureus*	Group B *Streptococcus*
–	–	–	2135
–	–	–	2271
–	–	2641	2639
2980	–	–	–
–	3067	3066	–
3118	3117	–	–
–	–	3386	3386
–	3416	3415	3416
–	3763	3762	3762
3863	3862	3860	3860
–	4112	4110	4109
4144	–	–	–
–	–	–	4426
4582	–	–	4578
4665	4665	–	4660
–	–	4995	4993
5003	–	–	–
5044	5040	5039	5038
5158	–	–	–
5606	–	–	–
–	–	–	6010
–	–	6053	6052
–	–	6102	6099
6196	6193	6191	6192
–	6246	6244	6244
–	6516	6510	–
–	–	–	6538
6622	6618	6615	6615
6827	–	–	–
–	6835	–	–
6883	–	–	6885
–	–	7003	–
–	7241	7238	–
–	8055	–	–
–	–	8138	–
–	–	8178	–
–	8533	8528	8528
–	9030	9025	9027
9045	–	–	–
–	9229	9227	9226
–	–	9552	–
–	9560	–	–
9573	–	–	–
	9682	–	–
10589	–	–	–
–	–	10848	–
11194	–	–	–
–	–	–	11209
11219	11216	–	–
–	11569	–	11564
11579	–	–	–

indicate that whole-cell MALDI-TOF MS may be useful for assessing specific macrophage responses to bacterial pathogens.

4. Discussion

We have recently used MALDI-TOF MS to classify intact eucaryotic cells without the extraction of cellular proteins. This method has a high resolution and detects circulating cells, such as monocytes, lymphocytes and neutrophils. It also detects murine and human macrophages and diverse macrophage-related cell lines [6]. Here, we investigated whether the accuracy of the whole-cell MALDI-TOF MS approach enabled the assessment of multifaceted activation of macrophages and, particularly, the conditions leading to M1/M2 polarisation. Analysis of the MALDI-TOF MS profiles of

Table 3 – Characteristic peaks of macrophages stimulated with intracellular bacteria.
The *m/z* ratio of specific peaks that resulted from the comparison of the reference spectra between stimulated and unstimulated macrophages is shown. Each row corresponds to peaks with different *m/z* values, and peaks that were considered identical are presented in the same row. The peaks that were specific for each experimental condition are underlined.

IFN-γ	IL-4	BCG	*O. tsutsugamushi*	*C. burnetii*
–	–	–	2283	2282
–	–	–	–	2339
–	–	–	–	2429
–	–	–	2666	2668
–	–	–	2780	2779
2980	–	–	–	–
–	3067	3071	–	–
–	–	–	3087	3087
3118	3117	–	–	–
–	–	–	–	3153
–	3416	3417	–	–
–	3763	3766	3768	3768
–	–	–	3791	–
3863	3862	3862	3865	3866
–	4112	4111	–	–
4144	–	–	–	–
–	–	4430	4432	–
4582	–	–	4583	4584
–	–	–	4607	–
4665	4665	–	–	–
–	–	–	4984	–
5003	–	5002	5006	5006
5044	5040	–	–	–
–	–	–	5071	–
5158	–	–	–	–
5606	–	–	–	–
–	–	–	–	5779
–	–	6014	–	6017
–	–	6054	–	–
–	–	–	–	6061
6196	6193	6195	6196	6195
–	6246	6247	6251	–
–	6516	6516	–	–
–	–	–	–	6544
6622	6618	–	6621	6627
6827	–	–	–	–
–	6835	6832	–	–
6883	–	–	–	–
–	7241	7240	–	7244
–	–	7454	7458	–
–	8055	–	–	–
–	–	8181	–	–
–	–	–	–	8272
–	8533	–	–	–
–	9030	–	–	–
9045	–	–	–	–
–	9229	–	–	–
–	9560	–	–	–
9573	–	–	–	–
–	–	9661	–	–
–	9682	–	–	–
–	–	9877	–	–
–	–	9921	–	–
–	–	–	–	9932
10589	–	–	–	–
–	–	10855	–	–
11194	–	–	–	–
11219	11216	–	–	–
–	11569	–	–	–

macrophages showed that the responses to IFN-γ and IL-4, two canonical inducers of M1 and M2 macrophages, respectively, clustered into distinct groups. The resulting spectra of the M1/M2 polarised macrophages were highly reproducible. Hence, MALDI-TOF MS profiles of macrophages stimulated with IFN-γ and IL-4 may be considered fingerprints of M1 and M2 macrophages, respectively. To our knowledge, only two studies have explored the ability of whole-cell MALDI-TOF MS to assess various states of a unique cell type. Small differences in MALDI-TOF MS spectra are sufficient to assess the viability of CHO cells [26]. Marvin-Guy et al. demonstrated that the spectra from T84 epithelial cells in the growth phase are very different from those of confluent cells [27]. Our results suggested that whole-cell MALDI-TOF MS could be used to assess the plasticity of cells, such as macrophages.

The inflammatory cytokine, TNF, and the bacterial component, LPS, are considered to be M1 agonists; thus, we investigated whether whole-cell MALDI-TOF MS could be used to study the activation of macrophages by TNF and LPS. The TNF and LPS responses were close to the classical M1 response induced by IFN-γ although the TNF and LPS responses exhibited specific features. This underlines that the accuracy of the technique allowed to detect distinct subgroups in the M1 polarised macrophages. The combination of IFN-γ and LPS also led to an M1-type response, and was closer to the profile induced by LPS alone. This finding may be a result of the differences between the priming and activation of macrophages. Indeed, it is well known that IFN-γ does not induce cytokine release or promote the microbicidal activity of macrophages, but it amplifies these functions in the macrophage response to LPS [28]. IFN-γ and LPS differentially modulate gene expression in macrophages [29], and it has recently been demonstrated that proteome profiles are different in human macrophages stimulated with IFN-γ, LPS and the combination of IFN-γ+LPS [18]. We also asked whether whole-cell MALDI-TOF MS could be used to discriminate different types of M2 macrophages. It has been suggested that M2 macrophages include at least three subsets with different phenotypic characteristics, repertoires of gene expression, abilities to produce cytokines and functional activities [30,31]. We found that IL-10 and TGF-β1 induced spectra that were close to but distinct from those induced by IL-4. Taken together, these results demonstrated that MALDI-TOF MS approach was able to discriminate different subtypes of M1 and M2 macrophages.

Macrophages are known to play essential roles in host defence by recognising, engulfing and killing microorganisms. They respond to a broad variety of bacteria through a unique pattern of gene expression changes, referred to as the "common host response" [12,32–34]. Evidence also indicates that bacterial pathogens can interfere with macrophage activation. We found that the MALDI-TOF MS spectra of macrophages stimulated with the extracellular bacteria such as *S. aureus* and group B *Streptococcus* evoked M2 profiles. These M2-type profiles may be a result of the production of IL-10 by macrophages stimulated with *S. aureus* [35] and the inhibition of the NF-κB pathway by group B *Streptococcus* [36]. The MALDI-TOF MS approach discriminated the responses to *S. aureus* and group B *Streptococcus*. The MALDI-TOF MS profiles of macrophages stimulated with intracellular bacteria were clustered into a group that included BCG- and cytokine-stimulated macrophages and a distinct cluster composed of *O. tsutsugamushi*, the agent of scrub typhus, *C. burnetii*, the agent of Q fever, and unstimulated macrophages. Interestingly, BCG-stimulated macrophages exhibited a more similar response to macrophage stimulated with IL-4 than with IFN-γ, suggesting an M2-type response. It has been demonstrated that bacteria, such as *Mycobacterium tuberculosis*, induce an M2 phenotype *in vitro* [37], which is consistent with our findings. We previously demonstrated that *O. tsutsugamushi* replicates in human monocytes and upregulates the expression of genes that are associated with the M1 polarisation of macrophages [22]. This apparent discrepancy with our current results may be attributed to a variety of causes. For example, exocytosis may interfere with the fingerprints observed in the MALDI-TOF MS analysis, as macrophages are known to produce high levels of cytokines in response to pathogens. Moreover, the response to heat-killed *O. tsutsugamushi* is dramatically different from that of live organisms [22], suggesting that the use of macrophages and heat-killed pathogens instead of monocytes and live organisms may affect the cellular response to bacterial aggression. This is highlighted by the transcriptional responses of monocytes and macrophages to *C. burnetii*. Indeed, *C. burnetii* induces a transcriptional M1-type response in monocytes and an atypical M2-type profile in macrophages [12]. Taken together, these results show that an easy assay using whole-cell MALDI-TOF was able to detect specific fingerprints of macrophages stimulated with various bacteria. Whole-cell MALDI-TOF may therefore be suitable to explore the immune response.

In conclusion, the accuracy and reproducibility of the whole-cell MALDI-TOF MS approach enables the analysis of different types of macrophage activation. This fast and inexpensive method permits the classification of M1- and M2-associated macrophage phenotypes and reveals the diversity of proteomic responses to cytokines and bacterial pathogens. The specific fingerprints we found may be useful for studying the activation of macrophages in pathological conditions.

Supplementary data to this article can be found online at http://dx.doi.org/10.1016/j.jprot.2012.07.046.

Conflict of interest

There is no financial/commercial conflict of interests.

Acknowledgments

Richard Ouedraogo was supported by a grant from the Ministère de la Santé (PHRC 2010).

REFERENCES

[1] Huang Q, Huang Q, Chen W, Wang L, Lin W, Lin J, et al. Identification of transgelin as a potential novel biomarker for gastric adenocarcinoma based on proteomics technology. J Cancer Res Clin Oncol 2008;134:1219-27.

[2] Visentin M, Simula MP, Sartor F, Petrucco A, De Re V, Toffoli G. Identification of proteins associated to multi-drug resistance in LoVo human colon cancer cells. Int J Oncol 2009;34:1281-9.

[3] Fan Y, Wang J, Yang Y, Liu Q, Fan Y, Yu J, et al. Detection and identification of potential biomarkers of breast cancer. J Cancer Res Clin Oncol 2010;136:1243-54.
[4] Welker M. Proteomics for routine identification of microorganisms. Proteomics 2011;11:3143-53.
[5] Buchanan CM, Malik AS, Cooper GJS. Direct visualisation of peptide hormones in cultured pancreatic islet alpha- and beta-cells by intact-cell mass spectrometry. Rapid Commun Mass Spectrom 2007;21:3452-8.
[6] Ouedraogo R, Flaudrops C, Ben Amara A, Capo C, Raoult D, Mege JL. Global analysis of circulating immune cells by matrix-assisted laser desorption ionization time-of-flight mass spectrometry. PLoS One 2010;5:e13691.
[7] Ishii KJ, Koyama S, Nakagawa A, Coban C, Akira S. Host innate immune receptors and beyond: making sense of microbial infections. Cell Host Microbe 2008;3:352-63.
[8] Mantovani A, Sica A, Locati M. Macrophage polarization comes of age. Immunity 2005;23:344-6.
[9] Martinez FO, Sica A, Mantovani A, Locati M. Macrophage activation and polarization. Front Biosci 2008;13:453-61.
[10] Mosser DM, Edwards JP. Exploring the full spectrum of macrophage activation. Nat Rev Immunol 2008;8:958-69.
[11] Murray PJ, Wynn TA. Protective and pathogenic functions of macrophage subsets. Nat Rev Immunol 2011;11:723-37.
[12] Benoit M, Desnues B, Mege JL. Macrophage polarization in bacterial infections. J Immunol 2008;181:3733-9.
[13] Biswas SK, Sica A, Lewis CE. Plasticity of macrophage function during tumor progression: regulation by distinct molecular mechanisms. J Immunol 2008;180:2011-7.
[14] Cassetta L, Cassol E, Poli G. Macrophage polarization in health and disease. Sci World J 2011;11:2391-402.
[15] Gordon S. Alternative activation of macrophages. Nat Rev Immunol 2003;3:23-35.
[16] Mantovani A, Sica A, Sozzani S, Allavena P, Vecchi A, Locati M. The chemokine system in diverse forms of macrophage activation and polarization. Trends Immunol 2004;25:677-86.
[17] Slomianny M-C, Dupont A, Bouanou F, Beseme O, Guihot AL, Amouyel P, et al. Profiling of membrane proteins from human macrophages: comparison of two approaches. Proteomics 2006;6:2365-75.
[18] Brown J, Wallet MA, Krastins B, Sarracino D, Goodenow MM. Proteome bioprofiles distinguish between M1 priming and activation states in human macrophages. J Leukoc Biol 2010;87:655-62.
[19] Kraft-Terry SD, Gendelman HE. Proteomic biosignatures for monocyte-macrophage differentiation. Cell Immunol 2011;271:239-55.
[20] Drancourt M, Roux V, Fournier PE, Raoult D. rpoB gene sequence-based identification of aerobic Gram-positive cocci of the genera *Streptococcus*, *Enterococcus*, *Gemella*, *Abiotrophia*, *and Granulicatella*. J Clin Microbiol 2004;42:497-504.
[21] Delaby A, Gorvel L, Espinosa L, Lépolard C, Raoult D, Ghigo E, et al. Defective monocyte dynamics in q Fever granuloma deficiency. J Infect Dis 2012;205:1086-94.
[22] Tantibhedhyangkul W, Prachason T, Waywa D, El Filali A, Ghigo E, Thongnoppakhun W, et al. *Orientia tsutsugamushi* stimulates an original gene expression program in monocytes: relationship with gene expression in patients with scrub typhus. PLoS Negl Trop Dis 2011;5:e1028.
[23] Ghigo E, Imbert G, Capo C, Raoult D, Mege JL. Interleukin-4 induces *Coxiella burnetii* replication in human monocytes but not in macrophages. Ann N Y Acad Sci 2003;990:450-9.
[24] Ryan CG, Clayton E, Griffin W, Sie S, Cousens D. SNIP, a statistics-sensitive background treatment for the quantitative analysis of PIXE spectra in geoscience applications. Nucl Inst Methods Phys Res B 1988;34:396-402.
[25] Biswas SK, Mantovani A. Macrophage plasticity and interaction with lymphocyte subsets: cancer as a paradigm. Nat Immunol 2010;11:889-96.
[26] Feng H, Sim LC, Wan C, Wong NSC, Yang Y. Rapid characterization of protein productivity and production stability of CHO cells by matrix-assisted laser desorption/ionization time-of-flight mass spectrometry. Rapid Commun Mass Spectrom 2011;25:1407-12.
[27] Marvin-Guy LF, Duncan P, Wagnière S, Antille N, Porta N, Affolter M, et al. Rapid identification of differentiation markers from whole epithelial cells by matrix-assisted laser desorption/ionisation time-of-flight mass spectrometry and statistical analysis. Rapid Commun Mass Spectrom 2008;22: 1099-108.
[28] Gifford GE, Lohmann-Matthes ML. Gamma interferon priming of mouse and human macrophages for induction of tumor necrosis factor production by bacterial lipopolysaccharide. J Natl Cancer Inst 1987;78:121-4.
[29] Yu SF, Koerner TJ, Adams DO. Gene regulation in macrophage activation: differential regulation of genes encoding for tumor necrosis factor, interleukin-1, JE, and KC by interferon-gamma and lipopolysaccharide. J Leukoc Biol 1990;48:412-9.
[30] Mantovani A, Sozzani S, Locati M, Allavena P, Sica A. Macrophage polarization: tumor-associated macrophages as a paradigm for polarized M2 mononuclear phagocytes. Trends Immunol 2002;23:549-55.
[31] Mège J-L, Mehraj V, Capo C. Macrophage polarization and bacterial infections. Curr Opin Infect Dis 2011;24:230-4.
[32] Nau GJ, Richmond JFL, Schlesinger A, Jennings EG, Lander ES, Young RA. Human macrophage activation programs induced by bacterial pathogens. Proc Natl Acad Sci USA 2002;99: 1503-8.
[33] Akira S, Uematsu S, Takeuchi O. Pathogen recognition and innate immunity. Cell 2006;124:783-801.
[34] Jenner RG, Young RA. Insights into host responses against pathogens from transcriptional profiling. Nat Rev Microbiol 2005;3:281-94.
[35] Frodermann V, Chau TA, Sayedyahossein S, Toth JM, Heinrichs DE, Madrenas J. A modulatory interleukin-10 response to staphylococcal peptidoglycan prevents Th1/Th17 adaptive immunity to *Staphylococcus aureus*. J Infect Dis 2011;204:253-62.
[36] Fong CHY, Bebien M, Didierlaurent A, Nebauer R, Hussell T, Broide D, et al. An antiinflammatory role for IKKbeta through the inhibition of "classical" macrophage activation. J Exp Med 2008;205:1269-76.
[37] Rajaram MVS, Brooks MN, Morris JD, Torrelles JB, Azad AK, Schlesinger LS. *Mycobacterium tuberculosis* activates human macrophage peroxisome proliferator-activated receptor gamma linking mannose receptor recognition to regulation of immune responses. J Immunol 2010;185:929-42.

Whole-cell MALDI-TOF mass spectrometry: a tool for immune cell analysis and characterization

Ouedraogo R, Textoris J, **Daumas A**, Capo C, Mege JL.

Methods Mol Biol. 2013;1061:197-209.

doi: 10.1007/978-1-62703-589-7_12.

Analysis and Characterization of Immune Cells and Their Activation Status by Whole-Cell MALDI-TOF Mass Spectrometry

Ouedraogo R, Textoris J, Gorvel L, **Daumas A**, Capo C, Mege JL.

Methods Mol Biol. 2019;2024:339-351.

Le protocole expérimental d'analyse des cellules eucaryotes et d'exploration de l'activation des macrophages en spectrométrie de masse MALDI-TOF a été publié. Une mise à jour du chapitre vient d'être publiée. Seule cette dernière version est présentée ci-dessous.

Certains résultats de la première publication de l'équipe [20] et de l'étude ci-dessous [**Article 1**] sont repris dans ces publications à visée didactique mais il est aussi fait mention de l'analyse détaillée des spectres à l'aide du logiciel R permettant de s'affranchir du logiciel associé au spectromètre de masse adapté à la microbiologie.

Chapter 12

Whole-Cell MALDI-TOF Mass Spectrometry: A Tool for Immune Cell Analysis and Characterization

Richard Ouedraogo, Julien Textoris, Aurélie Daumas, Christian Capo, and Jean-Louis Mege

Abstract

Matrix-assisted laser desorption/ionization time-of-flight mass spectrometry (MALDI-TOF MS) is widely used in proteomics. It has been recently demonstrated that MALDI-TOF MS can be used to identify and classify numerous bacterial species or subspecies. We applied MALDI-TOF MS directly to intact mammalian cells, and we found that this method is valuable to identify human circulating cells and cells involved in the immune response including macrophages. As macrophages are characterized by a high degree of plasticity in response to their microenvironment, we stimulated human macrophages with cytokines, bacterial products, and a variety of bacteria. We found that MALDI-TOF MS discriminated unstimulated and stimulated macrophages, and also detected multifaceted activation of macrophages. We conclude that whole-cell MALDI-TOF MS is an accurate method to identify various cell types and to detect subtle modifications in cell activity.

Key words Mass spectrometry, Matrix-assisted laser desorption/ionization time-of-flight, Intact cell, Macrophage, Cell activation

1 Introduction

Matrix-assisted laser desorption/ionization time-of-flight mass spectrometry (MALDI-TOF MS) is a powerful tool for the analysis of ionized molecules (i.e., proteins) by measuring their mass/charge (m/z) ratio. This technique is currently used in biochemistry to identify peptides, proteins, posttranslational modifications of proteins [1, 2], and nucleic acids [2, 3]. Typically, in cell biology, using MALDI-TOF MS to analyze cellular protein composition requires a critical cell lysis step, as well as a variety of fractionation and separation steps, including affinity separation methods, gel electrophoresis, chromatographic separations [4]. Combined with gel electrophoresis, MALDI-TOF MS allows for the study of the proteome [5] and the identification of a large number of proteins

Kelly M. Fulton and Susan M. Twine (eds.), *Immunoproteomics: Methods and Protocols*, Methods in Molecular Biology, vol. 1061,
DOI 10.1007/978-1-62703-589-7_12,

in the proteome, the secretome, and membranes from activated macrophages [6]. Seemingly, MALDI-TOF MS can identify M1 responses of macrophages, such as the response to interferon (IFN)-γ and lipopolysaccharide (LPS) [5]. Using pulse stable isotope labeling of amino acids in cell culture, Kraft-Terry et al. identified a bioprofile in *macrophage colony-stimulating factor*-differentiated monocytes that is consistent with an M2 profile [6]. However, these approaches based on cell component separation require large sample quantities and cannot be used to analyze clinical specimens. Various attempts have been made to study single mammalian cells by MALDI-TOF MS, but, to date, these methods have been proven fastidious, and the biological information extracted is limited [7].

New applications of the MALDI-TOF MS method have been introduced recently in bacteriology laboratories. The fingerprints of intact bacteria allow rapid identification and taxonomic classification of numerous bacterial species and subspecies [8–10]. Using databases established from isolated bacterial species, the identification of many bacterial species in clinical samples [11] is fast, easy to perform, and inexpensive.

The MALDI-TOF MS procedure for the identification of bacterial species was expanded to three mammalian cell lines in 2006 [4]. More recently, 66 cell lines, representing 34 species from insects to primates, have been identified by MALDI-TOF MS [12]; but this method involves ethanol inactivation and formic acid–acetonitrile extraction. We applied MALDI-TOF MS directly to intact cells, and found this method highly valuable to the identification of human circulating cells, and cells involved in the immune response, including macrophages [13]. In addition, macrophages have a high degree of plasticity, and adapt quickly in response to their microenvironment. They sense microorganisms through receptors that bind conserved and ubiquitous microbial motifs, such as LPS. Macrophages stimulated with type I cytokines, i.e., IFN-γ, Tumor Necrosis Factor (TNF), or bacterial products, i.e., LPS, adopt an M1 macrophage phenotype which is inflammatory, tumoricidal, and microbicidal. Macrophages stimulated with interleukin (IL)-4 or IL-10, adopt an M2 macrophage phenotype, which regulates inflammatory and immune responses, and is only weakly tumoricidal and microbicidal [14]. Hence, macrophages constitute a model of choice to assess the accuracy of whole-cell MALDI-TOF MS to detect subtle modifications in cell activity [15].

We describe here the effective use of MALDI-TOF MS to identify many intact eukaryotic cell populations by creating a database of known samples. The experimental protocol, bioinformatics analysis of whole-cell MALDI-TOF MS spectra, and the comparison of unknown samples to the database allow the identification of various cell types within heterogeneous samples [13] or multifaceted activation of macrophages [15].

2 Materials

The different cell types or stimulated cells were prepared separately to establish databases. Experiments with mixed cell types (circulating cells) are indicated. Prepare sterile solutions for cell isolation and culture. Prepare and store all reagents at 4 °C. Prepare MALDI-TOF matrix just before use.

2.1 Human Circulating Cells

1. Isolate peripheral blood mononuclear cells (PBMCs) from leukopacks (or blood donors) by Ficoll gradient (MSL, Eurobio), as previously described [16].
2. Prepare $CD14^+$ monocytes using CD14 MicroBeads and the MACS separation system (Miltenyi Biotec), according to the manufacturer's protocol.
3. Prepare T $CD3^+$ lymphocytes using CD3 MicroBeads and the MACS separation system (Miltenyi Biotec), according to the manufacturer's protocol.
4. Obtain monocyte-derived macrophages (MDMs) by incubating monocytes (10^6 cells in 6-well plates) in 3 mL of RPMI 1640 containing 20 mM HEPES, 10 % human serum AB^+, 2 mM L-glutamine, 100 IU/mL penicillin, and 100 μg/mL streptomycin for 4 days. Replace human serum with fetal calf serum (FCS) for 3 additional days. The obtained cell population was identified as macrophages (more than 95 %) by acquisition of membrane CD68 expression and CD14 down-modulation.
5. Obtain dendritic cells (DCs) by incubating monocytes with 1,000 U/mL human recombinant *granulocyte macrophage-colony stimulating factor* (GM-CSF) and 500 U/mL of human recombinant IL-4 in RPMI 1640 containing 10 % FCS, 2 mM L-glutamine, 100 IU/mL penicillin, and 50 μg/mL streptomycin for 7 days. Change the medium every 3 days and add again 1,000 U/mL GM-CSF and 500 U/mL IL-4. The obtained cells expressed high levels of CD11c and CD1a, and low levels of CD14 and CD68.
6. Obtain polymorphonuclear cells (PMNs) after Ficoll centrifugation, by sedimentation of red blood cells (RBCs) within dextran T500 (1.5 % (w/v), Pharmacosmos) (*see* **Note 1**).
7. Obtain red blood cells (RBCs) by 1/1,000 dilution of blood in Phosphate-buffered saline (PBS).

2.2 Noncirculating Cells

The preparation of several cell populations including mammalian primary cells and cell lines, one *Xenopus laevis* cell line (XTC-2 cells), and four types of amoebae (*Acanthamoeba polyphaga*, *Acanthamoeba castellanii*, *Hartmannella vermiformis*, *Poteriochromonas melhamensis*) is described in ref. 13.

2.3 Macrophage Stimulation

1. Stimulate MDMs with 20 ng/mL of human recombinant IFN-γ, IL-4, IL-10, or TNF (purchased from R&D Systems or other suppliers) for different time points. Also stimulate MDMs with 1 μg/mL LPS from *Escherichia coli* or heat-killed bacteria (50 bacteria per cell) including *Mycobacterium tuberculosis*, *Mycobacterium bovis*, *Mycobacterium avium*, *Rickettsia prowazekii*, and *Orientia tsutsugamushi* (*see* **Note 2**)
2. *M. tuberculosis* (CIP H37Rv strain 103471), *M. bovis* (Bacillus Calmette-Guérin, BCG CIP strain 671203), and a clinical isolate of *M. avium* subsp. *hominissuis* were obtained from the Laboratory of Microbiology of the Hospital La Timone (Marseille) [17].
3. *R. prowazekii* strain Breinl (ATCC VR-142), the agent of epidemic typhus [18], and *O. tsutsugamushi* strain Kato (CSUR R163) [19], the agent of scrub typhus, were propagated in L929 cells (*see* **Note 3**).
4. Heat-killed bacteria were obtained after heating microorganisms at 95 °C for 1 h.

2.4 Reagents and Materials for MALDI-TOF MS

1. The matrix solution consists of a 10 mg/mL solution of acid-α-cyano-4-hydroxy cinnamic (HCCA) diluted in 500 μL acetonitrile, 250 μL Milli-Q grade water, and 250 μL trifluoroacetic acid at 10 %. Mix and sonicate for at least 20 min. Centrifuge at 13,000 × *g* for 5 min. Discard the pellet and keep the supernatant. The matrix solution is ready for use (*see* **Note 4**).
2. AutoFlex II mass spectrometer (Bruker Daltonics).
3. Bruker MSP 384 software polished steel target (Bruker Daltonics).
4. FlexControl 3.0 software (Bruker Daltonics).
5. FlexAnalysis 3.3 software (Bruker Daltonics).
6. Biotyper 3.0 software (Bruker Daltonics).
7. ClinProTools 2.2 software (Bruker Daltonics).

3 Methods

3.1 MALDI-TOF Target Preparation

1. Moisten the Bruker MSP 384 polished steel target with hot tap water. Rub with KIMTECH paper. Rub with 70 % ethanol. Rinse with hot tap water by rubbing with KIMTECH paper. Rub finally with 70 % ethanol.
2. Immerse the target in 70 % ethanol and sonicate for at least 15 min.
3. Cover the target with 500 μL to 1 mL of trifluoroacetic acid. Rub with KIMTECH paper. Rinse with high performance liquid chromatography (HPLC) grade water without rubbing. Dry the target at room temperature (*see* **Note 5**).

3.2 Preparation of Deposits

1. Centrifuge cells (2×10^6 cells per assay) at $300 \times g$ for 5 min and wash them in PBS without Ca^{2+} or Mg^{2+} (*see* **Note 6**). Centrifuge to remove traces of culture medium. Collect cell pellets in 20 µL of PBS without Ca^{2+} or Mg^{2+}. Freeze cells for 2–3 days before analysis at –80 °C.
2. Thaw gently samples on ice (4 °C) (*see* **Note 7**).
3. Put the Bruker MSP 384 polished steel target on a horizontal support to obtain uniform deposits throughout the spot (*see* **Note 8**).
4. Homogenize cells in Eppendorf tubes before deposition of 1 µL on the MALDI target. Add 1 µL of the HCCA matrix to the sample on the target. Avoid mixing the spot with the pipette (*see* **Note 9**).
5. Drop 12–16 different spots of the same sample.
6. The evaporation takes place gradually at room temperature, and the formed HCCA crystals contain dispersed sample molecules.
7. Samples may be immediately analyzed or stored in the dark for several days before analysis.

3.3 Acquisition of Data

1. Insert the Bruker MSP 384 polished steel target containing samples in the Autoflex II mass spectrometer (Bruker Daltonics) outfitted with the Compass 1.2 software suite (consisting of FlexControl 3.0 and FlexAnalysis 3.3 from Bruker Daltonics). Run samples in positive mode, with 240 laser satisfactory shots in 40 shot steps intervals and 40 % laser power, performed in different regions of the analyzed sample spot. A signal-to-noise ratio of 3.0 was selected to define peaks, with a maximum of 100 peaks per spectrum. After the target plate calibration was complete, the AutoExecute command was used to analyze the samples. The processes described below are manufacturer or software defaults, and do not require adjusting.
2. Laser settings. Fuzzy Control, On; Weight, 2.00; Laser power, between 30 and 45 %; Matrix Blaster, 5.
3. Data Evaluation. Peak Selection Masses, 4,000–10,000; Mass Control List, Off; Peak Exclusion, ignore the largest peaks in the defined mass range; Peak Evaluation Processing Method, Default; Smoothing: On; Base-line Subtraction, On; Peak, Resolution higher than 400; Protein maximal resolution, ten times above the threshold.
4. Accumulation. Parent Mode, On; Sum up to 240 satisfactory shots in 40 shot steps; Dynamic Termination, On; Criteria Intensity, Early termination if reaching intensity value of 20,000 for ten peaks.

5. Movement. Spiral large, Maximal allowed number at one raster position; Parent Mode, 80; Quit sample after 25 subsequently failed judgments.
6. Processing. Flex analysis. Method, none; BioTools MS method, none.
7. Sample Carrier. Manual fine control speed, *x* (10,000 µm/s) *y* (20,000 µm/s); Relative *x* (5 µm) *y* (5 µm); Absolute *x* (−2,000 µm) *y* (−2,000 µm); State *x* (0) *y* (0); Random walk, 50 shots at raster spot; Mode, off.
8. Spectrometer. High voltage, switched On; Ion Source 1, 19,99 kV; Ion Source 2, 18,74 kV; Lens, 7 kV; Pulsed Ion Extraction, 330 ns; Polarity, Positive; Matrix Suppression, Mode Gaiting; Gaiting strength, height; Suppress up to, *m/z* 1,500 Da.
9. Detection. Mass range, 2,000–20,137; Mode, Medium Range; Detector Gain, Linear (18×); Sample Rate, 1.00 GS/s; Electronic Gain, Enhanced (100 mV); Real-time Smooth, High; Spectrum, Size (63,463 pts), Delay (29,412 pts).
10. Processing Method. MBT process.
11. Setup. Range, Medium; Laser Frequency, 25 Hz; Autoteaching, On; Instrument-specific Settings: Digitizer Trigger Level (2,000 mV), Digital off Linear (127 cnt), Digital off Reflector (127 cnt); Detector Gain Voltage Offset, Linear (1,300 V), Reflector, 1,400 V; Laser Attenuator, Offset (75 %), Range (15 %); Electronic Gain Button Definitions: Gain, regular (Offset Lin, 100 mV; Offset Ref 100 mV; 200 mV/full scale); enh. (Offset Lin, 51 mV; Offset Ref 51 mV; 100 mV/full scale); highest (Offset Lin, 25 mV; Offset Ref 25 mV; 50 mV/full scale).
12. Calibration. Calibration strategy, Interactive; Mass Control List, Bacterial test standard; Zoom Range, ±5 %; Peak Assignment Tolerance, User Defined (1,000 ppm); Mode, linear.

3.4 Data Analysis

3.4.1 Spectrum Analysis

1. The FlexAnalysis software 3.3 allows raw spectrum processing, baseline subtraction, smoothing, peak list editing, and displays several spectra into one window or superimposes spectra (for the comparison of different types of circulating cells, *see* Fig. 1).
2. The ClinProTools 2.2 software from Bruker Daltonics is used to analyze the variability between different samples. Load spectra of each cell category to create according classes.

   2D representation generated by ClinProTools 2.2. The software selects automatically two peaks that are present in each cell type but have different intensities (here, the peaks 2 and 30). This representation highlights the reproducibility of spectra between spectra of each class (here, ten spectra obtained from ten different blood donors), and the differences between

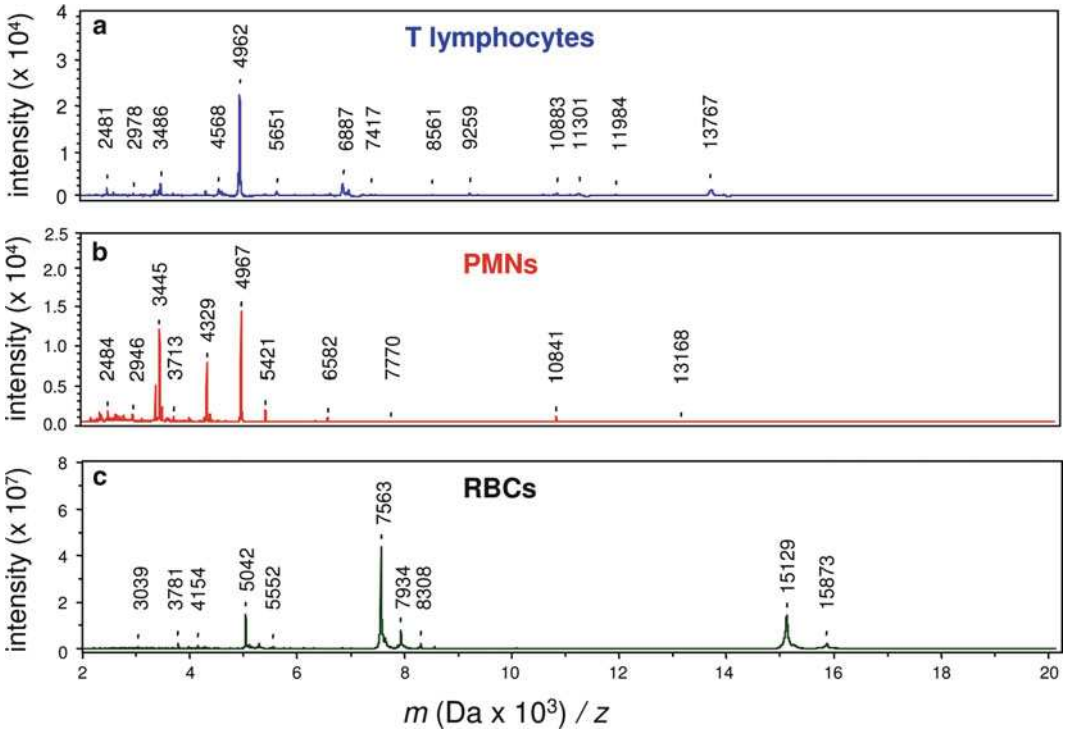

Fig. 1 MALDI-TOF MS spectra of circulating cells. T lymphocytes (**a**), PMNs (**b**), and RBCs (**c**) were isolated from a healthy blood donor. Representative MALDI-TOF MS spectra are shown. The figure is extracted from the ref. 13

the different classes (here, monocytes, T lymphocytes and PMNs) (*see* Fig. 2).

3. Gel-view representation generated by ClinProTools 2.2. This representation compares the reproducibility of spectra within the same class, and the differences between different classes. The different bands represent different peaks of each class. The intensity of bands corresponds to the intensity of detected peaks. This representation shows the reproducibility of spectra within each class (here, four spectra obtained from four different blood donors) and the peaks that are differentially expressed in different classes (here, monocytes and T lymphocytes isolated from each blood donor) (*see* Fig. 3).

3.4.2 Database Creation

1. The Biotyper 3.0 software from Bruker Daltonics is used to create and manage databases. An averaged spectrum for each cell category corresponds to at least ten individual spectra. Here, we created a database that includes 17 mammalian cell types, one *X. laevis* cell line (XTC-2 cells), and four types of amoebae (*A. polyphaga*, *A. castellanii*, *H. vermiformis*, *P. melhamensis*) (*see* **Note 10**).

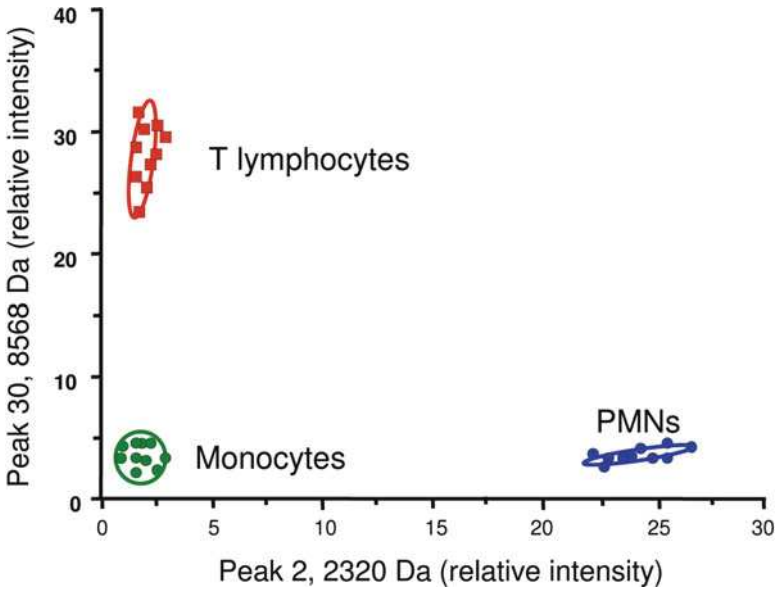

Fig. 2 Reproducibility of MALDI-TOF MS signatures. Monocytes, T lymphocytes, and PMNs were isolated from ten healthy blood donors. MALDI-TOF MS spectra were analyzed using 2D Peak Distribution View. The relative intensities of the two peaks automatically selected were homogenous among blood donors, and the *ellipses* represent the standard deviation within each cell population (monocytes, T lymphocytes, and PMNs, respectively). *See* ref. 13

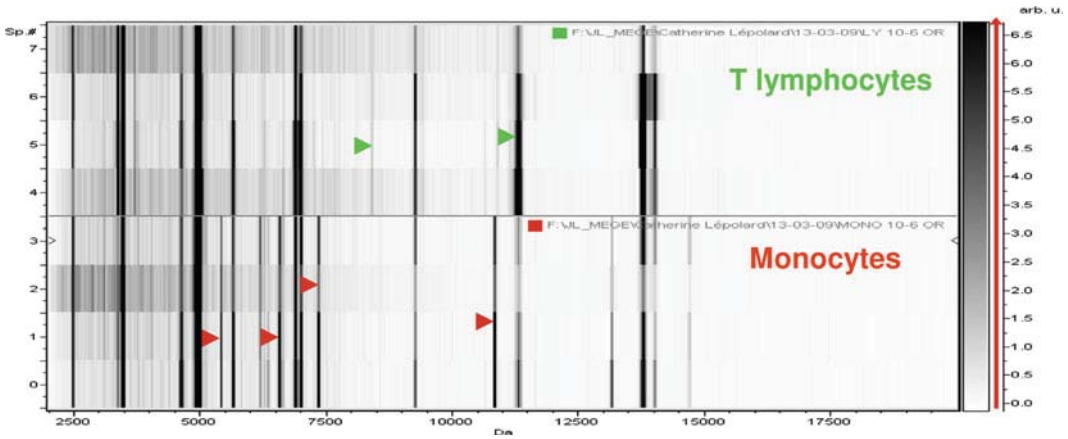

Fig. 3 Gel view representation of monocytes and T lymphocytes. Circulating cells were isolated from four different healthy blood donors. MALDI-TOF MS spectra are presented in Gel View representation. Spectra are shown with *m/z* values on the *x*-axis and the peak intensity (in arbitrary units) is coded with the grey scale presented on the *right*. Major differences between monocytes and T lymphocytes are indicated by *arrowheads*. *See* ref. 13

2. Baselines are automatically subtracted from spectra, and the background noise smoothed. An average spectrum is automatically created using default Biotyper method settings provided by the manufacturer. The sensitivity (the maximum tolerated

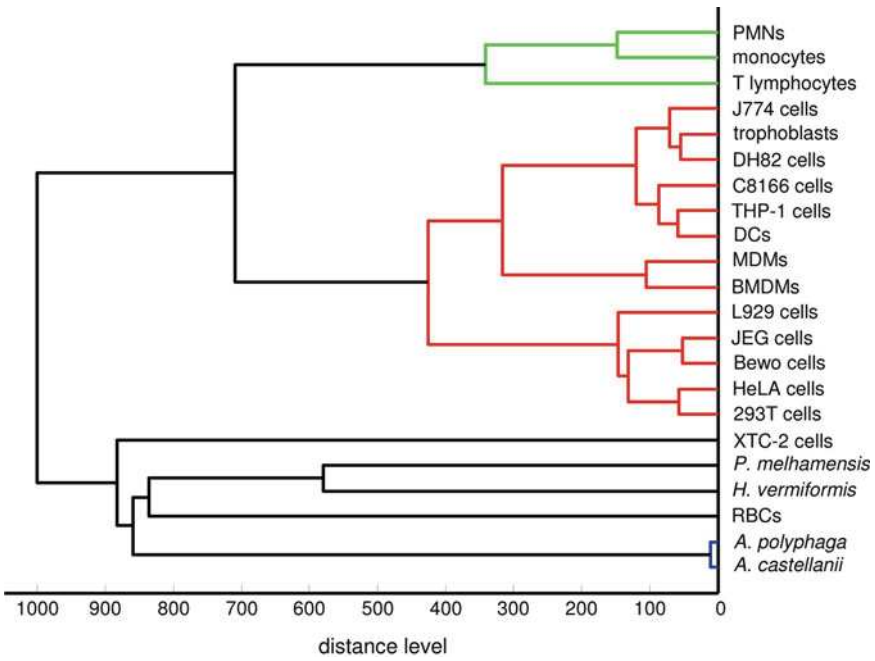

Fig. 4 Dendrogram of 22 eukaryotic cell types. MALDI-TOF MS was performed on 22 cell types with at least 20 spectra per cell type. A mean spectrum for each cell type was added to the database using the BioTyper 3.0 software and the dendrogram creation method. *See* ref. 13

error) of mass spectrum values and spectrum shifts was 200 particles per million. The minimum frequency to benchmark selection of peaks was 25 %, and only peaks with signal/noise intensity above background are automatically selected by the software. An average virtual spectrum consisting of 70 peaks is added to the database as a new reference.

3. The Biotyper 3.0 software is used to generate a dendrogram representation of cell categories according to their protein fingerprint (*see* Fig. 4). This figure shows that mammalian cells (in red and green) and nonmammalian cells (in black and blue) were in two distinct branches of the dendrogram. Circulating nucleated cells (in green) clustered within a subbranch distinct of primary cells (trophoblasts, DCs, MDMs, murine bone marrow-derived macrophages (BMDMs)) and cell lines. Note that human RBCs, which are unnucleated cells, clustered with nonmammalian cells.
4. The Biotyper 3.0 software is used to identify unknown spectra by comparison with database references. The sensitivity and the maximum error tolerated to determine the mean m/z values are 1 Da. Score values between 0.000 and 1.699 indicate that the unknown spectra did not match with known references. Values between 1.700 and 1.899 indicate probable cell identification.

Table 1
Identification of subpopulations by MALDI-TOF MS

Multiple cell population	Identification	Scores
Monocytes + T lymphocytes (equal concentration)	Monocytes	2,250
	T lymphocytes	2,247
PBMCs	Monocytes	2,078
	T lymphocytes	2,024
Whole blood (after hypotonic shock)	PMNs	2,049
	Monocytes	1,585
	T lymphocytes	1,654

The fingerprints of monocytes and T lymphocytes were identified in a mixed population (50 % monocytes, 50 % T lymphocytes) and in PBMCs. In blood, it was possible to identify PMNs (that represent about 70 % of total leukocytes), but not monocytes or T lymphocytes

Scores between 2.000 and 3.000 are considered statistically significant, and allow effective identification of the unknown spectra [13]. This procedure is currently used to identify bacterial species in clinical samples [11]. Here, we extend this method and the scores provided by Bruker Daltonics to identify the different cell populations present in a complex tissue. First, isolated monocytes and T lymphocytes were mixed, and the resulting fingerprint shows that monocytes and T lymphocytes are identified by MALDI-TOF MS (Table 1) The Table 1 also shows that the fingerprints of monocytes and lymphocytes T, respectively, are identified in peripheral blood mononuclear cells. In whole blood that contains leukocytes essentially composed of PMNs, the fingerprint of PMNs is identified, but not those of monocytes and T lymphocytes.

3.5 Macrophage Activation Analysis with R Software

The analysis of MALDI-TOF MS spectra described above is performed using Bruker Daltonics software. We present here a similar analysis performed with an open-source software (R), and specific algorithms that are presented as supplementary material in a recently published manuscript [15].

1. Load raw spectra in R (version 2.14) using the readBrukerFlexData library.
2. Analyze spectra using the MALDIquant library and specific algorithms. The square root of the intensities is used to enhance graphical visualization of the spectra.
3. Correct background using Statistics-sensitive Nonlinear Peak-clipping algorithm for baseline estimation [20]. Peaks are detected using a Signal-to-Noise Ratio of 6.0. The detected

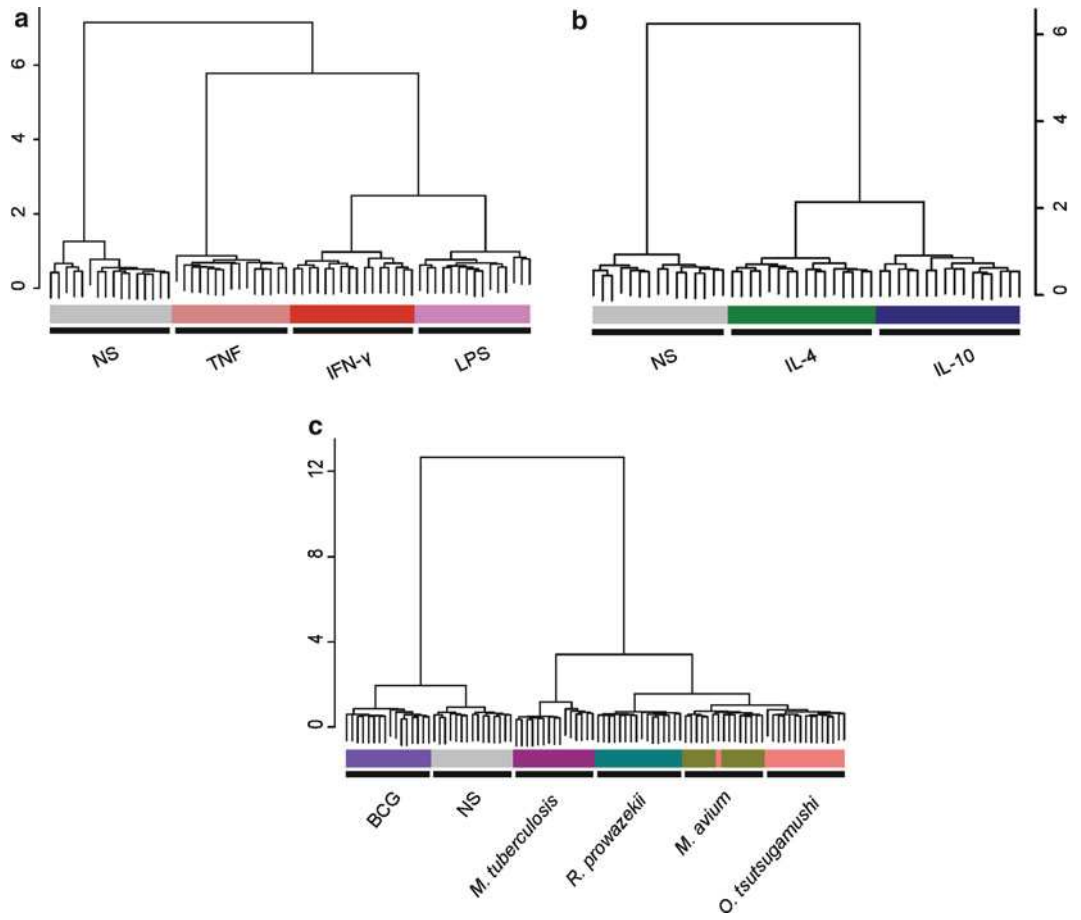

Fig. 5 Hierarchical clustering of activated macrophages. Monocyte-derived macrophages were stimulated with M1-related agonists (**a**), M2-related agonists (**b**), and intracellular bacteria (**c**) for 18 h. Unstimulated macrophages are presented in *grey* (NS)

peaks are considered similar across spectra when the m/z values are within a 2,000 ppm window.

4. Use hierarchical clustering to classify the spectra, ward algorithm for agglomeration, and a dissimilarity matrix based on the Jaccard distance. The Jaccard index measures similarity between boolean sample sets. The Jaccard distance, which measures dissimilarity between sample sets, is complementary to the Jaccard index and is obtained by subtracting the Jaccard coefficient from 1 or by dividing the difference of the sizes of the union and the intersection of two sets by the size of the union. This procedure was used to discriminate unstimulated (in grey) and stimulated macrophages (in colors) (*see* Fig. 5). Note that the responses of macrophages to different M1 agonists clustered but were not superimposable (*see* Fig. 5a). Similarly, the responses of macrophages to IL-4 and IL-10, two M2 agonists,

clustered compared to unstimulated macrophages but were distinct (*see* Fig. 5b). Different intracellular bacteria induced specific signatures (*see* Fig. 5c). Taken together, these results show that MALDI-TOF MS detected the multifaceted activation of macrophages.

4 Notes

1. PMNs must be isolated from remaining RBCs after dextran T500 sedimentation. Lyse RBCs by a 30 s hypotonic shock to obtain pure PMNs. In the absence of lysis, RBC signals were detected in MALDI-TOF MS and masked the detection of PMNs.
2. The stimulation of human MDMs is usually performed in RPMI 1640 supplemented with 10 % FCS, 100 UI/mL penicillin and 50 μg/mL streptomycin.
3. Wash bacteria with PBS to remove the components contained in growth media (such as serum proteins) that may interfere with MALDI-TOF MS spectra.
4. A matrix solution containing crystals does not allow a good ionization of sample molecules, and may affect the quality of spectra.
5. A target improperly cleaned may bias the results. It is therefore very important to take the time to carefully clean targets.
6. Cells may agglutinate in the presence of Ca^{2+} and Mg^{2+}. In addition, salts may interfere with MALDI-TOF MS.
7. Rapid and vigorous thawing alters samples, thus affecting the MALDI-TOF MS analysis.
8. Homogeneous deposits are necessary to obtain reproducible and high-quality spectra.
9. Mixing spots with pipettes alters spectrum quality. It is therefore important to respect the proportions and indicated details.
10. Each laboratory needs to construct its own databases before comparing cell populations and looking at unknown samples. We may export our databases to other laboratories.

Acknowledgments

We thank Nicolas Armstrong, Carine Couderc, Philippe Decloquement, and Christophe Flaudrops for their technical assistance.

References

1. Johnson RP, El-Yazbi AF, Hughes MF, Schriemer DC, Walsh EJ, Walsh MP et al (2009) Identification and functional characterization of protein kinase A-catalyzed phosphorylation of potassium channel Kv1.2 at serine 449. J Biol Chem 284:16562–16574
2. Li X, Cowles EA, Cowles RS, Gaugler R, Cox-Foster DL (2009) Characterization of immunosuppressive surface coat proteins from *Steinernema glaseri* that selectively kill blood cells in susceptible hosts. Mol Biochem Parasitol 165:162–169
3. Mellmann A, Cloud J, Maier T, Keckevoet U, Ramminger I, Iwen P et al (2008) Evaluation of matrix-assisted laser desorption ionization-time-of-flight mass spectrometry in comparison to 16S rRNA gene sequencing for species identification of nonfermenting bacteria. J Clin Microbiol 46:1946–1954
4. Zhang X, Scalf M, Berggren TW, Westphall MS, Smith LM (2006) Identification of mammalian cell lines using MALDI-TOF and LC-ESI-MS/MS mass spectrometry. J Am Soc Mass Spectrom 17:490–499
5. Brown J, Wallet MA, Krastins B, Sarracino D, Goodenow MM (2010) Proteome bioprofiles distinguish between M1 priming and activation states in human macrophages. J Leukoc Biol 87:655–662
6. Kraft-Terry SD, Gendelman HE (2011) Proteomic biosignatures for monocyte-macrophage differentiation. Cell Immunol 271: 239–255
7. Rubakhin SS, Churchill JD, Greenough WT, Sweedler JV (2006) Profiling signaling peptides in single mammalian cells using mass spectrometry. Anal Chem 78:7267–7272
8. Sauer S, Freiwald A, Maier T, Kube M, Reinhardt R, Kostrzewa M et al (2008) Classification and identification of bacteria by mass spectrometry and computational analysis. PLoS One 3:e2843
9. Dieckmann R, Helmuth R, Erhard M, Malorny B (2008) Rapid classification and identification of salmonellae at the species and subspecies levels by whole-cell matrix-assisted laser desorption ionization-time of flight mass spectrometry. Appl Environ Microbiol 74:7767–7778
10. Lay JO Jr, Holland RD (2000) Rapid identification of bacteria based on spectral patterns using MALDI-TOF MS. Methods Mol Biol 146:461–487
11. Seng P, Drancourt M, Gouriet F, La Scola B, Fournier PE, Rolain JM et al (2009) Ongoing revolution in bacteriology: routine identification of bacteria by matrix-assisted laser desorption ionization time-of-flight mass spectrometry. Clin Infect Dis 49:543–551
12. Karger A, Bettin B, Lenk M, Mettenleiter TC (2010) Rapid characterisation of cell cultures by matrix-assisted laser desorption/ionisation mass spectrometric typing. J Virol Methods 164:116–121
13. Ouedraogo R, Flaudrops C, Ben Amara A, Capo C, Raoult D, Mege JL (2010) Global analysis of circulating immune cells by matrix-assisted laser desorption ionization time-of-flight mass spectrometry. PLoS One 5:e13691
14. Benoit M, Desnues B, Mege JL (2008) Macrophage polarization in bacterial infections. J Immunol 181:3733–3739
15. Ouedraogo R, Daumas A, Ghigo E, Capo C, Mege JL, Textoris J (2012) Whole-cell MALDI-TOF MS: a new tool to assess the multifaceted activation of macrophages. J Proteomics 75:5523–5532
16. Delaby A, Gorvel L, Espinosa L, Lépolard C, Raoult D, Ghigo E et al (2012) Defective monocyte dynamics in Q fever granuloma deficiency. J Infect Dis 205:1086–1094
17. Mba Medie F, Ben Salah I, Henrissat B, Raoult D, Drancourt M (2011) *Mycobacterium tuberculosis* complex mycobacteria as amoeba-resistant organisms. PLoS One 6:e20499
18. Meghari S, Bechah Y, Capo C, Lepidi H, Raoult D, Murray PJ et al (2008) Persistent *Coxiella burnetii* infection in mice overexpressing IL-10: an efficient model for chronic Q fever pathogenesis. PLoS Pathog 4:e23
19. Tantibhedhyangkul W, Prachason T, Waywa D, El Filali A, Ghigo E, Thongnoppakhun W et al (2011) *Orientia tsutsugamushi* stimulates an original gene expression program in monocytes: relationship with gene expression in patients with scrub typhus. PLoS Negl Trop Dis 5:e1028
20. Ryan CG, Clayton E, Griffin WL, Sie SH, Cousens DR (1988) SNIP, a statistics-sensitive background treatment for the quantitative analysis of PIXE spectra in geoscience applications. Nucl Inst Meth Phys Res B 34:396–402

Whole-cell MALDI-TOF mass spectrometry is an accurate and rapid method to analyze different modes of macrophage activation

Ouedraogo R, **Daumas A**, Capo C, Mege JL, Textoris J.

J Vis Exp. 2013 Dec 26;(82):50926.

doi: 10.3791/50926.

L'équipe a eu l'opportunité de pouvoir présenter la spectrométrie de masse MALDI-TOF en tant qu'outil d'évaluation de l'activation macrophagique sous un format vidéo pour la revue JoVE.

JoVE (Journal of Visualized Experiments) est une revue scientifique en vidéo contrôlée par un comité éditorial. Créée en 2006, JoVE se destine à la publication sous forme audiovisuelle d'expérimentations et accroît ainsi la productivité et la reproductibilité des travaux de recherche scientifique. JoVE diffuse des vidéos montrant des expérimentations menées dans des laboratoires du plus haut niveau et les propose en ligne à des millions de chercheurs, d'enseignants et d'étudiants dans le monde.

La méthode présentée est explicitée dans la publication qui y est associée, présentée ci-dessous.

La vidéo est quant à elle disponible en suivant le lien http://www.jove.com/video/50926/

L'article et la vidéo explicitent le protocole expérimental utilisé pour analyser par spectrométrie de masse MALDI-TOF sur cellules entières différents modes d'activation des macrophages dérivés de monocytes : l'obtention des macrophages et leur stimulation par les différents agonistes, le traitement des échantillons pour leur analyse avec le spectromètre de masse MALDI-TOF et enfin, le traitement bio-informatique des résultats obtenus indépendamment des programmes d'analyse liés à l'appareil d'acquisition.

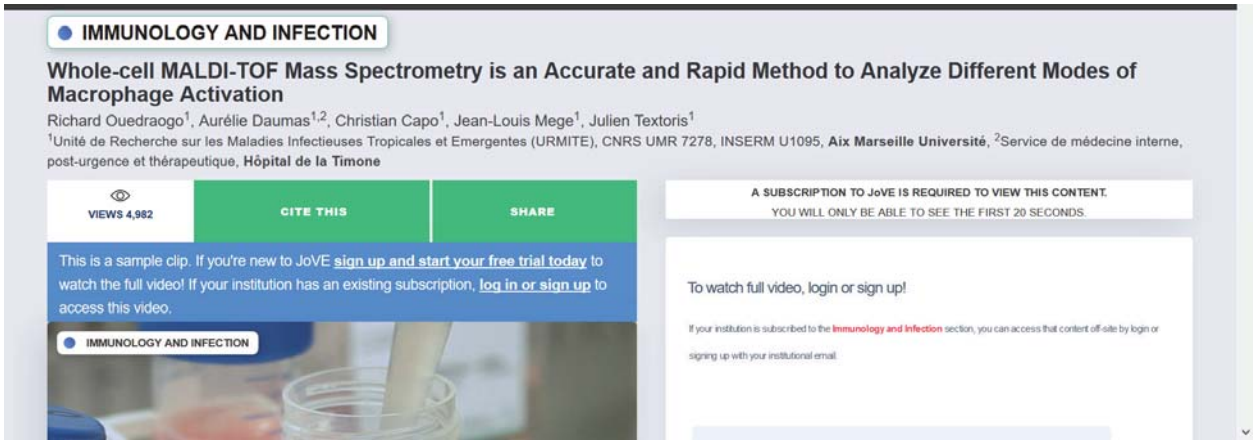
IMMUNOLOGY AND INFECTION
Whole-cell MALDI-TOF Mass Spectrometry is an Accurate and Rapid Method to Analyze Different Modes of Macrophage Activation
Richard Ouedraogo[1], Aurélie Daumas[1,2], Christian Capo[1], Jean-Louis Mege[1], Julien Textoris[1]
[1]Unité de Recherche sur les Maladies Infectieuses Tropicales et Emergentes (URMITE), CNRS UMR 7278, INSERM U1095, Aix Marseille Université, [2]Service de médecine interne, post-urgence et thérapeutique, Hôpital de la Timone
VIEWS 4,982
CITE THIS
SHARE
This is a sample clip. If you're new to JoVE sign up and start your free trial today to watch the full video! If your institution has an existing subscription, log in or sign up to access this video.
IMMUNOLOGY AND INFECTION
A SUBSCRIPTION TO JoVE IS REQUIRED TO VIEW THIS CONTENT.
YOU WILL ONLY BE ABLE TO SEE THE FIRST 20 SECONDS.
To watch full video, login or sign up!
If your institution is subscribed to the Immunology and Infection section, you can access that content off-site by login or signing up with your institutional email.

Video Article

Whole-cell MALDI-TOF Mass Spectrometry is an Accurate and Rapid Method to Analyze Different Modes of Macrophage Activation

Richard Ouedraogo[1], Aurélie Daumas[1,2], Christian Capo[1], Jean-Louis Mege[1], Julien Textoris[1]

[1]Unité de Recherche sur les Maladies Infectieuses Tropicales et Emergentes (URMITE), CNRS UMR 7278, INSERM U1095, Aix Marseille Université

[2]Service de médecine interne, post-urgence et thérapeutique, Hôpital de la Timone

Correspondence to: Julien Textoris at julien.textoris@ap-hm.fr

URL: http://www.jove.com/video/50926
DOI: doi:10.3791/50926

Keywords: Immunology, Issue 82, MALDI-TOF, mass spectrometry, fingerprint, Macrophages, activation, IFN-g, TNF, LPS, IL-4, bacterial pathogens

Date Published: 12/26/2013

Citation: Ouedraogo, R., Daumas, A., Capo, C., Mege, J.L., Textoris, J. Whole-cell MALDI-TOF Mass Spectrometry is an Accurate and Rapid Method to Analyze Different Modes of Macrophage Activation. *J. Vis. Exp.* (82), e50926, doi:10.3791/50926 (2013).

Abstract

MALDI-TOF is an extensively used mass spectrometry technique in chemistry and biochemistry. It has been also applied in medicine to identify molecules and biomarkers. Recently, it has been used in microbiology for the routine identification of bacteria grown from clinical samples, without preparation or fractionation steps. We and others have applied this whole-cell MALDI-TOF mass spectrometry technique successfully to eukaryotic cells. Current applications range from cell type identification to quality control assessment of cell culture and diagnostic applications. Here, we describe its use to explore the various polarization phenotypes of macrophages in response to cytokines or heat-killed bacteria. It allowed the identification of macrophage-specific fingerprints that are representative of the diversity of proteomic responses of macrophages. This application illustrates the accuracy and simplicity of the method. The protocol we described here may be useful for studying the immune host response in pathological conditions or may be extended to wider diagnostic applications.

Video Link

The video component of this article can be found at http://www.jove.com/video/50926/

Introduction

Matrix-Assisted Laser Desorption/Ionization Time-Of-Flight Mass Spectrometry (MALDI-TOF MS) is a popular mass spectrometry technique to study biological samples. Using a laser beam and an energy-absorbing matrix allows a soft ionization process: the evaporation and genesis of large mostly single-charged biomolecules. This process is called desorption/ionization, justifying the acronym MALDI. These ions are then accelerated by application of voltage and enter a TOF analyzer that allows the separation of these ions and the quantification of their respective masses[1].

MALDI-TOF MS has been extensively used in biology, chemistry, and medicine to identify molecules and biomarkers[2-4] or to monitor post-translational modifications on proteins[5,6]. Recently, several groups applied MALDI-TOF MS to the identification of microorganisms from clinical samples[7,8]. This microbiological application is now used routinely in the clinical settings. Whole cell MALDI-TOF has many advantages compared to classical applications of MALDI-TOF MS. Samples containing whole cells are directly processed, avoiding time consuming steps to fractionate or separate large amounts of material. Moreover, no characterization of the various peaks is needed: the whole spectrum is considered as a fingerprint of the sample, and matching algorithms compare the tested spectrum with a database of reference spectra.

We and others have applied this whole-cell analysis technique to eukaryotic cells. Many applications may be derived from this technique: (1) identify the main cell types from a mixed sample[9-11]; (2) assess the viability of cell cultures over time (including quality control industrial applications)[12]; (3) monitor activation states of a single cell type[13]; (4) assess the malignant transformation of a clinical sample[14,15].

Here, we describe the use of whole-cell MALDI-TOF MS to explore the various polarization phenotypes of macrophages in response to cytokines or heat-killed bacteria. Macrophages play a pivotal role in the immune response to microbial pathogens. They detect infectious agents in the tissues through pattern recognition receptors able to detect conserved microbial patterns, such as lipopolysaccharide (LPS)[16]. Macrophages are professional antigen-presenting cells that interact with T cells to mount the adaptive immune response. T cells influence macrophages by releasing cytokines that either reinforce or regulate the microbicidal activity of macrophages. By analogy to the Th1/Th2 lymphocyte polarization, inflammatory, microbicidal, and tumoricidal macrophages have been classified into M1 macrophages and immunoregulator macrophages as M2 macrophages[17-19]. The term M1 refers to the classical activation of macrophages by type I cytokines, such as interferon (IFN)-γ and tumor necrosis factor (TNF), or bacterial products, such as LPS[18,20-23], whereas macrophages activated by alternative pathways (interleukin (IL)-4, IL-10, Transforming Growth Factor-β1 are considered M2 macrophages[19,24,25]. The high phenotypic and functional plasticity of macrophages in response to their microenvironment renders these macrophages useful to analyze subtle changes by a MALDI-TOF MS approach.

Protocol

In the present protocol, the whole-cell MALDI-TOF technique is used to obtain a mass spectrum considered as a fingerprint of the sample. A bioinformatic analysis allowed the comparison and the classification of these fingerprints. There were three main parts in this protocol:

1. The preparation of the biological samples: control macrophages and macrophages stimulated with different agonists.
2. The analysis of each type of sample with technical replicates by whole-cell MALDI-TOF MS.
3. The bioinformatics analysis of raw data.

Prepare sterile solutions for cell isolation and culture. Prepare and store all reagents at 4 °C

1. Preparation of Human Monocytes

1. Prepare cell culture medium. Add 55 ml of human serum AB+ or fetal bovine serum (FBS) and 5 ml of the antibiotic solution (penicillin at 10,000 UI/ml and streptomycin at 10,000 µg/ml; final concentration of 100 UI/ml for penicillin and 100 µg/ml for streptomycin) to RPMI 1640 medium (500 ml).
    1. Isolate peripheral blood mononuclear cells (PBMCs) from leukopacks (leukocyte concentrates).
        1. Prepare 50 ml tubes containing 15 ml Ficoll. Dilute the blood in saline (vol/vol, 1/10). Deposit 30 ml diluted PBMCs on Ficoll as previously described[26].
        2. Centrifuge at 700 x g for 20 min. Recover PBMCs at the interface between Ficoll (density of 1.077 g/ml) and diluted plasma. Dilute PBMCs in culture medium and centrifuge at 300 x g for 5 min.
    2. Prepare CD14+ monocytes from PBMCs using magnetic beads coated with anti-CD14 antibodies.

        Note: Keep products and cells at 4 °C until monocyte obtention.
        1. Prepare running buffer consisting of phosphate-buffered saline (PBS) pH 7.2, 0.5% bovine serum albumin (BSA) and 2 mM ethylenediaminetetraacetic acid (EDTA).
        2. Gently dissociate pelleted PBMCs (10^7 cells per assay) into 80 µl of running buffer.
        3. Add 20 µl CD14 MicroBeads to PBMCs**.** Mix and incubate PBMCs for 15 min**.** Wash PBMCs with 5 ml of running buffer and centrifuge at 300 x g for 5 min. Gently dissociate pelleted PBMCs into 500 µl of running buffer for 10^8 PBMCs.

            Note: use 500 µl of running buffer for PBMC concentrations lower than 10^8 PBMCs.
        4. Proceed to magnetic separation.

            Note: for less than 2 x 10^8 PBMCs, use MS column; for more than 2 x 10^8 PBMCs and less than 2 x 10^9 PBMCs, use LS column.
        5. Rinse precolumn and column with running buffer (500 µl for MS column or 3 ml for LS column)**.** Add PBMCs into the precolumn (wait for unlabeled cells to pass through the column)**.** Rinse 3 times with running buffer (500 µl for MS column or 3 ml for LS column)**.** Remove the precolumn.
        6. Place the column on 15 ml tubes**.** Add running buffer (1 ml for MS column or 5 ml for LS column) on the column and elute CD14+ cells by applying a pressure on the column.
        7. Centrifuge the eluate at 300 x g for 5 min. Discard the supernatant**.** Wash monocyte pellet with 10 ml of culture medium.

            Note: Analyze the purity of monocyte preparation using anti-CD14 antibodies and flow cytometry (classically higher than 95%).

2. Differentiation of monocytes into macrophages.
    1. Incubate monocytes (10^6 monocytes per well in 6 well plates) in 3 ml of culture medium containing 10% human serum AB+ at 37 °C. After 4 days, replace the culture medium containing human serum by 3 ml culture medium containing 10% FBS for 3 additional days.
    2. Identify the obtained cell population as monocyte-derived macrophages (MDMs) by flow cytometry (see **Figure 1**).
        1. Replace the culture medium by 3 ml PBS. Scrape MDMs with a rubber policeman and collect MDM suspensions. Centrifuge at 400 x g for 5 min. Add PBS containing 2% BSA to pelleted MDMs and gently agitate cell suspension. Adjust the cell concentration (10^6 MDMs in 200 ml PBS) and incubate at 4 °C.
        2. Add 10 ml of anti-CD14 antibodies and 10 ml of anti-CD68 antibodies to MDM suspension and incubate at 4 °C for 20 min in the dark.

            Note: these antibodies must be labeled with two different fluorochromes consistent with flow cytometry analysis. For example, anti-CD14 antibodies may be conjugated with phycoerythrin coupled (for monocytes staining) and anti-CD68 antibodies with Alexa Fluor 647 coupled (for macrophages staining).
        3. Centrifuge MDMs at 400 x g for 5 min. Remove supernatants. Gently dissociate the cell pellet and incubate MDMs in 250 ml 3% paraformaldehyde (PFA) for 15 min at room temperature. Centrifuge PFA-fixed MDMs at 400 x g for 5 min. Wash MDMs with 3 ml PBS and centrifuge MDMs at 400 x g for 5 min. Gently dissociate MDM pellet in 400 ml PBS.
        4. Analyze the differentiation of monocytes (that express CD14 but not CD68) into monocytes (that express CD68 but not CD14). Note: classically more than 95% of cells are MDM.

3. 18 hr stimulation of MDMs.
    1. Replace the culture medium of adherent MDMs by fresh 3 ml culture medium (containing 10% FBS).

2. To induce a M1 or M2 polarization, use the following human recombinant cytokines: IFN-γ and TNF for M1 polarization, and IL-4 for M2 polarization. M1 macrophages are also obtained by stimulation with LPS. Note that stock-solutions of cytokines are conserved at -80 °C and that the stock-solution of LPS is conserved at -20 °C.
    1. Dilute the stock-solution of IFN-gγ (1 mg/ml) at 1/100 in culture medium to obtain a dilution of 10 ng/ml. Add 6 µl of this IFN-γ dilution to MDMs to obtain a final IFN-γ concentration of 20 ng/ml.
    2. Dilute the stock-solution of TNF (1 mg/ml) at 1/100 in culture medium to obtain a dilution of 10 ng/ml. Add 6 µl of this TNF dilution to MDMs to obtain a final TNF concentration of 20 ng/ml.
    3. Dilute the stock-solution of IL-4 (1 mg/ml) at 1/100 in culture medium to obtain a dilution of 10 ng/ml. Add 6 µl of this IL-4 dilution to MDMs to obtain a final IL-4 concentration of 20 ng/ml.
    4. Add 3 µl of the stock-solution of LPS (1 mg/ml) to MDMs to obtain a final LPS concentration of 1 µg/ml.

3. To stimulate MDMs with bacteria, use heat-killed bacteria. Wash living bacteria with PBS and heat them at 95 °C for 1 hr. Use *Orientia tsutsugamushi* (strain Kato (CSUR R163), *Mycobacterium bovis* (Bacillus Calmette-Guérin, BCG CIP strain 671203) and *Coxiella burnetii* (Nine Mile in phase I) were because these pathogens are known to infect macrophages. Thus, prepare a *O. tsutsugamushi* suspension at 10^9 bacteria/ml. Add 50 µl to MDMs . Repeat the same step for *M. bovis* and *C. burnetii.*

4. Preparation of biological samples for MALDI-TOF MS.
    1. Wash stimulated MDMs with PBS without Ca^{2+} or Mg^{2+} (cells may agglutinate in the presence of Ca^{2+} or Mg^{2+}). Scrape MDMs with a rubber policeman and collect MDM suspensions. Centrifuge MDMs. Wash again MDMs in PBS without Ca^{2+} or Mg^{2+} at 400 x g for 5 min to discard FBS contamination.
    2. Adjust the cell concentration (2 x 10^6 MDMs per assay). Centrifuge MDMs at 400 x g for 5 min and discard supernatants. Collect cell pellets in 20 µl of PBS without Ca^{2+} or Mg^{2+}.
    3. Analyze samples immediately or store them in PBS at -80 °C before analysis.

2. Analysis of Macrophages by Whole-Cell Maldi-TOF MS

1. Preparation of CHCA matrix.
    1. Add 500 µl of acetonitrile, 250 µl 10% trifluoroacetic acid, and 250 µl of high-performance liquid chromatography (HPLC) water to a vial. Dilute 10 mg of CHCA in this solution to a final concentration of 10 mg/ml. Mix and sonicate for at least 20 min.

        Note: sonication will improve the saturation of the matrix but this step is not mandatory.
    2. Centrifuge at 13,000 x g for 5 min. Discard the pellet and keep the supernatant.

        Note: prepare the matrix solution just before use. A matrix solution that contains crystals does not allow a good ionization of sample molecules, and this may affect the quality of the spectra.

2. Preparation of MALDI steel target.
    1. Moisten the polished steel target with hot tap water. Rub with precision wipe paper. Add 70% ethanol and rub. Rinse with water by rubbing. Add 70% ethanol and rub with precision paper.
    2. Immerse the target in 70% ethanol and sonicate for at least 15 min. Cover the target with 500 µl to 1 ml of trifluoroacetic acid at 80%. Rub and wipe with precision paper. Rinse with HPLC water without rubbing. Dry the target at room temperature.

        Note: an improperly cleaned target may affect the quality of the spectra.

3. Preparation of deposits.
    1. Place the clean target on a horizontal and level support to obtain uniform deposits.
    2. Gently thaw MDM samples on ice. Note: rapid and vigorous thawing may alter samples, thus affecting the quality of the spectra. Homogenize MDMs (by pipetting back and forth the cell suspension) before deposition of 1 µl (containing approximately 1 x 10^5 cells) on the MALDI target. Add 1 µl of the MALDI matrix solution on the sample. Avoid mixing spot with the pipette. Mixing spots with pipettes alters the quality of the spectra. Depose 12-16 samples/assay (technical replicates).
    3. Evaporate spontaneously at room temperature. Note: evaporation takes place gradually and leads to the formation of matrix/sample crystals. The deposits may be immediately analyzed or stored in the dark for several days before analysis (up to 2 weeks).
    4. User should control that the cytokines or heat-killed bacteria used in the experiment do not provide peaks within the range of stimulated macrophages' spectra. Here, we checked that the cytokines and heat-killed bacteria alone did not provide any signal within the studied range (0-20 kDa).

4. Mass spectrometer tuning and data acquisition.
    1. Insert the steel target containing samples in the mass spectrometer.
    2. Configure the mass spectrometer and run data acquisition. Use the default configuration for automated acquisition of the data.
    3. Note: a detailed view of the configuration of flexControl software is given in the appendix/**Table 1**. This may vary according to mass spectrometer and software used.

3. Bioinformatic Analysis

Note: the bioinformatic analysis was performed using the free and open source statistical analysis software R, along with specific analysis libraries (*MALDIquant*). R can be downloaded freely from its website http://cran.r-project.org/. A detailed description of the script is provided as supplementary material.

1. Loading and pretreatment of raw data.
    1. Store raw data on the computer associated with the mass spectrometer in multiple files and folders. Retrieve the root folder of the experiment with all subfolders. Copy root folder to personal computer for analysis.
    2. Use *readBrukerFlexData* and *MALDIquant* libraries to load and analyze raw data.

        Note: *readBrukerFlexData* allows the loading of raw data from the mass spectrometer into a specific object in R for further analysis. See *MALDIquant* description for further information[27].
    3. Analyze generated spectra.

        Note: each spectrum consists of a list of peaks with their respective masses and intensities (relative abundance). Use the square root of the intensities to enhance the graphical visualization of the spectra. Correct the background using a statistic-sensitive nonlinear peak-clipping algorithm for baseline estimation[27]. Use a signal-to-noise ratio of 6 to detect peaks. Consider that the detected peaks are similar across spectra when the mass/charge (*m/z*) values are within a 2,000 ppm window.
2. Score definition and computation. Classify the spectra using a hierarchical clustering with a ward algorithm for agglomeration and a dissimilarity matrix based on the Jaccard distance.

    Note: the Jaccard index measures the similarity between Boolean sample sets (*i.e.* the presence/absence of a list of peaks).
3. Comparison of spectra and viewing.
    1. Analyze raw spectra plots. Note: x-axis represents the *m/z* ratio (in Daltons) and the y-axis represents the intensity (relative abundance).
    2. Assess the similarity between spectra by hierarchical clustering. Represent similarity (or divergence) as dendrogram.
    3. Assess the reproducibility by the mean of virtual gel-view representation. Note: virtual gel-view representation is a modified heatmap plot where relative abundance is color-coded with increasing intensities of blue.

Representative Results

The aim of the present protocol is to demonstrate the accuracy of whole-cell MALDI-TOF MS to assess the responsiveness of macrophages to their microenvironment.

Figure 1 describe preparation of stimulated macrophages from blood samples. **Figure 2** represents the analysis of monocytes and MDMs by flow cytometry. Note that monocytes expressed CD14 but not CD68 (**Figure 1A**). Conversely, MDMs expressed CD68 but not CD14 (**Figure 1B**).

Figure 3 describes the principle of whole-cell MALDI-TOF MS. Cells are deposited with matrix on the target plate. Within the mass spectrometer, a laser beam induces the desorption and ionization of molecules by shooting multiple times on the sample (240 shots). The produced ions are accelerated by a magnetic field and separated according to their *m/z* ratio in the tube. The TOF analyzer records the impact of the various ions at the end of the tube. According to the time of flight, each impact is converted into a *m/z* ratio, and impacts corresponding to the same *m/z* ratio are summed up to generate the full raw spectrums.

Figure 4 illustrates the role of sample preparations in the interpretation of MALDI-TOF MS results. A good quality spectrum is represented in **Figure 4A**. It usually contains a major peak around 5 kD (*m/z* = 4,965). A minimum cell concentration is required to obtain good samples: **Figure 4B** shows a poor quality spectrum obtained with a low cell concentration. However, raising MDM concentration above 1 x 10^5/µl does not improve the quality of spectra. Similar poor results are obtained when the sample is mixed with matrix before deposition on the target plate. If mixing is done on the target plate, it may also result in heterogeneous crystallization, as shown in **Figure 4C**. Hence, deposition of the samples on the target is a tricky and critical step in this protocol.

The reproducibility of the spectra is shown in **Figure 5**. Here, spectra from various samples are represented as a heatmap. Relative abundance (intensity) is color-coded by intensities of blue. This virtual gel-view representation illustrates the reproducibility of the samples within each class. The normalization and alignment of the spectra is a critical step to obtain such results. An unsupervised analysis by hierarchical clustering is summarized as a dendrogram on the right hand side of the figure. It illustrates that all samples clustered within three different groups: unstimulated MDMs (NS), IFN-γ-stimulated or IL-4-stimulated MDMs.

Figure 6 illustrates the discrimination of M1 macrophages (MDMs stimulated with IFN-γ) from M2 macrophages (MDMs stimulated with IL-4) and unstimulated MDMs. Indeed, the peak representation of a reference spectrum for IFN-γ, IL-4 or unstimulated MDMs shows specific peaks for each class. This representation is obtained using the R *MALDIquant* library[27].

Figure 7 illustrates the specific fingerprints induced by several agonists. It is commonly accepted that IFN-γ, TNF and LPS induce an inflammatory (M1-type) response in macrophages. We used MDM samples stimulated with these cytokines alone or in combination to illustrate the accuracy of whole-cell MALDI-TOF MS. Indeed, spectra from all stimulated samples were clearly separated from those of unstimulated macrophages (**Figure 7A**). However, we obtained a specific fingerprint from each type of stimulation, as illustrated by the clustering of the samples according to the stimuli. Interestingly, MDMs also exhibited specific fingerprints induced by heat-killed bacteria (**Figure 7B**). These results support the hypothesis that MALDI-TOF MS may be used to analyze circulating cells to assess the host-response to infection or inflammatory diseases in the clinical setting.

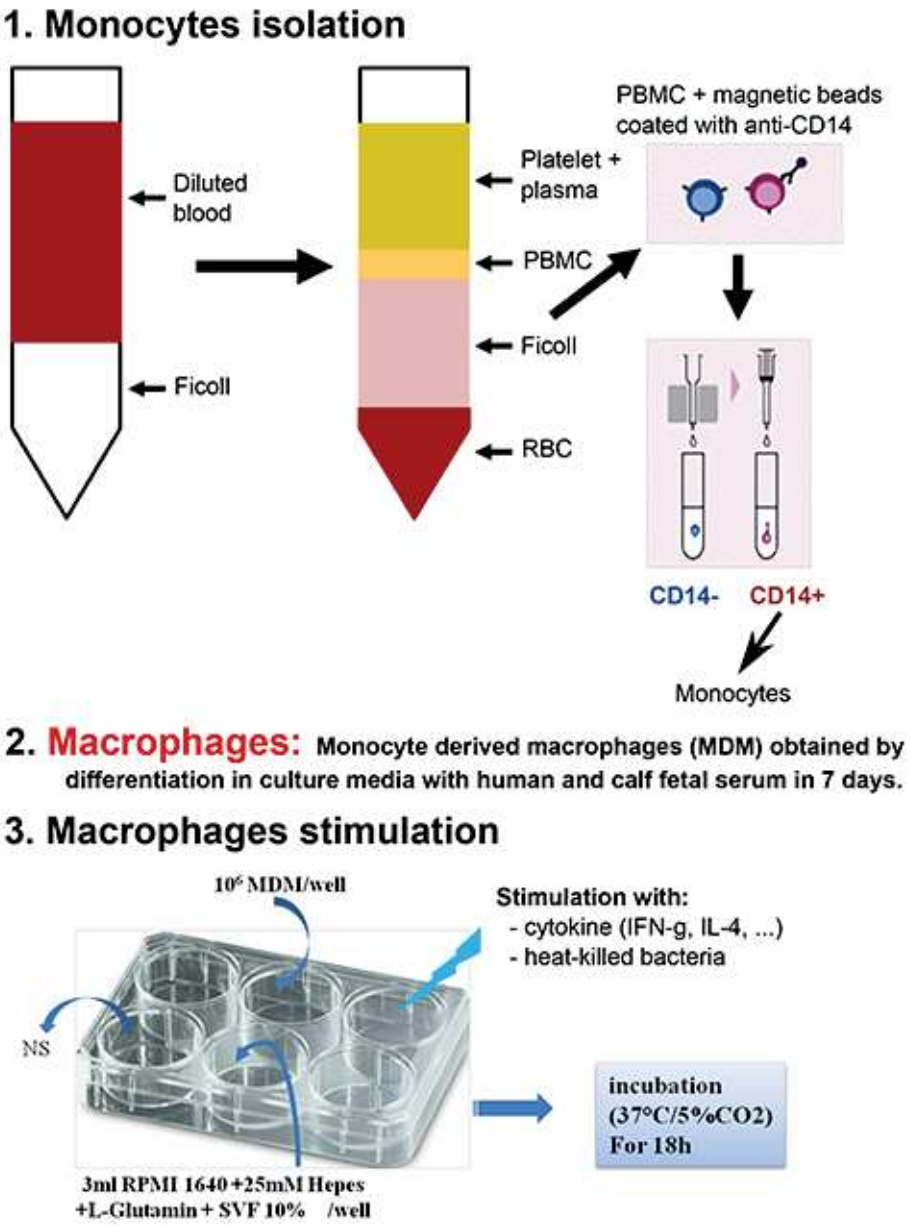

Figure 1. Preparation of biological samples. 1. Monocytes were selected from peripheral blood mononuclear cells (PBMC) by positive selection with magnetic beads coated with anti-CD14+ antibodies. **2.** Macrophages were obtained in 7 days by culture of monocytes in RPMI. **3.** Stimulated samples were obtained by adding either cytokines or heat-killed bacteria for 18h on differentiated macrophages. RBC: Red blood cells. Click here to view larger image.

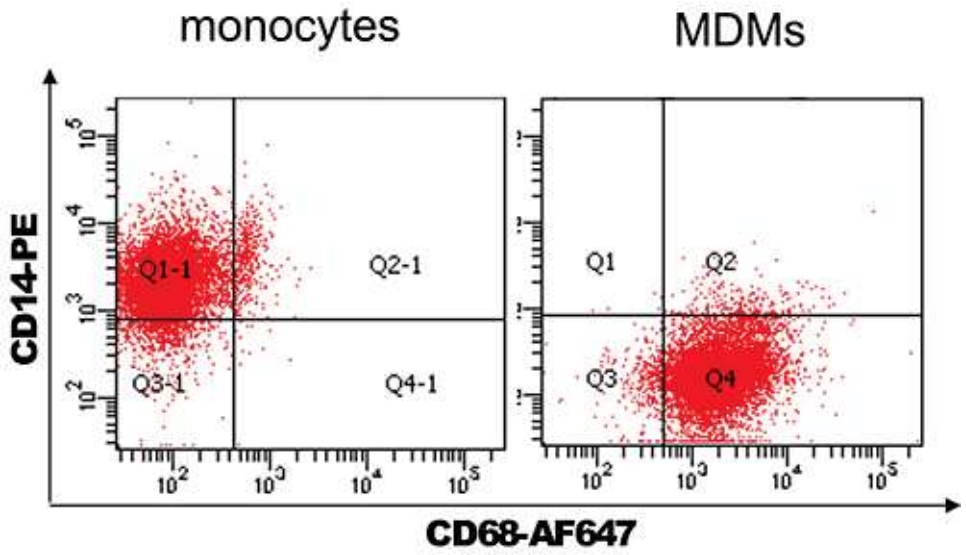

Figure 2. Assessment of CD14 and CD68 expression by flow cytometry. Monocytes (left panel) or MDMs (right panel) were labeled with anti-CD14-PE and anti-CD68-AF647 antibodies to assess membrane expression of these molecules. The differentiation of monocytes into MDMs is accompanied by the down-modulation of CD14 expression and the up-modulation of CD68 expression. Click here to view larger image.

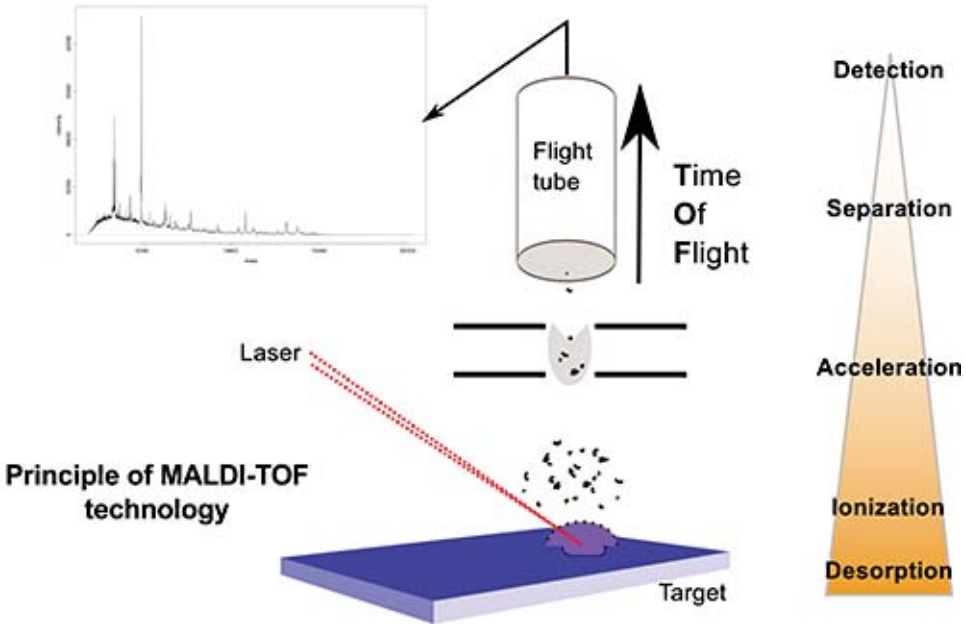

Figure 3. Principle of MALDI-TOF MS technology. This drawing describes the principle of the MALDI-TOF mass spectrometry. Click here to view larger image.

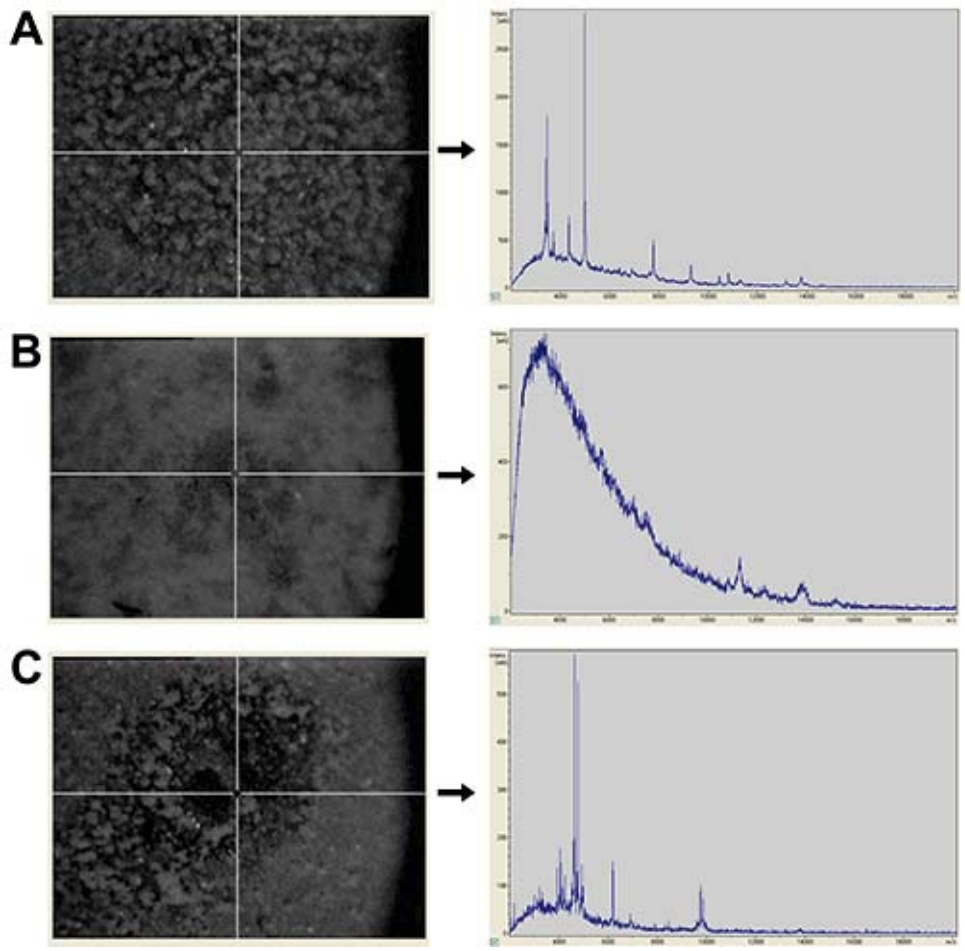

Figure 4. Whole-cell MALDI-TOF MS spectra. A zoomed view of spots deposited on the MALDI target (left panels) with corresponding spectra (right panels). Note that a good quality spot leads to an accurate spectra (**A**) whereas bad quality spots lead to spectra with a very poor signal to noise ratio (**B, C**). Click here to view larger image.

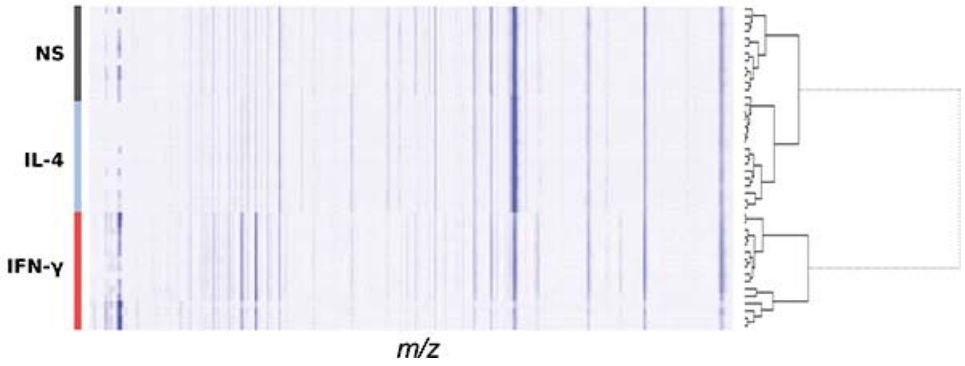

Figure 5. Reproducibility of MALDI-TOF MS spectra. Virtual gel-view of the whole spectra obtained from control and IL-4- or IFN-γ-stimulated MDMs are presented as a heatmap. Horizontal axis refers to the *m/z* ratio. Spectra are classified according to the presence/absence of peaks. NS: non stimulated; IFN-γ: interferon-gamma; IL-4: interleukin 4. This figure was reproduced from Ouedraogo *et al.*[13] with permission. Click here to view larger image.

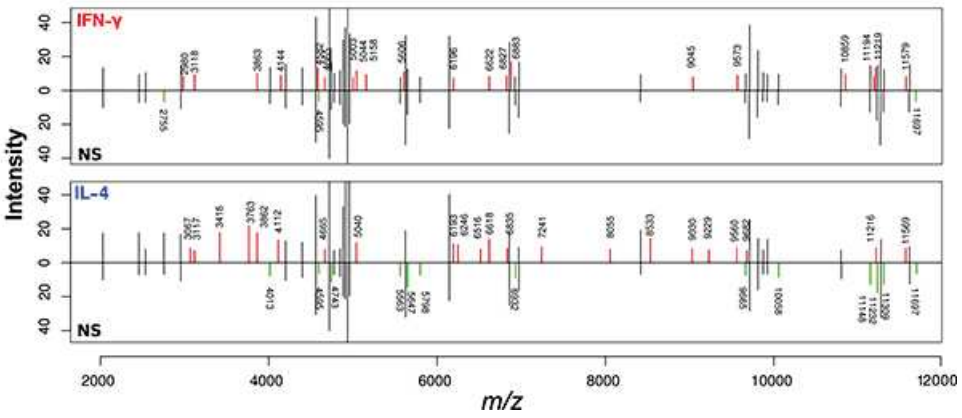

Figure 6. Reference spectra for M1 and M2 macrophages. The reference spectra for IFN-γ- and IL-4-stimulated MDMs are compared to the reference spectrum of nonstimulated (NS) MDMs. The peaks that are shared by stimulated and NS MDMs are in black. The peaks that are induced by stimulation are in red, whereas peaks that are detected only in NS MDMs are in green. *m/z*: mass/charge ratio; IFN-γ: interferon-gamma; IL-4: interleukin 4. This figure was reproduced from Ouedraogo *et al.*[13] with permission. Click here to view larger image.

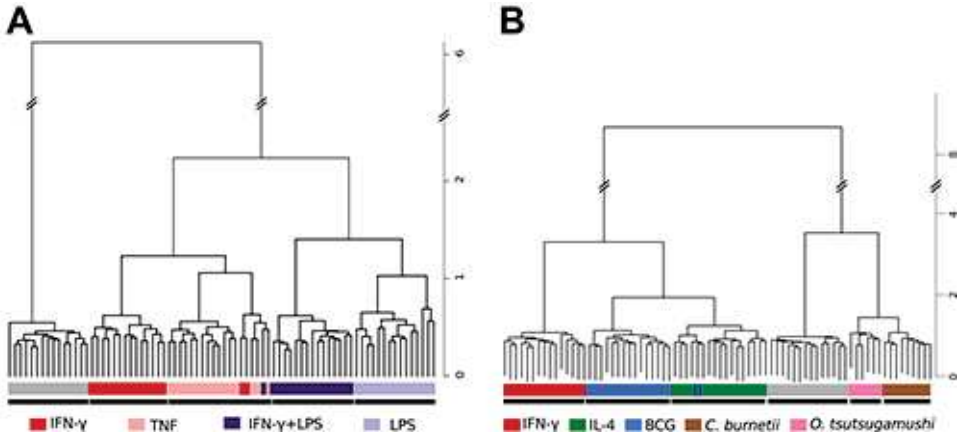

Figure 7. Hierarchical clustering of activated MDMs. MDMs were stimulated with different agonists for 18 hr. The results are shown as hierarchical clustering of the data. MDMs were activated with M1-related agonists (**A**) and intracellular bacteria or IL-4 (**B**). Unstimulated MDMs are presented in grey. IFN-γ: interferon-gamma; LPS: lipopolysaccharide from *Escherichia coli*; TNF: tumor necrosis factor, IL-4: interleukin 4; BCG; bacillus Calmette-Guérin; *C. burnetii*: *Coxiella burnetii*; *O. tsutsugamushi*: *Orientia tsutsugamushi*. This figure was reproduced from Ouedraogo *et al.*[13] with permission. Click here to view larger image.

Discussion

This protocol describes the use of MALDI-TOF-MS on eukaryotic whole cells. Here, we illustrate the accuracy of the method by analyzing the multiple activation states of macrophages in response to their microenvironment.

The success of the protocol relies on few critical steps. First, any solution contaminant may alter the spectra. For example, it is important to wash cells in PBS to remove culture medium and serum proteins before deposition on the target. A cell concentration of 1 x 10^5 cells/µl is also needed to ensure reproducible results. Second, the crystallization is an important step in the protocol. To ensure good quality results, the target plate must be carefully washed and the matrix should be prepared before the deposition of samples on the target. The best results are obtained when the samples are deposited on the target just before the matrix solution (avoid mixing the samples with the matrix before the deposition on the target). Correct spontaneous mixing between samples and the matrix solution needs homogeneous deposits. Third, whole-cell MALDI-TOF-MS is a high-throughput technique, which can rapidly result in high amounts of raw data. Bioinformatics analysis is thus a major tool to systematically analyze the data in a reasonable amount of time. Quality assessment, background correction and normalization can be automated. The selection of relevant peaks (*e.g.* above a given signal-to-noise ratio) and the comparison of spectra based on the presence/absence of these peaks require important computational steps. These methods are described in details in the supplementary material of this article.

Although the acquisition of a mass spectrometer may represent a significant investment, daily running costs are low, and a high number of biological and technical replicates may be easily obtained in one run. For example, our university hospital is able to routinely identify bacteria in 200 clinical samples each day with a similar whole-cell technique. The cell concentration may be a limit for specific clinical applications such as the analysis of needle biopsies or cells harvested from broncho-alveolar lavages. A recent article described an automated approach of whole-cell MALDI-TOF analysis that allowed the robust classification of samples with as few as 250 cells on each spot[11]. A proof of concept of the clinical application of this technique to the diagnosis of oral cancer has also been recently published[15]. The matrix choice may limit the type of analyzed molecules. Some matrices will favor the ionization of specific type of molecules (proteins, lipids, sugars…) and of a given mass

range. In our conditions, we were not able to retrieve good quality spectra with ions above 20 kDa. In our protocol, we focused on the analysis of whole spectra as a fingerprint of a given activation state of cells. Therefore, we did not try to identify the proteins that form the main peaks of the spectrum. The identification of specific biomarkers requires an alternative use of mass spectrometry.

In conclusion, we describe here the application of a whole-cell MALDI-TOF MS approach for the accurate and rapid analysis of macrophage activation. This method allowed the identification of macrophage-specific fingerprints that are representative of the diversity of proteomic responses to cytokines and bacterial pathogens. The protocol we described here may be useful for studying the immune host response in pathological conditions or may be extended to wider diagnostic applications.

Disclosures

The authors have no conflict of interest to declare. RO, JLM and CC are inventors of an international patent WO 2011/154650, named "Procédé d'identification de cellules de mammifères par spectrométrie de masse MALDI-TOF".

Acknowledgements

Richard Ouedraogo is supported by a grant from the Ministère de la Santé (PHRC 2010). We thank Laurent Gorvel, Christophe Flaudrops and Nicolas Amstrong for technical assistance.

References

1. Gross, J. *Mass Spectrometry: A Textbook*. Springer-Verlag, Berlin (2011).
2. Villanueva, J., *et al.* Serum Peptide Profiling by Magnetic Particle-Assisted, Automated Sample Processing and MALDI-TOF Mass Spectrometry. *Anal. Chem.* **76**(6), 1560–1570 (2004).
3. Diamandis, E. P. Mass Spectrometry as a Diagnostic and a Cancer Biomarker Discovery Tool Opportunities and Potential Limitations. *Molec. Cell. Proteomics.* **3**(4), 367–378 (2004).
4. Pusch, W. & Kostrzewa, M. Application of MALDI-TOF Mass Spectrometry in Screening and Diagnostic Research. *Curr. Pharm. Design.* **11**(20), 2577–2591 (2005).
5. Aebersold, R. & Mann, M. Mass spectrometry-based proteomics. *Nature*. **422**(6928), 198–207 (2003).
6. Domon, B. & Aebersold, R. Mass Spectrometry and Protein Analysis. *Science.* **312**(5771), 212–217 (2006).
7. Carbonnelle, E., *et al.* Robustness of two MALDI-TOF mass spectrometry systems for bacterial identification. *J. Microbiol. Methods.* **89**(2), 133–136 (2012).
8. Bizzini, A., Jaton, K., Romo, D., Bille, J., Prod'hom, G. & Greub, G. Matrix-Assisted Laser Desorption Ionization–Time of Flight Mass Spectrometry as an Alternative to 16S rRNA Gene Sequencing for Identification of Difficult-To-Identify Bacterial Strains. *J. Clin. Microbiol.* **49**(2), 693–696 (2011).
9. Buchanan, C. M., Malik, A. S. & Cooper, G. J. S. Direct visualisation of peptide hormones in cultured pancreatic islet alpha- and beta-cells by intact-cell mass spectrometry. *Rapid Commun. Mass Spectrom.* **21**(21), 3452–3458 (2007).
10. Ouedraogo, R., Flaudrops, C., Ben Amara, A., Capo, C., Raoult, D. & Mege, J.-L. Global analysis of circulating immune cells by matrix-assisted laser desorption ionization time-of-flight mass spectrometry. *PloS One.* **5**(10), e13691 (2010).
11. Munteanu, B., Reitzenstein, C. von, Hänsch, G. M., Meyer, B. & Hopf, C. Sensitive, robust and automated protein analysis of cell differentiation and of primary human blood cells by intact cell MALDI mass spectrometry biotyping. *Anal. Bioanal. Chem.* **404**(8), 2277–2286 (2012).
12. Feng, H., Sim, L. C., Wan, C., Wong, N. S. C. & Yang, Y. Rapid characterization of protein productivity and production stability of CHO cells by matrix-assisted laser desorption/ionization time-of-flight mass spectrometry. *Rapid Commun. Mass Spectrom.* **25**(10), 1407–1412 (2011).
13. Ouedraogo, R., Daumas, A., Ghigo, E., Capo, C., Mege, J.-L. & Textoris, J. Whole-cell MALDI-TOF MS: A new tool to assess the multifaceted activation of macrophages. *J. Proteomics.* **75**(18), 5523–5532 (2012).
14. Amann, J. M., *et al.* Selective profiling of proteins in lung cancer cells from fine-needle aspirates by matrix-assisted laser desorption ionization time-of-flight mass spectrometry. *Clin. Cancer Res.* **12**(17), 5142–5150 (2006).
15. Maurer, K., Eschrich, K., Schellenberger, W., Bertolini, J., Rupf, S. & Remmerbach, T. W. Oral brush biopsy analysis by MALDI-ToF Mass Spectrometry for early cancer diagnosis. *Oral Oncol.* **49**(2), 152–156 (2013).
16. Ishii, K. J., Koyama, S., Nakagawa, A., Coban, C. & Akira, S. Host innate immune receptors and beyond: making sense of microbial infections. *Cell Host Microbe.* **3**(6), 352–363 (2008).
17. Mantovani, A., Sica, A. & Locati, M. Macrophage polarization comes of age. *Immunity.* **23**(4), 344–346 (2005).
18. Martinez, F. O., Sica, A., Mantovani, A. & Locati, M. Macrophage activation and polarization. *Front. Biosci.* **13**, 453–461 (2008).
19. Mosser, D. M. & Edwards, J. P. Exploring the full spectrum of macrophage activation. *Nat. Rev. Immunol.* **8**(12), 958–969 (2008).
20. Murray, P. J. & Wynn, T. A. Protective and pathogenic functions of macrophage subsets. *Nat. Rev. Immunol.* **11**(11) 723–737 (2011).
21. Benoit, M., Desnues, B. & Mege, J.-L. Macrophage polarization in bacterial infections. *J. Immunol.* **181**(6), 3733–3739 (2008).
22. Biswas, S. K., Sica, A. & Lewis, C. E. Plasticity of macrophage function during tumor progression: regulation by distinct molecular mechanisms. *J. Immunol.* **180**(4), 2011–2017 (2008).
23. Cassetta, L., Cassol, E. & Poli, G. Macrophage polarization in health and disease. *Sci. World J.* **11**, 2391–2402 (2011).
24. Gordon, S. Alternative activation of macrophages. *Nat. Rev. Immunol.* **3**(1), 23–35 (2003).
25. Mantovani, A., Sica, A., Sozzani, S., Allavena, P., Vecchi, A. & Locati, M. The chemokine system in diverse forms of macrophage activation and polarization. *Trends Immunol.* **25**(12), 677–686 (2004).
26. Delaby, A., Gorvel, L., *et al.* Defective monocyte dynamics in Q fever granuloma deficiency. *J. Infect. Dis.* **205**(7), 1086–1094 (2012).
27. Gibb, S. & Strimmer, K. MALDIquant: a versatile R package for the analysis of mass spectrometry data. *Bioinformatics.* **28**(17), 2270–2271 (2012).

MALDI-TOF MS monitoring of PBMC activation status in sepsis

Daumas A, Alingrin J, Ouedraogo R, Villani P, Leone M, Mege JL.

BMC Infect Dis. 2018 Jul 31;18(1):355.

doi: 10.1186/s12879-018-3266-7.

Nous avons montré que la spectrométrie de masse MALDI-TOF permet de distinguer différents états d'activation des macrophages [**Article 1**]. Dans la même idée, Portevin et al. se sont intéressés à l'utilisation de la spectrométrie pour distinguer les sous-populations monocytaires à savoir classique, intermédiaire et non classique, qui sont habituellement caractérisées par leur niveau de cluster de différenciation (CD) 14 et CD16 expression en cytométrie de flux et monitorer leur état d'activation en réponse à différentes stimulations antigéniques (LPS et *Mycobacterium tuberculosis*) [124]. Confortant nos résultats préliminaires, leur travail met en lumière les avantages de la technique à savoir sa simplicité d'utilisation, la reproductibilité des analyses sur cellules entières, la sensibilité à distinguer différents profils d'activation cellulaire et l'indépendance de l'analyse bio-informatique des données puisqu'ils ont également utilisé le logiciel R et la bibliothèque open source MALDIquant Foreign R package. Cette technique pourrait permettre d'évaluer et mesurer l'état d'activation du système immunitaire dans différentes pathologies et d'apprécier la réponse aux traitements. Cependant la principale limite à notre étude et la leur dans l'idée d'une application en clinique, ce sont les manipulations nécessaires à l'obtention des monocytes ou des macrophages.

Nous nous sommes alors demandé si la technique pourrait s'appliquer à l'étude d'un mélange cellulaire tel que les PBMCs, facile à obtenir avec l'utilisation de Ficoll. L'interrogation in fine étant de savoir si dès les premières heures devant un patient présentant une réaction inflammatoire systémique (Systemic Inflammatory Response Syndrome = SIRS), par le biais de la spectrométrie, on arrive à confirmer ou infirmer l'origine infectieuse de cette réaction avant même les résultats éventuellement des prélèvements infectieux réalisés ou la réalisation d'autres explorations permettant d'identifier un foyer infectieux pas toujours présent initialement.

J'ai ainsi étudié dans un premier temps les signatures spectrales des PBMCs de 12 patients en sepsis sévère (2 présentant une bactériémie à *Staphylococcus aureus*, 4 une bactériémie à bacille Gram négatif et 6 n'ayant pas de documentation microbiologique bien qu'une infection soit fortement suspectée) et de sujets sains selon le même protocole qu'utilisé auparavant (Articles présentés précédemment).

Nous avons montré que les spectres des PBMCs de sujets sains étaient très différents des spectres des patients. Afin d'incrémenter le dendogramme réalisé par l'équipe, nous avons analysé le positionnement des spectres de 2 sujets sains et de 2 patients et observé que les spectres des patients se rapprochent le plus des spectres des polynucléaires et des monocytes alors que les spectres des sujets sains sont plus proches des lymphocytes. De façon rassurante en tout cas, les spectres des PBMCs sont très éloignés des spectres des autres cellules eucaryotes caractérisées par Ouedraogo et al. [20]. Nous avons pu mettre en évidence la présence ou absence spécifique de pics significatifs sur les spectres des patients et sujets sains.

Nous avons ensuite stimulé les PBMCs avec des cytokines (IFN-γ, IL-4 et IL-10), des motifs moléculaires associés aux micro-organismes (MAMPs) (LPS d'*Escherichia coli*, peptidoglycane de *Bacillus subtilis*, des oligonucléotides CpG et poly I :C pour les virus) et enfin des bactéries inactivées *(Staphylococcus aureus, Streptococcus agalactiae, Pseudomonas aeruginosa et Escherichia coli*).

Nous avons obtenu des signatures spécifiques et reproductibles pour chaque condition d'activation. Les spectres des PBMCs stimulés par les agonistes pro-inflammatoires (IFN-γ et LPS) se regroupent dans un même cluster bien distinct du cluster des spectres des PBMCs stimulés par les cytokines anti-inflammatoires à savoir IL-4 et IL-10. On observe également que les spectres des PBMCs stimulés par les MAMPs et les bactéries sont proches et qu'ils se différencient nettement des spectres des PBMCs non stimulés ou stimulés par poly I:C.

Les signatures obtenues étant spécifiques, nous avons créé une référence spectrale pour chaque état d'activation dans l'idée d'une banque de données. Nous avons ensuite comparé les spectres des patients avec ces spectres de référence sur le modèle de l'identification des micro-organismes avec un score de concordance.

Nous retrouvons clairement une signature IFN-γ et IL-10 chez tous les patients septiques prévisible du fait de la réponse inflammatoire et antiinflammatoire concomitante au cours du sepsis. Mais le résultat le plus marquant est que l'on identifie aussi chez tous les patients septiques indépendamment de la documentation microbiologique, une signature CpG ODN faisant évoquer une activation à un pathogène bactérien. Nous n'avons par contre pas retrouvé de concordance étroite entre le spectre des PBMCs stimulés par *Staphylococcus aureus* et les spectres des patients infectés à *Staphylococcus aureus,* de même qu'entre le spectre des PBMCs stimulés par le LPS d'*Escherichia coli* et les spectres des patients infectés à *Escherichia coli.*

Malgré les limites de cette première étude, la spectrométrie de masse pourrait permettre de distinguer un SIRS en lien avec une pathologie inflammatoire ou infectieuse ou encore d'aider le clinicien dans un contexte de SIRS non infectieux à dépister l'apparition d'une complication infectieuse avant même la clinique et bien avant l'éventuelle identification d'un micro-organisme sur des prélèvements. La sensibilité de la technique ne permet pas par contre d'aller à une caractérisation plus précise du stimulus bactérien.

Des études de confirmation sont nécessaires mais l'application de la technique au monitorage de la réponse immunitaire semble prometteuse.

Daumas et al. BMC Infectious Diseases (2018) 18:355
https://doi.org/10.1186/s12879-018-3266-7

BMC Infectious Diseases

RESEARCH ARTICLE Open Access

MALDI-TOF MS monitoring of PBMC activation status in sepsis

Aurélie Daumas[1,2*], Julie Alingrin[1,3], Richard Ouedraogo[1], Patrick Villani[2], Marc Leone[1,3] and Jean-Louis Mege[1]

Abstract

Background: MALDI-TOF mass spectrometry (MS) on whole cells enables the detection of different cell types and cell activation. Here, we wondered whether this approach would be useful to investigate the host response in sepsis.

Methods: Peripheral blood mononuclear cells (PBMCs) from patients with severe sepsis and healthy donors were analyzed with MALDI-TOF MS. PBMCs from healthy donors were also stimulated with lipopolysaccharide, peptidoglycan, CpG oligonucleotides, polyinosinic polycytidylic acid, and with heat-inactivated bacteria. Averaged spectra of PBMCs stimulated in vitro by different agonists were generated from the database using the Biotyper software and matching scores between each spectrum from patients and averaged spectra from the database were calculated.

Results: We show that the MALDI-TOF MS signature of PBMCs from septic patients was specific, compared with healthy controls. As the fingerprints observed in patients may be related to PBMC activation, PBMCs from healthy controls were stimulated with cytokines, soluble Pathogen-Associated Molecular Patterns (PAMPs) and heat-killed bacteria, and we created a database of reference spectra. The MALDI-TOF MS profiles of PBMCs from septic patients were then compared with the database. No differences were found between patients with documented infection ($n = 6$) and those without bacteriological documentation ($n = 6$). The spectra of PBMCs from septic patients matched with those of interferon-γ- and interleukin-10-stimulated PBMCs, confirming that sepsis is characterized by both inflammatory and immunoregulatory features. Interestingly, the spectra of PBMCs from septic patients without documented infection matched with the reference spectrum of PBMCs stimulated by CpG oligonucleotides, suggesting a bacterial etiology in these patients.

Conclusions: Despite the limits of this preliminary study, these results indicate that the monitoring of functional status of PBMCs in peripheral blood by whole cell MALDI-TOF MS could provide unique opportunities to assess disease progression or resolution in clinical settings.

Keywords: Sepsis, Mass spectrometry, MALDI-TOF, Mononuclear cells, IFN-γ, Interleukin-10, CpG oligonucleotides

Background

Sepsis is the combination of a systemic inflammatory response syndrome (SIRS) and infection [1]. Sepsis can progress to severe sepsis and septic shock, with mortality rates of 25 to 30% and 40 to 70%, respectively [2, 3]. The clinical manifestations of the early stages of sepsis are often similar to those of a patient with SIRS caused by sterile inflammation [3], leading to frequent underappreciation of sepsis in clinical practice. The traditional approach to sepsis diagnosis is based on the clinical signs and symptoms of sepsis, supported by relevant microbiological data. Unfortunately, up to 40% of the infections suspected in patients with sepsis are not microbiologically documented [4–6]. Consequently, physicians often use empiric antibiotic therapy, which has three major drawbacks: increased antibiotic resistance, patient toxicity, and elevated costs [7].

Two important challenges for physicians are to determine if the patient is infected or not in the absence of microbiological documentation, and when to begin antimicrobial therapy [8–10]. Numerous molecules, such as procalcitonin, are unable to discriminate between sepsis and SIRS [11, 12]. Cytokine imbalance has been thought to be useful for defining sepsis. Indeed, the recognition of soluble Pathogen-Associated Molecular Patterns (PAMPs) such as lipopolysaccharide (LPS), peptidoglycan (PGN),

* Correspondence: aurelie.daumas@ap-hm.fr
[1]Aix-Marseille Université, URMITE, IHU Méditerranée Infection, UMR CNR 7278, IRD 198, INSERM 1095, Marseille, France
[2]Service de Médecine Interne et Thérapeutique, Hôpital de la Timone, Assistance Publique-Hôpitaux de Marseille, Marseille, France
Full list of author information is available at the end of the article

CpG oligonucleotides (CpG-ODN), and polyinosinic polycytidylic acid (poly I:C) by pathogen recognition receptors (PRRs) induces the release of inflammatory cytokines, such as gamma interferon (IFN-γ) and the concomitant liberation of immunoregulatory cytokines, including interleukin (IL)-10 and IL-4. However, cytokine profiles are also unable to discriminate sepsis, and seem more related to SIRS severity than to sepsis [13].

MALDI-TOF mass spectrometry (MS) has emerged as a fast, reliable and inexpensive tool for bacterial identification and diagnosis [14, 15]. Interestingly, bacterial identification does not require previous fractionation steps [16]. Recently, we and others have applied the whole-cell MALDI-TOF MS technique to identify eukaryotic cells, including circulating cells [17–19]. Our team has also shown that whole-cell MALDI-TOF MS detects the multifaceted activation of monocyte-derived macrophages in response to various cytokines and bacterial pathogens [20]. Portevin et al. [21] demonstrated recently that MALDI-TOF MS fingerprints distinguish human monocyte sub-populations activated by distinct microbial ligands.

Our goal was to analyze peripheral blood mononuclear cells (PBMCs) in septic patients through whole-cell MALDI-TOF MS. This approach enabled the detection of a specific PBMC signature in septic patients. The analysis of the signature of healthy PBMCs stimulated with cytokines, soluble PAMPs and bacteria, frequently involved in sepsis, showed that the spectra of PBMCs from septic patients matched with those of PBMCs stimulated by IFN-γ, IL-10 and CpG-ODN. These findings evoked an infectious activation in septic patients regardless of documented or undocumented infection. Despite the limits of this preliminary study, this is the first report describing the use of a whole-cell MALDI-TOF MS approach to identify PBMC activation in septic patients.

Methods

Ethics statement

The study was approved by the Ethics Committee of the Assistance Publique-Hôpitaux de Marseille, France. Blood was collected after informed and written consent of healthy donors and septic patients.

Patients and healthy controls

Patient recruitment was provided from an ancillary study to the project "De-escalation of Empirical Antibiotics in Severe Sepsis" (Comité de Protection des Personnes Sud Méditerranée No. 2011–002297-22). Twelve patients (aged 18 and over) were enrolled in the polyvalent intensive care unit (North Hospital, Marseille, France). A single blood sample was collected at the time of empirical antibiotic initiation. Eligibility criteria were the presence of severe sepsis requiring empirical antimicrobial treatment. Severe sepsis was defined as the criteria for SIRS and suspected infection with at least one organ failure. SIRS was defined by two or more of the following conditions: temperature > 38 °C or < 36 °C, heart rate > 90 beats per minute, respiratory rate > 20 breaths per minute or PaCO2 < 32 mmHg, white blood cell count >12G/l, < 4G/l, or > 10% immature cells. Two patients with SIRS had *Staphylococcus aureus* bacteremia, 4 had gram-negative bacillus bacteremia and 6 had a strongly suspected infection clinically but not microbiologically documented. PBMCs from healthy donors were isolated from leukopacks (Etablissement Français du Sang).

Isolation and in vitro activation of PBMCs

Blood was collected in EDTA-containing tubes and PBMCs were isolated using Ficoll cushions (MSL, Eurobio). After centrifugation, PBMCs were washed in sterile phosphate buffered saline (PBS) without Ca^{2+} and Mg^{2+}, and 1×10^6 cells were suspended in 10 μL of PBS and frozen at − 80 °C for 2 to 3 days before analysis. In some experiments, PBMCs from healthy donors (1×10^6 cells in 6-well plates) were incubated in 2 mL of RPMI 1640 containing 10% fetal calf serum (FCS) and stimulated with 20 ng/mL IFN-γ (PeproTech), 20 ng/mL IL-4 or IL-10 (R&D Systems) for 18 h [22]. PBMCs were also stimulated with LPS from *Escherichia coli* (1 μg/mL, Sigma-Aldrich), peptidoglycan (PGN) from *Bacillus subtilis* (10 μg/mL, Sigma-Aldrich), CpG-ODN (2 μg/mL, InvivoGen) and poly I:C (25 μg/mL, InvivoGen). Finally, PBMCs were stimulated with heat-inactivated bacteria (10 bacteria per cell). Bacteria included oxacillin-sensitive *S. aureus*, community strain group B streptococcus, *Pseudomonas aeruginosa* (ATCC 27853) and *E. coli* (ATCC 25922). PBMCs stimulated for 18 h were pelleted in 10 μl of PBS and frozen as unstimulated PBMCs for MALDI-TOF MS analysis.

MALDI-TOF MS analysis

After thawing of the PBMCs, 1 μL of cell suspension was added to 1 μL of matrix solution (saturated solution of α-cyano-4-hydroxy-cynnamic acid in a mixture of 50% acetonitrile, 25% trifluoroacetic acid and water) as previously described [17, 20, 23]. The mixture was deposited on the MALDI target. The evaporation that gradually took place at room temperature allowed the formation of α-cyano-4-hydroxy-cynnamic acid crystals containing the dispersed samples. Measurements were performed using an Autoflex II mass spectrometer (Bruker Daltonics, Wissembourg, France) equipped with a 337-nm nitrogen laser. Each sample was irradiated with a laser for desorption and ionization. Each spectrum resulted from the sum of positive ions obtained after 525 laser shots in different regions of the analyzed spot (automatic mode). All the positive-ion mass spectra were acquired in the linear mode

at an acceleration voltage of 20 kV in the delayed extraction mode. A signal-to-noise of 3.0 was selected to define peaks, with a maximum of 100 peaks per spectrum. Spectra were automatically acquired with a mass/charge (*m/z*) ranging from 2000 to 20,000 Da using FlexControl and FlexAnalysis 2.4 software (Bruker Daltonics). The x-axis of spectra represented the *m/z* ratio (in daltons) of ionized molecules, and the y-axis indicated the intensity (relative abundance) of these ions.

Spectrum analysis

Analyses and graphical outputs were performed using the free and open source statistical analysis software R (version 2.13), along with specific analysis libraries (MALDIquant) as previously described [20]. The gel view representation indicates the reproducibility of the spectra. A hierarchical clustering with a ward algorithm for agglomeration and a dissimilarity matrix based on the Jaccard distance were used to classify the spectra. The MALDI Biotyper 3 software (Bruker Daltonics) was used to create an average reference spectrum for each PBMC sample, corresponding to at least 10 individual spectra. The Biotyper software realigns acquired spectra and automatically creates an average spectrum using default Biotyper software settings provided by the manufacturer, and we created a database as previously described [20]. The Biotyper software also allows the identification of unknown spectra as shown in clinical samples by comparison with reference spectra, for the identification and classification of microorganisms [14]. The score values proposed by the manufacturer have been used for microorganism identification. The score values between 0.000 and 1.699 do not allow reliable microbe identification; the values between 1.700 and 1.999 allow probable cell identification and score values higher than 2.0 are considered statistically significant; they allow the confident identification of different microbe species. We extended this method to assess PBMC activation status in septic patients. As the score values provided by Bruker Daltonics ranged from 0.000 to 2.000 when we used control samples and reference spectra, we considered that medians of matching scores higher than 1.5 allowed reliable identification of the activation profile of patient PBMCs and could be clinically relevant. Differences between conditions were tested with the Mann-Whitney *U* test and a cutoff value of 0.05 was chosen to consider a difference statistically significant.

Results

Signatures of PBMCs

As compared to phenotype studies that require panels of antibodies to characterize circulating cells, MALDI-TOF MS enables simple and rapid measurement of cell status. First, we wondered if PBMCs from healthy controls were characterized by a specific whole-cell MALDI-TOF MS signature. The spectra of PBMCs from ten healthy donors were composed of numerous peaks ranging from 2000 to 15,000 Da, with a major peak at 4961 Da. Note that the spectra of the ten donors were highly reproducible (Fig. 1a). Second, we found that the signatures of PBMCs from ten septic patients were similar but they were distinct from those of PBMCs from healthy controls. Because MALDI-TOF MS profiles were specific for PBMCs from healthy controls and septic patients, the dendrogram constructed by Ouedraogo et al. [17] was implemented with reference spectra of PBMCs from two healthy donors and two septic patients. As expected, the PBMCs from the two healthy donors were similar and clustered with T lymphocytes and, to a lesser extent, with monocytes and polymorphonuclear cells (PMNs). Likewise, the PBMCs from the two septic patients were similar and formed a specific cluster. This cluster was close to that of monocytes and PMNs but was away from the T lymphocyte cluster (Fig. 2). This specific pattern underlines the prominent role of the innate immune response in sepsis. Taken together, these results demonstrated that PBMC fingerprints distinguished patients with sepsis from healthy controls.

Peak characteristics of PBMCs in sepsis

We wondered if the analysis of individual peaks enables stratification of patients with sepsis, microbiologically documented or not. When the spectra were analyzed by comparing the presence or absence of peaks, we found that 10 peaks were present only in controls, 12 peaks were common to healthy donors and septic patients and 18 peaks were specific in septic patients (Table 1). Taking into account the limitations related to the limited number of patients in this preliminary study, among these 18 specific peaks, 15 were common to all septic patients independently of microbiological documentation. Concerning the three other peaks, the peak at 5415 Da was found in patients with gram-negative bacillus bacteremia (4/4) and one patient without microbiological documentation. The peak at 3329 Da was present in 3/4 patients with gram-negative bacillus bacteremia and the same patient without bacteriological documentation, suggesting that these two peaks could be associated with gram-negative bacillus bacteremia and that this patient without microbiological documentation could have gram-negative bacillus sepsis. Finally, the peak at 2942 Da was found in the two patients with *S. aureus* bacteremia and in one patient without microbiological documentation, suggesting that this peak could be related to *S. aureus* bacteremia (Table 1). Despite the limits of the study, these results show that the signature of septic patients is very similar, regardless of documented or undocumented infection.

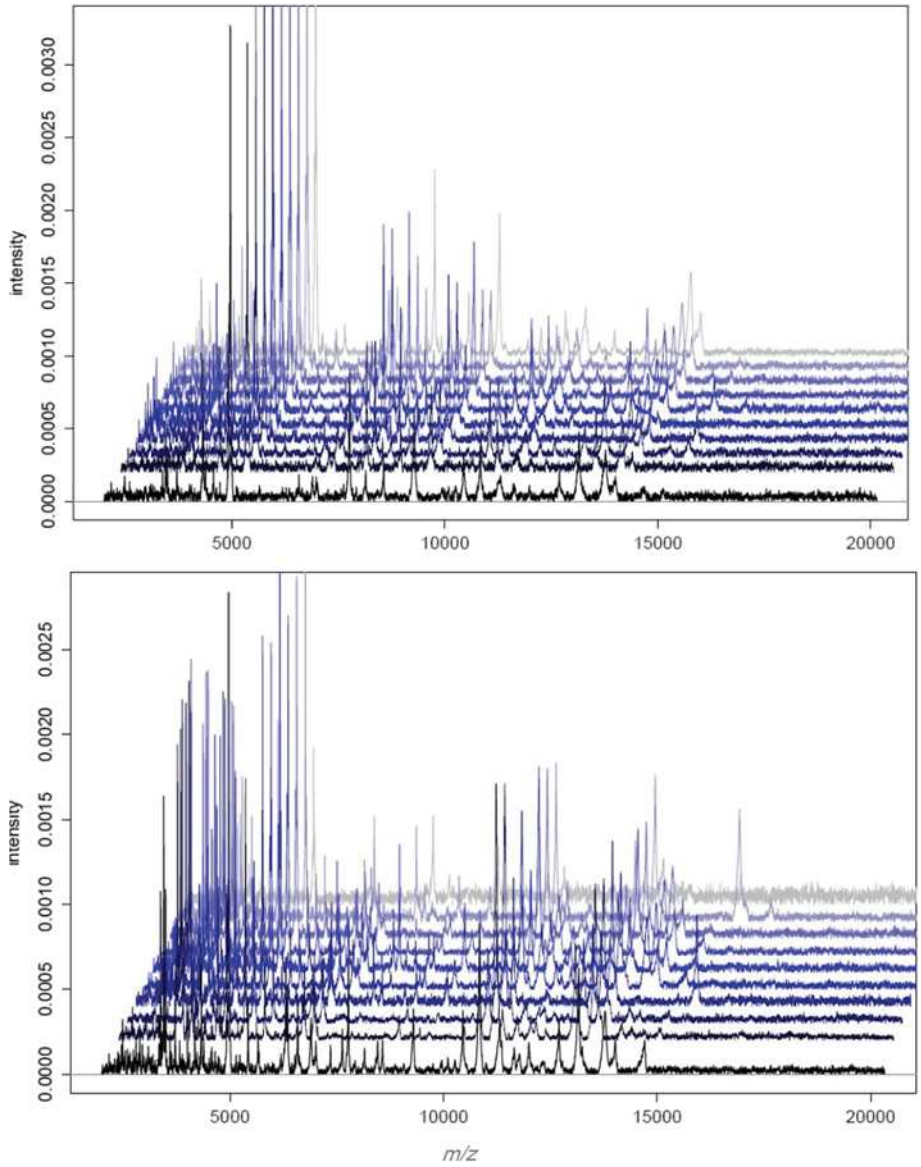

Fig. 1 MALDI-TOF MS spectra of PBMCs. The PBMCs (1×10^6 cells) from ten healthy donors (**a**) and ten septic patients (**b**) were suspended in 10 μL of PBS, and 1 μL was deposited onto the MALDI target. Representative MALDI-TOF MS spectra are shown. MALDI-TOF MS spectra were analyzed using statistical analysis software R (version 2.13)

Signatures of PBMCs activated in vitro

Because the differences between the signatures of healthy and septic PBMCs may be related to their activation state, we stimulated PBMCs with various agonists to determine if PBMC activation results in specific profiles. The stimulation of PBMCs with IFN-γ, LPS, IL-4 and IL-10 led to specific and reproducible responses, as shown using a virtual gel view representation (Fig. 3). The spectra from all stimulated samples were clearly separated from those of unstimulated PBMCs. Each type of stimulation led to specific fingerprints. The spectra from the PBMCs stimulated with inflammatory molecules (IFN-γ/LPS) clustered together. Similarly, immunoregulatory cytokines induced the clustering of PBMCs. The existence of these three major clusters (unstimulated, IFN-γ/LPS-, IL-4/IL-10-stimulated PBMCs) suggests that MALDI-TOF MS may be used to analyze the inflammatory response of PBMCs in the clinical setting.

We also investigated the responses of PBMCs to PAMPs and bacteria often found in sepsis. For that purpose, we used unstimulated PBMCs as controls and we compared the fingerprints induced by PAMPs and bacteria to these controls. Two very different clusters were clearly identified: one including unstimulated and poly I:C-stimulated PBMCs and the other with PBMCs

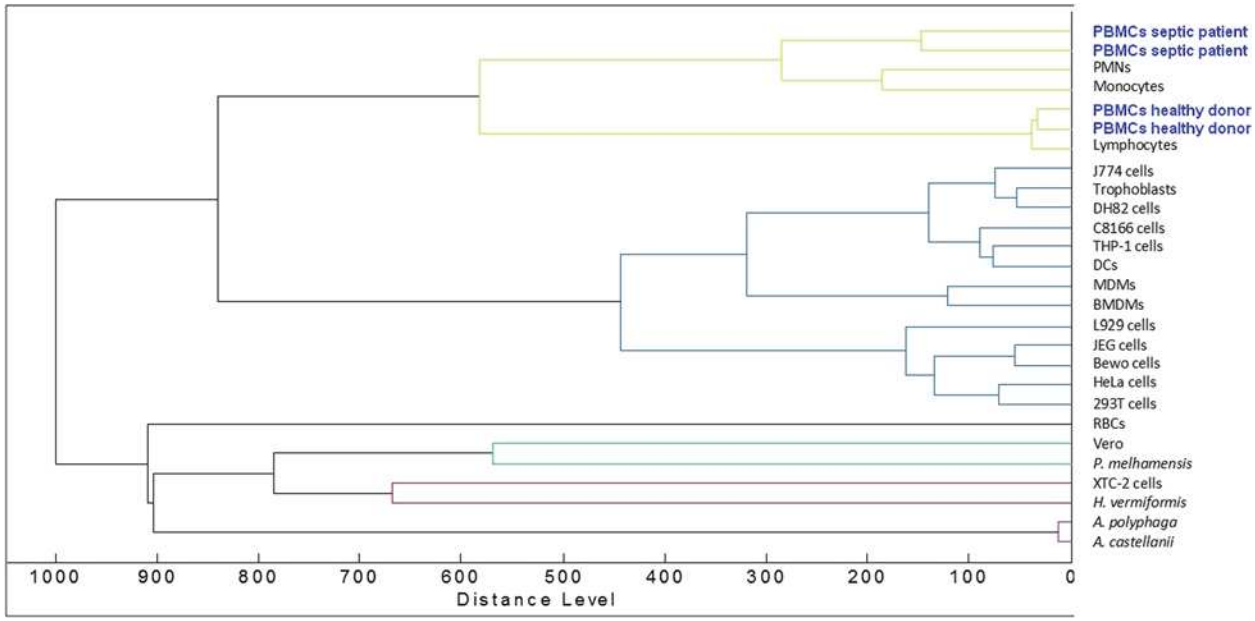

Fig. 2 Dendrogram representation of PBMCs**.** The dendrogram constructed by Ouedraogo et al. [17] was implemented with reference spectra of PBMCs from two healthy donors and two septic patients. The Biotyper (Bruker Daltonics) software was used to create an averaged spectrum for each patient, corresponding to at least 10 individual spectra. The averaged spectra were added to the database using the Biotyper software and the dendrogram creation method. Peripheral blood mononuclear cells (PBMCs); polymorphonuclear cells (PMNs); dendritic cells (DCs); monocyte-derived macrophages (MDMs); bone marrow-derived macrophages (BMDMs); red blood cells (RBCs)

stimulated with bacteria and other PAMPs (Fig. 4). Among the bacterial signatures, we observed that the signatures induced by *P. aeruginosa* and *E. coli* (Gram negative bacteria) were coupled to the signature induced by LPS from *E. coli.* Similarly, the signatures induced by *S. agalactiae* group B and *S. aureus* (gram-positive bacteria) were associated and close to the signature induced by PGN from *B. subtilis*. These results suggest that MALDI-TOF MS may be useful to assess a series of specific responses of PBMCs to varied agonists.

Finally, we used matching scores to compare the different modes of PBMC activation after having created averaged spectra of stimulated PBMCs. The MALDI-TOF MS profiles of PBMCs from septic patients were then compared with the database. None of the septic patients matched with the averaged spectrum of healthy donors, while the spectra of septic patients significantly matched with IFN-γ and IL-10 spectra regardless of whether the infection was documented ($n = 6$) or not (n = 6), confirming that sepsis is characterized by both inflammatory and immunoregulatory features (Fig. 5 and Additional file 1: Figure S1). It is noteworthy that the scores obtained by comparing the spectra of *E. coli*- and *S. aureus*-infected patients with the reference spectrum of *E. coli*- and *S. aureus*-stimulated PBMCs were significantly lower ($p < 0.05$) than those obtained with IL-10- and IFN-γ-specific spectra, respectively (see Fig. 5a, b), suggesting the prominence of the activation profile as a specific response to pathogens. Importantly, we found that the spectra of PBMCs from septic patients significantly ($p < 0.05$) matched with CpG-ODN, independently of a documented infection. Clearly, the activation profile found in the patients with unknown infection was similar to that of the patients with documented infection (see Fig. 5c), suggesting that these patients had a bacterial infection. Taken together, these results are consistent with that septic PBMCs were activated in a specific way and suggest a bacterial infection in septic patients without documented infection.

Discussion

Sepsis is a frequent and serious complication in intensive care unit patients. Despite many years of active research to find effective and specific therapies, the only true treatment still relies on organ system support and effective antimicrobial eradication with antibiotics and/or surgical intervention. An important factor in optimizing survival rates in these patients is the speed of diagnosis [2–5]. However, diagnosing sepsis is not always straightforward, particularly in patients who have complex ongoing disease processes. In addition, many of these patients received antimicrobial therapy that rendered microbial cultures negative. Hence, 30–40% of intensive care unit patients with severe sepsis had negative bacterial cultures [4–6]. Even when cultures are positive, results take several days to become available, thus slowing

Table 1 Peak characteristics of PBMCs

Healthy donors	Gram-negative bacillus bacteremia	*S. aureus* bacteremia	Patients without documented infection
2165			
2227			
2302			
2503			
	2617	2617	2617
	2631	2631	2631
	2646	2646	2646
2777			
	2795	2795	2795
		2942	2942
	3329		3329
	3355	3355	3355
3363			
3369	3369	3369	3369
	3398	3398	3398
	3426	3426	3426
3441	3441	3441	3441
3455			
	3467	3467	3467
3485	3485	3485	3485
	3708	3708	3708
3881			
	3998	3998	3998
	4323	4323	4323
4642			
4935	4935	4935	4935
4961	4961	4961	4961
4983	4983	4983	4983
5023			
	5415		5415
	6298	6298	6298
	6342	6342	6342
6574	6574	6574	6574
	7621	7621	7621
7762	7762	7762	7762
8561	8561	8561	8561
9285	9285	9285	9285
10,259	10,259	10,259	10,259
	10,441	10,441	10,441
10,831	10,831	10,831	10,831

The PBMCs from healthy donors and septic patients were analyzed by MALDI-TOF MS

The *m/z* ratio of peaks is shown. The peaks that were common to septic patients are underlined

the diagnostic process. Many biomarkers have been proposed over the years, but the diagnostic value of these molecules remains uncertain [24, 25].

We reasoned that a more integrated approach such as MALDI-TOF MS may be used to detect sepsis specifically in patients without microbiological documentation. As expected, we found that the signature of PBMCs from different healthy subjects was highly reproducible. It clustered with T lymphocytes but was largely different from the signature of numerous non-circulating cells. The signatures of PBMCs from septic patients largely differed from that of PBMCs from healthy controls. Interestingly, they clustered with the signature of monocytes and PMNs but not with T lymphocytes. The absence of clustering with T lymphocytes may be related to the lymphopenia associated with systemic inflammation syndromes [26]. This specific pattern underlines the prominent role of the innate immune response in sepsis.

We postulated that the fingerprints of septic patients may be related to specific activation of PBMCs. To assess the activation of PBMCs, we stimulated PBMCs from healthy controls with cytokines, PAMPs and bacteria. First, we identified both inflammatory (IFN-γ and LPS) and immunoregulatory (IL-4 or IL-10) signatures in PBMCs. Second, we also found that gram-negative bacteria and LPS induced specific signatures compared to those induced by gram-positive bacteria and PGN. Interestingly, the signatures induced by bacterial PAMPs were separate from a poly I:C, a PAMP known to strongly stimulate type 1 interferon as do most of viruses. This result might be useful in discriminating bacterial and viral infections, such as in pneumonia, for which no clinical, radiological and laboratory data differentiate bacterial from viral pneumonia [27].

Finally, we attempted to relate in vitro data and the fingerprints of septic PBMCs. We clearly identified IFN-γ and IL-10 signatures in septic patients. This result is consistent with the natural history of sepsis, where both inflammatory and immunoregulatory responses are observed [28]. We did not detect the signals delivered in vitro by heat-inactivated bacteria and bacterial ligands such as LPS and PGN, even when microbiological infection was documented. We can hypothesize that the lack of LPS and PGN signatures in sepsis may be related to anergy (endotoxin tolerance) [29]. In contrast, we found an intense CpG-ODN signature in septic patients, even in patients without microbiological documentation, suggesting the prominence of the activation profile as a specific response to pathogens. The Biotyper score cutoffs of 1.5 can be considered as unacceptably low for functions such as microbial identification. However, no comparison is possible because no score has so far been validated to discriminate specific responses of PBMCs to varied agonists. This is the first report describing the use

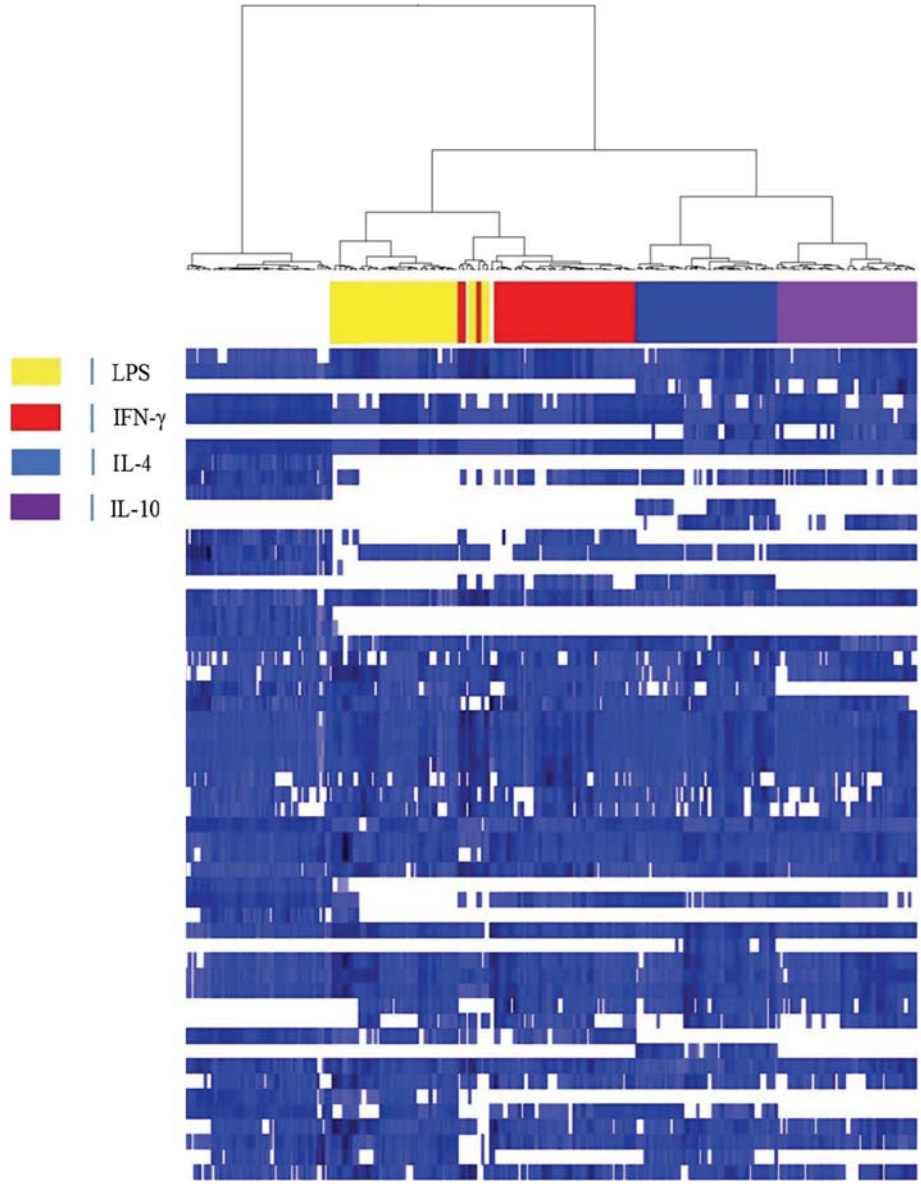

Fig. 3 Gel view representation of activated PBMCs. The PBMCs from healthy donors were stimulated with 20 ng/ml IFN-γ, IL-4, IL-10 or 1 μg/mL LPS for 18 h. The spectra were arranged in a pseudo-gel format using a gel view representation. Vertical axis refers to the m/z ratio. Spectra are classified according to the presence/absence of peaks. Unstimulated PBMCs are presented in white

of a whole-cell MALDI-TOF MS approach to identify PBMC activation in septic patients. As the score values provided by Bruker Daltonics ranged from 0.000 to 2.000 when we used control samples and reference spectra, we considered that medians of matching scores higher than 1.5 allowed reliable identification of the activation profile of patient PBMCs. Despite the choice of this score cutoff, we did not detect the signals delivered in vitro by heat-inactivated bacteria or bacterial ligands such as LPS and PGN in septic patients even with documented microbiological infection. Obviously, we observed a distinct and reproductible IFN-γ, IL-10 and CpG-ODN. The preliminary nature of the findings requires nevertheless confirmation of results.

To our knowledge, this is the first report describing the use of whole-cell MALDI-TOF MS analysis to identify mass spectra that discriminate specific responses of PBMCs to varied agonists and to study functional and activation status of septic patients with and without documented bacterial infection.

Conclusions

This study shows that MALDI-TOF MS of patient PBMCs is easy and fast to perform and may be

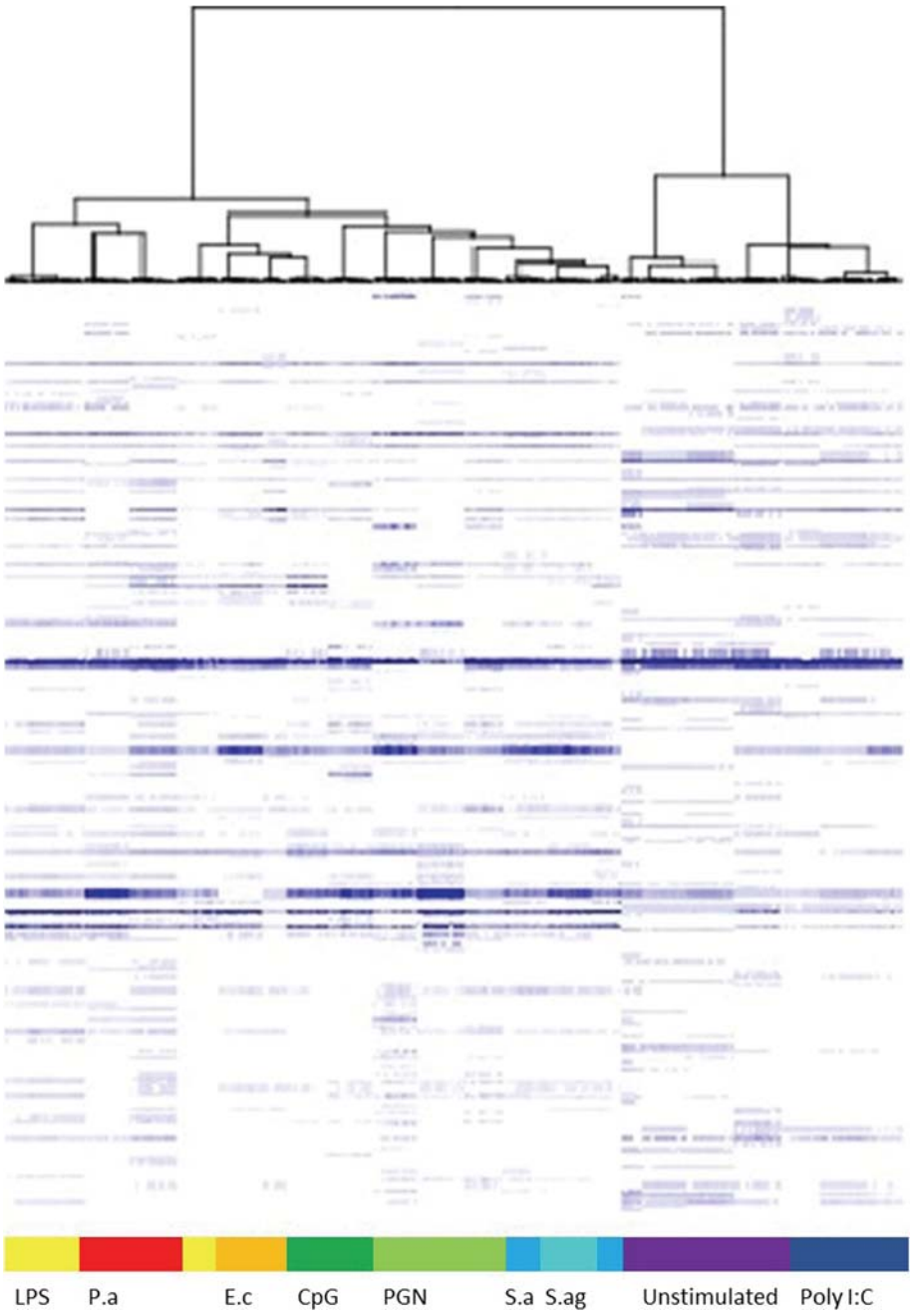

Fig. 4 Hierarchical clustering of activated PBMCs. PBMCs were stimulated with different agonists for 18 h. The results are shown as hierarchical clustering. Vertical axis refers to the m/z ratio. Spectra are classified according to the presence/absence of peaks. PBMCs stimulated with LPS from *Escherichia coli* are presented in yellow, with *Pseudomonas aeruginosa* (*P.a*) in red, *Escherichia coli* (*E.c*) in orange, CpG ODN in dark green, PGN in green, *Staphylococcus aureus* (*S.a*) in blue, *Streptococcus agalactiae* (*S.ag*) in turquoise, unstimulated PBMCs in purple and PBMCs stimulated with poly I:C in dark blue

considered as a routine method for the detection of sepsis. The reproducibility and accuracy of this approach enables the analysis of several types of PBMC activation and shows a similar activation signature for septic patients with and without documented bacterial infection. Consequently, this innovative approach may be promising in helping physicians in the identification and prognosis of septic patients and/or their treatment. This proof of concept could easily be translated to clinical studies to monitor the functional status of PBMCs from patients under treatment and to study the activation status of PBMCs from patients suffering from systemic and

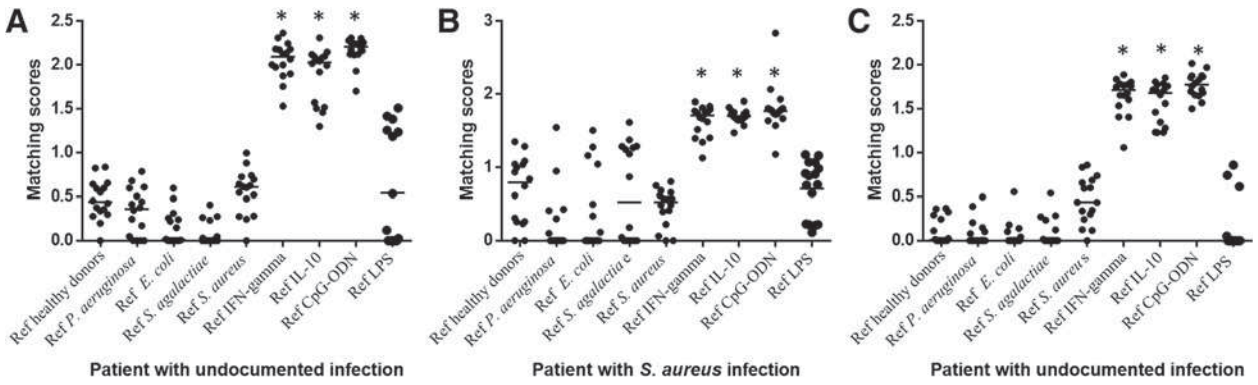

Fig. 5 Comparison between in vitro and in vivo data. Averaged spectra of PBMCs stimulated in vitro by different agonists were generated from the database using the Biotyper software. The spectra ($n = 16$) from four patients with *E. coli* bacteremia, two patients with *S. aureus* bacteremia and six patients with undocumented infection were then compared with the averaged spectra of the database. Scatter plots of one representative septic patient with *E. coli* infection (**a**), *S. aureus* infection (**b**) or without microbiological documentation (**c**) are presented. Matching scores between each spectrum from patients and averaged spectra from the database are represented with circles. Horizontal lines represent the medians of matching scores; a value higher than 1.5 was considered significant and allowed confident identification of the activation status of PBMCs. The nonparametric Mann-Whitney *U* test was used to compare scores with the averaged spectra of the database

chronic inflammatory disorders. However, the preliminary nature of the findings requires confirmation of results. As a next step, larger studies would confirm whether this new technique can improve the medical management of patients. High throughput monitoring of functional status of PBMCs in peripheral blood based on whole cell MALDI-TOF MS could provide unique opportunities to monitor disease progression and resolution in clinical settings.

Additional file

Additional file 1: Figure S1. Comparison between in vitro and in vivo data. Averaged spectra of PBMCs stimulated in vitro by different agonists were generated from the database using the Biotyper software. The spectra ($n = 16$) from 2 other patients with gram-negative bacillus bacteremia, the second patients with *S. aureus* bacteremia and three other patients with undocumented infection were then compared with the averaged spectra of the database. Matching scores between each spectrum from patients and averaged spectra from the database are represented with circles. Horizontal lines represent the medians of matching scores; a value higher than 1.5 was considered significant and allowed confident identification of the activation status of PBMCs. (JPG 320 kb)

Abbreviations

CpG-ODN: CpG oligonucleotides; *E. coli*: *Escherichia coli*; IFN-γ: Gamma interferon; IL: Interleukin; LPS: Lipopolysaccharide; MS: Mass spectrometry; PBMCs: Peripheral blood mononuclear cells; PGN: Peptidoglycan; Poly I:C: Polyinosinic polycytidylic acid; PRRs: Pathogen recognition receptors; *S. aureus*: *Staphylococcus aureus*; SIRS: Systemic inflammatory response syndrome

Acknowledgements

We thank Christian Capo for his attentive reading of our manuscript. RO was financially supported by "Infectiopôle Sud" foundation.

Availability of data and materials

The datasets used and/or analysed during the current study are available from the corresponding author on reasonable request.

Authors' contributions

AD, RO and JLM designed the study. AD, RO and JA carried out the experiments. AD, PV, ML and JLM carried out the statistical analysis and drafted the manuscript. All authors read and approved the final version of the manuscript.

Ethics approval and consent to participate

Patient recruitment was provided from an ancillary study to the project "De-escalation of Empirical Antibiotics in Severe Sepsis". Written informed consent was obtained from the participants or their parents. The study was approved by the Ethics Committee Sud Méditerranée (No. 2011–002297-22). Confidentiality of the participants' details was assured.

Consent for publication

Not applicable.

Competing interests

The authors declare that they have no competing interests.

Publisher's Note

Author details

[1]Aix-Marseille Université, URMITE, IHU Méditerranée Infection, UMR CNR 7278, IRD 198, INSERM 1095, Marseille, France. [2]Service de Médecine Interne et Thérapeutique, Hôpital de la Timone, Assistance Publique-Hôpitaux de Marseille, Marseille, France. [3]Service d'Anesthésie et Réanimation polyvalente, Hôpital Nord, Assistance Publique-Hôpitaux de Marseille, Marseille, France.

Received: 24 December 2017 Accepted: 23 July 2018
Published online: 31 July 2018

References

1. Singer M, Deutschman CS, Seymour CW, Shankar-Hari M, Annane D, Bauer M, Bellomo R, Bernard GR, Chiche JD, Coopersmith CM, Hotchkiss RS, Levy MM, Marshall JC, Martin GS, Opal SM, Rubenfeld GD, van der Poll T, Vincent JL, Angus DC. The Third International Consensus Definitions for Sepsis and Septic Shock (Sepsis-3). JAMA. 2016;315:801–10.
2. Annane D, Aegerter P, Jars-Guincestre MC, Guidet B. Current epidemiology of septic shock: the CUB-Rea network. Am J Respir Crit Care Med. 2003;168:165–72.
3. Cohen J, Brun-Buisson C, Torres A, Jorgensen J. Diagnosis of infection in sepsis: an evidence-based review. Crit Care Med. 2004;32:S466–94.

4. Dellinger RP, Levy MM, Rhodes A, Annane D, Gerlach H, Opal SM, Sevransky JE, Sprung CL, Douglas IS, Jaeschke R, Osborn TM, Nunnally ME, Townsend SR, Reinhart K, Kleinpell RM, Angus DC, Deutschman CS, Machado FR, Rubenfeld GD, Webb S, Beale RJ, Vincent JL, Moreno R, Surviving Sepsis Campaign Guidelines Committee including The Pediatric Subgroup. Surviving Sepsis Campaign: international guidelines for management of severe sepsis and septic shock, 2012. Intensive Care Med. 2013;39:165–228.
5. Adrie C, Alberti C, Chaix-Couturier C, Azoulay E, De Lassence A, Cohen Y, Meshaka P, Cheval C, Thuong M, Troché G, Garrouste-Orgeas M, Timsit JF. Epidemiology and economic evaluation of severe sepsis in France: age, severity, infection site, and place of acquisition (community, hospital, or intensive care unit) as determinants of workload and cost. J Crit Care. 2005;20:46–58.
6. Levy MM, Fink MP, Marshall JC, Abraham E, Angus D, Cook D, Cohen J, Opal SM, Vincent JL, Ramsay G. 2001 SCCM/ESICM/ACCP/ATS/SIS international Sepsis definitions conference. Crit Care Med. 2003;3: 1250–6.
7. Birmingham MC, Hassett JM, Schentag JJ, Paladino JA. Assessing antibacterial pharmacoeconomics in the intensive care unit. Pharmacoeconomics. 1997;12:637–47.
8. Rivers E, Nguyen B, Havstad S, Ressler J, Muzzin A, Knoblich B, Peterson E, Tomlanovich M, Early Goal-Directed Therapy Collaborative Group. Early goal-directed therapy in the treatment of severe sepsis and septic shock. N Engl J Med. 2001;345:1368–77.
9. Dellinger RP. The Surviving Sepsis Campaign: where have we been and where are we going? Cleve Clin J Med. 2015;82:237–44.
10. Bochud PY, Bonten M, Marchetti O, Calandra T. Antimicrobial therapy for patients with severe sepsis and septic shock: an evidence-based review. Crit Care Med. 2004;32:S495–512.
11. Tang BM, Eslick GD, Craig JC, McLean AS. Accuracy of procalcitonin for sepsis diagnosis in critically ill patients: systematic review and meta-analysis. Lancet Infect Dis. 2007;7:210–7.
12. Adib-Conquy M, Monchi M, Goulenok C, Laurent I, Thuong M, Cavaillon JM, Adrie C. Increased plasma levels of soluble triggering receptor expressed on myeloid cells 1 and procalcitonin after cardiac surgery and cardiac arrest without infection. Shock. 2007;28:406–10.
13. Bozza FA, Salluh JI, Japiassu AM, Soares M, Assis EF, Gomes RN, et al. Cytokine profiles as markers of disease severity in sepsis: a multiplex analysis. Crit Care. 2007;11:R49.
14. Drancourt M. Detection of microorganisms in blood specimens using matrix-assisted laser desorption ionization time-of-flight mass spectrometry: a review. Clin Microbiol Infect. 2010;16:1620–5.
15. Ferreira L, Sánchez-Juanes F, González-Avila M, Cembrero-Fuciños D, Herrero-Hernández A, González-Buitrago JM, Muñoz-Bellido JL. Direct identification of urinary tract pathogens from urine samples by matrix-assisted laser desorption ionization-time of flight mass spectrometry. J Clin Microbiol. 2010;48:2110–5.
16. Singhal N, Kumar M, Kanaujia PK, Virdi JS. MALDI-TOF mass spectrometry: an emerging technology for microbial identification and diagnosis. Front Microbiol. 2015;6:791.
17. Ouedraogo R, Flaudrops C, Ben Amara A, Capo C, Raoult D, Mege JL. Global analysis of circulating immune cells by matrix-assisted laser desorption ionization time-of-flight mass spectrometry. PLoS One. 2010;27(5):e13691.
18. Buchanan CM, Malik AS, Cooper GJ. Direct visualisation of peptide hormones in cultured pancreatic islet alpha- and beta-cells by intact-cell mass spectrometry. Rapid Commun Mass Spectrom. 2007;21:3452–8.
19. Munteanu B, von Reitzenstein C, Hänsch GM, Meyer B, Hopf C. Sensitive, robust and automated protein analysis of cell differentiation and of primary human blood cells by intact cell MALDI mass spectrometry biotyping. Anal Bioanal Chem. 2012;8:2277–86.
20. Ouedraogo R, Daumas A, Ghigo E, Capo C, Mege JL, Textoris J. Whole-cell MALDI-TOF MS: a new tool to assess the multifaceted activation of macrophages. J Proteome. 2012;75:5523–32.
21. Portevin D, Pflüger V, Otieno P, Brunisholz R, Vogel G, Daubenberger C. Quantitative whole-cell MALDI-TOF MS fingerprints distinguishes human monocyte sub-populations activated by distinct microbial ligands. BMC Biotechnol. 2015;15:24.
22. Mehraj V, Textoris J, Ben Amara A, Ghigo E, Raoult D, Capo C, Mege JL. Monocyte responses in the context of Q fever: from a static polarized model to a kinetic model of activation. J Infect Dis. 2013;208:942–51.
23. Ouedraogo R, Daumas A, Capo C, Mege JL, Textoris J. Whole-cell MALDI-TOF mass spectrometry is an accurate and rapid method to analyze different modes of macrophage activation. J Vis Exp. 2013;26:50926.
24. Biteker FS, Çaylak SD, Sözen H. Biomarkers in sepsis. Am J Emerg Med. 2016; 34:924-5.
25. Biron BM, Ayala A, Lomas-Neira JL. Biomarkers for Sepsis: what is and what might be? Biomark Insights. 2015;10:7–17.
26. Markwart R, Condotta SA, Requardt RP, Borken F, Schubert K, Weigel C, Bauer M, Griffith TS, Förster M, Brunkhorst FM, Badovinac VP, Rubio I. Immunosuppression after sepsis: systemic inflammation and sepsis induce a loss of naïve T-cells but no enduring cell-autonomous defects in T-cell function. PLoS One. 2014;9:e115094.
27. Engel MF, Paling FP, Hoepelman AI, van der Meer V, Oosterheert JJ. Evaluating the evidence for the implementation of C-reactive protein measurement in adult patients with suspected lower respiratory tract infection in primary care: a systematic review. Fam Pract. 2012;29:383–93.
28. Hotchkiss RS, Karl IE. The pathophysiology and treatment of sepsis. N Engl J Med. 2003;348:138–50.
29. Peng Q, O'Loughin JL, Humphrey MB. DOK 3 negatively regulates LPS responses and endotoxin tolerance. PLoS One. 2012;7:e39967.

Figure S1

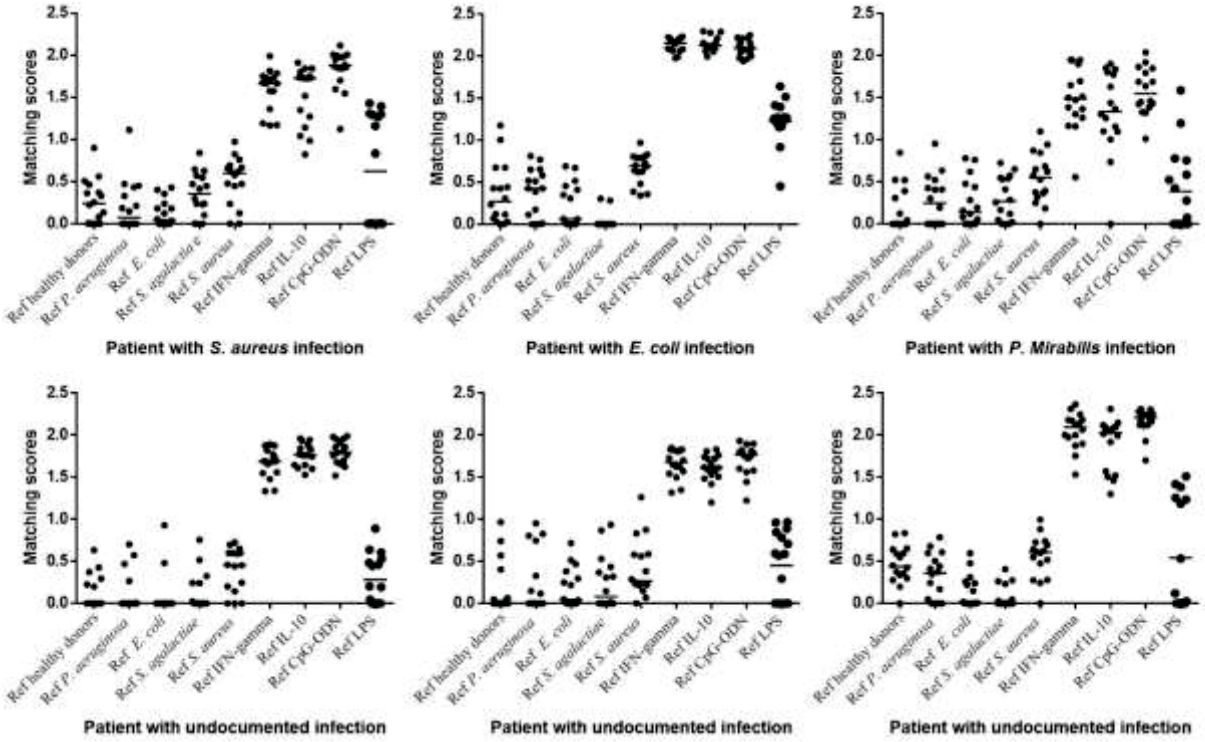
Matching scores
2.5
2.0
1.5
1.0
0.5
0.0
Ref healthy donors
Ref P. aeruginosa
Ref E. coli
Ref S. agalactiae
Ref S. aureus
Ref IFN-gamma
Ref IL-10
Ref CpG-ODN
Ref LPS
Patient with S. aureus infection
Patient with E. coli infection
Patient with P. Mirabilis infection
Patient with undocumented infection
Patient with undocumented infection
Patient with undocumented infection

Granulomatous response to Coxiella burnetii, the agent of Q fever: the lessons from gene expression analysis

Faugaret D, Ben Amara A, Alingrin J, **Daumas A**, Delaby A, Lépolard C, Raoult D, Textoris J, Mège JL.

Front Cell Infect Microbiol. 2014 Dec 15;4:172.

doi: 10.3389/fcimb.2014.00172. eCollection 2014.

Le granulome est le résultat d'une coopération intense entre les cellules de la réponse innée et adaptative dans le but d'éliminer des agents infectieux plutôt rebelles. La formation de granulomes constitue la signature histologique de diverses pathologies infectieuses, telles que la fièvre Q et la tuberculose.

La fièvre Q est une zoonose causée par une bactérie intracellulaire, *Coxiella burnetti,* transmise par voie respiratoire et plus rarement par voie digestive ou piqûre de tiques. Elle n'est symptomatique que dans 10 % des cas : c'est la fièvre Q aiguë. Elle est alors responsable de syndrome pseudo-grippal, de pneumopathie atypique et d'hépatite aiguë [125,126]. Dans la majorité des cas, la maladie est spontanément résolutive. Sur le plan anatomopathologique, on retrouve des granulomes inflammatoires centrés par une vacuole lipidique réalisant la classique « image en beignet » [127]. Dans 5 % des cas environ, la bactérie n'est pas contrôlée par le système immunitaire et va persister, principalement au niveau des valves cardiaques, des prothèses ou anévrismes vasculaires, mais aussi de façon plus rare au niveau pulmonaire, utérin, ostéoarticulaire ou ganglionnaire [125,126]. Une caractéristique commune de ces infections persistantes est leur évolution lente sur plusieurs mois à années et le plus souvent de façon asymptomatique. L'immunodépression favorise ces infections persistantes. La fièvre Q chronique est caractérisée par l'absence de granulome et la présence d'infiltrats leucocytaires bordant des zones de nécrose [128].

La tuberculose, qui demeure la 3ème cause infectieuse de mortalité dans le monde, touche principalement les populations des pays en voie de développement où vivant dans la précarité. Elle est due à *Mycobacterium tuberculosis*, un bacille aérobie transmis par voie respiratoire.

L'histoire naturelle de la maladie comprend 3 étapes : contamination, tuberculose-infection, tuberculose-maladie. La primo-infection tuberculeuse ou tuberculose-infection se manifeste par le développement d'une réponse immunologique plus ou moins intense vis à vis du bacille tuberculeux avec la formation de granulomes « tuberculeux » caractérisés par la présence de nécrose caséeuse [106, 120]. Le développement des granulomes est asymptomatique (aucun signe clinique et radiologique). La seule manifestation est le virage des réactions cutanées à la tuberculine (après intradermo-réaction ou la positivité des tests IGRA (Quantiféron® et TspotTB® qui explorent la production d'IFN-γ de l'individu en réponse à des antigènes spécifiques de *Mycobacterium tuberculosis*). Dans 90 % des cas, l'infection est maîtrisée par la réaction immunitaire de l'individu. Certains granulomes peuvent persister des années, voire même toute la vie, ils sont souvent calcifiés et ainsi visibles radiologiquement. Les bacilles dans ces foyers persistent mais ne se multiplient pas activement. Ils ont un métabolisme ralenti (bacilles dormants). On parle d'infection tuberculeuse latente. Dans les 10 % de cas restant (quantité abondante de la bactérie, enfant ou état d'immunodépression), l'infection n'est pas maitrisée et le bacille continue de se multiplier évoluant vers la tuberculose-maladie symptomatique à la fois sur le plan clinique et radiologique. Une tuberculose-maladie peut aussi survenir à distance de la tuberculose-infection. Il s'agit de réactivations soit en lien avec le vieillissement, soit dans un contexte d'immunodépression [129].

Afin d'explorer la réponse immunitaire granulomateuse à *Coxiella burnetti* et *Mycobacterium bovis* (BCG), l'évaluation *in vitro* de la formation des granulomes représente une approche globale simple. J'ai pu participer à l'étude de D. Faugaret sur l'analyse du transcriptome des cellules des granulomes formés en réponse à *Coxiella burnetti* et *Mycobacterium bovis* (BCG). Il a été mis en évidence qu'environ 60% des gènes modulés étaient communs aux granulomes induits par ces 2 agents pathogènes. Un quart des gènes était spécifiquement lié à la réponse à *Coxiella burnetti* et 14% à la réponse à *Mycoplasma bovis* (BCG).

Parmi les gènes modulés de façon similaire, on retient des gènes impliqués dans le recrutement des cellules mononuclées confirmant le rôle majeur des chémokines notamment CLL2 et CLL5 qui inhibées empêchent la formation des granulomes. Cependant le rôle de CLL2 semble prédominant puisque le blocage de CCR5 n'affecte pas par contre leur formation. Une signature transcriptionnelle de 206 gènes dont l'expression est modulée entre les granulomes à *Coxiella burnetti* et *Mycobacterium bovis* (BCG) a été étudiée. Parmi ces gènes, on retrouve des gènes impliqués dans la reconnaissance des pathogènes, la réponse inflammatoire et anti-

inflammatoire, l'activité microbicide mais aussi la mort cellulaire. Ainsi, de nombreux gènes de l'inflammation sont down-régulés avec *Coxiella burnetti* et up-régulés avec BCG. Une modulation inverse est retrouvée pour les gènes de la réponse anti-inflammatoire. Cependant, on observe aussi une surexpression de gènes codant pour des médiateurs de l'inflammation avec *Coxiella burnetti* comme *EPHB2*. L'expression des gènes impliqués dans la microbicidie est augmentée en réponse à *Coxiella burnetti* avec notamment des gènes de la réponse à l'IFN type I ou ISGs (rencontrés dans la réponse antivirale mais aussi en réponse à des bactéries ou composants bactériens comme le LPS), et diminuée pour BCG. En effet, l'expression d'*IFIT1 et d'OAS2* est significativement augmentée dans les cellules des granulomes induits par *Coxiella burnetti* par rapport à BCG. Enfin, *Coxiella burnetti* diminue l'expression de gènes impliqués dans la mort cellulaire alors qu'ils sont surexprimés avec BCG. Ainsi, *FASLG* et *GNLY* sont significativement surexprimés dans les cellules des granulomes induits par BCG par rapport à *Coxiella burnetti.*

Enfin, les macrophages représentant environ 40% des cellules constituant les granulomes, on s'est intéressé à leur polarisation au sein des granulomes à travers l'étude de la modulation des gènes activés lors de la stimulation des macrophages par l'IFN-γ (9 gènes M1) ou par l'IL-4 et l'IL-10 (9 gènes M2) sélectionnées à partir de données publiques. Des macrophages stimulés par ces cytokines ont été pris pour contrôles. Cette analyse a montré que les cellules des granulomes expriment un profil plutôt M1 correspondant à un phénotype inflammatoire et microbicide concordant avec les taux élevés de TNF et IFN-γ mesurés dans les surnageants.

Cette analyse du transcriptome des cellules des granulomes semble dans la fièvre Q correspondre à l'évolution naturelle de la maladie qui est l'élimination de *Coxiella burnetti* et la guérison alors que l'absence de formation de granulomes est retrouvée dans les formes chroniques de la maladie.

frontiers in
CELLULAR AND INFECTION MICROBIOLOGY

ORIGINAL RESEARCH ARTICLE
published: 15 December 2014
doi: 10.3389/fcimb.2014.00172

Granulomatous response to *Coxiella burnetii*, the agent of Q fever: the lessons from gene expression analysis

Delphine Faugaret[1,2], Amira Ben Amara[1], Julie Alingrin[1], Aurélie Daumas[1], Amélie Delaby[1,3], Catherine Lépolard[1], Didier Raoult[1], Julien Textoris[1,4] and Jean-Louis Mège[1]*

[1] *Aix Marseille Université, URMITE, UMR CNRS 7278, IRD 198, INSERM 1095, Marseille, France*
[2] *AltraBio SAS, Lyon, France*
[3] *Centre d'Immunologie de Marseille-Luminy, Parc Scientifique et Technologique, Marseille, France*
[4] *Unité Mixte BioMérieux-HCL, Hôpital Edouard Herriot - Pav P, Lyon, France*

Edited by:
Benjamin Coiffard, Hôpital Nord, France

Reviewed by:
Janakiram Seshu, The University of Texas at San Antonio, USA
Subramanian Dhandayuthapani, Texas Tech Health Sciences Center, USA

***Correspondence:**
Jean-Louis Mège, Aix Marseille Université, URMITE, UMR CNRS 7278, IRD 198, INSERM 1095, 27 Bld. Jean Moulin, 13005 Marseille, France
e-mail: jean-louis.mege@univ-amu.fr

The formation of granulomas is associated with the resolution of Q fever, a zoonosis due to *Coxiella burnetii*; however the molecular mechanisms of granuloma formation remain poorly understood. We generated human granulomas with peripheral blood mononuclear cells (PBMCs) and beads coated with *C. burnetii*, using BCG extracts as controls. A microarray analysis showed dramatic changes in gene expression in granuloma cells of which more than 50% were commonly modulated genes in response to *C. burnetii* and BCG. They included M1-related genes and genes related to chemotaxis. The inhibition of the chemokines, CCL2 and CCL5, directly interfered with granuloma formation. *C. burnetii* granulomas also expressed a specific transcriptional profile that was essentially enriched in genes associated with type I interferon response. Our results showed that granuloma formation is associated with a core of transcriptional response based on inflammatory genes. The specific granulomatous response to *C. burnetii* is characterized by the activation of type 1 interferon pathway.

Keywords: granuloma, Q fever, *Coxiella burnetii*, BCG, transcriptome, type 1 interferon pathway

INTRODUCTION

Q fever is a worldwide zoonosis caused by *Coxiella burnetii* (Mege et al., 1997). The primary *C. burnetii* infection leads to isolated fever, pneumonia, or hepatitis in 40% of exposed individuals. *C. burnetii* infection may become chronic in patients with valvular lesions, pregnant women, or immuno-compromised patients. In contrast with acute Q fever where the outcome is usually favorable, chronic Q fever is characterized by a long-term drug treatment and persistent risk of relapses. Interestingly, tissue granulomas are present in patients with acute Q fever. In chronic Q fever, granulomas are absent, replaced by lymphocyte infiltrates (Raoult et al., 2005), suggesting that granulomas play an important role in the resolution of Q fever.

Granulomas, defined as tissue collections of macrophages, are generated in response to various microorganisms (Zumla and James, 1996). Their organization varies according to the type of microorganism. In humans, *C. burnetii*-induced granulomas, which are paucibacillary, are composed of a lipid vacuole surrounded by a fibrinoid ring, the "doughnut granuloma" (Srigley et al., 1985; Travis et al., 1986). In contrast, tuberculous granulomas, which are multibacillary, consist of a necrotic core containing bacilli, enclosed by macrophages and surrounded by lymphocytes (Ulrichs and Kaufmann, 2006).

Granulomas are not static organizations but are characterized by continual remodeling and interactions between cell partners (Ramakrishnan, 2012; Shaler et al., 2013). After initial uptake of microorganisms by resident macrophages, the granuloma formation is initiated by recruiting macrophages and blood-derived myeloid cells. The recruitment of activated T-cells by these nascent granulomas completes granuloma formation, and renders them functional (Egen et al., 2008). The main function of granulomas is to contain infectious agents within a limited area, thus restricting the spread of pathogens. Once the infection is contained, the granuloma cells participate in the destruction of infectious agents. Indeed, wild type mice clear mycobacterial infection through granuloma formation whereas mycobacteria disseminate and granulomas are absent in mice that do not express interferon-γ (Cooper et al., 1993). In the majority of patients with tuberculosis, the presence of calcified granulomatous lesions is associated with a controlled infection (Ulrichs and Kaufmann, 2006). However, in others, mycobacteria induce the necrosis of infected macrophages, resulting in a caseum at the center of granulomas. This accumulation of caseum leads to collapsing granulomas and the spread of bacteria (Russell et al., 2009).

Studying granuloma formation in mice requires invasive methods that are not appropriate for human studies. A method was recently developed to generate human granulomas *in vitro* using peripheral blood mononuclear cells (PBMCs) co-cultured with beads coated with BCG (Puissegur et al., 2004; Delaby et al., 2010) or *C. burnetii* extracts (Delaby et al., 2010). This method enables to follow the initial events of granuloma formation and to investigate the molecular mechanisms of granulomas (Egen et al., 2008; Delaby et al., 2012). In this study, we used a

high throughput transcriptomic approach to characterize human granulomas induced *in vitro* by *C. burnetii* and to compare them with those induced by BCG. We found that numerous modulated genes were shared by *C. burnetii*- and BCG-induced granulomas, including chemotaxis-associated genes and M1 genes. *C. burnetii* induced a specific repertoire of upmodulated and downmodulated genes that included the activation of interferon-stimulated genes (ISGs), which confers a new role for this pathway in host response to *C. burnetii*.

MATERIALS AND METHODS

PATIENTS WITH Q FEVER

The study was approved by the Ethics Committee of the Aix-Marseille University. Written informed consent was obtained from each subject. Four patients with acute Q fever and 5 patients with Q fever endocarditis were selected. The diagnostic of acute Q fever was based on serological determination of anti-phase II *C. burnetii* antibodies (Abs). The suspicion of Q fever endocarditis was based on standardized questionnaire that included pathological evidence of endocarditis, positive echocardiograms, positive blood cultures, high titers of IgG specific for phase I *C. burnetii* (Raoult, 2012). The average age of patients with acute Q fever was 43 years old (ranging from 30 to 57 years old). The average age of patients with Q fever endocarditis was 54 years old (ranging from 40 to 74 years old). Six healthy individuals (with a mean age of 37 years, ranging from 28 to 56 years old) were used as controls.

PREPARATION OF CIRCULATING CELLS

PBMCs were prepared from leukopacks (Etablissement Français du Sang) or blood collected in ethylene-diamine-tetraacetic acid (EDTA) tubes from donors and patients after centrifugation through a Ficoll density cushion. Monocytes were isolated from PBMCs by CD14 positive selection using magnetic beads coated with anti-CD14 antibodies (Miltenyi Biotec). $CD14^+$ monocytes were differentiated into macrophages by cell culture (Ghigo et al., 2010). To obtain M1 macrophages, macrophages were stimulated with 20 ng/mL recombinant human IFN-γ (Tebu-bio) for 18 h. M2 macrophages were obtained by incubating macrophages with 10 ng/mL IL-10 or 20 ng/mL IL-4 (R&D Systems) for 18 h.

IN VITRO GENERATION OF GRANULOMAS

Granulomas were induced by using two procedures. First, sepharose beads were coated with bacterial extracts from phase I *C. burnetii* or BCG as previously described (Delaby et al., 2010). PBMCs recovered from leukopacks (2×10^6 per assay) were cultured with 800 coated beads for 8–12 days in the presence of mAbs against CCL2 and CCL5 or control isotypes (R&D Systems). Individual granulomas were then collected by micromanipulation and incubated in 2 mM EDTA, allowing cells to dissociate (Delaby et al., 2012). Second, the granuloma formation in patients with Q fever and healthy donors was determined by incubating PBMCs with *C. burnetii* (Puissegur et al., 2004). PBMCs (2×10^6 cells per assay) were cultured with 2×10^7 heat-killed bacteria (100°C, 1 h) in RPMI 1640 supplemented with fetal calf serum, L-glutamine and antibiotics in 6-well culture plates at 37°C. Cell aggregation was observed every 2 days under light microscopy, and cells were recovered after 8–10 days when the size of aggregates was the highest.

RNA EXTRACTION AND MICROARRAY

Total RNA was extracted from granuloma cells using the RNeasy Mini kit (Qiagen) and DNAse treatment. The granuloma cell gene expression was analyzed using 45,000 probes microarray chips (4×44K whole human genome G4112F, Agilent Technologies) and One-color Microarray Based Gene Expression Analysis kit, as previously described (Ben Amara et al., 2010). Three samples per experimental conditions were included in the analysis. Following array scans, image analysis and correction of intra-array signals were performed with Feature Extraction Software A.10.5.1.1 (Agilent Technologies) using default parameters. Minimum Information About a Microarray Experiment-compliant data are provided in the Gene Expression Omnibus (GEO) (Moal et al., 2013) at the National Center for Biotechnology Information (http://www.ncbi.nlm.nih.gov/geo/), and can be accessed with the GEO series accession number (GSE37666).

MICROARRAY ANALYSIS

Raw signal data were normalized with a False Discovery Rate below 0.1 and an absolute fold change (FC) value of 3.0. All analyses were performed using R software (version 3) with the bioconductor libraries (Gentleman et al., 2004). Functional annotation was performed using ClueGO plug-in (Bindea et al., 2009) and selecting terms belonging to GO Biological (Moal et al., 2013) in Cytoscape software (Smoot et al., 2011). An enrichment/depletion test, along with the Benjamin-Hochberg correction method, was performed for statistic analysis. GO terms from levels 6 to 8 in GO tree were selected, with a kappa score above 0.44, to create functional annotation network. Each node represents a GO term and contains at least 3 genes. The leading group term of a functional group was defined as the group containing the largest number of genes. Identification of biological groups depicted in the pie chart was established by manual selection of articles from Pubmed database, filtered to show those describing gene functions in immune cells. The identification of M1 and M2 signatures in granuloma cells was performed using the gene profiles of macrophages stimulated with IL-4, IL-10, and IFN-γ referenced in Gene Expression Omnibus database (GSE36537).

REAL-TIME QUANTITATIVE RT-PCR (qRT-PCR)

Reverse transcription of 100 ng of total RNA was performed as previously described (Ben Amara et al., 2010). Primers were designs using Primer3 (Moal et al., 2013) and their sequences were listed in Table 1. Quantitative PCR was performed with Light Cycler Fast Start DNA master^{PLUS} SYBR Green I (Roche applied Science). The results were normalized with the housekeeping gene β-actin. The FC of target genes relative to β-actin was computed using the formula $FC = 2^{-\Delta\Delta Ct}$, where $\Delta\Delta Ct = [(Ct_{Target} - Ct_{Actin})_{stimulated} - (Ct_{Target} - Ct_{Actin})_{unstimulated}]$ (Moal et al., 2013). The agreement between qRT-PCR and microarray data was assessed by Pearson correlation coefficient.

STATISTICAL ANALYSIS

Comparisons between two groups were performed using the Mann-Whitney *U*-test.

RESULTS

GLOBAL GENE PROGRAM OF GRANULOMA CELLS

We previously reported that PBMCs are capable to form granulomas when they are incubated with beads coated with bacterial extracts (Delaby et al., 2012). We wondered if granuloma formation was associated with specific changes in gene expression programs. We compared the transcriptional profiles of granuloma cells with that of naïve PBMCs using whole genome microarrays. Correspondence analysis was conducted to assess the reproducibility of data. The first axis of variance showed large differences between PBMCs and granuloma cells, while the second axis of variance revealed smaller differences between granuloma cells generated in response to *C. burnetii* and BCG (**Figure 1A**). Hierarchical clustering also showed that the transcriptional responses of granuloma cells were different from that of PBMCs (**Figure 1B**). Most probes that were upmodulated (1337) and downmodulated (1183) were common in *C. burnetii* and BCG challenges. The probes that were specifically modulated by *C. burnetii* included 524 upmodulated probes and 530 downmodulated probes. Conversely, 345 and 247 probes were upmodulated and downmodulated, respectively, by BCG. The expression of only one probe, the *CD163* gene, increased after *C. burnetii* challenge but decreased after BCG challenge (**Figure 1C**). These data showed that about 60% of modulated genes were shared by granuloma cells but that the granulomatous responses to *C. burnetii* and BCG were, in part, specific.

M1/M2 POLARIZATION OF GRANULOMA CELLS

The macrophages are known to be polarized into M1 or M2 cells, which is associated with microbicidal response or permissive response for intracellular bacteria respectively (Benoit et al., 2008). We wondered whether granuloma macrophages, which represent about 40% of granuloma cells (Delaby et al., 2012), were polarized. Nine M1- and 9 M2-related genes (corresponding to 12 and 17 probes, respectively) were selected according to published data (Martinez et al., 2006). Hierarchical clustering analysis showed that granuloma cells clustered with IFN-γ-stimulated macrophages (M1 macrophages) but not with IL-4- or IL-10-stimulated macrophages (M2 macrophages) (**Figure 2A**), demonstrating that granuloma cells exhibited inflammatory/microbicidal phenotype. This finding was confirmed by the measurement of inflammatory cytokines, TNF and IFN-γ, which were released after 9 days (IFN-γ: 204 ± 53 pg/ml; TNF: 1250 ± 250 pg/ml). However, the granulomatous responses to *C. burnetii* and BCG included some features of M2 macrophages. Indeed, *C. burnetii* upmodulated the expression of *CCL23* and *CCL13* genes, and BCG that of *FN1* and *SLCA47* genes. Other differences were evident: *C. burnetii* caused a slight increase in the expression of *TNF* and *EDN1* genes, but increased greatly the expression of *HESX1* and *CXCL9* genes, in comparison with BCG. To confirm microarray results, qRT-PCR was performed on M1 genes (**Figure 2B**). The profiles of each gene were significantly correlated in qRT-PCR and microarray ($R^2 = 0.64$, $p < 0.008$). In addition, the expression of *HESX1* and *TNFSF10* genes was greater in *C. burnetii*-induced granulomas than in BCG-induced granulomas. Conversely, BCG induced a higher increase in the expression of *IDO1* and *TNF* genes

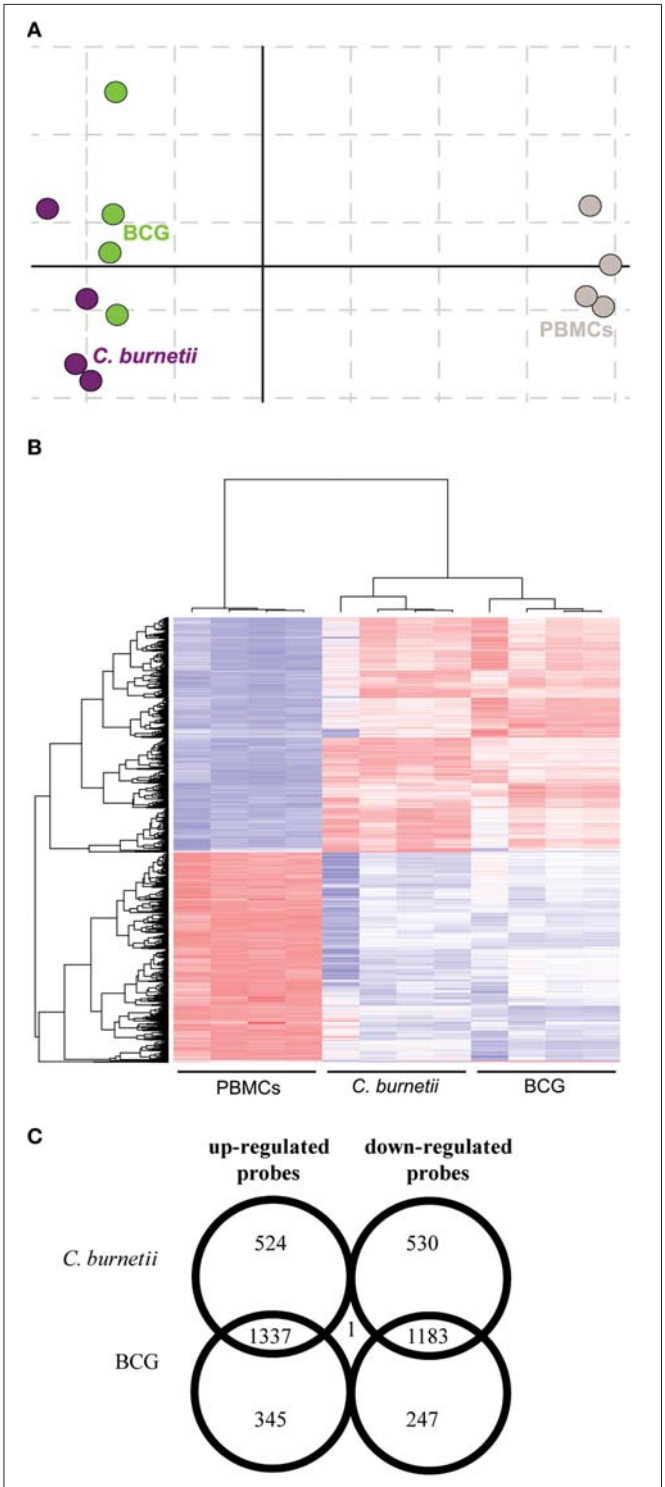

FIGURE 1 | Transcriptional responses of granuloma cells. Granuloma cells and PBMCs were analyzed by microarray. **(A)** The correspondence analysis of the probeset signature revealed that *C. burnetii* and BCG-induced granulomas were clearly separated from PBMCs. **(B)** The hierarchical clustering analysis showed specific clusters of upmodulated and downmodulated probes in granuloma cells compared to PBMCs. Gene expression level is color-coded from blue (downregulation) to red (upregulation). **(C)** The Venn diagram represents the expression of

(Continued)

FIGURE 1 | Continued
upmodulated and downmodulated probes in *C. burnetii* and BCG granuloma compared with PBMCs. The numbers in overlapping regions indicate the number of probes commonly modulated in granuloma cells obtained in response to *C. burnetii* and BCG. The numbers in non-overlapping regions indicate the number of probes specifically modulated in response to *C. burnetii* or BCG.

than *C. burnetii*. Taken together, these results suggest that granuloma macrophages were rather polarized into M1 macrophages, with subtle differences between *C. burnetii*- and BCG-induced granulomas.

FUNCTIONAL ANNOTATION OF *C. BURNETII*-SPECIFIC TRANSCRIPTIONAL PROGRAM

The gene expression program specifically induced by *C. burnetii* was analyzed by retaining only genes differentially modulated between *C. burnetii* and BCG (absolute $FC > 3.0$). We found that 206 genes were specifically modulated, and their roles were studied using GO Biological Process annotation and according to immune function. Nearly 50% of them were related to inflammatory mediators (17%), microbicidal activity (12%), anti-inflammatory mediators (9%) and pathogen recognition (8%). Other cell functions, such as chemotaxis, cell death, and metabolism were also differentially modulated (**Figure 3A**). Taken together, the genes that were specifically modulated by *C. burnetii* were organized into functional networks, suggesting a role in granuloma function.

Next, we investigated how these 206 genes were differently modulated in response to BCG or *C. burnetii* relative to PBMCs. A number of genes involved in chemotaxis were similarly modulated in granuloma cells in response to BCG or *C. burnetii* (**Figure S1**). The genes involved in chemotaxis play a critical role in granuloma formation. This is illustrated by the inhibition of granuloma formation when *C. burnetii*-coated beads were incubated with PBMCs in the presence of mAb directed against CLL2 and CCL5 but not with control isotypes. The mAb directed against CCR5 did not affect granuloma formation (**Figure 3B**). The functional groups associated with inflammation were differently modulated in granulomas induced by *C. burnetii* or BCG. Many genes related to inflammation were downmodulated by *C. burnetii* and upmodulated by BCG. The genes belonging to anti-inflammatory mediators were weakly upmodulated in response to *C. burnetii* but were strongly downmodulated by BCG. Nevertheless, *C. burnetii*-induced granulomas were not only characterized by anti-inflammatory program; indeed, *C. burnetii* did induce several genes related to inflammation such as *TNFSF13*, *CH25H*, and *IRF7* genes. The expression of genes related to cell death was also decreased in *C. burnetii*-generated granulomas, but increased in BCG-induced granulomas. Finally, *C. burnetii* strongly upmodulated the expression of genes involved in microbicidal response and, especially, ISGs including *MX1*, *MX2*, *IFI44*, *IFI6*, *IFIT1*, *IFITM2*, *IFITM3*, *ISG15*, *OAS1*, *OAS2*, *OAS3*, and *HERC5* genes, whereas BCG had little effect on these genes. The transcriptional differences between granulomas induced by *C. burnetii* and BCG compared with PBMCs were confirmed by qRT-PCR performed on several genes. Indeed, the expression of genes encoding inflammatory mediators such as *EPHB2* gene and *EDN1* gene was highly increased in response to *C. burnetii* and BCG, respectively. The expression of genes involved in cell death, such as *FASLG* and *GNLY*, was increased

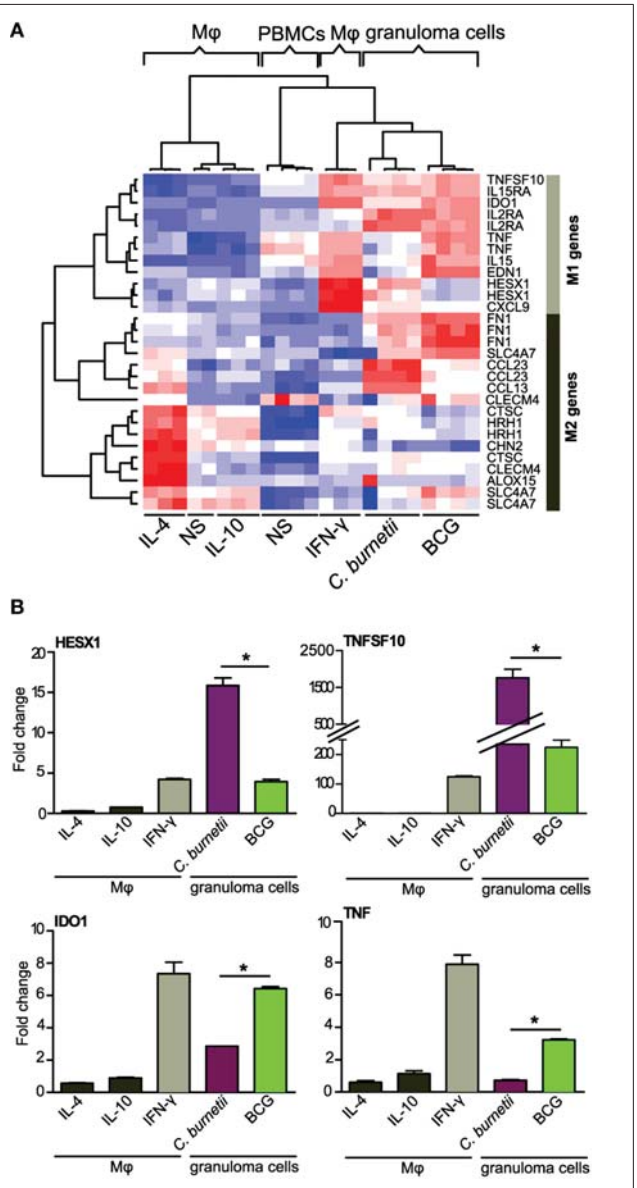

FIGURE 2 | Atypical M1 polarization of granuloma cells. The M1/M2 polarization of granuloma cells was studied using macrophages stimulated with IFN-γ (M1), IL-10, IL-4 (M2) as controls of M1 and M2 polarization. Microarrays **(A)** and qRT-PCR **(B)** were performed on M1/M2 macrophages and granuloma cells. **(A)** The hierarchical clustering of specific markers of M1 or M2 polarization indicates that granuloma cells induced by *C. burnetii* and BCG were located within a unique cluster near M1 macrophages. Note that M2 genes were modulated in granuloma cells as well. Gene expression level is color-coded from blue (downregulation) to red (upregulation). **(B)** The expression of *HESX1, TNFSF10, IDO1,* and *TNF* (M1 genes) was increased in *C. burnetii*- and BCG-induced granulomas, but their expression was differentially modulated in both types of granulomas. $^*p < 0.05$ for the comparison between *C. burnetii* and BCG using Mann-Whitney *U*-test. Mφ, Macrophages; NS, unstimulated.

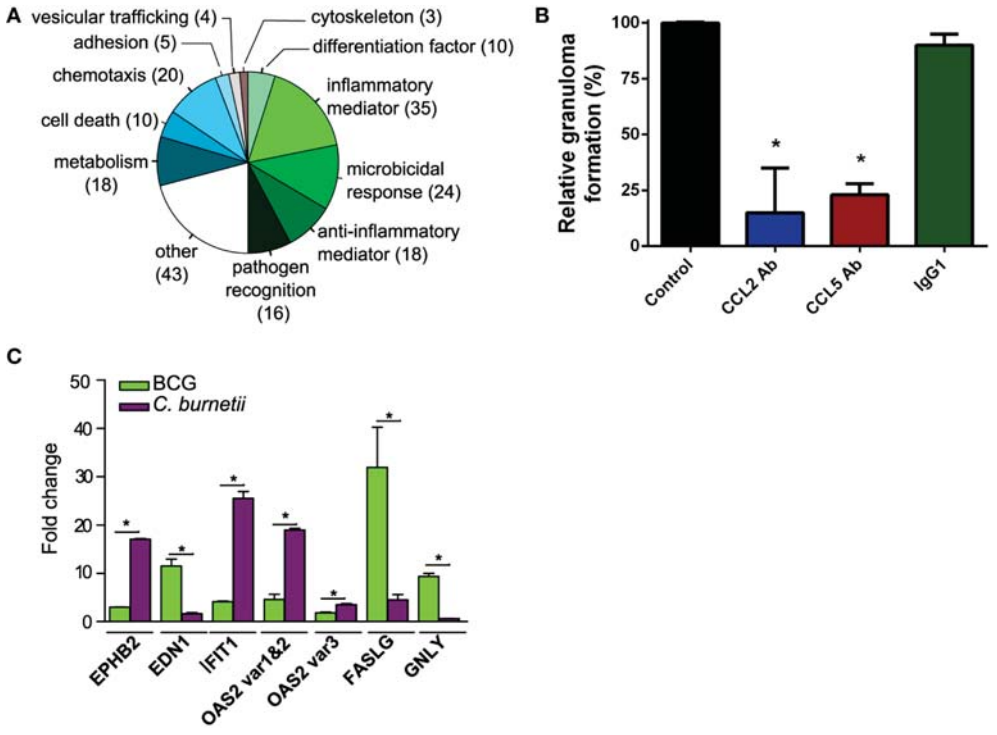

FIGURE 3 | Genes related to immune response in granuloma cells. (A) The genes that were modulated in granulomas induced by *C. burnetii* compared with BCG-induced granulomas were manually classified according to functions previously reported in immune response. The pie chart represents the distribution of modulated genes in each biological group. **(B)** PBMCs were incubated with *C. burnetii*-coated beads in the presence of CCL2 Ab, CCL5 Ab, and IgG1 or in their absence (Control) and the formation of granulomas was measured. Results were expressed as relative granuloma formation. $*p < 0.05$ for the comparison of conditions with and without antibodies. **(C)** The expression of *EPHB2, EDN1, IFIT1, OAS2, FASLG,* and *GNLY* genes in granuloma cells was confirmed by qRT-PCR. $*p < 0.05$ for the comparison between *C. burnetii* and BCG using Mann-Whitney *U*-test.

in response to BCG. In contrast, the expression of ISGs (*IFIT1* and *OAS2*) was highly upmodulated in granulomas induced by *C. burnetii* (**Figure 3C**). Taken together, these results showed that the granulomatous response shared common features, but also included specific characteristics, according to the nature of the pathogen. They also showed that the granulomas induced by *C. burnetii* were characterized by the activation of type 1 IFN genes.

TRANSCRIPTIONAL RESPONSE OF GRANULOMAS IN Q FEVER PATIENTS

We finally inquired whether the granulomatous response of patients with Q fever was associated with alteration in type 1 IFN pathway. First, we developed a simple method to obtain granulomas by incubating control PBMCs with *C. burnetii* to simplify the recovery of isolated granulomas using *C. burnetii*-coated beads. Cell aggregates were observed after a few days. Their size progressively increased and was greatest at 8–10 days, demonstrating that the time course of granuloma formation was similar when granulomas were generated *in vitro* using beads coated with bacterial extracts (Delaby et al., 2012) or heat-killed bacteria. We investigated the expression of *IFIT1* and *OAS2*, two genes belonging to type 1 IFN pathway which were specifically modulated in *C. burnetii*-induced granulomas. The expression of *IFIT1* (**Figure 4A**) and *OAS2* (**Figure 4B**) genes was strongly upmodulated in stimulated PBMCs, but not in unstimulated PBMCs. We noted that the levels of expression of *IFIT1* and *OAS2* genes were similar to those obtained with isolated granuloma cells (see **Figure 3C**). The expression of *IFIT1* genes (**Figure 4C**) and *OAS2* genes (**Figure 4D**) was similar in *C. burnetii*-induced granulomas from patients with Q fever and healthy controls. These results demonstrated that type 1 IFN pathway was not altered in Q fever granulomas.

DISCUSSION

The favorable outcome of Q fever is associated with the presence of granulomas (Raoult et al., 2005), but the real functions of granulomas during *C. burnetii* infection remain unknown. Therefore, we employed a technique that generated *in vitro* human granulomas (Delaby et al., 2010), then performed whole genome transcriptional profile of *C. burnetii*-induced granulomas and we compared it to that induced by BCG.

More than 50% of genes that were modulated in granulomas, were commonly modulated by *C. burnetii* and BCG. First, they included genes involved in chemotaxis, especially those related to the recruitment of monocytes and lymphocytes, such as *CCL2* (Loetscher et al., 1994), *CCL8* (Loetscher et al., 1994), *CCL13* (Garcia-Zepeda et al., 1996), *CCL17* (Cronshaw et al., 2006), and *CCL18* (Adema et al., 1997) genes. This finding is consistent with the critical role of the recruitment of monocytes and lymphocytes

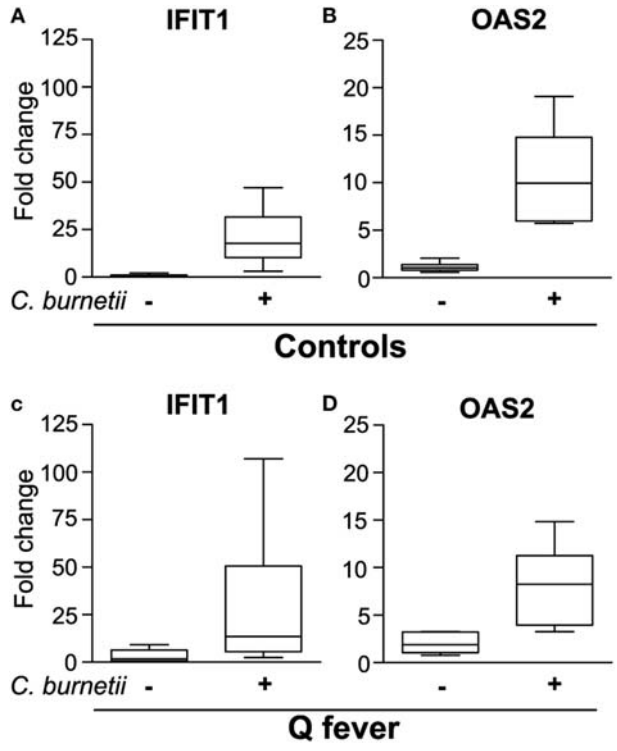

FIGURE 4 | Expression of ISGs in granulomas generated in Q fever patients. PBMCs from healthy donors **(A,B)** and patients with Q fever **(C,D)** were stimulated with heat-killed *C. burnetii* for 9 days and analyzed for the expression of IFIT1 **(A,C)** and OAS2 **(B,D)** by qRT-PCR.

in *in vitro*-generated granulomas (Delaby et al., 2012). Our data extend to human granulomas the role of chemokines initially described in animal models (Chensue, 2013). Hence, in mice deficient for CCR2, a receptor for CCL2 and CCL8, the number and size of granulomas, as well as monocyte recruitment at site of infection, are decreased (Jinnouchi et al., 2003). We provided evidence that the neutralization of CCL2 was sufficient to prevent the formation of granulomas in response to *C. burnetii* and BCG. As reported above in CCR2 deficient mice, it is likely that CCL2 is involved in the initial stages of granuloma formation. Similar results were obtained with the neutralization of CCL5. This result may be related to the model of CCL5 ko mice in which granuloma function is transiently impaired (Vesosky et al., 2010). In addition, granuloma cells in intestinal tissues from patients with Crohn's disease express CCL5 (Oki et al., 2005). It has been suggested that CCL5 via its interaction with CCR5 augments type 2 granuloma formation (Chensue, 2013). The role of CCL2 and CCL5 in granuloma formation in response to *C. burnetii* is likely not redundant. We hypothesize that a temporal regulation of chemokines is necessary for granuloma formation. Second, granulomas are essentially composed of macrophages, which were similarly polarized in response to *C. burnetii* and BCG. Indeed, granuloma cells expressed M1 profile with some features of M2 cells. This finding is markedly distinct from isolated macrophages infected with *C. burnetii* that express an atypical M2 profile (Benoit et al., 2008). This difference between isolated macrophages and macrophages involved in a functional unit such as granulomas has been reported in mice infected with *Mycobacterium tuberculosis*. Indeed, granuloma-associated macrophages are polarized into M1 cells whereas macrophages surrounding granulomas shift from an M1 to an M2 profile (Redente et al., 2010). In addition, the loss of M2 macrophages during *Leishmania major* infection delays disease progression and increases resistance to pathogens (Hölscher et al., 2006). We hypothesize that the microenvironment of granulomas sustains M1 polarization to eradicate pathogens.

The transcriptional response of *C. burnetii*-generated granulomas was, in part, specific. First, inflammatory genes were differentially modulated. Indeed, *C. burnetii* downmodulated the expression of *TNF*, *NCR3*, *EDN1* and genes related to the Th1 profile, such as *IFNG, TBX21*, which encodes the transcription factor tbet, *IL18RAP*, *IL26*, and *HOPX* genes. Murine macrophages infected with *Leishmania major*, a granuloma-inducing pathogen, are unable to produce EDN1 (Wahl et al., 2005). A dramatic decrease in inflammatory cytokines (IFN-γ, IL12-p40) was observed in granulomas from BCG-vaccinated guinea pigs induced by *M. tuberculosis* (Ly et al., 2007). Second, *C. burnetii* specifically induced the expression of *CH25H*, *TNFSF13*, and *IRF7* genes, known to be related to type 1 IFN pathway (Park and Scott, 2010; Tezuka et al., 2011) and likely involved in microbicidal response of granuloma cells. For instance, CH25H is an enzyme involved in production of oxysterol, 25-hydroxycholesterol. Oxysterols are known to bind liver X receptor (LXR) and its deficiency is associated with loss of microbicidal competence and apoptosis (Joseph et al., 2004). TNFSF13 likely plays a role in Th1 polarization and TNFSF13-deficient mice exhibit defective bacterial clearance (Xiao et al., 2008). Taken together, these results suggest that the activation of inflammatory genes may limit *C. burnetii* infection in specific granulomas directly or indirectly via type 1 IFN pathway.

The granuloma cells induced by *C. burnetii* exhibited upmodulated expression of numerous genes belonging to type 1 IFN pathway; most of these genes were ISGs. Although ISGs have been associated initially with antiviral response (Schoggins et al., 2011), many recent studies report their upregulation in response to bacteria and bacterial components, such as lipopolysaccharide (Textoris et al., 2012). Type 1 IFN signaling has also been implicated in efficient clearance of group B *Streptococcus*, *S. pneumoniae*, and *Escherichia coli* (Textoris et al., 2012). Indeed, injection of *C. burnetii* components in mice induces a transient IFN-α/β production, and a steady synthesis of OAS for several days (Zvilich et al., 1995). This finding is potentially important for the defense against *C. burnetii* since type 1 IFN was either not detected or its pathway was defective in macrophages or dendritic cells stimulated by *C. burnetii*, respectively (Gorvel et al., 2014). This may be related to previous reports, which state that a BCG mucoprotein is unable to induce the expression of interferon-inducible antiviral proteins (Ishii et al., 2005). The stimulation of type 1 IFN pathway (*OAS2* and *IFIT1* genes) was similar in granulomas from healthy controls or patients with Q fever. ISGs may therefore play an important role in the anti-infectious activity of *C. burnetii* granulomas.

In conclusion, the transcriptional response of *C. burnetii* granulomas includes a common part shared with other infectious granulomas and a part specific for *C. burnetii*. The specific response to *C. burnetii* involved the activation of genes involved in inflammation including type 1 IFN related genes, microbicidal activity, and apoptosis. This transcriptional program may account for the granuloma-mediated elimination of *C. burnetii*, in accordance with the natural history of Q fever where granulomas are associated with a protective immune response and resolution of the disease, whereas the absence of granulomas is associated with the chronic evolution of the disease.

ACKNOWLEDGMENTS

The authors would like to thank Olivia DeLozier for editing the English language manuscript.

SUPPLEMENTARY MATERIAL

The Supplementary Material for this article can be found online at: http://www.frontiersin.org/journal/10.3389/fcimb.2014.00172/abstract

Figure S1 | Functional annotation of *C. burnetii*- and BCG-modulated genes. The expression of the modulated genes in *C. burnetii*- and BCG-induced granulomas was compared to their expression in PBMCs. The functional groups that contain the largest number of distinctly modulated genes were selected, and genes were depicted. The direction of gene regulation is color-coded, with blue indicating downregulation, and red indicating upregulation.

REFERENCES

Adema, G. J., Hartgers, F., Verstraten, R., de Vries, E., Marland, G., Menon, S., et al. (1997). A dendritic-cell-derived C-C chemokine that preferentially attracts naive T cells. *Nature* 387, 713–717. doi: 10.1038/42716

Ben Amara, A., Ghigo, E., Le Priol, Y., Lépolard, C., Salcedo, S. P., Lemichez, E., et al. (2010). *Coxiella burnetii*, the agent of Q fever, replicates within trophoblasts and induces a unique transcriptional response. *PLoS ONE* 5:e15315. doi: 10.1371/journal.pone.0015315

Benoit, M., Barbarat, B., Bernard, A., Olive, D., and Mege, J.-L. (2008). *Coxiella burnetii*, the agent of Q fever, stimulates an atypical M2 activation program in human macrophages. *Eur. J. Immunol.* 38, 1065–1070. doi: 10.1002/eji.200738067

Bindea, G., Mlecnik, B., Hackl, H., Charoentong, P., Tosolini, M., Kirilovsky, A., et al. (2009). ClueGO: a Cytoscape plug-in to decipher functionally grouped gene ontology and pathway annotation networks. *Bioinformatics* 25, 1091–1093. doi: 10.1093/bioinformatics/btp101

Chensue, S. W. (2013). Chemokines in innate and adaptive granuloma formation. *Front. Immunol.* 4:43. doi: 10.3389/fimmu.2013.00043

Cooper, A. M., Dalton, D. K., Stewart, T. A., Griffin, J. P., Russell, D. G., and Orme, I. M. (1993). Disseminated tuberculosis in interferon gamma gene-disrupted mice. *J. Exp. Med.* 178:2243. doi: 10.1084/jem.178.6.2243

Cronshaw, D. G., Kouroumalis, A., Parry, R., Webb, A., Brown, Z., and Ward, S. G. (2006). Evidence that phospholipase-C dependent, calcium-independent mechanisms are required for directional migration of T-lymphocytes in response to the CCR4 ligands CCL17 and CCL22. *J. Leukoc. Biol.* 79, 1369–1370.

Delaby, A., Espinosa, L., Lépolard, C., Capo, C., and Mège, J.-L. (2010). 3D reconstruction of granulomas from transmitted light images implemented for long-time microscope applications. *J. Immunol. Methods* 360, 10–19. doi: 10.1016/j.jim.2010.06.008

Delaby, A., Gorvel, L., Espinosa, L., Lépolard, C., Raoult, D., Ghigo, E., et al. (2012). Defective monocyte dynamics in Q fever granuloma deficiency. *J. Infect. Dis.* 205, 1086–1094. doi: 10.1093/infdis/jis013

Egen, J. G., Rothfuchs, A. G., Feng, C. G., Winter, N., Sher, A., and Germain, R. N. (2008). Macrophage and T cell dynamics during the development and disintegration of mycobacterial granulomas. *Immunity* 28, 271–284. doi: 10.1016/j.immuni.2007.12.010

Garcia-Zepeda, E. A., Combadiere, C., Rothenberg, M. E., Sarafi, M. N., Lavigne, F., Hamid, Q., et al. (1996). Human monocyte chemoattractant protein (MCP)-4 is a novel CC chemokine with activities on monocytes, eosinophils, and basophils induced in allergic and nonallergic inflammation that signals through the CC chemokine receptors (CCR)-2 and -3. *J. Immunol.* 157, 5613–5626.

Gentleman, R. C., Carey, V. J., Bates, D. M., Bolstad, B., Dettling, M., Dudoit, S., et al. (2004). Bioconductor: open software development for computational biology and bioinformatics. *Genome Biol.* 5:R80. doi: 10.1186/gb-2004-5-10-r80

Ghigo, E., Barry, A. O., Pretat, L., Al Moussawi, K., Desnues, B., Capo, C., et al. (2010). IL-16 promotes *T. whipplei* replication by inhibiting phagosome conversion and modulating macrophage activation. *PLoS ONE* 5:e13561. doi: 10.1371/journal.pone.0013561

Gorvel, L., Textoris, J., Banchereau, R., Ben Amara, A., Tantibhedhyangkul, W., von Bargen, K., et al. (2014). Intracellular bacteria interfere with dendritic cell functions: role of the type I interferon pathway. *PLoS ONE* 9:e99420. doi: 10.1371/journal.pone.0099420

Hölscher, C., Arendse, B., Schwegmann, A., Myburgh, E., and Brombacher, F. (2006). Impairment of alternative macrophage activation delays cutaneous leishmaniasis in nonhealing BALB/c mice. *J. Immunol.* 176, 1115–1121. doi: 10.4049/jimmunol.176.2.1115

Ishii, K., Kurita-Taniguchi, M., Aoki, M., Kimura, T., Kashiwazaki, Y., Matsumoto, M., et al. (2005). Gene-inducing program of human dendritic cells in response to BCG cell-wall skeleton (CWS), which reflects adjuvancy required for tumor immunotherapy. *Immunol. Lett.* 98, 280–290. doi: 10.1016/j.imlet.2004.12.002

Jinnouchi, K., Terasaki, Y., Fujiyama, S., Tomita, K., Kuziel, W. A., Maeda, N., et al. (2003). Impaired hepatic granuloma formation in mice deficient in C-C chemokine receptor 2. *J. Pathol.* 200, 406–416. doi: 10.1002/path.1362

Joseph, S. B., Bradley, M. N., Castrillo, A., Bruhn, K. W., Mak, P. A., Pei, L., et al. (2004). LXR-dependent gene expression is important for macrophage survival and the innate immune response. *Cell* 119, 299–309. doi: 10.1016/j.cell.2004.09.032

Loetscher, P., Seitz, M., Clark-Lewis, I., Baggiolini, M., and Moser, B. (1994). Monocyte chemotactic proteins MCP-1, MCP-2, and MCP-3 are major attractants for human $CD4^+$ and $CD8^+$ T lymphocytes. *FASEB J.* 8, 1055–1060.

Ly, L. H., Russell, M. I., and McMurray, D. N. (2007). Microdissection of the cytokine milieu of pulmonary granulomas from tuberculous guinea pigs. *Cell. Microbiol.* 9, 1127–1136. doi: 10.1111/j.1462-5822.2006.00854.x

Martinez, F. O., Gordon, S., Locati, M., and Mantovani, A. (2006). Transcriptional profiling of the human monocyte-to-macrophage differentiation and polarization: new molecules and patterns of gene expression. *J. Immunol.* 177, 7303–7311. doi: 10.4049/jimmunol.177.10.7303

Mege, J. L., Maurin, M., Capo, C., and Raoult, D. (1997). *Coxiella burnetii*: the "query" fever bacterium. A model of immune subversion by a strictly intracellular microorganism. *FEMS Microbiol. Rev.* 19, 209–217. doi: 10.1016/S0168-6445(96)00030-7

Moal, V., Textoris, J., Ben Amara, A., Mehraj, V., Berland, Y., Colson, P., et al. (2013). Chronic hepatitis E virus infection is specifically associated with an interferon-related transcriptional program. *J. Infect. Dis.* 207, 125–132. doi: 10.1093/infdis/jis632

Oki, M., Ohtani, H., Kinouchi, Y., Sato, E., Nakamura, S., Matsumoto, T., et al. (2005). Accumulation of $CCR5^+$ T cells around $RANTES^+$ granulomas in Crohn's disease: a pivotal site of Th1-shifted immune response? *Lab. Invest.* 85, 137–145. doi: 10.1038/labinvest.3700189

Park, K., and Scott, A. L. (2010). Cholesterol 25-hydroxylase production by dendritic cells and macrophages is regulated by type I interferons. *J. Leukoc. Biol.* 88, 1081–1087. doi: 10.1189/jlb.0610318

Puissegur, M.-P., Botanch, C., Duteyrat, J.-L., Delsol, G., Caratero, C., and Altare, F. (2004). An *in vitro* dual model of mycobacterial granulomas to investigate the molecular interactions between mycobacteria and human host cells. *Cell. Microbiol.* 6, 423–433. doi: 10.1111/j.1462-5822.2004.00371.x

Ramakrishnan, L. (2012). Revisiting the role of the granuloma in tuberculosis. *Nat. Rev. Immunol.* 12, 352–366. doi: 10.1038/nri3211

Raoult, D. (2012). Chronic Q fever: expert opinion versus literature analysis and consensus. *J. Infect.* 65, 102–108. doi: 10.1016/j.jinf.2012.04.006

Raoult, D., Marrie, T., and Mege, J. L. (2005). Natural history and pathophysiology of Q fever. *Lancet Infect. Dis.* 5, 219–226. doi: 10.1016/S1473-3099(05)70052-9

Redente, E. F., Higgins, D. M., Dwyer-Nield, L. D., Orme, I. M., Gonzalez-Juarrero, M., and Malkinson, A. M. (2010). Differential polarization of alveolar macrophages and bone marrow-derived monocytes following chemically and pathogen-induced chronic lung inflammation. *J. Leukoc. Biol.* 88, 159–168. doi: 10.1189/jlb.0609378

Russell, D. G., Cardona, P.-J., Kim, M.-J., Allain, S., and Altare, F. (2009). Foamy macrophages and the progression of the human tuberculosis granuloma. *Nat. Immunol.* 10, 943–948. doi: 10.1038/ni.1781

Schoggins, J. W., Wilson, S. J., Panis, M., Murphy, M. Y., Jones, C. T., Bieniasz, P., et al. (2011). A diverse range of gene products are effectors of the type I interferon antiviral response. *Nature* 472, 481–485. doi: 10.1038/nature09907

Shaler, C. R., Horvath, C. N., Jeyanathan, M., and Xing, Z. (2013). Within the Enemy's Camp: contribution of the granuloma to the dissemination, persistence and transmission of *Mycobacterium tuberculosis*. *Front. Immunol.* 4:30. doi: 10.3389/fimmu.2013.00030

Smoot, M. E., Ono, K., Ruscheinski, J., Wang, P.-L., and Ideker, T. (2011). Cytoscape 2.8: new features for data integration and network visualization. *Bioinformatics* 27, 431–432. doi: 10.1093/bioinformatics/btq675

Srigley, J. R., Vellend, H., Palmer, N., Phillips, M. J., Geddie, W. R., Van Nostrand, A. W., et al. (1985). Q-fever. The liver and bone marrow pathology. *Am. J. Surg. Pathol.* 9, 752–758. doi: 10.1097/00000478-198510000-00007

Textoris, J., Capo, C., and Mège, J.-L. (2012). "Type I interferons and bacterial infectious diseases: new features," in *Recent Research Developments in Immunology*, ed S. G. Pandalai (Trivandrum: Research Signpost), 49–74.

Tezuka, H., Abe, Y., Asano, J., Sato, T., Liu, J., Iwata, M., et al. (2011). Prominent role for plasmacytoid dendritic cells in mucosal T cell-independent IgA induction. *Immunity* 34, 247–257. doi: 10.1016/j.immuni.2011.02.002

Travis, L. B., Travis, W. D., Li, C. Y., and Pierre, R. V. (1986). Q fever. A clinicopathologic study of five cases. *Arch. Pathol. Lab. Med.* 110, 1017–1020.

Ulrichs, T., and Kaufmann, S. H. E. (2006). New insights into the function of granulomas in human tuberculosis. *J. Pathol.* 208, 261–269. doi: 10.1002/path.1906

Vesosky, B., Rottinghaus, E. K., Stromberg, P., Turner, J., and Beamer, G. (2010). CCL5 participates in early protection against *Mycobacterium tuberculosis*. *J. Leukoc. Biol.* 87, 1153–1165. doi: 10.1189/jlb.1109742

Wahl, J. R., Goetsch, N. J., Young, H. J., Van Maanen, R. J., Johnson, J. D., Pea, A. S., et al. (2005). Murine macrophages produce endothelin-1 after microbial stimulation. *Exp. Biol. Med. (Maywood)* 230, 652–658.

Xiao, Y., Motomura, S., and Podack, E. R. (2008). APRIL (TNFSF13) regulates collagen-induced arthritis, IL-17 production and Th2 response. *Eur. J. Immunol.* 38, 3450–3458. doi: 10.1002/eji.200838640

Zumla, A., and James, D. G. (1996). Granulomatous infections: etiology and classification. *Clin. Infect. Dis.* 23, 146–158. doi: 10.1093/clinids/23.1.146

Zvilich, M., Williams, J. C., Waag, D., Rill, W. R., Malli, R. J., Bell, P., et al. (1995). Characterization of the non-specific humoral and cellular antiviral immunity stimulated by the chloroform-methanol residue (CMR) fraction of *Coxiella burnetii*. *Antiviral Res.* 27, 389–404. doi: 10.1016/0166-3542(95)00022-E

Conflict of Interest Statement: The Guest Associate Editor, Benjamin Coiffard, declares that, despite having collaborated with author, Aurélie Daumas, the review process was handled objectively. The authors declare that the research was conducted in the absence of any commercial or financial relationships that could be construed as a potential conflict of interest.

Received: 29 July 2014; accepted: 21 November 2014; published online: 15 December 2014.

*Citation: Faugaret D, Ben Amara A, Alingrin J, Daumas A, Delaby A, Lépolard C, Raoult D, Textoris J and Mège J-L (2014) Granulomatous response to Coxiella burnetii, the agent of Q fever: the lessons from gene expression analysis. Front. Cell. Infect. Microbiol. **4**:172. doi: 10.3389/fcimb.2014.00172*

This article was submitted to the journal Frontiers in Cellular and Infection Microbiology.

Figure S1

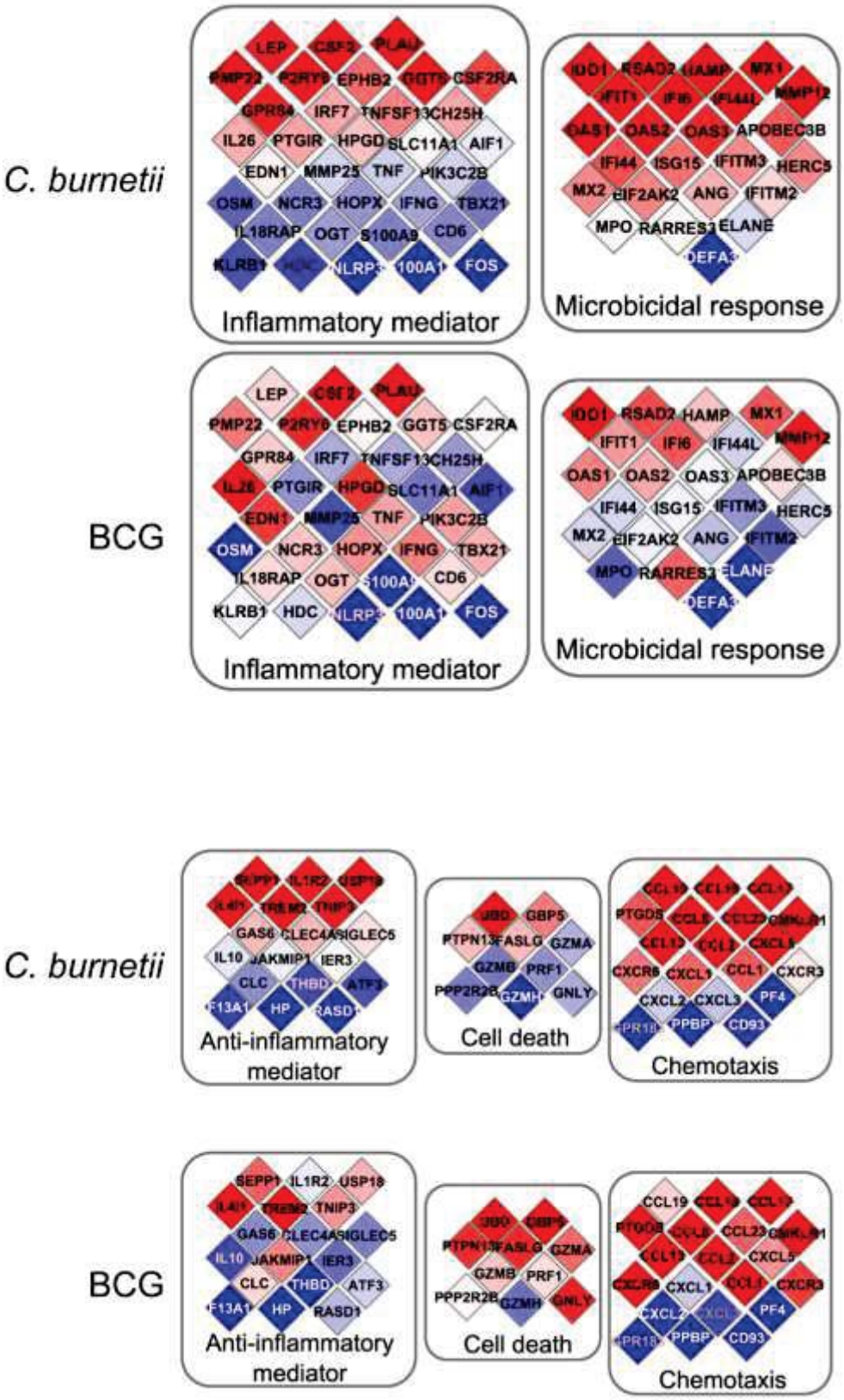
C. burnetii
LEP
CSF2
PLAU
PMP22
P2RY6
EPHB2
GGT5
CSF2RA
GPR84
IRF7
TNFSF13
CH25H
IL26
PTGIR
HPGD
SLC11A1
AIF1
EDN1
MMP25
TNF
PIK3C2B
OSM
NCR3
HOPX
IFNG
TBX21
IL18RAP
OGT
S100A9
CD6
KLRB1
HDC
NLRP3
S100A12
FOS
Inflammatory mediator
IDO1
RSAD2
HAMP
MX1
IFIT1
IFI6
IFI44L
MMP12
OAS1
OAS2
OAS3
APOBEC3B
IFI44
ISG15
IFITM3
HERC5
MX2
EIF2AK2
ANG
IFITM2
MPO
RARRES3
ELANE
DEFA3
Microbicidal response
BCG
Inflammatory mediator
Microbicidal response
C. burnetii
SEPP1
IL1R2
USP18
IL4I1
TREM2
TNIP3
GAS6
CLEC4A
SIGLEC5
IL10
JAKMIP1
IER3
CLC
THBD
ATF3
F13A1
HP
RASD1
Anti-inflammatory mediator
JUD
GBP5
PTPN13
FASLG
GZMA
GZMB
PRF1
PPP2R2B
GZMH
GNLY
Cell death
CCL19
CCL18
CCL23
PTGDS
CCL5
CXCL5
CXCR6
CXCL1
CCL1
CXCR3
CXCL2
CXCL3
PF4
PPBP
CD93
Chemotaxis
BCG
Anti-inflammatory mediator
Cell death
Chemotaxis

Impaired Granuloma Formation in Sepsis: Impact of Monocytopenia

Alingrin J, Coiffard B, Textoris J, Belenotti P, **Daumas A**, Leone M, Mege JL.

PLoS One. 2016 Jul 21;11(7):e0158528.

doi: 10.1371/journal.pone.0158528. eCollection 2016.

La mise en jeu normale des défenses de l'organisme contre une infection implique une réponse inflammatoire initiale. Néanmoins, chez certains patients, cette réponse est disproportionnée entrainant des défaillances d'organe (sepsis sévère) voire un état de choc [130]. De manière logique, cette réponse inflammatoire est rapidement associée à une intense réponse anti-inflammatoire conduisant à une baisse de l'hypersensibilité retardée et une incapacité de juguler l'infection, et prédisposant à la survenue d'infections nosocomiales [131]. La méconnaissance jusqu'à il y a une dizaine d'années de l'importance et de la précocité d'apparition de cette immunodépression (le terme de « paralysie immunitaire » est également utilisé) explique au moins en partie les échecs des stratégies thérapeutiques étudiées par le passé qui visaient à corriger les désordres inflammatoires en inhibant encore plus le système immunitaire des patients [132]. Dans ce contexte de défaillance immunitaire, les patients qui vont normaliser rapidement leurs fonctions immunitaires restent le plus souvent indemnes d'infections nosocomiales et évoluent favorablement. A l'inverse, les patients qui présentent des dysfonctions immunitaires persistantes au cours du temps, ont un risque élevé d'infections liées aux soins et de décès. Nous savons aujourd'hui que l'ensemble des mécanismes immunitaires est touché aussi bien la réponse innée qu'adaptative avec un défaut de réponse monocytaire et une anergie lymphocytaire cependant variable en fonction des patients [131,133]. Tout l'enjeu est donc de pouvoir monitorer la réponse immunitaire des patients grâce à un panel de biomarqueurs de la réponse de l'hôte pour permettre de proposer une prise en charge personnalisée avec des thérapies ciblées visant à restaurer spécifiquement leurs fonctions immunitaires.

Le granulome est la résultante d'une coopération intense entre les cellules de la réponse innée et adaptative dans le but d'éliminer un agent pathogène rebelle. L'évaluation *in vitro* de sa

formation permet ainsi d'explorer la fonctionnalité des différents acteurs du système immunitaire et leurs interactions et de mieux comprendre les complications de son dysfonctionnement. Cette méthode déjà utilisée au sein du laboratoire pour l'étude de la fièvre Q, est apparue séduisante pour évaluer l'état d'immunodépression des patients en sepsis sévère et éventuellement étudier l'effet de thérapies immunomodulatrices. J'ai participé à l'étude de Julie Alingrin alors que je réalisais la même évaluation chez les patients âgés.

Dix-neuf patients en sepsis sévère, 9 patients avec un antécédent de fièvre Q guérie et 9 volontaires sains ont été étudiés. L'isolement des cellules mononucléées du sang périphérique (PBMCs) a été effectué à partir d'échantillons sanguins par une technique manuelle utilisant un gradient de Ficoll. Les PBMCs ont ensuite été incubés avec les billes couplées aux extraits bactériens (*Mycobacterium bovis* et *Coxiella burnetii*). La formation des granulomes a été quantifiée après 3, 6 et 9 jours de culture, par le compte du nombre de billes nues, de granulomes partiels et de granulomes complets.

Quatre conditions expérimentales ont tout d'abord été testées en raison d'une quantité limitée de cellules afin de définir le rapport nombre de cellules/ nombre de billes optimal qui s'est avéré être 2,5 x 10^5 cellules avec 50 billes par puit.

Cette étape de mis au point de la méthode réalisée, nous avons ensuite pu comparer la formation de granulome dans nos différentes populations. En raison d'une probable immunisation des patients par *Mycobactérium bovis*, il a été décidé d'étudier également des patients immunisés par *Coxiella burnetii.*

Le premier résultat de cette étude est un défaut de formation de granulomes chez les patients septiques aux différents temps d'analyse quels que soient les extraits bactériens utilisés. A noter cependant que 6 patients septiques sur 19 arrivent à former des granulomes mais avec une cinétique plus lente pour 3 d'entre eux et qu'un sujet contrôle sain ne forme pas de granulomes. Aucune différence significative n'a été retrouvée entre les patients septiques formant des granulomes et ceux n'y arrivant pas. Ainsi, la formation *in vitro* de granulomes pourrait servir à évaluer le degré d'immunosuppression et le monitorer en réponse à un traitement voir évaluer le pronostic.

Pour expliquer le défaut de formation de granulomes, les taux de monocytes et de lymphocytes circulants ont été comparés. Les patients septiques ne formant pas de granulome présentaient

des taux de monocytes significativement plus faibles et/ou une lymphopénie bien que cette anomalie ne soit pas significativement associée à l'absence de formation de granulomes. Du fait d'exceptions donc, la formule leucocytaire ne peut pas permettre de prédire la capacité de formation de granulomes.

Le dosage du TNF dans les surnageants a mis en évidence des taux significativement plus faibles chez les patients qui ne forment pas de granulomes sans augmentation de l'IL-10 en parallèle. Pour confirmer le rôle du TNF dans la formation des granulomes, qui en clinique a du sens (susceptibilité des patients sous anti-TNF aux infections), l'ajout de TNF ou d'un anticorps monoclonal anti-TNF a été étudié sans aucun impact sur les résultats obtenus préalablement.

Ainsi, cette méthode permet de mettre en évidence la défaillance immunitaire de la plupart des patients septiques et confirme le rôle central des monocytes dans la formation du granulome comme déjà rapporté [22]. En ce qui concerne l'imputabilité du TNF dans la formation des granulomes, la réalité est plus complexe que ce que l'on peut imaginer car l'ajout de TNF ne suffit pas à reverser le processus.

.

PLOS | ONE

RESEARCH ARTICLE

Impaired Granuloma Formation in Sepsis: Impact of Monocytopenia

Julie Alingrin[1,2], Benjamin Coiffard[1,2], Julien Textoris[1¤], Pauline Belenotti[1], Aurélie Daumas[1,3], Marc Leone[1,2], Jean-Louis Mege[1]*

1 Unité de Recherche sur les Maladies Infectieuses Tropicales et Emergentes, UMR 63, CNRS 7278, IRD 198, INSERM U1095, Aix-Marseille Université, Marseille, France, **2** Service d'Anesthésie et de Réanimation, Hôpital Nord, Assistance Publique-Hôpitaux de Marseille, Aix-Marseille Université, Marseille, France, **3** Service de Médecine Interne, Gériatrie et Thérapeutique, Hôpital de la Timone, Assistance Publique-Hôpitaux de Marseille, Aix-Marseille Université, Marseille, France

¤ Current address: Institut BioMerieux, Unité Mixte BioMérieux-HCL, Hôpital Edouard Herriot—Pav P, 5, Place d'Arsonval, 69437, Lyon Cedex 03, France
* jean-louis.mege@univ-amu.fr

Citation: Alingrin J, Coiffard B, Textoris J, Belenotti P, Daumas A, Leone M, et al. (2016) Impaired Granuloma Formation in Sepsis: Impact of Monocytopenia. PLoS ONE 11(7): e0158528. doi:10.1371/journal.pone.0158528

Editor: Alain Haziot, INSERM, FRANCE

Received: February 9, 2016

Accepted: June 16, 2016

Published: July 21, 2016

Data Availability Statement: All relevant data are within the paper and its Supporting Information files.

Funding: The authors have no support or funding to report.

Competing Interests: The authors have declared that no competing interests exist.

Abstract

Granulomas are a collection of immune cells considered to be protective in infectious diseases. The *in vitro* generation of granulomas is an interesting substitution to invasive approaches of granuloma study. The monitoring of immune response through the determination of *in vitro* granuloma formation in patients with severe sepsis may be critical to individualize treatments. We compared the *in vitro* generation of granulomas by co-culturing circulating mononuclear cells from 19 patients with severe sepsis, 9 patients cured from Q fever and 12 healthy subjects as controls, and Sepharose beads coated either with BCG or *Coxiella burnetii* extracts to analyze both immune and innate granulomas, respectively. We showed that the great majority of patients with severe sepsis were unable to form granulomas in response to BCG and *C. burnetii* extracts whereas more than 80% of healthy controls and patients cured from Q fever formed granulomas. We also found that monocytopenia and defective production of tumor necrosis factor were associated with reduced formation of granulomas in patients with severe sepsis even if TNF did not seem to be involved in the defective granuloma formation. Taken together, these results suggest that the deficiency of granuloma formation may be a measurement of altered recruitment and activation of monocytes and lymphocytes in patients with severe sepsis.

Introduction

Granulomas are a tissue collection of macrophages and lymphocytes, which are generated in response to various microorganisms [1], toxic molecules and foreign materials [2]. The first step of granuloma formation is the recruitment of macrophages and blood-derived myeloid cells, which is completed by the recruitment of activated T cells. Macrophages within granulomas undergo a maturation program leading to the formation of multinucleated giant cells (MGCs) and foamy cells [3,4]. The formation of granulomas is conditioned by the cytokine

context. Indeed, type 1 cytokines such as interferon (IFN)-γ, interleukin (IL)-12, and tumor necrosis factor (TNF) are necessary for the formation of granulomas in response to bacteria [5]. The granulomas evolve from "innate granulomas" that do not require T cells to "immune granulomas" in which T cells are required [6].

The study of tissue granulomas requires invasive methods that are not convenient for the investigation of patients. A method was recently developed to generate granulomas *in vitro* using the co-culture of peripheral blood mononuclear cells (PBMCs) and Sepharose beads coated with bacterial extracts from BCG [7] or *Coxiella burnetii* (CB) [8]. The monocytes migrate to the beads and maturate into macrophages and MGCs in the presence of lymphocytes [8]. Hence, the *in vitro* assay of granuloma formation measures the activation and the ability of monocytes to migrate towards the source of infection and could be used in clinics. For instance, this assay has been used to study the ability of invasive *Escherichia coli* from patients with Crohn disease to elicit the aggregation of macrophages and lymphocytes [9]. A similar assay combined with high-content screening technology allows investigating anti-tuberculous compound activities [10]. In brain-injured patients who develop nosocomial pneumonia, PBMCs generate fewer mature granulomas than those of controls in response to BCG [11]. PBMCs from a large proportion of patients with Q fever endocarditis are unable to form granulomas in the presence of beads coated with CB extracts. This is related to altered recruitment of monocytes since the distance covered by monocytes was lower in Q fever endocarditis than in controls [12]. Hence, the *in vitro* assay can mimic the lack of granulomas found in patients with chronic evolution of Q fever and suggests that impaired monocyte migration is involved in defective formation of granulomas. Taken together, these data suggest that the *in vitro* formation of granulomas could be a new method to assess recruitment and activation of immune cells in patients.

Severe sepsis is defined as the combination of a systemic inflammatory response syndrome and suspected infection with at least one organ failure including hypotension, respiratory failure, coma, liver failure, thrombocytopenia and acute renal failure [13]. It is characterized by an uncontrolled inflammatory response that leads to immune system failure including a loss of delayed hypersensitivity, an inability to clear infections and a predisposition to nosocomial infections [14]. Some cytokines such as circulating TNF have been correlated with the prognosis of severe sepsis [15] and such findings have served as a basis for immunotherapy of sepsis targeting TNF. Unfortunately, this strategy was unsuccessful [16]. Few molecules have been proposed to assess the prognosis of severe sepsis and to identify patients who can benefit from innovative treatments. For instance, the expression of HLA-DR is used before the administration of granulocyte-macrophage colony-stimulating factor in patients with a defective immune response [17]. Although these tools investigate some features of the immune response, we need bioassays that enable us to assess the activation of immune cells in patients to adapt immune therapy.

Here, we assessed the ability of PBMCs from patients with severe sepsis to generate granulomas. To exonerate our data from the constraints of prior immunization, we compared granuloma formation in response to BCG and CB (a majority *vs*. a minority of patients specifically immunized). We found that 13 of 19 patients with severe sepsis were unable to form granulomas, suggesting severe impairment of their ability to recruit and activate immune cells. We also demonstrated a relationship between the impairment of granuloma formation and monocytopenia.

Materials and Methods

Study population

Patient recruitment was provided from an ancillary study to the "De-escalation of Empirical Antibiotics in Severe Sepsis" project (Comité de Protection des Personnes Sud Méditerranée no. 2011-002297-22) [18]. Patients were enrolled from February 1st, 2012, to April 8th, 2013, at the polyvalent intensive care unit (ICU) (15 beds) of the North Hospital (968 beds), Marseille, France. Written informed consent was obtained from the patients and their relatives. Eligibility criteria were the presence of severe sepsis requiring an empirical antimicrobial treatment. At the time of blood collection, we collected demographic variables, causes of ICU admission, source of infection, use of vasopressors, need for mechanical ventilation, lymphocyte and monocyte blood counts determined by numeration formula of leukocytes the first day of sepsis (cells/l), the simplified acute physiology score (SAPS) 2 [19] and the sequential organ failure assessment (SOFA) score reflecting the number of organ failures [20]. On ICU discharge, we collected the number of ICU days, the number of days with mechanical ventilation, the number of days with vasopressors and the ICU mortality rate. A total of 19 patients with severe sepsis (17 males and two females) were enrolled in the study with a median age of 57 years [49–66] with the lungs as primary infection site (16 patients) (Table 1). Lymphopenia and

Table 1. Patient features.

Variables	Values
Clinical features	
Patients (males/females)	19 (17/2)
Age [years]	57 [49–66]
SOFA	8 [6–10]
SAPS II	38 [30–48]
Number of ICU days	12 [8–17]
Mechanical ventilation (days)	8 [5–13]
Causes of ICU admission (%)	
Sepsis	7 (37)
Head trauma	4 (21)
Coma	2 (11)
Stroke	2 (11)
Active bleeding	2 (11)
Acute respiratory failure	2 (11)
Sources of infection (%)	
Lung	16 (84)
Urinary tract	2 (11)
Abdomen	1 (5.2)
Microbiological findings (%)	
MSSA	7 (37)
Streptococcus pneumoniae	3 (16)
Other Gram positive bacteria	1 (5)
Enterobacteria	5 (26)
Other Gram negative bacteria	5 (26)

SOFA: sequential organ failure assessment; SAPS: simplified acute physiology score; ICU: intensive care unit; MSSA: Methicillin susceptible *Staphylococcus aureus*. Results are expressed as absolute number and percentage or median and interquartiles, as required.

doi:10.1371/journal.pone.0158528.t001

monocytopenia are defined as cell counts lower than 1×10^9 cells/l and 0.2×10^9 cells/l, respectively. An historical cohort of 21 individuals as controls including 12 healthy donors and 9 patients with cured Q fever was defined on clinical (history of acute Q fever) and serological recovery (residual levels of anti-*C. burnetii* antibodies (Abs)).

PBMC isolation

The EDTA-anticoagulated blood samples (5 ml) were withdrawn the day of empirical antibiotic onset. The PBMCs were isolated after centrifugation on Ficoll cushion, as previously described [21]. The PBMCs were then suspended (about 5×10^6 cells/ml) in RPMI 1640 containing 20% fetal calf serum (FCS, Invitrogen) and 10% dimethyl sulfoxide and conserved at -80°C.

Bacteria and bead preparation

BCG (*Mycobacterium bovis*, American Type Culture Collection, stub 35734) was cultured on agarose (Middlebrook 7H10 agar medium). *C. burnetii* (Nine Mile strain RSA496) was cultured as previously described [22]. The bacteria (10^9 per assay) were sonicated in a coupling buffer ($NaHCO_3$ 0.1 M pH 8.3 with NaCl 0.5 M) and their protein content was determined by Bradford's method as previously described [12]. Activated 4B Sepharose beads (about 4×10^4 beads, 40–100 μm diameter, GE Healthcare) were coated with bacterial extracts (0.5 mg of proteins). The coupling efficiency was determined by measuring the protein content of supernatants.

Granuloma formation

The formation of granulomas was studied using a modified method adapted from Delaby *et al.* to investigate patients with severe sepsis [12]. For that purpose, different concentrations of PBMCs (1×10^5 and 2.5×10^5 per well) were incubated in 96-well microplates in the presence of 50 or 100 beads coated with BCG or CB in 200 μl of RPMI 1640 containing 10% FCS and antibiotics at 37°C. The formation of granulomas was measured after 3, 6 and 9 days in duplicates and evaluated by reverse microscopy. Only beads that were completely covered by cells were considered granulomas and the results were expressed as the percentage of granulomas. The reproducibility was assessed in 3 individuals who were assayed 3 times with similar results. To assess the impact of freezing on the ability to forming granulomas, PBMCs from three individuals were frozen or immediately used, and the formation of granulomas was measured. In some experiments, PBMCs from patients who did not form granulomas were incubated with beads coated with BCG or CB extracts and 10 ng/ml of human recombinant TNF (R&D Systems) while control PBMCs were incubated with coated beads and 10 ng/ml monoclonal Ab (mAb) directed against TNF (Adalimumab kindly provided by Professor J. Roudier, Marseille) and granuloma formation was measured. Crude data are available in the S1 Table.

Cytokine measurement

PBMCs (2.5×10^5 cells/well) were incubated with beads coated with bacterial extracts (50 beads/well) for 1 day of culture. Each experiment was performed in duplicate. Cell supernatants were collected and TNF and IL-10 were assayed in duplicates (100 μl each) using specific immunoassays (R&D Systems). The results were expressed as pg/ml. The detection limits of immunoassays were of 5.5 and 3.9 pg/ml for TNF and IL-10, respectively. The intra- and inter-specific coefficients of variation ranged from 5% to 10%. Crude data are available in S2 Table.

Statistical analysis

Quantitative data are presented as the medians and interquartile ranges [IQRs], and mean and standard deviation. Qualitative data are presented as absolute counts and percentages. Differences between groups were tested with the Student *t* test and a cutoff value of 0.05 was chosen to consider a difference to be statistically significant. Data analysis and plots were performed using R software (v.3.1.2) with "stats" and "*ggplot2*" libraries (Bioconductor software suite).

Results

In vitro generation of granulomas in patients with severe sepsis

In a first series of experiments, we defined the experimental conditions of granuloma formation using three healthy controls. We found that the culture of 2.5×10^5 PBMCs with 50 BCG- or CB-coated beads in 96-well microplates led to the formation of 75% and 90% of granulomas after 6 and 9 days, respectively. We also measured the effect of PBMC freezing on granuloma formation. The ability to form granuloma was not significantly different in unfrozen and frozen PBMCs (92 ± 5% *vs*. 80 ± 7% after 9 days, respectively). In addition, we assayed the ability of three control PBMCs to form granulomas three times. The variations in granuloma formation did not exceed 10%. Hence, these conditions, which reduced blood sampling and provided a reproducible assay for routine investigation of frozen PBMCs from septic patients, were used in the subsequent experiments.

Then, we investigated the formation of granulomas in patients with severe sepsis. Severe sepsis was characterized by a dramatic decrease in granuloma formation as compared with healthy controls and individuals with cured Q fever. Indeed, after 3 days of culture of PBMCs with BCG-coated beads, the formation of granulomas was low (16 ± 33%) in septic patients whereas it already reached 65 ± 30% in healthy controls ($p < 0.001$). Note that one healthy control was unable to form granulomas and two subjects form only a small number of granulomas. The defective formation of granulomas in septic patients was not due to a delayed formation of granulomas since it remained lower in the septic patients than in the healthy controls after 6 (25 ± 41% *vs*. 81 ± 30%, $p < 0.001$) and 9 days (22 ± 39% *vs*. 79 ± 30%, $p < 0.001$). It was clearly related to severe sepsis because the patients cured from Q fever were fully able to form BCG-specific granulomas; the percentage was close to 100% (75 ± 41%; 98 ±2%; 99 ±1%; $p < 0.001$ at days 3, 6 and 9, respectively) (Fig 1A). The deficient formation of granulomas did not affect all the patients with severe sepsis because six among the 19 (31%) patients kept the ability to form granulomas. Note that granuloma formation was delayed in 3 of these patients. The patients with SOFA ≥ 7 tended to have a defective granuloma formation, but no significant correlation was found (S1 Fig). No significant difference was found between the patients with and without granuloma formation (S3 Table).

Because the deficiency of granuloma formation in severe sepsis was related to the immune granulomas, we wondered if innate granulomas were also affected. We determined the ability of PBMCs from patients with severe sepsis to form innate granulomas using beads covered with CB extracts. We showed that the patients with severe sepsis were unable to form innate granulomas (14 ± 32%; 25 ± 42%; 24 ± 40%) compared with the healthy controls (58 ± 31%; 84 ± 24%; 84 ± 28%; $p < 0.001$) and with the patients cured from Q fever (79 ± 41%; 99 ± 1%; 98 ± 2%; $p < 0.001$) at days 3, 6, and 9, respectively. Note that the patient who did not form granulomas in response to BCG extracts was unable to mount a granuloma response to CB extracts. The level of the deficiency in patients with severe sepsis was similar to that found for immune granulomas (Fig 1B). Taken together, these results showed that the patients with severe sepsis exhibited a defective formation of innate and immune granulomas.

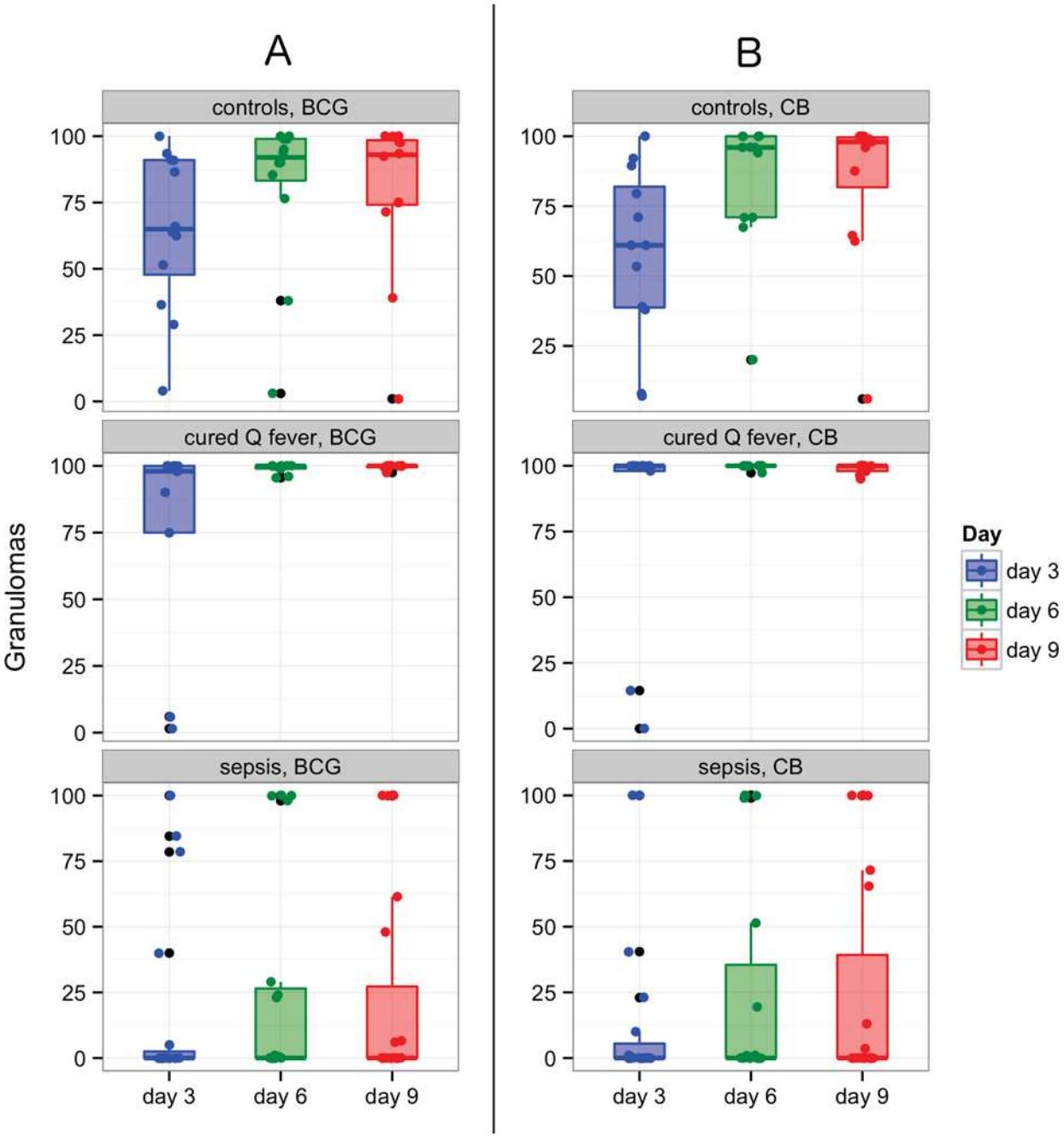

Fig 1. Granuloma formation in controls, cured Q fever and patients with severe sepsis. PBMCs (2.5×10^5) were cultured during 3, 6 and 9 days in the presence of 50 beads coated with BCG (A) or CB (B) extracts. PBMCs were isolated from controls (upper part), patients cured from Q fever (medium part) and patients with severe sepsis (lower part). Granuloma formation is expressed as the percentage of beads entirely covered by PBMCs. The boxplots represent the medians with the first and third quartiles. The whiskers represent the highest value that is within 1.5* IQR*. Data beyond the end of the whiskers are outliers and plotted as black points. Color points represent the mean value of the duplicates.

doi:10.1371/journal.pone.0158528.g001

Mechanisms of defective granuloma formation in septic patients

We previously reported that monocytes, but not lymphocytes, are required for granuloma formation [12]. Defective granuloma formation may be the result of the impaired recruitment of

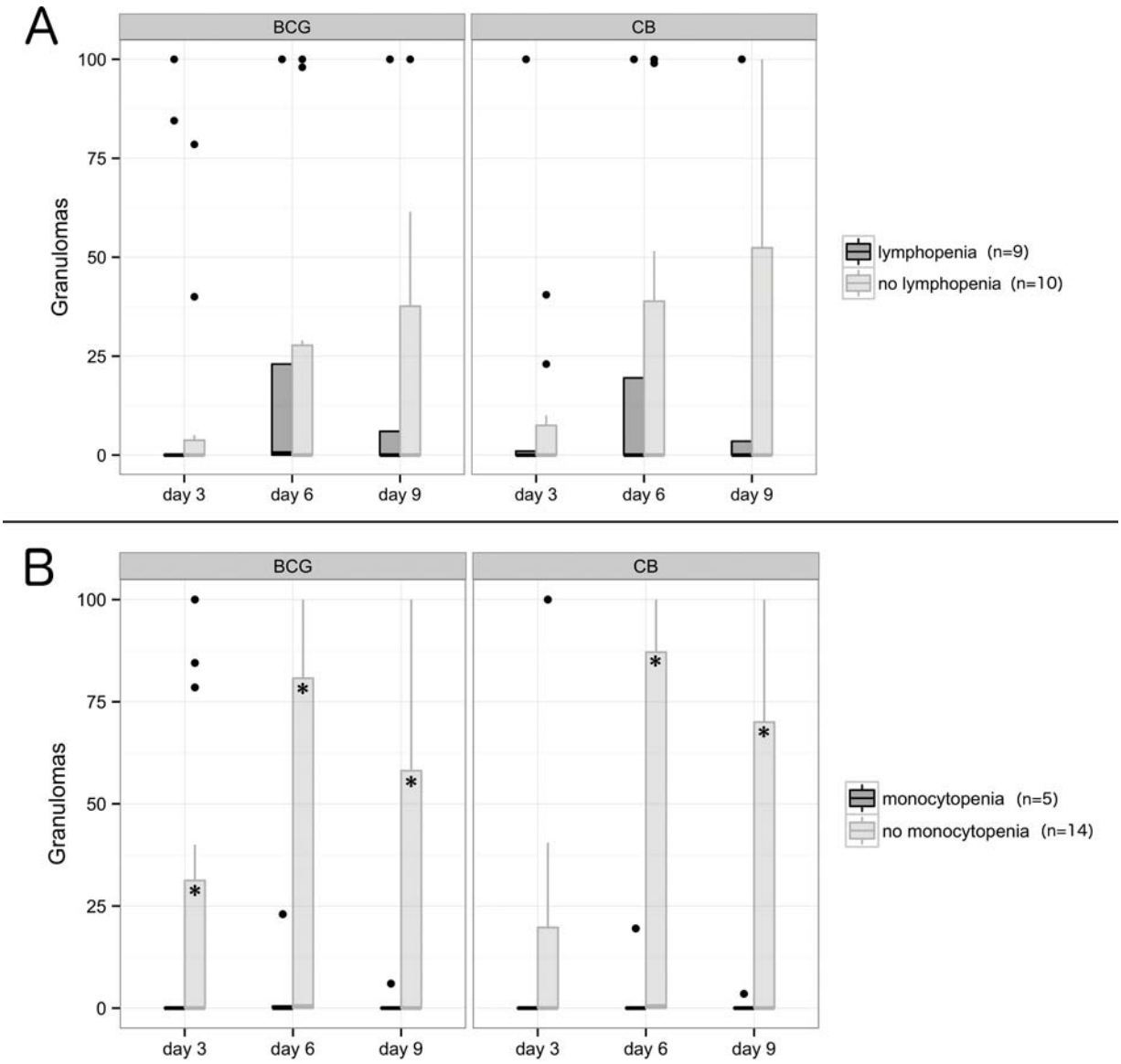

Fig 2. Granuloma formation according to lymphopenia or monocytopenia. Granuloma formation with BCG-coated beads (left) and CB-coated beads (right) was measured during 9 days in PBMCs from patients with severe sepsis. Patients were classified according to lymphopenia (A) and monocytopenia (B). The results are expressed as the percentage of beads entirely covered by PBMCs. The boxplots represent the medians with the first and third quartiles. The whiskers represent the highest value that is within 1.5*IQR. Data beyond the end of the whiskers are outliers and plotted as black points. * $p < 0.05$ represents the differences between patients with and without monocytopenia.

doi:10.1371/journal.pone.0158528.g002

monocytes. We wondered if changes in monocyte and lymphocyte circulating levels impacted granuloma formation in patients with severe sepsis. The cohort of septic patients consisted of 11 patients with an abnormal formula, including 9 patients who did not form granulomas. The alteration of circulating mononuclear cells consisted of lymphopenia for 9 patients and monocytopenia for 5 patients. Three patients were both lymphopenic and monocytopenic. Lymphopenia in patients with severe sepsis was not significantly associated with the impaired formation of immune and innate granulomas although 7 patients with lymphopenia did not form granulomas (Fig 2A). In contrast, the five patients with monocytopenia ($0.12 \pm 0.08 \times 10^9$

cells/l) were unable to form immune and innate granulomas (Fig 2B), showing that monocytopenia was associated with defective granuloma formation.

As monocytopenia did not account for all the patients with defective granuloma formation, we wondered whether alterations in cytokine imbalance interfered with granuloma formation. As TNF is associated with granuloma formation, we measured its release by PBMCs from septic patients. The amounts of TNF in supernatants from BCG-stimulated PBMCs were significantly ($p = 0.02$ and $p = 0.03$, respectively) lower in the patients with severe sepsis (54 [36–150] pg/ml) than in the healthy controls (295 [198–626] pg/ml) and the patients with cured Q fever (362 [279–443] pg/ml). Similarly, the amounts of TNF in supernatants from CB-stimulated PBMCs were significantly ($p = 0.04$ and $p = 0.05$, respectively) lower in the patients with severe sepsis (59 [35–290] pg/ml) than in the healthy controls (311 [169–791] pg/ml) and the patients with cured Q fever (480 [292–647] pg/ml) (Fig 3A). The decreased production of TNF may be related to the hyporesponsiveness of PBMCs from patients with severe sepsis or the increased production of an immunosuppressive cytokine such as IL-10. To discriminate between these hypotheses, we determined the release of IL-10 by PBMCs in the presence of BCG- or CB-coated beads. The release of IL-10 by control PBMCs stimulated with BCG- or CB-coated beads did not exceed 40 pg/ml in healthy controls and patients cured from Q fever. The release of IL-10 by PBMCs from septic patients was rather lower than that found in controls and patients with cured Q fever (Fig 3A), suggesting that the decreased release of TNF in severe sepsis was not related to the overproduction of an immunosuppressive cytokine such as IL-10. Finally, we studied the relationship between the capacity to form granulomas and the production of TNF in septic patients. The release of TNF (182 [104–349] and 232 [109–564] pg/ml, respectively) by PBMCs from the patients who formed immune (BCG) and innate (CB) granulomas was significantly ($p < 0.05$) higher than that of PBMCs from patients unable to form immune and innate granulomas (36 [23–46] and 38 [18–50] pg/ml, respectively) (Fig 3B). Taken together, these results showed that the defective formation of innate and immune granulomas in patients with severe sepsis was related to monocytopenia and associated with reduced production of TNF.

To tempt to relate defective granuloma formation and reduced production of TNF, we performed additional experiments. First, we added recombinant TNF to PBMCs from 3 patients who did not form granulomas: TNF was unable to increase the formation of immune and innate granulomas. Indeed, the percentage of immune granulomas observed when PBMCs were incubated in the presence of TNF was of 18 ± 25%; 27 ± 38%; 28 ± 42% at days 3, 6 and 9, respectively. Similarly, TNF did not increase the percentage of innate granulomas in patients unable to form granulomas (20 ± 25%, 27 ± 38%; 28 ± 42% at days 3, 6 and 9, respectively). Second, we added mAb directed against TNF to control PBMCs cultured for 9 days in the presence of beads coated with BCG or CB extracts. We found that such treatment had no effect on granuloma formation. Indeed, the percentage of immune granulomas remained high in the presence of anti-TNF mAb (55 ± 37%, 75 ± 35% and 87 ± 24% at days 3, 6 and 9, respectively. Similarly, anti-TNF mAb did not affect the percentage of innate granulomas (48 ± 42%, 78 ± 32% and 88 ± 21% at days 3, 6 and 9, respectively). Taken together, these results showed that the formation of granulomas was not directly related to TNF.

Discussion

The study of immune response through the measurement of individual biomarkers to predict the evolution of patients with severe sepsis has been unsuccessful to date. We are proposing an alternative method, measurement of the *in vitro* formation of granulomas. It has been shown that PBMCs are able to form *in vitro* granulomas using beads covered with BCG [7] or CB [12]

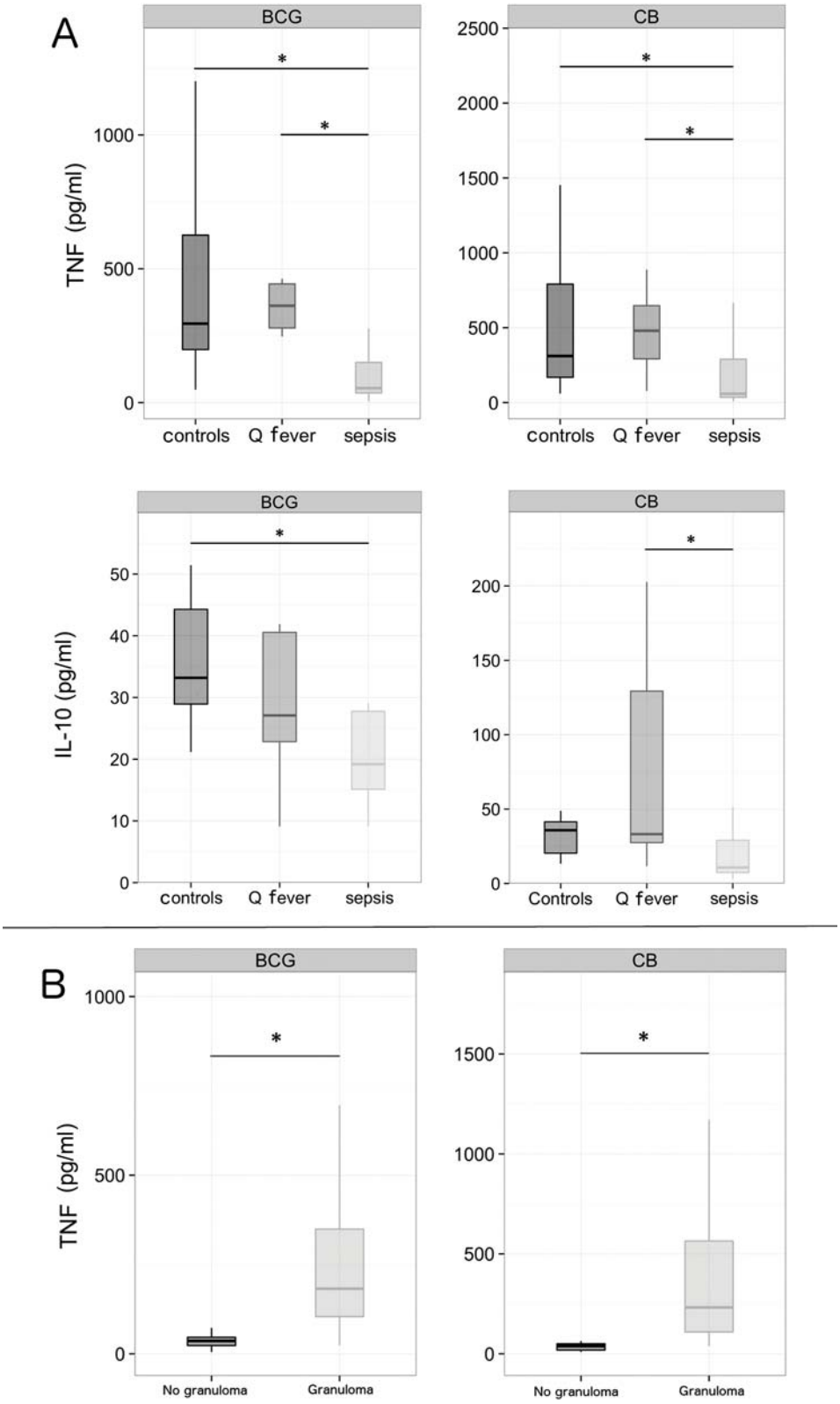

Fig 3. Cytokine production by PBMCs. PBMCs (2.5×10^5 cells/well) isolated from patients with severe sepsis, cured Q fever and healthy controls were cultured in the presence of beads (50 beads/well) coated with BCG (left) or CB (right) extracts for 24 h. Each experiment was performed in duplicate. The presence of

TNF and IL-10 in cell supernatants was assayed twice. The results were expressed as pg/ml. In A, TNF and IL-10 were measured in 8 Controls, 7 Q fever, and 14 samples of Sepsis. In B, TNF was measured in patients with severe sepsis who formed (6 samples) or did not form (8 samples) granulomas. The boxplots represent the medians with the first and third quartiles. The whiskers represent the highest value that is within 1.5 *IQR. * $p < 0.05$.

doi:10.1371/journal.pone.0158528.g003

extracts. Here, we developed an *in vitro* assay to measure granuloma formation with low-size blood samples. In addition, using beads coated with BCG or CB extracts enabled us to investigate innate and immune responses in patients. The assay was distinct from the measurement of isolated biomarkers such as membrane antigens or soluble cytokines but could be related to whole blood stimulation assay. Nevertheless, while the former assesses activation and recruitment of PBMCs, the latter measures the ability of circulating cells to produce soluble mediators.

We found that granuloma formation was impaired in patients with severe sepsis. As the BCG vaccinal status of healthy subjects and septic patients was unknown, this may be a limit of the study. However, it is likely that most of them were immunized due to the inclusion criteria in France (affiliation to the national health system for being included in clinical trials). We also used samples of patients cured from Q fever as controls in order to have a population with specific immunization. The defective formation of granulomas with BCG-coated beads reflects a defective cell-mediated immune response. It may be related to loss of the delayed hypersensitivity response to common recall antigens associated with sepsis-induced immunosuppression [14]. Impaired granuloma formation with CB-coated beads in patients with severe sepsis who are not sensitized to CB suggests an immunoparalysis state [14]. Nevertheless, a minority of patients with severe sepsis was able to form granulomas, although we ignore if these granulomas are functionally competent. Conversely, one healthy control was unable to form granulomas. As the age of this control was 70 years, we suggest that the inability to form granulomas may be related to immunosenescence because about 10% of healthy aged individuals were unable to form granulomas (manuscript in preparation). Defective granuloma formation may be associated with the severity of sepsis or patient outcomes. We assessed granuloma formation according to severity including the severity score (SOFA) and survival. There is a tendency between defective granuloma formation and high SOFA but no significant correlation was found, likely due to the size of samples.

We then investigated the mechanisms involved in the defective granuloma formation in patients with severe sepsis. First, we showed that defective granuloma formation was associated with monocytopenia, but not with lymphopenia. This is consistent with our previous report in which we showed that monocytes, but not lymphocytes, are required for the initial phases of granuloma formation including the migration toward beads coated with bacterial extracts [12]. This may be also related to the role of macrophage supply in the maintain of granuloma integrity as demonstrated in a zebrafish model of granuloma formation [23]. Nevertheless, defective granuloma formation related to monocytopenia did not account for all the septic patients who did not form granulomas. Second, the defective granuloma formation in septic patients may depend on an inflammatory process or bacterial infection. We investigated the hypothesis based on cytokine imbalance because sepsis-induced immunosuppression is associated with decreased production of inflammatory cytokines and a high IL-10-to-TNF ratio [24]. We found that the TNF release induced by BCG or CB extracts was decreased in PBMCs from patients with severe sepsis. This finding is consistent with initial papers that showed the role of TNF in granuloma formation [5]. The decrease of TNF production occurs without IL-10 increase, suggesting that the modulation of TNF release was not related to the overproduction of IL-10, as in sepsis-induced immunosuppression based on LPS tolerance [25]. Our results are

also distinct from those concerning patients with traumatic brain injury associated with defective granuloma formation in which a strong inflammatory response was observed [11]. The decrease in TNF release may result from a decreased number of TNF-producing cells in the blood, especially monocytes, rather than a repolarization of the immune response toward an anti-inflammatory profile. However, TNF adding to PBMCs from septic patients unable to form granulomas did not restore the formation of immune and innate granulomas. Similarly, adding anti-TNF mAb to control PBMCs did not inhibit the formation of immune and innate granulomas. These results suggest that TNF is dispensable or acts in synergy with other cytokines in granuloma formation. We hypothesize that the defective granuloma formation in septic patients may depend on bacterial infection. Indeed, Deknuydt *et al*. included patients with traumatic brain injury before the occurrence of nosocomial pneumonia and showed that impaired granuloma formation in these patients is associated with an increased frequency of secondary infections [11], suggesting that bacterial infection plays a major role in the defective formation of granulomas in patients with severe sepsis.

Conclusion

In conclusion, this study showed that the assay of *in vitro* granuloma formation was convenient to study small blood samples in clinical practice. It also demonstrated that granuloma formation was impaired in a large proportion of patients with severe sepsis, as well as the role of monocytes. This study also suggests that immune response impairment is somewhat heterogeneous in patients with severe sepsis and use of this assay with larger cohorts of patients will be necessary.

Supporting Information

S1 Fig. Granuloma formation according to ICU discharge and SOFA score. PBMCs isolated from patients with severe sepsis were cultured in the presence of beads coated with BCG (left) or CB (right) extracts for 9 days. Patients were classified according to ICU discharge (dead or alive) (A) and SOFA score (≥ 7 or <7) (B). The results are expressed as the percentage of beads entirely covered by PBMCs. The boxplots represent the medians with the first and third quartiles. The whiskers represent the highest value that is within 1.5* IQR. Data beyond the end of the whiskers are outliers and plotted as black points.
(TIFF)

S1 Table. Granuloma data. Represents each value (in percentage) of granuloma formation, at day 3, 6, 9, from controls, cured Q fever, or sepsis PBMCs, coated with CB or BCG beads, in duplicates.
(PDF)

S2 Table. Cytokine data. Represents TNF and IL-10 values (in pg/ml) in cells supernatants for 1 day of culture, according granuloma formation, from controls, cured Q fever, or sepsis PBMCs, coated with CB or BCG beads, in duplicates.
(PDF)

S3 Table. Patient features according to granuloma formation or no granuloma formation. SOFA: sequential organ failure assessment; SAPS: simplified acute physiology score; ICU: intensive care unit. Results are expressed as absolute number and percentage or median and interquartiles, as required.
(DOCX)

Author Contributions

Conceived and designed the experiments: JT ML JLM. Performed the experiments: JA AD PB. Analyzed the data: BC JT ML JLM. Contributed reagents/materials/analysis tools: JA BC JT PB AD ML JLM. Wrote the paper: JA JT ML JLM.

References

1. Zumla A, James DG. Granulomatous infections: etiology and classification. Clin Infect Dis Off Publ Infect Dis Soc Am. 1996; 23(1):146–58.
2. Molina-Ruiz AM, Requena L. Foreign Body Granulomas. Dermatol Clin. 2015; 33(3):497–523. doi: 10.1016/j.det.2015.03.014 PMID: 26143429
3. Egen JG, Rothfuchs AG, Feng CG, Winter N, Sher A, Germain RN. Macrophage and T cell dynamics during the development and disintegration of mycobacterial granulomas. Immunity. 2008; 28(2):271–84. doi: 10.1016/j.immuni.2007.12.010 PMID: 18261937
4. Russell DG, Cardona PJ, Kim MJ, Allain S, Altare F. Foamy macrophages and the progression of the human TB granuloma. Nat Immunol. 2009; 10(9):943–8. doi: 10.1038/ni.1781 PMID: 19692995
5. Ramakrishnan L. Revisiting the role of the granuloma in tuberculosis. Nat Rev Immunol. 2012; 12 (5):352–66. doi: 10.1038/nri3211 PMID: 22517424
6. Shaler CR, Horvath CN, Jeyanathan M, Xing Z. Within the Enemy's Camp: contribution of the granuloma to the dissemination, persistence and transmission of Mycobacterium tuberculosis. Front Immunol. 2013; 4:30. doi: 10.3389/fimmu.2013.00030 PMID: 23420646
7. Puissegur MP, Botanch C, Duteyrat JL, Delsol G, Caratero C, Altare F. An in vitro dual model of mycobacterial granulomas to investigate the molecular interactions between mycobacteria and human host cells. Cell Microbiol. 2004; 6(5):423–33. PMID: 15056213
8. Delaby A, Espinosa L, Lépolard C, Capo C, Mège JL. 3D reconstruction of granulomas from transmitted light images implemented for long-time microscope applications. J Immunol Methods. 2010; 360(1–2):10–9. J Immunol Methods. 2010 Aug 31;360(1–2):10–9. doi: 10.1016/j.jim.2010.06.008 PMID: 20561526
9. Meconi S, Vercellone A, Levillain F, Payré B, Al Saati T, Capilla F, et al. Adherent-invasive Escherichia coli isolated from Crohn's disease patients induce granulomas in vitro. Cell Microbiol. 2007; 9(5):1252–61. PMID: 17223928
10. Silva-Miranda M, Ekaza E, Breiman A, Asehnoune K, Barros-Aguirre D, Pethe K, et al. High-content screening technology combined with a human granuloma model as a new approach to evaluate the activities of drugs against Mycobacterium tuberculosis. Antimicrob Agents Chemother. 2015; 59 (1):693–7. doi: 10.1128/AAC.03705-14 PMID: 25348525
11. Deknuydt F, Roquilly A, Cinotti R, Altare F, Asehnoune K. An In vitro model of mycobacterial granuloma to investigate the immune response in brain-injured patients. Crit Care Med. 2013; 41(1):245–54. doi: 10.1097/CCM.0b013e3182676052 PMID: 23128384
12. Delaby A, Gorvel L, Espinosa L, Lépolard C, Raoult D, Ghigo E, et al. Defective monocyte dynamics in Q fever granuloma deficiency. J Infect Dis. 2012; 205(7):1086–94. doi: 10.1093/infdis/jis013 PMID: 22351939
13. Calandra T, Cohen J, International Sepsis Forum Definition of Infection in the ICU Consensus Conference. The international sepsis forum consensus conference on definitions of infection in the intensive care unit. Crit Care Med. 2005; 33(7):1538–48. PMID: 16003060
14. Hotchkiss RS, Monneret G, Payen D. Sepsis-induced immunosuppression: from cellular dysfunctions to immunotherapy. Nat Rev Immunol. 2013; 13(12):862–74. doi: 10.1038/nri3552 PMID: 24232462
15. Debets JM, Kampmeijer R, van der Linden MP, Buurman WA, van der Linden CJ. Plasma tumor necrosis factor and mortality in critically ill septic patients. Crit Care Med. 1989; 17(6):489–94. PMID: 2721208
16. Hotchkiss RS, Karl IE. The Pathophysiology and Treatment of Sepsis. N Engl J Med. 2003; 348 (2):138–50. PMID: 12519925
17. Meisel C, Schefold JC, Pschowski R, Baumann T, Hetzger K, Gregor J, et al. Granulocyte-macrophage colony-stimulating factor to reverse sepsis-associated immunosuppression: a double-blind, randomized, placebo-controlled multicenter trial. Am J Respir Crit Care Med. 2009; 180(7):640–8. doi: 10.1164/rccm.200903-0363OC PMID: 19590022
18. Leone M, Bechis C, Baumstarck K, Lefrant JY, Albanèse J, Jaber S, et al. De-escalation versus continuation of empirical antimicrobial treatment in severe sepsis: a multicenter non-blinded randomized

noninferiority trial. Intensive Care Med. 2014; 40(10):1399–408. doi: 10.1007/s00134-014-3411-8 PMID: 25091790

19. Le Gall JR, Loirat P, Alperovitch A, Glaser P, Granthil C, Mathieu D, et al. A simplified acute physiology score for ICU patients. Crit Care Med. 1984; 12(11):975–7. PMID: 6499483

20. Vincent JL, Sakr Y, Sprung CL, Ranieri VM, Reinhart K, Gerlach H, et al. Sepsis in European intensive care units: results of the SOAP study. Crit Care Med. 2006; 34(2):344–53. PMID: 16424713

21. Honstettre A, Imbert G, Ghigo E, Gouriet F, Capo C, Raoult D, et al. Dysregulation of cytokines in acute Q fever: role of interleukin-10 and tumor necrosis factor in chronic evolution of Q fever. J Infect Dis. 2003; 187(6):956–62. PMID: 12660942

22. Gorvel L, Textoris J, Banchereau R, Ben Amara A, Tantibhedhyangkul W, von Bargen K, et al. Intracellular bacteria interfere with dendritic cell functions: role of the type I interferon pathway. PloS One. 2014; 9:e99420. doi: 10.1371/journal.pone.0099420 PMID: 24915541

23. Pagán AJ, Yang CT, Cameron J, Swaim LE, Ellett F, Lieschke GJ, et al. Myeloid Growth Factors Promote Resistance to Mycobacterial Infection by Curtailing Granuloma Necrosis through Macrophage Replenishment. Cell Host Microbe. 2015; 18(1):15–26. doi: 10.1016/j.chom.2015.06.008 PMID: 26159717

24. Boomer JS, To K, Chang KC, Takasu O, Osborne DF, Walton AH, et al. Immunosuppression in patients who die of sepsis and multiple organ failure. JAMA. 2011; 306(23):2594–605. doi: 10.1001/jama.2011.1829 PMID: 22187279

25. Biswas SK, Lopez-Collazo E. Endotoxin tolerance: new mechanisms, molecules and clinical significance. Trends Immunol. 2009; 30(10):475–87. doi: 10.1016/j.it.2009.07.009 PMID: 19781994

Figure S1

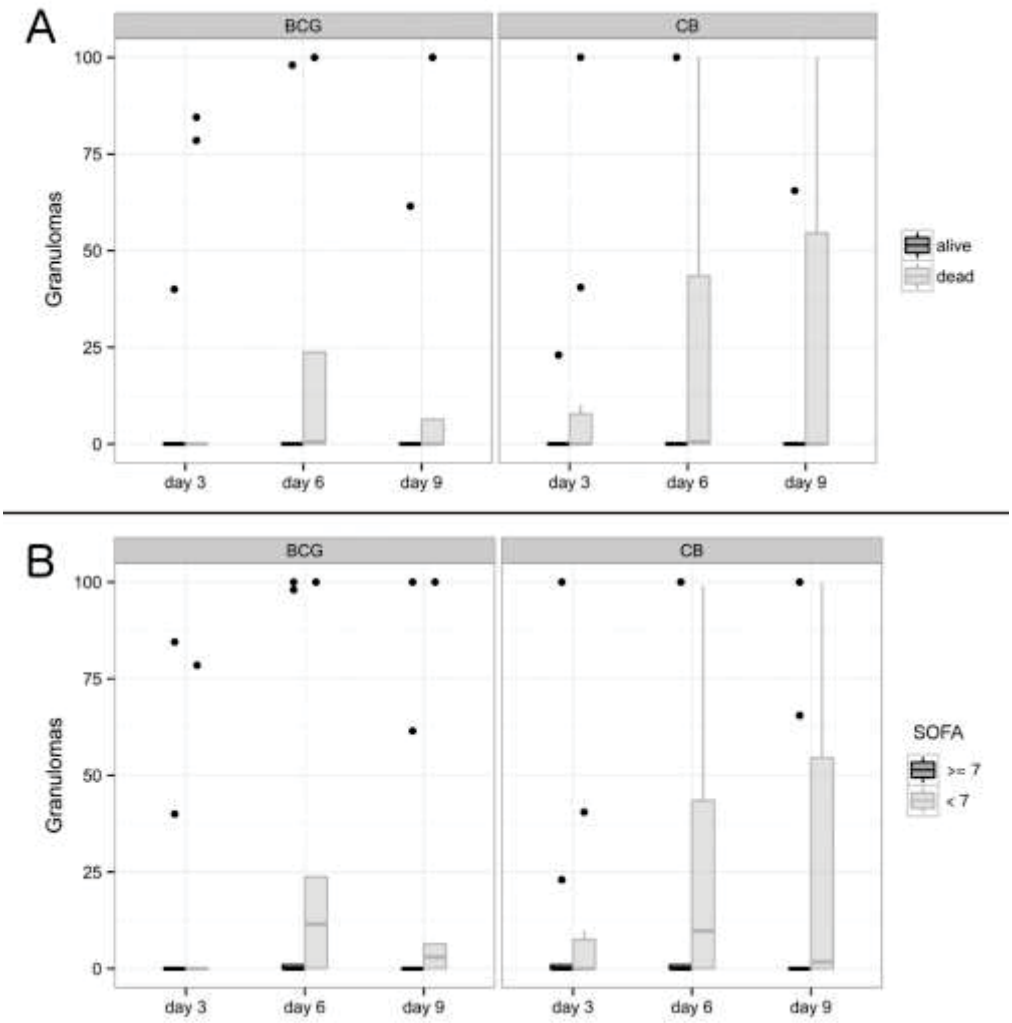
A
BCG
CB
Granulomas
100
75
50
25
0
day 3
day 6
day 9
alive
dead
B
BCG
CB
Granulomas
SOFA
>= 7
< 7

S3 Table. Patient features according according to granuloma formation or no granuloma formation.

Clinical features	Granulomas	No granulomas
Patients (Males/Females)	13 (11/2)	6 (6/0)
Age [Years]	57 [50-70]	54 [46-61]
SAPS II	40 [31-45]	37 [32-49]
SOFA	8 [6-11]	8 [5-9]
Number of ICU days	12 [6-16]	13 [9-18]
Mechanical ventilation (days)	7 [4-10]	13 [9-26]
Vasopressors use (days)	3 [3-5]	4 [2-6]
ICU Mortality (%)	5 (38)	1 (17)
Normal formula (%)	4 (31)	4 (67)
Lymphopenic (%)	7 (54)	2 (33)
Monocytopenic (%)	5 (38)	0 (0)

SOFA: sequential organ failure assessment; SAPS: simplified acute physiology score; ICU: intensive care unit. Results are expressed as absolute number and percentage or median and interquartiles, as required.

Defective granuloma formation in elderly infected patients

Aurélie Daumas[1,2], Benjamin Coiffard[1], Céline chartier[1], Amira Ben amara[1], Julie Alingrin[3], Patrick Villani[2], Jean-Louis Mege[1]

[1] Aix-Marseille Univ, IRD, APHM, MEPHI, IHU-Méditerranée Infection, Marseille, France.

[2] Service de Médecine Interne, Gériatrie et Thérapeutique, Hôpital de la Timone, Assistance Publique-Hôpitaux de Marseille

[3] Service d'Anesthésie et de Réanimation, Hôpital Nord, Assistance Publique-Hôpitaux de Marseille

Corresponding author:

Professor Jean-Louis MEGE

Aix-Marseille Université, IRD, APHM, MEPHI, IHU-Méditerranée Infection

Marseille, France

jean-louis.mege@univ-amu.fr

Soumis à Frontiers in Cellular and Infection Microbiology

La population vieillie, notamment dans les pays industrialisés avec un triplement de la population âgée de plus de 60 ans d'ici 2050. Le vieillissement est complexe associant modifications physiologiques et pathologies chroniques qui entraînent une diminution des capacités de réserve du sujet. Le vieillissement est hétérogène. En effet, tous les organes ne vieillissent pas de la même manière au sein d'une même personne et tous les individus ne sont pas égaux face au vieillissement. Le vieillissement est associé à un déclin des capacités du système immunitaire, appelé immunosénescence, touchant à la fois le compartiment inné et adaptatif. Il s'y associe un autre phénomène appelé « inflamm-aging » caractérisé par une production accrue de cytokines pro-inflammatoires [134]. L'ensemble de ces modifications diminue les capacités du patient âgé à produire une réponse immune efficace contre les agressions.

Ainsi, le sepsis est beaucoup plus fréquent dans la population âgée et est associé à deux fois plus de mortalité [135]. Deux phases sont décrites dans le sepsis à savoir tout d'abord une phase pro-inflammatoire puis une phase immunodépressive permettant le retour à l'homéostasie [136]. Des altérations du fonctionnement du système immunitaire ont été décrites au cours de la phase immunodépressive notamment une altération fonctionnelle des monocytes, une augmentation des lymphocytes T régulateurs et l'augmentation de cytokines suppressives telles que l'IL-10 [136]. La persistance de cet état est associée à un mauvais pronostic avec un risque élevé d'infections et une augmentation de la mortalité. L'avenir se tourne donc vers des traitements immunomodulateurs, cependant, l'impact du sepsis sur le système immunitaire sénescent humain est encore mal compris et nécessite d'être étudié.

Nous avons donc décidé d'utiliser la méthode de formation in vitro de granulomes pour étudier l'impact du sepsis sur le déroulement de la réponse immunitaire. Nous avons ainsi étudié la capacité de sujets âgés en bonne santé et infectés à former des granulomes en réponse à des extraits de *Coxiella burnetii* et de BCG. Nous avons inclus 23 patients âgés en sepsis et 24 patients âgés non infectés comme contrôles. La formation des granulomes a été étudiée durant les 9 jours suivant la mise en culture des PBMCs des patients avec les billes de sépharose couplées aux extraits bactériens de *Coxiella burnetii* ou *Mycobacterium bovis* (BCG).

Le résultat principal est que plus de la moitié des sujets infectés (52%) sont incapables de former des granulomes contre seulement 8% des sujets sains que ce soit en réponse à *Coxiella burnetii*

ou BCG. Sur le plan clinique, une dénutrition étaient significativement retrouvée chez les patients ne formant pas de granulome. Contrairement à l'étude chez les patients en sepsis, les sujets âgés incapables de former des granulomes ne présentaient pas de monocytopénie et/ou de lymphopénie. Ce défaut de formation était associé à un défaut de différenciation des macrophages en cellules épithélioides et en cellules géantes multinucléés. En outre, la production de TNF était diminuée sans lien avec une surexpression d'IL-10. Au niveau du transcriptome, tous les gènes décrits et étudiés dans la formation des granulomes [**Article 5**], à l'exception d'un gène impliqué dans la polarisation M1 des macrophages, étaient sous-exprimés chez les patients ne formant pas de granulome par rapport aux patients en formant.

Ainsi, cette méthode semble être un excellent outil d'évaluation de la capacité du système immunitaire dans son ensemble à répondre à une agression. En objectivant dès J3, l'incapacité des PBMCs d'un patient à former des granulomes, cela pourrait amener à adapter la prise en charge du patient.

Abstract

Granulomas are compact structures formed in tissues by the immune system in response to aggressions. The *in vitro* generation of granulomas using circulating mononuclear cells is an innovative method to easily assess the immune status of patients. Monitoring the immune response in infected elderly patients would help improve their therapeutic management. Circulating mononuclear cells from 23 elderly patients with sepsis and 24 healthy elderly patients were incubated with Sepharose beads coated with either BCG or *Coxiella burnetii* extracts. The formation of granulomas was measured over 9 days.

Most healthy elderly patients (92%) were able to form granulomas in response to BCG and *C. burnetii* extracts compared to only 48% of infected elderly patients. Malnutrition was significantly associated with impaired granuloma formation in healthy and infected patients. Granulomas typically comprise epithelioid cells and multinucleated giant cells, however, these cells were not detected in samples obtained from patients unable to form granulomas. We also found that the impairment of granuloma formation was associated with reduced production of tumor necrosis factor without overproduction of interleukin-10. Finally, all genes specifically modulated in granulomatous cells were down-modulated in patients with defective granuloma formation. TNFSF10 was the only M1 gene markedly upregulated in patients who did not form granulomas. These results suggest that defective granuloma formation may be a marker of altered activation of immune cells in elderly patients accounting for the difficulty in clearing infections and the predisposition to nosocomial infections.

Keywords: sepsis, elderly patient, granuloma, tumor necrosis factor, multinucleated giant cell

INTRODUCTION

Granulomas are organized collections of immune cells that reflect tissue immune response to aggressions. They are dynamic structures based on the recruitment of monocytes, macrophages, and T lymphocytes, and the subsequent differentiation of macrophages into epithelioid cells and multinuclear giant cells (MGCs). Granulomas have a significant protective function but can also be pathogenic [1,2]. Their main function is to isolate bacteria or other pathogens from the body and facilitate their destruction by granulomatous cells. Tuberculous granulomas contain primarily monocyte-derived macrophages and epithelioid cells surrounded by a ring of $CD4^+$ and $CD8^+$ T cells. These granulomas are also rich in MGCs generated by the fusion of activated macrophages. Cytokines and chemokines play a critical role in granuloma formation through their control of the recruitment and activation of immune cells [3]. Indeed, type 1 cytokines such as interferon (IFN)-γ, tumor necrosis factor (TNF), and interleukin (IL)-12 are involved in the acquisition of the microbial competence of macrophages and contribute substantially to the ability of the host to eradicate pathogens. Conversely, IL-10, an anti-inflammatory cytokine, negatively regulates the protective immune response [4]. In intracellular bacterial infections, $CD4^+$ T cells differentiate into T helper type 1 (Th1) effector cells that secrete IFN-γ and TNF; these mediate protection by stimulating the microbial activity of macrophages [1]. In a mouse model of mycobacterial infection, the absence of TNF and IFN-γ leads to impaired granuloma formation and increases bacterial infection [5,6]. Furthermore, the use of anti-TNF antibodies in patients highlights the role of TNF in granuloma formation. Clinical observations have revealed that anti-TNF-α treatment is associated with a risk of tuberculosis reactivation. However, we recently reported that anti-TNF antibodies do not affect the formation of granulomas but that of MGCs [7]. In humans, impaired IL12/IFN-γ predisposes patients to

mycobacterial infections and interferes with granuloma formation depending on the severity of IFN-γ impairment [8].

The study of tissue granulomas in patients requires biopsies, which cannot be performed routinely. Recently, an *in vitro* alternative was proposed. The method is based on the culture of peripheral blood mononuclear cells (PBMCs) with Sepharose beads coated with bacterial extracts from BCG, an attenuated strain derived from *Mycobacterium bovis* [9], and from *Coxiella burnetii* (CB), the causative agent of Q fever [10]. This method is convenient to study the initial phases of granuloma formation and the transcriptional signature. More than 50% of genes are commonly modulated in response to CB and BCG. They include M1-related genes such as HESX1, TNFSF10, IDO1 and TNF, and genes related to chemotaxis (CCL2, CCL5). CB strongly upmodulates the expression of genes involved in microbicidal response, especially ISGs including IFIT1. Furthermore, the expression of genes such as FASLG and GNLY involved in cell death is increased in response to BCG [11]. This approach enables the formation of granulomas to be investigated in clinical practice. Indeed, the *in vitro* formation of granulomas is defective in the majority of patients with chronic Q fever; this is related to the impaired migration of monocytes toward CB-coated beads [12]. In brain injury patients, the defective *in vitro* formation of granulomas involving monocytes, natural killer cells, and γδ T cells, is associated with increased nosocomial pneumonia [13]. In patients with severe sepsis, the defective *in vitro* formation of granulomas is related to monocytopenia and associated with reduced production of TNF [14].

Elderly individuals are at risk of contracting infectious diseases due to their declining immune system known as "immunosenescence". If the latter affects both innate and adaptive immunity, other factors likely contribute to the increased risk; these include malnutrition, comorbidities, diminished mucosal barriers, decreased cough reflex, and mechanical changes to the urinary

tract system [15,16]. The most common comorbidities that have been linked to an increased risk of infection are congestive heart failure, chronic kidney disease, diabetes mellitus, cirrhosis, chronic obstructive lung disease, and malignancies [17]. In infectious diseases, patient outcome is determined by a complex interplay between pro- and anti-inflammatory host responses [18]. In most patients, the pro-inflammatory response is self-limited. However, in patients who develop sepsis, the response is exaggerated (or "hyper-inflammatory") and leads to a compensatory downregulation of the immune system during which the patient is susceptible to organ dysfunction and nosocomial infection. The mechanisms of resistance or susceptibility of individuals are not well understood. A major risk factor appears to be some degree of pre-existing immune dysfunction. For instance, elderly patients and immunosuppressed patients both have a higher incidence of sepsis, as well as a higher mortality rate [18]. Martin et al. [19] showed that the incidence of sepsis is disproportionately higher in elderly adults and age is an independent predictor of mortality.

We hypothesized that infected elderly patients would be unable to mount an efficient immune response against pathogens. To test this hypothesis, we assessed the ability of PBMCs to generate granulomas *in vitro* in response to BCG and CB.

We found that the ability to develop an *in vitro* granulomatous response to BCG or CB was impaired in a majority (52%) of infected elderly patients whereas only 8% of healthy patients did not form granulomas. The defective formation of granulomas was associated with decreased formation of epithelioid cells and MGCs and reduced production of TNF. In addition, the impairment of granuloma formation was associated with a marked alteration in the activation of granuloma cells without polarization of macrophages.

MATERIALS AND METHODS

Study population

Patients recruitment was provided from an ancillary study to NCT02734017. Written informed consent was obtained from the patients or their relatives. Patients from the geriatric unit at Timone Hospital in Marseille, France were enrolled from January 1st 2015 to April 30th 2016 according to the following criteria: aged over 65 years with at least three chronic illnesses or over 75 years and with presence or absence of sepsis without organ failure lasting for less than 48 hours requiring empirical antimicrobial treatment. We included 23 infected patients with different pathogens and sources of infection and 24 patients without infection as healthy patients. The latter were devoid of immunodeficiency, cancer in the previous 5 years, and immunosuppressive and immunomodulatory drugs. At the time of blood collection, we also collected demographic variables, comorbidities, biological data, and the source of infection for the infected patients. The main clinical characteristics of the 47 patients enrolled are summarized in **Table 1**.

Mononuclear cell isolation

EDTA-anticoagulated blood samples (5 mL) were collected (on day of initiation of empirical antibiotic treatment for infected patients) and immediately sent to the laboratory. Peripheral blood mononuclear cells (PBMCs) from infected patients and controls were isolated from whole blood using a Ficoll gradient (MSL, Eurobio) and suspended in RPMI 1640 containing 25 mM HEPES and 2 mM L-glutamine (Invitrogen) [14]. After centrifugation at 500 × *g,* PBMCs were washed in sterile phosphate-buffered saline (PBS, Life Technologies) and suspended (about 5 × 10^6 cells/ml) in RPMI 1640 containing 20% fetal calf serum (FCS, Invitrogen) and 10% dimethylsulfoxide, and preserved at -80°C.

Coupling of beads with bacterial extracts

CB organisms (Nine Mile strain, RSA 495) and BCG (CIP 105050) were cultured as described previously [9]. The bacteria (10^9 per assay) were sonicated in a coupling buffer (0.1 M NaHCO3 pH 8.3 containing 0.5 M NaCl) and their protein content was determined using Bradford's method (BioRad protein assay). Cyanogen-bromide (CN-Br)-activated Sepharose 4B beads 40 to 100 μm in diameter (GE Healthcare, France) were suspended in 1 mM HCl for 15 min and then washed in a coupling buffer according to the manufacturer's instructions.

Bacterial extracts (0.5 mg of protein corresponding to about 2.5×10^8 bacteria) were added to 10 mg (4×10^4 beads) of beads and the mixture was rotated overnight at 4 °C in a coupling buffer. After centrifugation at 120 × *g* for 10 min, the coupling efficiency of the bacterial extracts was determined by measuring the protein content of the supernatants. The beads were then extensively washed, and the remaining CN-Br active groups were blocked by incubating the beads with 0.1 M Tris–HCl buffer pH 8.0 for 2 h. After centrifugation at 120 × *g* for 10 min, the beads were washed again three times in acetate and Tris-HCl buffers. The beads were finally stored at 4 °C in phosphate-buffered saline for a month.

Granuloma formation

In vitro granuloma formation was assessed after incubation of 2.5 x 10^5 PBMCs with 50 Sepharose beads coated with either CB or BCG extracts in 96-well plates containing RPMI 1640 medium supplemented with 25 mM HEPES, 2 mM of L-glutamine, 10% FCS, and antibiotics at 37°C. The formation of granulomas was evaluated after 3, 6, and 9 days of culture using inverse microscopy (DIM3000 B, Leica). Only beads completely covered with cells were considered granulomas. All the wells (3 per experiment) were examined under an optical microscope to determine the number of granulomas. The results were expressed as the percentage of granulomas in relation to the number of beads in the well.

Cell characterization

May-Grünwald Giemsa (Sigma, France) staining was used to identify epithelioid cells and MGCs in dissociated granuloma cells. The percentage of epithelioid cells and MGCs was quantified using an inverted microscope after 3, 6, and 9 days of culture.

Dissociated granuloma cells (5 x 10^5) were also analyzed using flow cytometry. PBMCs were labeled with a mixture of the following fluorescent antibodies: CD3-PC5 (Beckman Coulter, France), CD4-APC (Dako, France), CD8-PE (Beckman Coulter, France), CD68-FTIC (Dako, France), and CD45-APC H7 (Becton Dickinson Biosciences, France) with isotype-matched fluorophore-conjugated immunoglobulin G (IgG) for the controls. Cell populations were identified using a CANTO II flow cytometer (Becton Dickinson Biosciences) and DIVA BD software (San Jose, CA) was used to analyze the data.

In patients unable to form granulomas, the cells were recovered and analyzed in the same way as the granuloma cells.

Cytokine measurement

PBMCs (2.5 x 10^5 cells/well) were incubated with coated beads (50 beads/well) and the supernatants were collected after 1 and 3 days. TNF and IL-10 production were measured in the supernatants using enzyme immunoassays (R&D Systems, Quantinine® ELISA kit) according to the manufacturer's instructions. The results were expressed as pg/ml. The intra- and inter-specific coefficients of variation ranged from 5% to 10%.

RNA Extraction and Real-time quantitative RT-PCR *(qRT-PCR)*

Granuloma cells were dissociated by incubation in PBS buffer containing 2 mM EDTA (Invitrogen). Total RNA from granuloma cells was extracted and treated with DNase using the RNeasy® Mini Kit (Qiagen). Reverse transcription of 150 ng of total RNA was performed as

described previously [20]. We assessed the expression of nine M1 (TNFSF10, IL15RA, IDO1, IL2RA, TNF, IL15, EDN1, HESX1, CXCL29), seven M2 (ALOX15, FN1, CCL23, CCL13, CLEC4, CSTE, HRH1), and four granulomatous genes (EPBH2, FASLG, GNLY, IFIT1) in granuloma cells in response to CB and BCG, as previously studied [11]. All selected primers were designed using Primer3 (version 0.4.0; http://bioinfo.ut.ee/primer3/). Quantitative PCR was performed using LightCycler FastStart DNA Master^{PLUS} SYBR Green I (Roche). The results were normalized with the housekeeping gene β-actin. The fold change (FC) of the target genes relative to β-actin was computed using the formula $FC = 2^{-\Delta\Delta Ct}$, where $\Delta\Delta Ct = (Ct_{Target} - Ct_{Actin})_{stimulated} - (Ct_{Target} - Ct_{Actin})_{unstimulated}$ [20].

Statistical Analysis

Quantitative data are presented as the mean with range or standard deviation. Qualitative data are presented as absolute counts and percentages. Results between groups were compared using the Mann-Whitney U test. Differences were considered significant when $p < 0.05$. Data analysis was performed, and plots were generated using GraphPad Prism 5 (GraphPad Software Inc).

RESULTS

Patient characteristics

The characteristics of the study population are shown in **Table 1.** Twenty-three infected patients (14 women and 9 men) with an average age of 81.7 years and 24 healthy patients (13 women and 11 men) with an average age of 84.6 years were included. The leukocyte and neutrophil counts were significantly ($p < 0.001$) higher in infected patients than in healthy patients, whereas the monocyte and lymphocyte counts were not significantly different. C-reactive protein and albumin levels were significantly ($p < 0.001$) higher and lower, respectively, in infected patients. The most frequent infections were urinary tract infections (8 patients) and

pneumonia (6 patients). The microbial etiology was identified in only 50% of infected patients and consisted mainly of gram-negative bacilli (n = 8). No patient had a medical history of tuberculosis or Q fever.

Defective formation of granulomas in infected patients

We wondered if the occurrence of infection in elderly subjects was associated with impaired granuloma formation. PBMCs from healthy patients and infected patients were incubated with beads coated with BCG and granuloma formation was measured for 9 days (**Figure 1A**). The great majority of healthy patients (22 out of 24, 92%) were able to form granulomas, whereas only 48% of infected patients were. The defective formation of granulomas in infected patients was not due to a delayed formation because the formation of granulomas was significantly lower in infected patients than in healthy patients at days 3, 6, and 9 ($p < 0.001$) (**Figure 1B**). After cultivating PBMCs with BCG-coated beads for 3 days, the formation of granulomas was significantly lower in infected patients (22 ± 36%), whereas it reached 42 ± 40% in healthy patients. The defective formation of granulomas was not due to a delayed formation because it remained lower in infected patients than in healthy patients after 6 days (50 ± 42% vs 74 ± 31%) and 9 days (49 ± 45% vs 72 ± 33%). Interestingly, when CB-coated beads were used instead of BCG-beads, the patients who did not form granulomas in response to BCG extracts were also unable to form granulomas in response to CB extracts. After 3 days of culture of PBMCs with CB-coated beads, the formation of granulomas was also significantly low in infected patients. The defective formation of granulomas was not due to a delayed formation since it remained lower in infected patients than healthy patients after 6 and 9 days (**Figure 1C**). The comparison of granuloma formation in response to BCG and CB extracts did not show any significant difference, except at day 9 for healthy patients for whom the granuloma percentage was significantly lower in response to CB extracts than in response to BCG (**Figure**

2). Taken together, these results show that the ability to develop an *in vitro* granulomatous response to BCG or CB extracts was altered in infected elderly patients. Given these results, the following experiments were performed with BCG-coated beads only.

Granuloma formation and patient characteristics

As infected patients were partitioned into two populations able or unable to form granulomas, we wondered if impaired granuloma formation was associated with some clinical and/or biological features of patients (**Tables S1 and S2**). We found that infected female patients were more prone to forming granulomas than their male counterparts. This gender effect was not observed in healthy patients. Among the clinical parameters, malnutrition was significantly associated with impaired granuloma formation in both healthy and infected patients ($p = 0.02$). The inflammatory status as assessed by the CRP level was not significantly different in infected patients who did or did not form granulomas. Leukocyte and neutrophil counts were significantly higher in healthy patients who formed granulomas than in patients who did not form granulomas. No difference was found in infected patients. So, except malnutrition, no significant difference was found between patients with and without granuloma formation. Hence, clinical and biological parameters were not sufficient to account for impaired granuloma formation.

Cell composition of granulomas

We wondered whether the cellular composition of granulomas was altered in patients. First, we measured the proportion of cell populations placed in culture from patients who would form granulomas and those who would not. The proportion of monocytes and $CD4^+$ and $CD8^+$ T lymphocytes determined using flow cytometry was similar between healthy patients and infected patients regardless of their capacity to form granulomas or not (data not shown).

In the absence of granuloma formation, the proportion of monocytes and T cells did not change during the culture. In the presence of granuloma formation in response to BCG, $CD4^+$ T lymphocytes steadily increased during the culture with BCG-coated beads, whereas $CD8^+$ T cells moderately decreased during the same time. No difference was observed between infected and healthy patients. Monocytes from each group decreased during the 9 days of culture; this is related to their macrophage maturation (data not shown).

As granulomas are known to be rich in epithelioid cells and MGCs (**Figures 3A and 3B**), their presence was assessed using May-Grünwald-Giemsa staining after 3, 6, and 9 days. When cultured mononuclear cells were unable to form granulomas, especially in infected patients, neither epithelioid cells nor MGCs were found. When granulomas were formed, epithelioid cells and MGCs were detected from day three and reached almost 25% and 4% of granulomatous cells, respectively, on day 9 in healthy patients (**Figure 3C**). In infected patients, epithelioid cells represented on average 13% of the granuloma cells on day six then decreased to reach about 10% after 9 days. Concerning MGCs, they did not exceed 2% after 6 days of culture then decreased (**Figure 3D**). Thus, granulomas of healthy patients contained significantly more epithelioid cells and MGCs than granulomas of infected patients ($p = 0.04$ and $p = 0.02$, respectively). Taken together, these results showed that the defective formation of granulomas was associated with deficient epithelioid cell and MGC formation.

Cytokines and deficient granuloma formation in infected patients

As the defective formation of granulomas in infected patients may be associated with a decrease in inflammatory cytokines, we measured the release of TNF and IL-10 by cells incubated with BCG-coated beads for 1 and 3 days. First, we noticed that the amounts of TNF in the supernatants were lower on day 3 compared with the results on day 1. The amounts were significantly lower in healthy patients and infected patients who did not form granulomas than

in healthy patients and infected patients with granuloma formation on day 1 as well as on day 3 ($p < 0.05$ for healthy patients and $p < 0.001$ for infected patients) (**Figure 4**). The decrease in production of TNF may be related to an increase in production of an immunosuppressive cytokine such as IL-10. Therefore, the amounts of IL-10 in the supernatants were measured. They were low and similar in infected and healthy patients with or without granuloma formation (**Figure 4**). Taken together, these results suggested that the defective formation of granulomas was associated with a decrease in TNF production and not an increase in IL-10 production.

Gene expression programs and deficient granuloma formation in infected patients

As the alteration in granuloma formation was related to TNF deficiency, we investigated the activation status of granulomatous cells in individuals who formed granulomas. We collected cells from granulomas after dissociation in eight patients who formed granulomas (5 infected patients and 3 healthy patients) and assessed the expression of a panel of nine M1, seven M2, and four granulomatous genes, as reported previously [11]. In patients who formed granulomas, M1, M2, and granulomatous genes were upregulated, suggesting strong activation of granulomatous cells without M1 or M2 polarization (**Figure 5A**). It is noteworthy that in patients who did not form granulomas (n=3), the expression of M1, M2, and granulomatous genes was markedly depressed, with the exception of TNFSF10 (**Figure 5B**). Hence, the granulomas formed in healthy individuals and infected patients exhibited normal activation profiles. Healthy and infected patients with impaired formation of granulomas are associated with a profound alteration in the activation program of immune cells.

DISCUSSION

Elderly patients are susceptible to infection and the risk of complications is higher when they are infected. Several factors affect the prognosis of infected elderly patients such as immunosenescence-associated immunosuppression, age-related organ changes, comorbidities,

malnutrition or polypharmacy [21]. We hypothesized that infected elderly patients were unable to mount an efficient immune response against pathogens and we proposed answering this question by measuring the *in vitro* formation of granulomas using beads covered with BCG [8] and CB [9] extracts.

We showed that granuloma formation was impaired in infected patients compared to healthy patients in response to both BCG and CB extracts. To exempt our data from the constraints of prior immunization, we compared granuloma formation in response to BCG to which a majority of individuals are immunized and CB to which a minority of individuals are immunized. Clearly, our results are not dependent on prior immunization as the modulation of BCG and CB granulomas was similar. This result is consistent with defective granuloma formation observed in patients with severe sepsis [14]. Likewise, PBMCs from brain-injured patients with nosocomial pneumonia generated significantly fewer granulomas compared with brain-injured patients without nosocomial pneumonia and healthy donors [13].

Deficient granuloma formation was observed in a large proportion (48%) of infected patients and a minority of healthy patients (8%). No relationship was found between defective granuloma formation and age, sex or comorbidities. Clinically, only malnutrition was significantly associated with the impairment of granuloma formation. Malnutrition can be defined as the state of being poorly nourished. The causes of malnutrition are extremely varied, and can be divided into three main types: medical, social, and psychological. For example, ageing is frequently associated with decreases in taste acuity and smell, deteriorating dental health, and decreases in physical activity, which may all affect nutrient intake. Malnutrition primarily leads to a decrease in T cells. The number of $CD4^+$ T cells from spleens of fasted mice is 40 to 50% lower compared to fed control animals [22]. Other studies have shown that mice fed a protein-deficient diet exhibit lower T cell numbers compared to chow-fed control mice [23,24]. A similar observation was made in humans. Malnourished children have lower

circulating $CD4^+$ and $CD8^+$ T cell numbers compared to well-nourished children [25]. The decrease in immune cell numbers during malnutrition contributes to a devastating effect on the ability of the immune system to mount a successful immune response to infection. This accounts for increased susceptibility to microbial pathogens such as influenza, *M. tuberculosis*, *Streptococcus pneumonia*, and gastrointestinal infection microbes in malnourished individuals [26,27]. A relationship between defective granuloma formation and monocyte and lymphocyte counts has been reported in the absence of malnutrition. In patients with severe sepsis, we showed that defective granuloma formation was associated with monocytopenia, whereas brain-injured patients experienced lymphopenia with a non-significant trend toward a lower lymphocyte count in patients with nosocomial pneumonia compared with patients without infection [13,14].

We showed previously that monocytes migrate to the beads, mature into macrophages, then progress to epithelioid cells and MGCs under the influence of lymphocytes [10]. We wondered if the cell composition of granulomas was affected by infection in elderly patients. We found that when mononuclear cells did not form granulomas, neither epithelioid cells nor MGCs were found. When mononuclear cells formed granulomas, the number of epithelioid cells and MGCs in infected elderly patients was lower than in granulomas of healthy patients. This alteration of granuloma organization is consistent with other reports. In brain-injured patients, the percentage of MGCs was lower in patients, especially with infection, compared with healthy donors [13]. These results suggest that the maturation process of macrophages is impaired in infected patients.

As many reports have established a relationship between cytokine production and granuloma formation, including the presence of epithelioid cells and MGCs, we investigated pro/anti-inflammatory cytokine imbalance. TNF is necessary for the formation of granulomas and Il-10 is involved in the inhibition of macrophage activation and high levels are associated with a

disorganization of granulomas [2,28]. We found that TNF release decreased in PBMCs from patients unable to form granulomas with no increase in IL-10, suggesting that the modulation of TNF production was not related to the overproduction of IL-10. The same results were obtained in patients with severe sepsis [14]. Several studies have highlighted through the use of TNF deficient mice or anti-TNF-α drugs that TNF-α is essential for the formation and maintenance of granulomas [29,30]. Recently, we showed that etanercept slightly delayed the formation of granulomas and reduced the generation of MGCs by inhibiting cell fusion in the same way as adalimumab treatment [7]. As the transformation and fusion of macrophages require autocrine stimulation by TNF production, the low production of TNF can explain the defective differentiation of granuloma macrophages we observed [31].

We previously reported that BCG- and CB-induced granulomas were characterized by the expression of genes related to M1 macrophage polarization and chemotaxis [11]. First, we found that polarization and granuloma formation-associated gene expression was dramatically decreased in mononuclear cells that did not form granulomas. M1, M2, and granulomatous gene expression was upregulated without polarization in patients who formed granulomas. The lack of polarization may be related to immunosenescence.

Altogether, we have shown that infection in elderly patients decreases granuloma formation and reduces the production of TNF-α and the formation of epithelioid cells and MGCs. This study also suggests that the impact of infection on the immune response is heterogeneous in elderly patients. Further studies are necessary to understand why some patients form granulomas and others do not when they are infected.

TABLE 1. Characteristics of the Study Population

	Patients with infection (n=23)	**Patients without infection (n=24)**	***p***
Age (years) mean (min-max)	81.7 (62-100)	84.6 (74-100)	0.78
Male, n (%)	9 (39.1)	11 (45.8)	0.25
Medical history, n (%)			
Diabetes Mellitus	10 (43.5)	4 (16.6)	0.06
Malnutrition	4 (17.4)	1 (4.2)	0.16
Chronic lung disease	1 (4.3)	2 (8.3)	0.56
Cardiac insufficiency	6 (26.1)	7 (29.2)	0.75
Dementia	5 (21.7)	9 (37.5)	0.21
Number of circulating cells on admission			
Leukocytes (Giga/L) mean [min-max]	10.3 [4.4-20]	6.7 [4.4-11]	<0.001 *
Lymphocytes (Giga/L) mean [min-max]	1.3 [0.44-3.6]	1.7 [0.62-3.6]	0.09
Neutrophils (Giga/L) mean [min-max]	8.1 [3-17]	4.4 [2.1-9.6]	<0.001 *
Monocytes (Giga/L) mean [min-max]	0.7 [0.21-1.6]	0.7 [0.22-3.8]	0.75
CRP (mg/L) mean [min-max]	163.3 [10-449.8]	10.1 [0-48]	<0.001 *
Albumin (g/L) mean [min-max]	28.7 [18-41.8]	36.1 [29-44.3]	<0.001 *
Sources of infection, n	Urinary infection (n=8) Pneumonia (n=6) Digestive infection (n=3) Sepsis (n=3) Skin infection (n=2) Spondylitis (n=1)		
Pathogens involved, n	*Escherichia Coli (n=6)* *Proteus Mirabilis (n=1)* *Methicillin-sensitive Staphylococcus aureus (n=2)* *Klebsiella pneumoniae (n=1)* Metapneumovirus *(n=1)*		

p values for comparisons between patients with infection and healthy controls.

*$p < 0.05$

TABLE S1. Granuloma formation and characteristics of infected patients

	Infected patients forming granulomas	**Infected patients not forming granulomas**	***p***
Number of patients	11/23 (48%)	12/23 (52%)	0.77
Patients (female/male)	9/2	4/7	1
Age (years) mean (min-max)	82.9 [65-100]	80.7 [65-93]	0.59
Medical history, n Diabetes Mellitus Malnutrition Chronic lung disease Cardiac insufficiency Dementia	 3/11 0/11 0/11 3/11 2/11	 7/12 4/12 0/12 2/12 4/12	 0.14 0.02 * 1 0.56 0.43
Leukocytes (Giga/L) mean [min-max]	12 [5.9-20]	9.2 [6.7-12]	0.12
Neutrophils (Giga/L) mean [min-max]	9.8 [4.5-17]	7.0 [3.9-10]	0.06
Monocytes (Giga/L) mean [min-max]	0.9 [0.33-1.6]	0.6 [0.21-1.3]	0.1
Lymphocytes (Giga/L) mean [min-max]	1.3 [0.44-3.6]	1.4 [0.8-2.3]	0.8
C-reactive protein (mg/L) mean [min-max]	195.3 [36.2-449.8]	143.1 [10-337]	0.25
Albumin (g/L) mean [min-max]	29.5 [19-41.8]	27.9 [18-34.6]	0.57
Sources of infection, n	Urinary infection (n=2) Pneumonia (n=3) Digestive infection (n=2) Skin infection (n=2) Spondylitis (n=1) Sepsis (n=1)	Urinary infection (n=5) Pneumonia (n=4) Digestive infection (n=1) Sepsis (n=2)	
Pathogens involved, n	4/10 *E. coli* (n=3) *S. aureus* (n=1)	7/12 *E. coli* (n=3) *S. aureus* (n=1) *P. mirabilis* (n=1) *K. pneumoniae* (n=1) Metapneumovirus (n=1)	

p values for comparisons between infected patients that formed granulomas and infected patients that did not form granulomas

*$p < 0.05$

TABLE S2. Granuloma formation and characteristics of healthy patients

	Healthy patients forming granulomas	Healthy patients not forming granulomas	*p*
Number of patients	22/24 (92%)	2/24 (8%)	
Patients (female/male)	12/10	2/0	0.23
Age (years) mean (min-max)	83.1 [74-100]	84 [81-87]	0.82
Medical history, n Diabetes Mellitus Malnutrition Chronic lung disease Cardiac insufficiency Dementia	 4/22 1/22 2/22 2/22 7/22	 0/2 2/2 0/2 0/2 0/2	 0.53 0.02 * 0.67 0.67 0.36
Leukocytes (Giga/L) mean [min-max]	6.8 [4.4-11]	5.55 [5.4-5.7]	0.002 *
Neutrophils (Giga/L) mean [min-max]	4.4 [2.9-9.6]	2.9 [2.6-3.2]	0.02 *
Monocytes (Giga/L) mean [min-max]	0.71 [0.29-3.8]	0.4 [0.22-0.61]	0.34
Lymphocytes (Giga/L) mean [min-max]	1.65 [0.62-3.6]	1.75 [1.2-2.3]	0.89
C-reactive protein (mg/L) mean [min-max]	8.7 [0-33]	25.0 [2-48]	0.61
Albumin (g/L) mean [min-max]	36.3 [29-44.3]	34.1 [32.3-36]	0.44

p values for comparisons between healthy patients forming granulomas and healthy patients not forming granulomas

*$p < 0.05$

Figure 1. Granuloma formation in infected and healthy patients

A

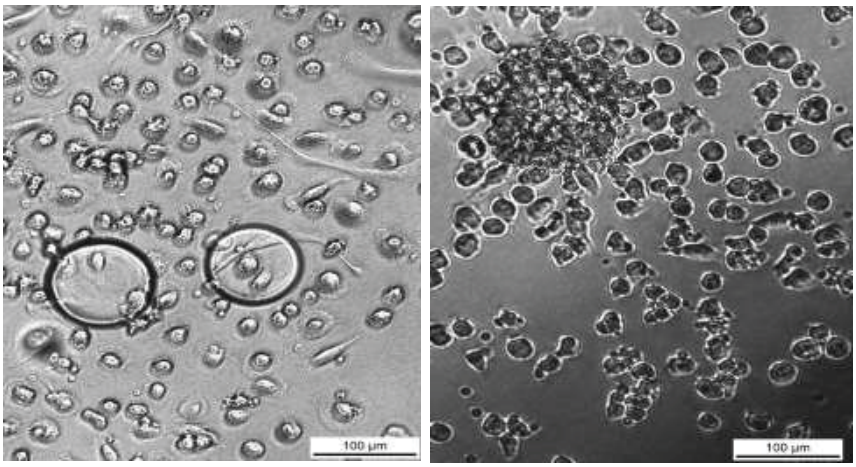

B

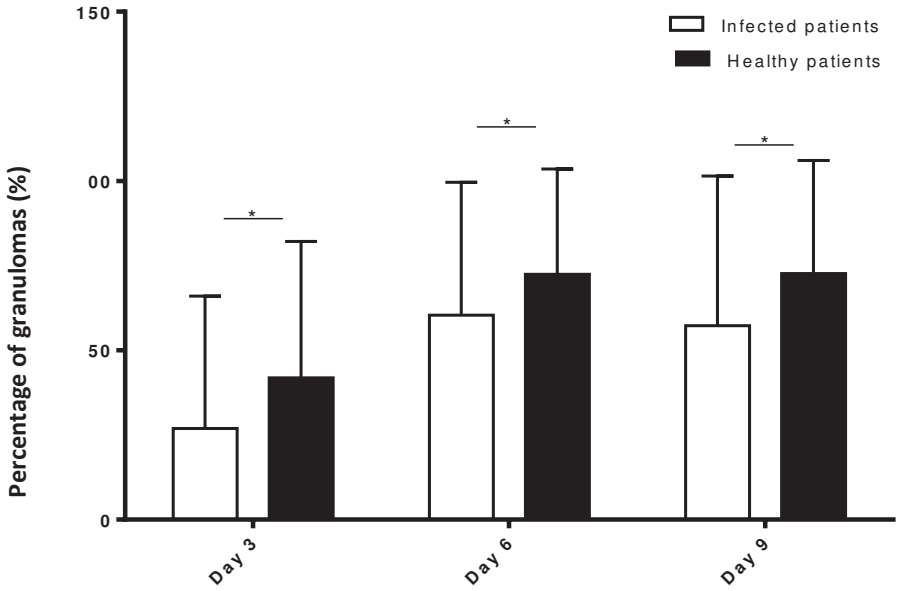

C

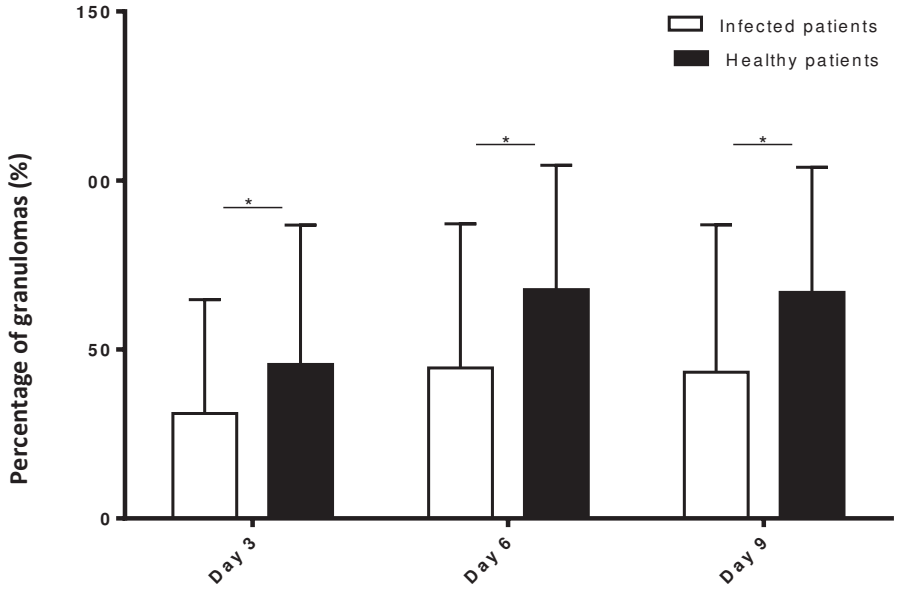

PBMCs (2.5 x $10^{5)}$ from healthy and infected patients were incubated with 50 Sepharose beads coated with bacterial extracts for 9 days. The entire content of three wells per experiment was examined under an optical microscope to determine the number of granulomas. Only beads completely covered by cells were considered granulomas.

A. Representative micrographs of beads coated with BCG with PBMCs from an infected patient with no granuloma (left) and from a healthy patient with a representative granuloma (right).

B and C. The number of generated granulomas in response to BCG extracts (B) and CB extracts (C) was enumerated and the results are expressed in percentage of bead-associated granulomas and presented as the mean ± SD. *$p < 0.05$.

Figure 2. Comparison of granuloma formation in response to BCG and CB extracts

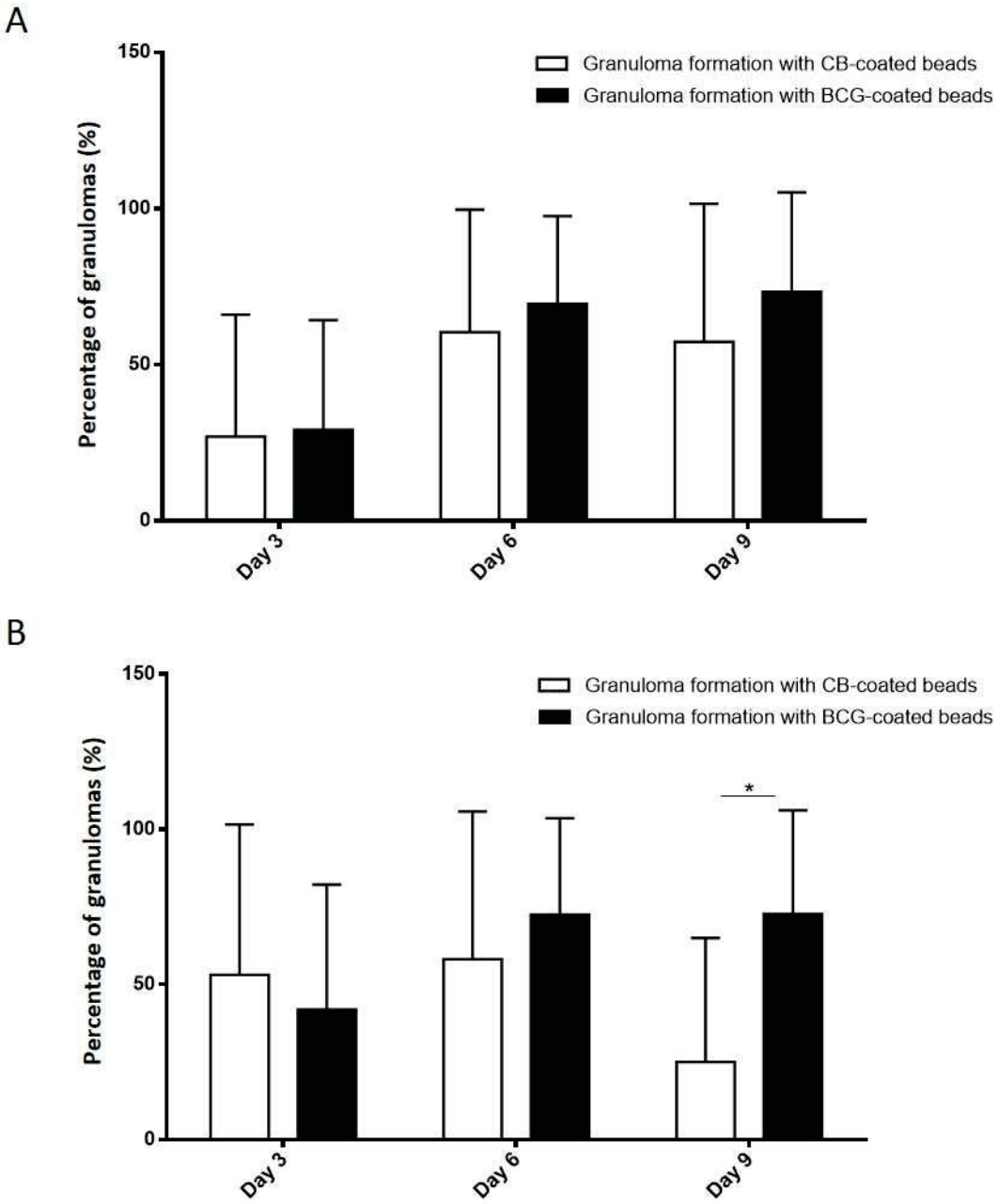

PBMCs (2.5 x $10^{5)}$ from healthy and infected patients were incubated with 50 Sepharose beads coated with bacterial extracts for 9 days. The entire content of three wells per experiment was examined under an optical microscope to determine the number of granulomas. Only beads completely covered by cells were considered granulomas. The results are expressed in percentage of bead-associated granulomas and presented as the mean ± SD. *$p < 0.05$.

A. There was no significant difference in granuloma formation in infected patients, regardless of the beads used.

B. In healthy patients, the percentage of granulomas on day 9 was significantly lower with the CB-coated beads than the BCG-coated beads.

Figure 3. Cell composition of granulomas

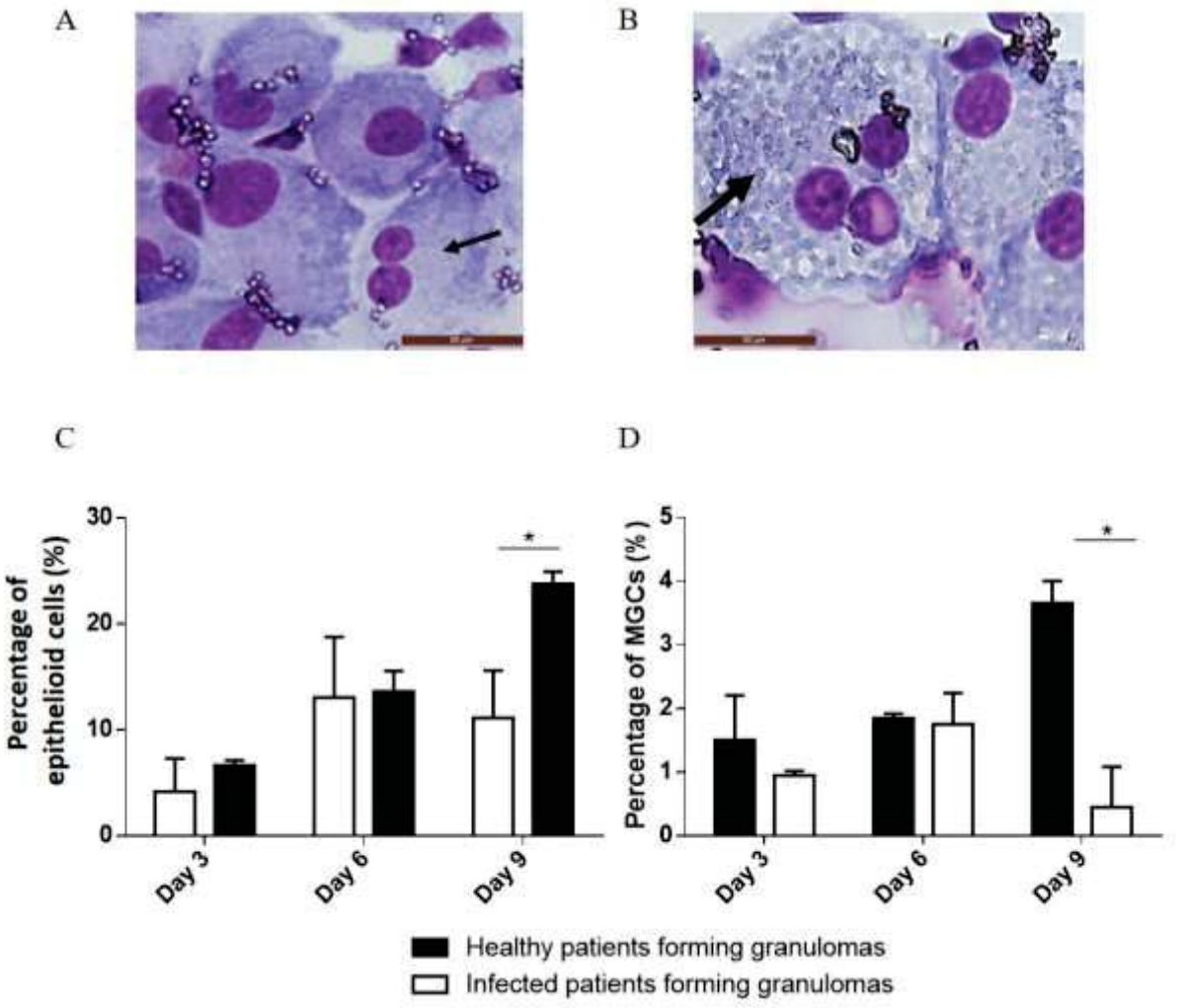

BCG-granulomas were recovered and the cells were dissociated from the beads by mechanical agitation. They were then stained using May-Grünwald Giemsa staining and observed under an optical microscope. The percentages of cells were compared between six infected patients and six healthy patients. Each experiment was performed in duplicate.

A. The black arrow indicates a typical epithelioid cell

B. The thick black arrow indicates a typical MGC

C and D. The proportion of epithelioid cells and MGCs relative to the granuloma cells was determined after 3, 6, and 9 days. The results are presented as the mean ± SD.

Figure 4. Cytokine production

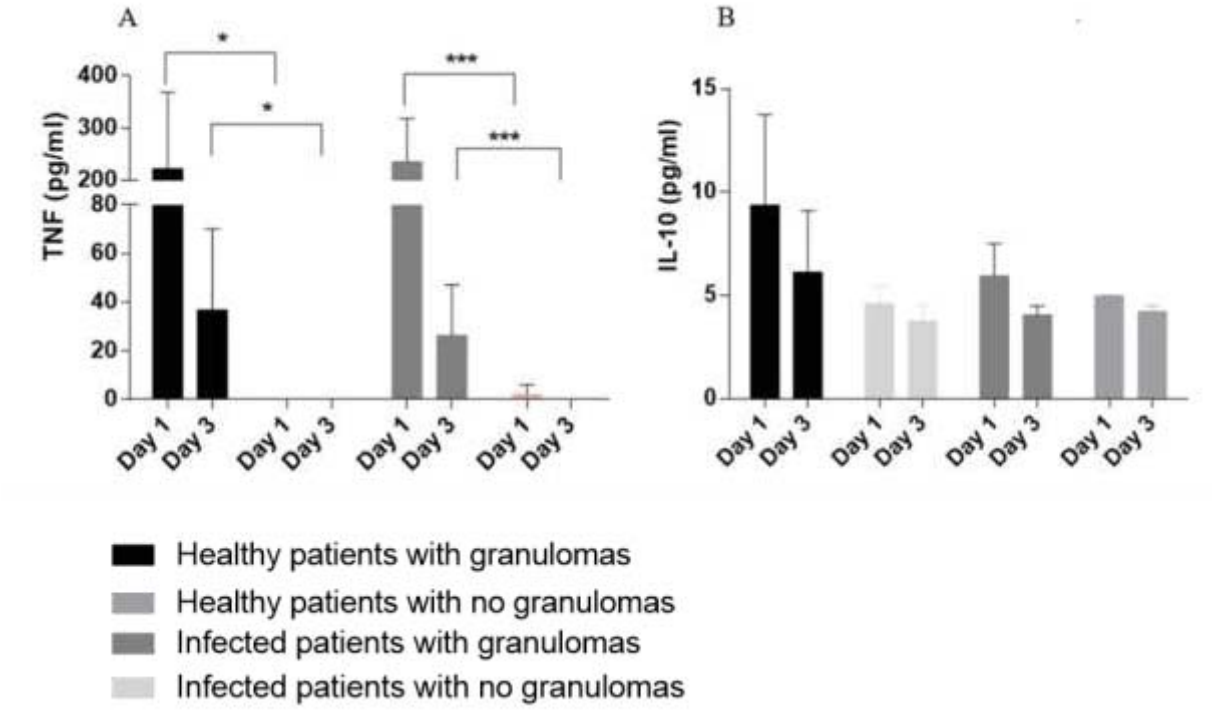

PBMCs (2.5 x $10^{5)}$ from 13 healthy patients (11 who formed granulomas and 2 who did not form granulomas) and 16 infected patients (7 who formed granulomas and 9 unable to form granulomas) were incubated with 50 Sepharose beads coated with BCG extracts for 1 and 3 days. The supernatants were collected after 1 and 3 days. TNF and IL-10 production were determined using enzyme immunoassays. The results are expressed as pg/mL and presented as the mean ± SD. * $p < 0.05$, *** $p < 0.0001$

Figure 5. Gene expression program in infected patients

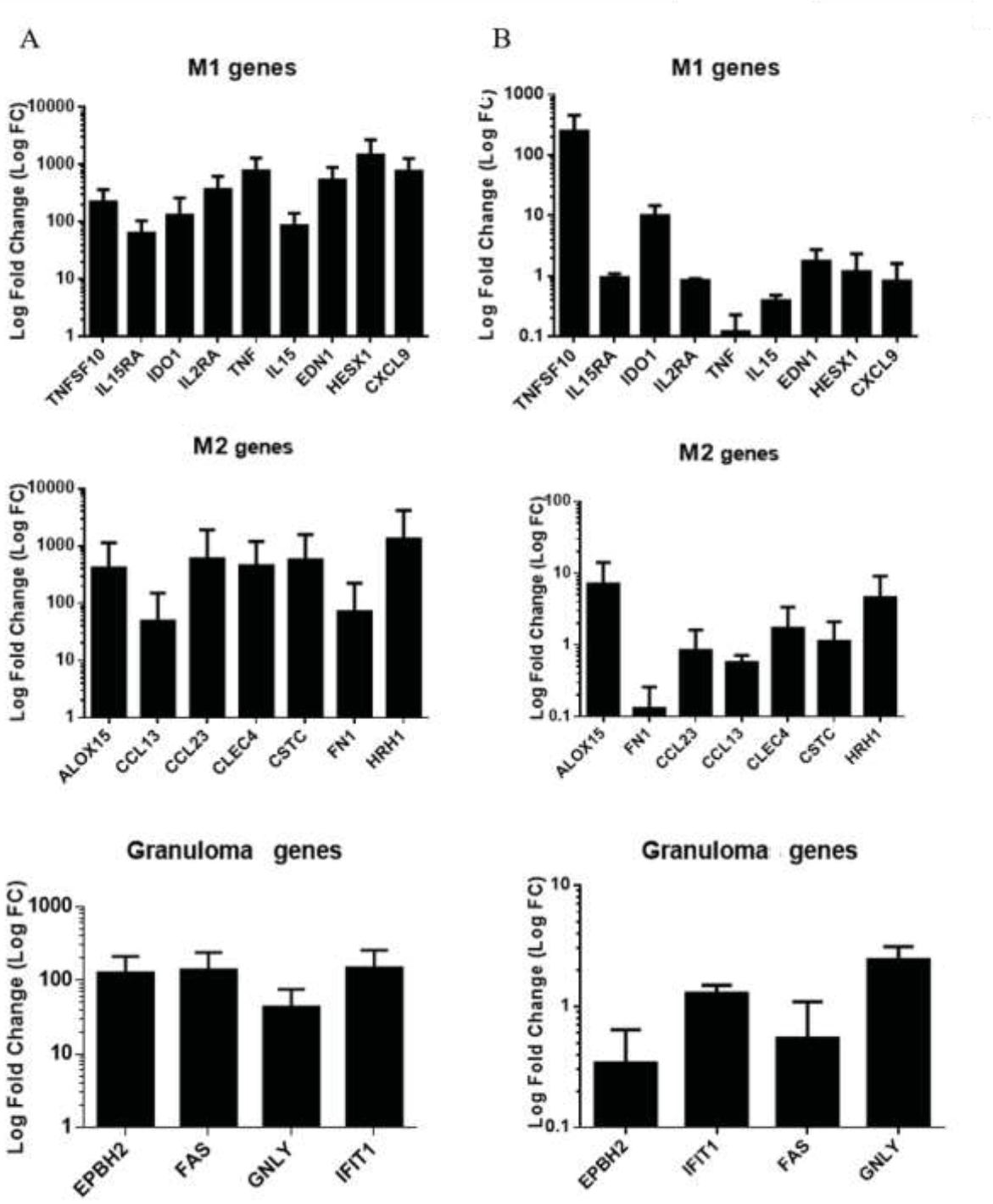

qRT-PCR was performed on a panel of M1, M2, and granulomatous genes. Gene expression was analyzed in cells from granulomas after dissociation in eight individuals (5 were infected)

who formed granulomas (A) and in mononuclear cells in three patients who did not form granulomas (2 were infected) (B). The results were normalized with the housekeeping gene β-actin. The FC of the target genes relative to β-actin was computed using the formula $FC = 2^{-\Delta\Delta Ct}$, where $\Delta\Delta Ct = (Ct_{Target} - Ct_{Actin})_{stimulated} - (Ct_{Target} - Ct_{Actin})_{unstimulated.}$ The results are expressed as the log fold change ± SD.

REFERENCES

[1] Saunders BM, Britton WJ. Life and death in the granuloma: immunopathology of tuberculosis. Immunol Cell Biol. 2007;85:103-11.

[2] Pagán AJ, Ramakrishnan L. The Formation and Function of Granulomas. Annu Rev Immunol. 2018;36:639-65.

[3] Turner MD, Nedjai B, Hurst T, Pennington DJ. Cytokines and chemokines: At the crossroads of cell signalling and inflammatory disease. Biochim Biophys Acta. 2014;1843:2563-2582.

[4] Silva Miranda M, Breiman A, Allain S, Deknuydt F, Altare F. The tuberculous granuloma: an unsuccessful host defence mechanism providing a safety shelter for the bacteria? Clin Dev Immunol. 2012;2012:139127.

[5] Gallegos AM, van Heijst JW, Samstein M, Su X, Pamer EG, Glickman MS. A gamma interferon independent mechanism of CD4 T cell mediated control of M. tuberculosis infection in vivo. PLoS Pathog. 2011;7:e1002052.

[6] Beham AW, Puellmann K, Laird R, Fuchs T, Streich R, Breysach C, Raddatz D, Oniga S, Peccerella T, Findeisen P, Kzhyshkowska J, Gratchev A, Schweyer S, Saunders B, Wessels JT, Möbius W, Keane J, Becker H, Ganser A, Neumaier M, Kaminski WE. A TNF-regulated recombinatorial macrophage immune receptor implicated in granuloma formation in tuberculosis. PLoS Pathog. 2011;7:e1002375.

[7] Mezouar S, Diarra I, Roudier J, Desnues B, Mege JL. Tumor Necrosis Factor-Alpha Antagonist Interferes with the Formation of Granulomatous Multinucleated Giant Cells: New Insights Into Mycobacterium tuberculosis Infection. Front Immunol. 2019;10:1947.

[8] Naranbhai V. The role of host genetics (and genomics) in Tuberculosis. Microbiol Spectr. 2016;4.

[9] Puissegur MP, Botanch C, Duteyrat JL, Delsol G, Caratero C, Altare F. An *in vitro* dual model of mycobacterial granulomas to investigate the molecular interactions between mycobacteria and human host cells. Cell Microbiol. 2004;6:423-33.

[10] Delaby A, Espinosa L, Lépolard C, Capo C, Mège JL. 3D reconstruction of granulomas from transmitted light images implemented for long-time microscope applications. J Immunol Methods. 2010;360:10-9.

[11] Faugaret D, Ben Amara A, Alingrin J, Daumas A, Delaby A, Lépolard C, Raoult D, Textoris J, Mège JL. Granulomatous response to Coxiella burnetii, the agent of Q fever: the lessons from gene expression analysis. Front Cell Infect Microbiol. 2014;4:172.

[12] Delaby A, Gorvel L, Espinosa L, Lépolard C, Raoult D, Ghigo E, Capo C, Mege JL. Defective monocyte dynamics in Q fever granuloma deficiency. J Infect Dis. 2012;205:1086-94.

[13] Deknuydt F, Roquilly A, Cinotti R, Altare F, Asehnoune K. An *in vitro* model of mycobacterial granuloma to investigate the immune response in brain-injured patients. Crit Care Med. 2013;41:245-254.

[14] Alingrin J, Coiffard B, Textoris J, Belenotti P, Daumas A, Leone M, Mege JL. Impaired Granuloma Formation in Sepsis: Impact of Monocytopenia. PLoS One. 2016;11:e0158528.

[15] Gavazzi G, Krause KH. Ageing and infection. Lancet Infect Dis. 2002;2:659-66.

[16] Hepper HJ, Sieber C, Walger P, Bahrmann P, Singler K. Infections in the elderly. Crit Care Clin. 2013;29:757-74.

[17] Esper AM, Moss M, Lewis CA, Nisbet R, Mannino DM, Martin GS. The role of infection and comorbidity; factors that influence disparities in sepsis. Crit Care Med. 2006;34:2576-82.

[18] Faix JD. Biomarkers of sepsis Crit Rev Clin Lab Sci. 2013;50:23-36.

[19] Martin GS, Mannino DM, Moss M. The effect of age on the development and outcome of adult sepsis. Crit Care Med. 2006;34:15-21.

[20] Ben Amara A, Ghigo E, Le Priol Y, Lépolard C, Salcedo SP, Lemichez E, Bretelle F, Capo C, Mege JL. Coxiella burnetii, the agent of Q fever, replicates within trophoblasts and induces a unique transcriptional response. PLoS One. 2010;5:e15315.

[21] Tannaou T, Koeberle S, Manckoundia P, Aubry R. Multifactorial immunodeficiency in frail elderly patients: Contributing factors and management. Med Mal Infect. 2019;49:167-72.

[22] Saucillo DC, Gerriets VA, Sheng J, Rathmell JC, Maciver NJ. Leptin metabolically licenses T cells for activation to link nutrition and immunity. J Immunol. 2014;192:136-44.

[23] Pena-Cruz V, Reiss CS, McIntosh K. Sendai virus infection of mice with protein malnutrition. J Virol. 1989;63:354164.

[24] Taylor AK, Cao W, Vora KP, De La Cruz J, Shieh WJ, Zaki SR, et al. Protein energy malnutrition decreases immunity and increases susceptibility to influenza infection in mice. J Infect Dis. 2013;207:501-10.

[25] Najera O, Gonzalez C, Toledo G, Lopez L, Ortiz R. Flow cytometry study of lymphocyte subsets in malnourished and well-nourished children with bacterial infections. Clin Diagn Lab Immunol. 2004;11:577-80.

[26] Cegielski JP, McMurray DN. The relationship between malnutrition and tuberculosis: evidence from studies in humans and experimental animals. Int J Tuberc Lung Dis. 2004;8:286-98.

[27] Verhagen LM, Gomez-Castellano K, Snelders E, Rivera-Olivero I, Pocaterra L, Melchers WJ, et al. Respiratory infections in Enepa Amerindians are related to malnutrition and *Streptococcus pneumoniae* carriage. J Infect. 2013;67:273-81.

[28] Boomer JS, Green JM, Hotchkiss RS. The changing immune system in sepsis: is individualized immuno-modulatory therapy the answer? Virulence. 2014;5:45-56.

[29] Kindler V, Sappino AP, Grau GE, Piguet PF, Vassalli P. The inducing role of tumor necrosis factor in the development of bactericidal granulomas during BCG infection. Cell. 1989;56:731-40.

[30] Roach DR, Bean AG, Demangel C, France MP, Briscoe H, Britton WJ. TNF regulates chemokine induction essential for cell recruitment, granuloma formation, and clearance of mycobacterial infection. J Immunol. 2000;168:4620-7.

[31] Takashima T, Ohnishi K, Tsuyuguchi I, et al: Differential regulation of formation of multinucleated giant cells from concanavalin A-stimulated human blood monocytes by IFN-gamma and IL-4. J Immunol. 1993;150:3002-10

Phenotypic diversity and emerging new tools to study macrophage activation in bacterial infectious diseases

Ka MB, **Daumas A**, Textoris J, Mege JL.

Front Immunol. 2014 Oct 10;5:500.

doi: 10.3389/fimmu.2014.00500. eCollection 2014. Review.

Nous avons abordé dans la plupart des articles précédents le sujet de l'état d'activation des cellules notamment des monocytes/macrophages dans différentes situations pathologiques mais aussi normales. Il semble à cet égard que le concept de polarisation M1/M2 des macrophages semble plutôt maintenant être un continuum d'états fonctionnels dépendant de l'agression, de l'environnement et évoluant ainsi dans le temps, reflétant par conséquent mieux la variabilité et complexité des réponses aux agressions. En effet, une classification M1/M2 des macrophages a été proposée il y a une vingtaine d'année sur le modèle de la polarisation lymphocytaire Th1/Th2 qui a montré depuis ses limites. Alors que les macrophages M1 sont inflammatoires, microbicides et promoteurs d'une réponse immunitaire adaptative de type Th1, les macrophages M2 régulent la réponse inflammatoire et sont fortement impliqués dans le retour à l'homéostasie. Dans la réalité, les mêmes macrophages peuvent être, dans un premier temps, inflammatoires, avant de participer à la résolution de l'inflammation. Il apparaît également que certains pathogènes comme les bactéries intracellulaires promeuvent une polarisation M2 pour pouvoir survivre dans les macrophages. De même, l'évolution chronique de certaines maladies infectieuses est liée à une reprogrammation des macrophages vers des profils M2. Ainsi, bien plus que 2 visages, les macrophages peuvent exprimer tout un panel de profils d'activation en fonction du contexte.

La tentation est également souvent grande d'appliquer cette distinction M1/M2 aux monocytes circulants, considérant qu'ils répondent de la même façon que les macrophages aux stimuli. En fait, différentes études montrent que la réponse des monocytes est différente de celle des macrophages et que leur polarisation n'est pas aussi affirmée que celle des macrophages.

A travers cette revue, nous avons voulu montrer les nombreux visages de l'activation des macrophages dans la lutte contre les infections.

frontiers in
IMMUNOLOGY

REVIEW ARTICLE
published: 10 October 2014
doi: 10.3389/fimmu.2014.00500

Phenotypic diversity and emerging new tools to study macrophage activation in bacterial infectious diseases

Mignane B. Ka[1], Aurélie Daumas[1], Julien Textoris[2] and Jean-Louis Mege[1]*

[1] *Unité de Recherche sur les Maladies Infectieuses Tropicales et Emergentes, UMR 63, CNRS 7278, IRD 198, INSERM U1095, Aix-Marseille Université, Marseille, France*

[2] *Unité Mixte bioMérieux-HCL, Hôpital Edouard Herriot, Lyon, France*

Edited by:
Laurel L. Lenz, University of Colorado School of Medicine, USA

Reviewed by:
Fulvio D'Acquisto, Queen Mary University of London, UK
Kingston H. Mills, Trinity College Dublin, Ireland

Correspondence:
Jean-Louis Mege, Faculté de Médecine, URMITE, 27 Bld. Jean Moulin, Marseille 13005, France
e-mail: jean-louis.mege@univ-amu.fr

Macrophage polarization is a concept that has been useful to describe the different features of macrophage activation related to specific functions. Macrophage polarization is responsible for a dichotomic approach (killing vs. repair) of the host response to bacteria; M1-type conditions are protective, whereas M2-type conditions are associated with bacterial persistence. The use of the polarization concept to classify the features of macrophage activation in infected patients using transcriptional and/or molecular data and to provide biomarkers for diagnosis and prognosis has most often been unsuccessful. The confrontation of polarization with different clinical situations in which monocytes/macrophages encounter bacteria obliged us to reappraise this concept. With the exception of M2-type infectious diseases, such as leprosy and Whipple's disease, most acute (sepsis) or chronic (Q fever, tuberculosis) infectious diseases do not exhibit polarized monocytes/macrophages. This is also the case for commensals that shape the immune response and for probiotics that alter the immune response independent of macrophage polarization. We propose that the type of myeloid cells (monocytes vs. macrophages) and the kinetics of the immune response (early vs. late responses) are critical variables for understanding macrophage activation in human infectious diseases. Exploring the role of these new markers will provide important tools to better understand complex macrophage physiology.

Keywords: macrophage, activation, polarization, infectious diseases, bacteria

INTRODUCTION

Why a new review about macrophage polarization during bacterial infectious diseases? The initial analysis of macrophage activation, based on *in vitro* experiments and the use of animal models, suggested a dichotomic classification based on the production of canonical molecules associated with a specific function. The production of nitric oxide is associated with the killing of microorganisms or tumor cells and characterizes M1-type macrophage response whereas the expression of arginase (production of ornithine) is associated with the repair and characterizes M2-type macrophage responses (1). The concept of M1/M2 polarization has been largely popularized because macrophage polarization was considered the reflection of Th1 and Th2 polarization of lymphocytes, although the idea that activation by T cells is required for macrophage polarization is likely incorrect (1). As the Th1/Th2 paradigm has progressively been replaced by several functional statuses over the past years, the meaning of a similar dichotomy of macrophage activation is unknown. During the last years, numerous transcriptional and/or molecular markers associated with M1- or M2-type macrophage responses were found but they did not have a clear relationship with macrophage functions, which has been a source of controversies. We feel that these new markers could provide additional important tools to better understand complex macrophage physiology. In addition, recent advances suggest that monocytes readily available in humans are not able to polarize like mature tissue macrophages. As a consequence, the increasing number of publications in which clinical cohorts are investigated with new tools of macrophage investigation allows a global analysis of the cell responses, which results in a more precise overview of the clinical data. It is likely that the concept of M1/M2 macrophages is likely insufficient to describe human infectious diseases. While M2-type infectious diseases such as leprosy and Whipple's disease represent a clinical exception; most acute (sepsis) or chronic (Q fever, tuberculosis) bacterial diseases do not exhibit polarized monocytes/macrophages. According to the analysis of Thomas Kuhn, the "paradigm" of macrophage polarization applied to human bacterial diseases suffers from abnormalities that could lead to a paradigm shift to a kinetic vision of macrophage activation.

THE MACROPHAGE POLARIZATION CONCEPT

The molecular concept of the polarization of human macrophages has been initially based on the selective expression of a few markers that have poor specificity when expressed alone. The development of high-throughput profiling technologies that enable the investigation of complex macrophage states (2) has increased the number of biomarkers associated with the M1 or M2 status (**Figure 1**). Among the papers reporting transcriptomic analysis of activated macrophages that of Martinez et al. was the most contributive (3). The authors showed that M1 and M2 polarization affect 5.2 and 0.3% of transcripts, respectively. The functional annotation reveals the enrichment with categories such as DNA transcription, protein

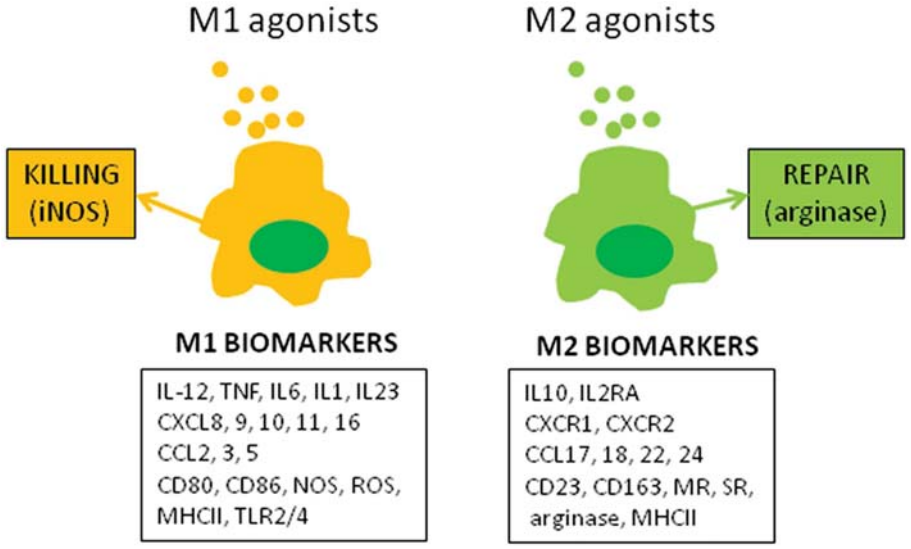

FIGURE 1 | M1 and M2 macrophage polarization. The figure represents canonical M1 and M2 agonists that induce the production of M1 and M2 markers by human macrophages *in vitro*. These markers, isolated or combined, have been used to describe the polarization of monocytes and macrophages in clinical investigations.

metabolism, G protein coupled-receptors, and lipid metabolism in addition to well-identified cytokine and chemokine families. Hence, the polarization of human macrophages has become more complex than the initial descriptions.

A recent transcriptomic analysis of human macrophages stimulated by a large panel of agonists allowed a description of macrophage activation as a spectrum. This spectrum of activation was more complex than the M1 vs. M2 model of activation because at least nine distinct activation programs were identified. The use of network analyses demonstrated a central transcriptional regulator present in all activation conditions that was complemented by regulators associated with the programs stimulated by each agonist (4). The authors used this model of activation to analyze human alveolar macrophages from patients who were smokers or from patients with chronic obstructive pulmonary disease (COPD). They found that the activation program of macrophages was more complex than predicted in smokers and in patients with COPD. They did not find enrichment with modules associated with interleukin (IL)-4/IL-13 activation in patients with COPD, as was expected, but did find a decrease in the modules associated with interferon (IFN)-γ (4). This report clearly demonstrates that the prominent, popular point of view that cigarette smoke and COPD increase M2-like characteristics (5) was not supported when high-throughput approaches were used.

A proteomics approach has also been used to investigate macrophage polarization. The MALDI-TOF mass spectrometry (MS) technique combined with gel electrophoresis permitted the identification of a large number of soluble or membrane proteins in activated macrophages. This double approach allowed the identification of an M1 signature in human macrophages stimulated with LPS and IFN-γ (6). Recently, we used MALDI-TOF MS to characterize whole eukaryotic cells (7) and the activation status of human macrophages (8). We found that whole-cell MALDI-TOF MS analysis was able to discriminate macrophages according to the type of M1 or M2 agonists and allowed for the identification of different subtypes of M1 or M2 macrophages. The MALDI-TOF MS analysis of pathogen-stimulated macrophages also enabled the detection of pathogen-associated fingerprints that did not correspond to the standard M1/M2 polarization model (8). Taken together, the use of polarization markers other than iNOS and arginase has been controversial. Recently, we proposed guidelines for macrophage activation in which we favored an approach based on a combination of markers instead of isolated canonical markers of polarization (9).

The exploration of tissue macrophages, excepted alveolar macrophages, requires biopsies in infected patients even if it is possible to identify M1 and M2 macrophages in tissues using proteomic or immunohistochemical approaches. Recently, macrophage polarization was investigated in tissues from patients with diseases characterized by a Th1 or Th2 response. M1 macrophages were defined as those expressing CD68 or CD163 with phosphorylated STAT1 (pSTAT1), and M2 macrophages were defined on the basis of the co-expression of CMAF (macrophage activation factor) with CD68 or CD163 (10). The pSTAT1 and CMAF are preferentially associated with M1 and M2 macrophages, respectively. In contrast, CD163, which was considered by several authors as an M2 specific-marker (11), was unable to discriminate M1 and M2 macrophages within pathological tissues. These findings were confirmed by a recent study in which macrophages were differentiated by granulocyte macrophage-colony stimulating factor (GM-CSF) or macrophage-colony stimulating factor (M-CSF) and secondarily polarized by IFN-γ or IL-4/IL-13; CD163 was unable to discriminate the M1 status from the M2 status (12). The investigation of macrophage activation in infected patients concerns essentially circulating monocytes that are accessible after blood collection and purification from blood, but the situation

regarding their M1/M2 polarization is complex. Using a microarray approach, we showed that M1/M2 polarization, defined by comparison with the IFN-γ and IL-4 signatures of macrophages, was transient in human monocytes, and gene expression data from published reports showed that not even small signatures of polarized macrophages were found in monocytes (13). Hence, the study of activation in tissue macrophages or circulating monocytes suffers from the lack of convenient tools, suggesting that the concept of macrophage polarization is not convenient. Among the recommendations for reporting macrophage activation, the recommendation precising how macrophages are isolated and which marker combinations are used to measure macrophage activation is likely a solution for the investigation of monocytes *ex vivo* (9).

MACROPHAGE POLARIZATION AND MICROBIOTA

The microorganisms present at the surfaces of mucosa mainly consist of commensals that have developed mutualistic relationships with hosts such as human beings. Indeed, during steady-state conditions, the microbiota influences the efficiency of digestion, controls metabolism, and affects the differentiation and functions of intestinal immune cells, including macrophages. This coevolution has been illustrated by numerous reports based on studies on germ-free animals or antibiotic-treated hosts (14–16). It has been established that the intestinal microbiota maintains a tolerant environment that allows the development of M2-like intestinal macrophages. Indeed, the macrophages from lamina propria show down-regulated expression of innate response receptors and inflammatory functions, but they retain phagocytosis and bactericidal activities (17). It is likely that commensals may directly or indirectly shape the polarization status of intestinal macrophages. Hence, *Bacteroides fragilis* and intestinal *Clostridia* are known to stimulate regulatory T cells (Tregs) and polarization toward an M2 phenotype (14). The exopolysaccharide from *Bacillus subtilis* prevents the intestinal disease associated with *Citrobacter rodentium,* and protection is transferred by peritoneal macrophages (18). The probiotic *Clostridium butyricum* promotes the development of IL-10-producing macrophages that prevent inflammatory colitis (19). Some end-products of bacterial anaerobic fermentation, such as short-chain fatty acids (α-butyrate), inhibit the inflammatory response of macrophages via a mechanism based on the inhibition of histone deacetylase (20). In contrast, intestinal commensals such as *Enterococcus faecalis* polarize colon macrophages to an M1 phenotype in a murine model in which macrophages are depleted with clodronate (21). These findings suggest that the diversity of commensal bacteria accounts for the diversity of macrophage responses. Probiotics such as *Lactobacillus* sp. or *Bifidobacterium* sp. may benefit the host (14), but we ignore their effect on macrophage polarization. The strain G-101 of *Lactobacillus brevis* inhibits the inflammatory response of mice treated by trinitrobenzenesulfonic acid. This anti-inflammatory property is related to the ability of the bacteria to prevent the expression of M1 markers and to favor M2 markers, likely via the production of IL-10 (22). For other authors, probiotics have either no effect on the polarization of RAW 264.7 macrophages as a readout (23), or these bacteria promote an activation profile of the M1-like type in THP-1 cells stimulated with lipopolysaccharide (LPS) (24). It is noteworthy that all of these studies are limited to *in vitro* experiments or animal models, and the extrapolation to human beings must be careful.

If the hypothesis that a breach of intestinal homeostasis is true, the presence of pathogenic bacteria would interfere with the polarization status of intestinal and systemic macrophages. Hence, an M1 profile would be found in patients with acute typhoid fever due to *Salmonella enterica* serovar Typhi, whereas an M2 signature would be observed in convalescent patients. The M2 response does not mean eradication of the pathogen because persistence of the M2 status favors re-infection, relapses, and development of a carrier state (25, 26). On the other hand, there is an increase in M1 and M2 markers in antrum from patients infected with *Helicobacter pylori* and uncomplicated gastritis. The presence of atrophic gastritis is associated with the expression of M1 polarization. It is predictable that shifting macrophage polarization from the M1 to M2 status is protective in chronic *H. pylori* infection. This may be reminiscent of the association of high levels of CCL18, a typical M2 marker, with prolonged survival of patients with gastric carcinoma (26, 27).

Imbalances in gut microbiota have also been associated with systemic diseases such as allergy. Recently, Kim et al. reported the induction of allergen-induced infiltration of inflammatory cells in mice treated with antibiotics. This treatment alters macrophage functions but reorients alveolar macrophages and circulating monocytes toward an M2 phenotype. This latter response is involved in allergic airway inflammation induced by allergens. Antibiotic treatment facilitates fungal overgrowth that exacerbates airway inflammation. The prostaglandin E2 produced by gut fungi is responsible for eosinophil-mediated inflammation and M2 polarization of macrophages (28). If the concept of macrophage polarization is useful for analyzing the host response to intestinal pathogens, there is no clear evidence that it is a convenient tool to measure the response to commensals and probiotics.

MACROPHAGE POLARIZATION AND ACUTE INFECTIOUS DISEASES

As sepsis is a consequence of the systemic inflammatory response to infectious aggression, it was tantalizing to consider sepsis as an M1-associated disease (25). Sepsis can also associate a secondary immunodeficiency in which the polarization of macrophages may be altered, as in LPS tolerance. Indeed, LPS-tolerant macrophages express M2 markers, but not M1 markers, and this phenotype can be reversed by IFN-γ (29). It is thought that the evolution of sepsis is characterized by a transition from an initial M1 response to a secondary M2 response. The interaction of macrophages with pathogens accounts for their initial polarization, and the M1-to-M2 transition should rather involve mechanisms of activation control such as suppressors of cytokine signaling (SOCS) proteins; SOCS1 and SOCS2 are associated with M2 macrophages whereas SOCS3 is overexpressed in M1 cells. A high SOCS1/SOCS3 expression ratio might be a biomarker of M2 cells *in vivo* (30). The fact that M2 bias is associated with the resistance of mice does not account for the poor prognosis of patients who exhibit secondary immune deficiency with an M2 phenotype. Indeed, this latter phase, named immune paralysis, is associated with increased susceptibility to nosocomial infections and late lethality (31). In patients with sepsis, the percentage of monocytes

expressing CD163 and CD206 is increased. The increase in monocytes expressing M2-like markers has been associated with a lower proportion of IFN-γ-producing T cells or with a higher proportion of Tregs in patients with sepsis. Nevertheless, enrichment with M2-type monocytes has no impact on sepsis prognosis (32). In others reports, the expression of CD163 by monocytes is accurate for discriminating patients with inflammatory presentation from those with sepsis (33), suggesting that CD163 may be a biomarker of prognosis and that the expression of CD163 by monocytes is higher in non-survivors than in survivors (34). Soluble forms of M2-type markers such as CD163 and CD206 are also increased in patients with sepsis, and their high levels are associated with poor prognosis in sepsis. Although membrane and soluble forms of CD163 share the ability to be biomarkers of prognosis in sepsis, circulating CD163 reflecting the polarization of monocytes or their activation independently of M1/M2 polarization tends to be ignored (34, 35). The measurement of monocyte activation is a partial reflection of the altered immune functions in tissues from patients with sepsis and does not assess the diversity of stimuli that they encounter from the initial pathological event. It is probably more pertinent to consider the level of monocyte activation and not the bias toward a polarized status as a biomarker.

INTERFERENCE WITH M1 POLARIZATION IN CHRONIC INFECTIOUS DISEASES: Q FEVER

As intracellular bacteria subvert host microbicidal effectors *in vitro*, we proposed that they have evolved specific strategies to interfere with M1 polarization (25). The example of Q fever is informative as we have assessed the concept of macrophage polarization in *in vitro* experiments, animal models, and patients. Q fever is a zoonosis caused by *Coxiella burnetii*, an intracellular bacterium related to *Legionellae* species, and for which the major targets are monocytes and macrophages. The severity of the infectious disease is chronic evolution with a risk of endocarditis or vascular infection (36).

The circulating monocytes exhibit a pro-inflammatory M1-type response, which is consistent with epidemiological data showing bacterial clearance in most infected patients when they are challenged by *C. burnetii in vitro*. More surprisingly, monocyte-derived macrophages are polarized toward an atypical M2-type in response to bacterial stimulation. This latter effect is characterized by the release of IL-10, transforming growth factor (TGF)-β, and CCL18 and the expression of the mannose receptor (MR) and of arginase-1, but macrophages also express IL-6 and CXCL8, two molecules that are associated with M1 polarization (37). These differences in monocyte/macrophage activation may account for the unexplained differences in bacterial survival: *C. burnetii* are unable to replicate in monocytes but replicate within macrophages (38). Similar findings were found *in vitro* with *Mycobacterium tuberculosis*, which prevents M1 polarization and activates peroxisome proliferator-activated receptor (PPAR)-γ, which is characteristic of macrophage M2 polarization (25, 39).

Nevertheless, we identified IL-10 as the only cytokine able to induce the replication of *C. burnetii* in monocytes and macrophages, suggesting that IL-10-associated M2 polarization is involved in bacterial replication and tissue persistence. The role of IL-10 in the pathogenesis of chronic infection is strengthened by the correlation of the amount of IL-10 and the chronic evolution of Q fever with the restoration of the microbicidal competence of monocytes when IL-10 was neutralized (40, 41). The engulfment of apoptotic cells by monocytes and macrophages is associated with an M2 program induced by IL-10 and favors the intracellular replication of *C. burnetii*. In contrast, treatment of these M2 polarized myeloid cells with IFN-γ and the uptake of necrotic cells suggest that the M1 program is sufficient to clear *C. burnetii* (42). The role of IL-10 is demonstrated in transgenic mice that constitutively overexpress IL-10 in the macrophage compartment and exhibit sustained infection, as in chronic Q fever. Macrophages from IL-10-overexpressing mice are unable to clear *C. burnetii* infection and exhibit an M2-type transcriptional program in which arginase, MR and Yim1/2 are increased and inflammatory markers are down-modulated (43). The infection of mice overexpressing IL-10, which mimics tuberculosis reactivation, reveals features of M2 macrophages, as reported above in *C. burnetii* infection of mice (26).

Concomitantly, we found that mice deficient for vanin-1, a membrane-anchored pantetheinase that controls tissue inflammation, are permissive for *C. burnetii* and exhibit an activation program in macrophages that is skewed toward an IL-10-associated M2 phenotype (44). Hence, IL-10-mediated polarization of macrophages is necessary for *C. burnetii* persistence in tissues.

To test the relevance of these findings in patients, we selected M1- and M2-related genes from the microarray analyses of IFN-γ and IL-4-stimulated macrophages (**Figure 2**). The expression of these genes was not different in patients with acute Q fever and healthy controls. These findings did not support the hypothesis that patients with acute Q fever, who are able to control the infection, should exhibit an M1-type phenotype. The expression of a minority of M1/M2 genes was increased in patients with Q fever endocarditis and who were unable to clear *C. burnetii* and who were expected to exhibit an M2-type phenotype (13). The analysis of the transcriptional profiles of patients with active tuberculosis shows the modulation of M1-related genes, but not that of M2 genes. Similar results were obtained in infants vaccinated with Calmette–Guerin bacillus (26, 45, 46).

In conclusion, the activation program of monocytes from patients with acute and chronic Q fever and tuberculosis cannot be reduced to an M1/M2 dichotomy. We cannot rule out that macrophages in tissues such as endocardium, lungs, or liver are polarized, as suggested by *in vitro* studies and animal models. This is illustrated by the example of pleural macrophages. Tuberculous pleural effusion, an extra-pulmonary form of tuberculosis, is associated with the M1 profile in pleural fluid that is characterized by an increase in M1 macrophages and inflammatory cytokines (47).

M2 POLARIZATION IN CHRONIC INFECTIOUS DISEASES: LEPROSY AND WHIPPLE'S DISEASE

Two infectious diseases, leprosy and Whipple's disease, which share several features such as the tropism for macrophages of *Mycobacterium leprae* and *Tropheryma whipplei*, and the role of the immune response into features of pathogenesis, are associated with M2 polarization (26). The overexpression of IL-10 is found in

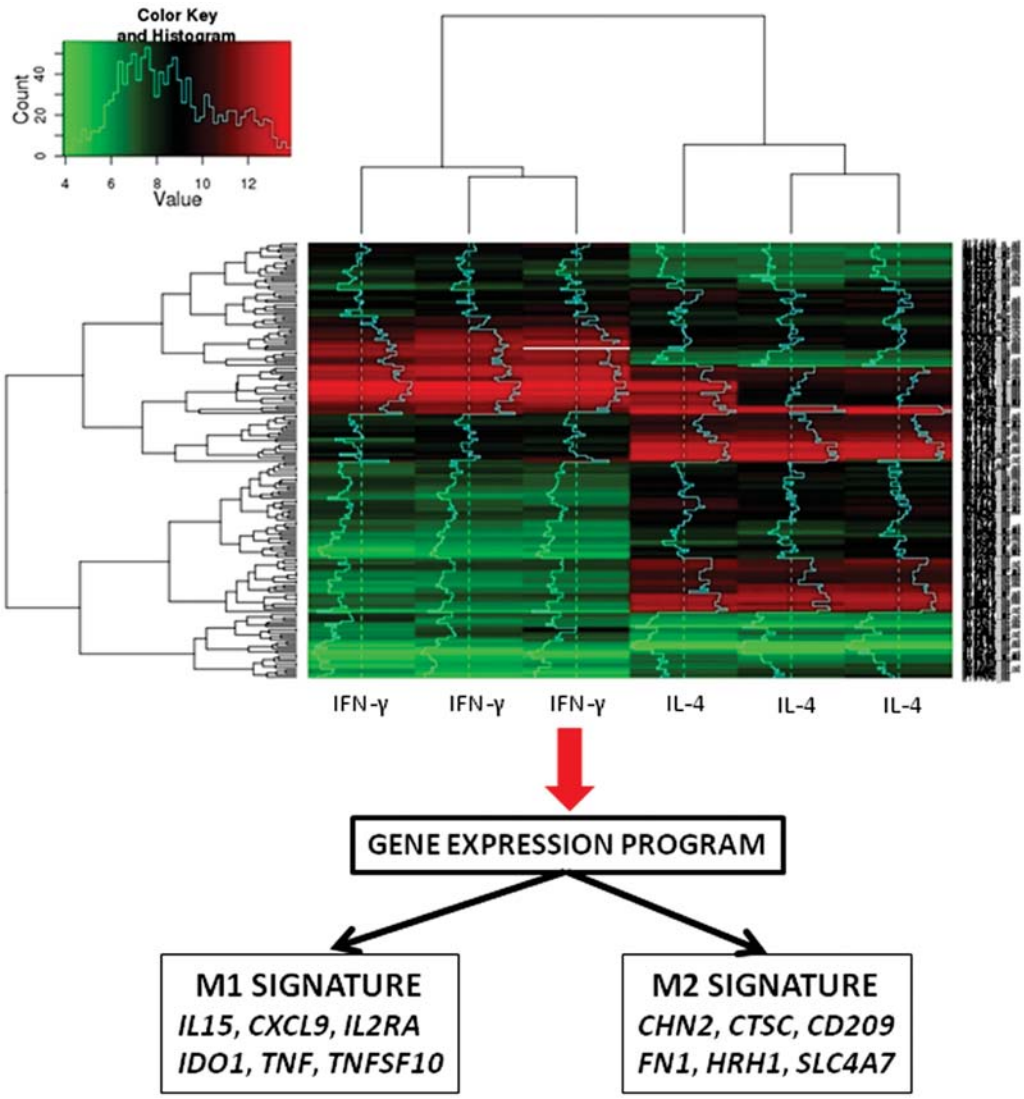

FIGURE 2 | Transcriptomic assessment of macrophage polarization. The figure represents the heat map of gene expression in IFN-γ- and IL-4-stimulated macrophages. The use of microarray enables the identification of the original M1 and M2 signatures.

lepromatous lesions and likely reflects M2 polarization. The transcriptional analysis of these lesions reveals an enrichment of M2 genes, which is in contrast to what occurs in tuberculoid lesions (48). The expression of CD163 by foamy macrophages in lepromatous lesions but not by macrophages from tuberculoid lesions has been considered strong evidence of M2 polarization in lepromatous leprosy (26). Whether this polarization is a consequence of the production of IL-10 or if it reflects a Th2 response is often ignored.

Whipple's disease is characterized by the presence of macrophages with periodic acid-Schiff inclusions within the lamina propria; these macrophages exhibit some features of macrophages from mycobacterial lesions. As described above for lepromatous leprosy, there is converging evidence that Th2 polarization of the immune response is critical for the pathophysiology of Whipple's disease. An M2 macrophage signature was observed in duodenal biopsies from one patient with intestinal Whipple's disease (49). Moos et al. reported the increased expression of CD163 on duodenal macrophages and circulating monocytes, and this finding was strengthened by an increase in IL-10 and a decrease in inducible NO synthase expression in these cells, suggesting a functional polarization toward an M2 profile (50, 51). The conclusion that IL-10 may be critical for *T. whipplei* pathogenicity was not confirmed by *in vitro* studies, in which we found an increase in IL-1β, IL-16, and type I IFN production, but not in IL-10 (52, 53). It is likely that type I IFN prevents the IFN-γ-protective effect, as reported for mycobacterial infections (54). This finding underlines the caution that must be taken regarding conclusions about polarization when based on a limited number of markers.

COMPLEXITY OF MACROPHAGE ACTIVATION IN INFECTIOUS DISEASES

The analysis of infectious disease literature (see above) reveals that modulation of monocyte/macrophage activation is frequently observed, whereas clear-cut M1/M2 polarization is rather a rare event. This observation is related to the history of infected patients. Indeed, the stage of the disease is a critical parameter. For instance, the activation of monocytes/macrophages is different in patients with initial sepsis and those with delayed complications. In addition, numerous patients are distributed between two extreme situations: between patients with acute Q fever and those with Q fever endocarditis, there is a population of patients with valvular disease and Q fever associated with a risk of chronic evolution, and these patients overproduce IL-10 in a sustained manner. However, the measurement of IL-10 at a given time of Q fever evolution is not sufficient to assess the prognosis of patients with Q fever (55). In patients with tuberculosis, the transcriptional signature is transient at the beginning of the disease and is finished 1 year later (45). Clearly, the analysis of the transcriptional pattern of patients with tuberculosis will be dramatically different according to the time of the inclusion, and such an analysis is often difficult to assess at the beginning of the disease. These different clinical and experimental situations drove us to propose a model of monocyte/macrophage activation in which the kinetic component of the disease was integrated. This model is based on the comparison of the transcriptomes from activated monocytes and macrophages. The responses of monocytes to polarizing ligands are characterized by two early and late phases of monocyte activation. The hallmarks of the M1/M2 status are found in the early phase but are absent from the late phase of activation. We selected a series of early and late genes and measured their expression in monocytes from patients with acute and chronic Q fever. Most of the early genes were found to be up-regulated in monocytes from patients with acute Q fever, two of them, NLRC5 and RTP4, were up-regulated by IFN-γ, suggesting that IFN-γ plays a role in the host response during acute Q fever. In contrast, the late genes were up-regulated in chronic Q fever, and some early genes were down-modulated. There was a specific association between late genes such as *ALOX15*, *CLEC4F*, *CCL13*, and *CCL23* and chronic Q fever (13). It is noteworthy that some of them have been associated with the M2 program, which is a result that might lead to incorrect conclusions about monocyte activation. We are unable to assign a function to the modulated genes.

In conclusion, the analysis of macrophage polarization through clinical situations revealed that the mechanisms underlying the activation of monocytes and macrophages are distinct. This point is critical because most clinical investigations are based on monocytes and the conclusions are extrapolated on data obtained with macrophages. The second observation is the importance of activation kinetics in the assessment of infected patients who are at different stages of disease history. Therefore, early and late genes may be alternative biomarkers for analyzing infectious and inflammatory diseases. The lessons from the investigation of infected patients do not invalidate the functional model of M1/M2 polarization. They revealed the difficulty to relate a signature and a function. In addition, the finding of a role for these genes in the activation of macrophages will be useful to understand the complexity of macrophage physiology in normal and pathological conditions.

REFERENCES

1. Mills CD, Ley K. M1 and M2 macrophages: the chicken and the egg of immunity. *J Innate Immun* (2014). doi:10.1159/000364945
2. Kidd BA, Peters LA, Schadt EE, Dudley JT. Unifying immunology with informatics and multiscale biology. *Nat Immunol* (2014) **15**(2):118–27. doi:10.1038/ni0914-894c
3. Martinez FO, Gordon S, Locati M, Mantovani A. Transcriptional profiling of the human monocyte-to-macrophage differentiation and polarization: new molecules and patterns of gene expression. *J Immunol* (2006) **177**(10):7303–11. doi:10.4049/jimmunol.177.10.7303
4. Xue J, Schmidt SV, Sander J, Draffehn A, Krebs W, Quester I, et al. Transcriptome-based network analysis reveals a spectrum model of human macrophage activation. *Immunity* (2014) **40**(2):274–88. doi:10.1016/j.immuni.2014.01.006
5. Hussell T, Bell TJ. Alveolar macrophages: plasticity in a tissue-specific context. *Nat Rev Immunol* (2014) **14**(2):81–93. doi:10.1038/nri3600
6. Brown J, Wallet MA, Krastins B, Sarracino D, Goodenow MM. Proteome bioprofiles distinguish between M1 priming and activation states in human macrophages. *J Leukoc Biol* (2010) **87**(4):655–62. doi:10.1189/jlb.0809570
7. Ouedraogo R, Flaudrops C, Ben Amara A, Capo C, Raoult D, Mege JL. Global analysis of circulating immune cells by matrix-assisted laser desorption ionization time-of-flight mass spectrometry. *PLoS One* (2010) **5**(10):e13691. doi:10.1371/journal.pone.0013691
8. Ouedraogo R, Daumas A, Ghigo E, Capo C, Mege JL, Textoris J. Whole-cell MALDI-TOF MS: a new tool to assess the multifaceted activation of macrophages. *J Proteomics* (2012) **75**(18):5523–32. doi:10.1016/j.jprot.2012.07.046
9. Murray PJ, Allen JE, Biswas SK, Fisher EA, Gilroy DW, Goerdt S, et al. Macrophage activation and polarization: nomenclature and experimental guidelines. *Immunity* (2014) **41**(1):14–20. doi:10.1016/j.immuni.2014.06.008
10. Barros MH, Hauck F, Dreyer JH, Kempkes B, Niedobitek G. Macrophage polarisation: an immunohistochemical approach for identifying M1 and M2 macrophages. *PLoS One* (2013) **8**(11):e80908. doi:10.1371/journal.pone.0080908
11. Buechler C, Ritter M, Orso E, Langmann T, Klucken J, Schmitz G. Regulation of scavenger receptor CD163 expression in human monocytes and macrophages by pro- and antiinflammatory stimuli. *J Leukoc Biol* (2000) **67**(1):97–103. doi:10.1189/jlb.0813437
12. Kittan NA, Allen RM, Dhaliwal A, Cavassani KA, Schaller M, Gallagher KA, et al. Cytokine induced phenotypic and epigenetic signatures are key to establishing specific macrophage phenotypes. *PLoS One* (2013) **8**(10):e78045. doi:10.1371/journal.pone.0078045
13. Mehraj V, Textoris J, Ben Amara A, Ghigo E, Raoult D, Capo C, et al. Monocyte responses in the context of Q fever: from a static polarized model to a kinetic model of activation. *J Infect Dis* (2013) **208**(6):942–51. doi:10.1093/infdis/jit266
14. Ivanov II, Honda K. Intestinal commensal microbes as immune modulators. *Cell Host Microbe* (2012) **12**(4):496–508. doi:10.1016/j.chom.2012.09.009
15. Hooper LV, Macpherson AJ. Immune adaptations that maintain homeostasis with the intestinal microbiota. *Nat Rev Immunol* (2010) **10**(3):159–69. doi:10.1038/nri2710
16. Round JL, Mazmanian SK. The gut microbiota shapes intestinal immune responses during health and disease. *Nat Rev Immunol* (2009) **9**(5):313–23. doi:10.1038/nri2515
17. Smith PD, Ochsenbauer-Jambor C, Smythies LE. Intestinal macrophages: unique effector cells of the innate immune system. *Immunol Rev* (2005) **206**:149–59. doi:10.1111/j.0105-2896.2005.00288.x
18. Jones SE, Paynich ML, Kearns DB, Knight KL. Protection from intestinal inflammation by bacterial exopolysaccharides. *J Immunol* (2014) **192**(10):4813–20. doi:10.4049/jimmunol.1303369
19. Hayashi A, Sato T, Kamada N, Mikami Y, Matsuoka K, Hisamatsu T, et al. A single strain of *Clostridium butyricum* induces intestinal IL-10-producing macrophages to suppress acute experimental colitis in mice. *Cell Host Microbe* (2013) **13**(6):711–22. doi:10.1016/j.chom.2013.05.013
20. Chang PV, Hao L, Offermanns S, Medzhitov R. The microbial metabolite butyrate regulates intestinal macrophage function via histone deacetylase

inhibition. *Proc Natl Acad Sci U S A* (2014) **111**(6):2247–52. doi:10.1073/pnas.1322269111
21. Yang Y, Wang X, Huycke T, Moore DR, Lightfoot SA, Huycke MM. Colon macrophages polarized by commensal bacteria cause colitis and cancer through the bystander effect. *Transl Oncol* (2013) **6**(5):596–606. doi:10.1593/tlo.13412
22. Jang SE, Hyam SR, Han MJ, Kim SY, Lee BG, Kim DH. *Lactobacillus brevis* G-101 ameliorates colitis in mice by inhibiting NF-κB, MAPK and AKT pathways and by polarizing M1 macrophages to M2-like macrophages. *J Appl Microbiol* (2013) **115**(3):888–96. doi:10.1111/jam.12273
23. Christoffersen TE, Hult LT, Kuczkowska K, Moe KM, Skeie S, Lea T, et al. In vitro comparison of the effects of probiotic, commensal and pathogenic strains on macrophage polarization. *Probiotics Antimicrob Proteins* (2014) **6**(1):1–10. doi:10.1007/s12602-013-9152-0
24. Habil N, Al-Murrani W, Beal J, Foey AD. Probiotic bacterial strains differentially modulate macrophage cytokine production in a strain-dependent and cell subset-specific manner. *Benef Microbes* (2011) **2**(4):283–93. doi:10.3920/BM2011.0027
25. Benoit M, Desnues B, Mege JL. Macrophage polarization in bacterial infections. *J Immunol* (2008) **181**(6):3733–9. doi:10.4049/jimmunol.181.6.3733
26. Mege JL, Mehraj V, Capo C. Macrophage polarization and bacterial infections. *Curr Opin Infect Dis* (2011) **24**(3):230–4. doi:10.1097/QCO.0b013e328344b73e
27. Quiding-Jarbrink M, Raghavan S, Sundquist M. Enhanced M1 macrophage polarization in human *Helicobacter pylori*-associated atrophic gastritis and in vaccinated mice. *PLoS One* (2010) **5**(11):e15018. doi:10.1371/journal.pone.0015018
28. Kim YG, Udayanga KG, Totsuka N, Weinberg JB, Nunez G, Shibuya A. Gut dysbiosis promotes M2 macrophage polarization and allergic airway inflammation via fungi-induced PGE2. *Cell Host Microbe* (2014) **15**(1):95–102. doi:10.1016/j.chom.2013.12.010
29. Chen J, Ivashkiv LB. IFN-γ abrogates endotoxin tolerance by facilitating Toll-like receptor-induced chromatin remodeling. *Proc Natl Acad Sci U S A* (2010) **107**(45):19438–43. doi:10.1073/pnas.1007816107
30. Wilson HM. SOCS proteins in macrophage polarization and function. *Front Immunol* (2014) **5**:357. doi:10.3389/fimmu.2014.00357
31. Hotchkiss RS, Karl IE. The pathophysiology and treatment of sepsis. *N Engl J Med* (2003) **348**(2):138–50. doi:10.1056/NEJMra021333
32. Brunialti MK, Santos MC, Rigato O, Machado FR, Silva E, Salomao R. Increased percentages of T helper cells producing IL-17 and monocytes expressing markers of alternative activation in patients with sepsis. *PLoS One* (2012) **7**(5):e37393. doi:10.1371/journal.pone.0037393
33. Moller HJ, Moestrup SK, Weis N, Wejse C, Nielsen H, Pedersen SS, et al. Macrophage serum markers in pneumococcal bacteremia: prediction of survival by soluble CD163. *Crit Care Med* (2006) **34**(10):2561–6. doi:10.1097/01.CCM.0000239120.32490.AB
34. Kjaergaard AG, Rodgaard-Hansen S, Dige A, Krog J, Moller HJ, Tonnesen E. Monocyte expression and soluble levels of the haemoglobin receptor (CD163/sCD163) and the mannose receptor (MR/sMR) in septic and critically ill non-septic ICU patients. *PLoS One* (2014) **9**(3):e92331. doi:10.1371/journal.pone.0092331
35. Rodgaard-Hansen S, Rafique A, Christensen PA, Maniecki MB, Sandahl TD, Nexo E, et al. A soluble form of the macrophage-related mannose receptor (MR/CD206) is present in human serum and elevated in critical illness. *Clin Chem Lab Med* (2014) **52**(3):453–61. doi:10.1515/cclm-2013-0451
36. Raoult D, Marrie T, Mege JL. Natural history and pathophysiology of Q fever. *Lancet Infect Dis* (2005) **5**(4):219–26. doi:10.1016/S1473-3099(05)70052-9
37. Benoit M, Barbarat B, Bernard A, Olive D, Mege JL. *Coxiella burnetii*, the agent of Q fever, stimulates an atypical M2 activation program in human macrophages. *Eur J Immunol* (2008) **38**(4):1065–70. doi:10.1002/eji.200738067
38. Ben Amara A, Bechah Y, Mege JL. Immune response and *Coxiella burnetii* invasion. *Adv Exp Med Biol* (2012) **984**:287–98. doi:10.1007/978-94-007-4315-1_15
39. Rajaram MV, Brooks MN, Morris JD, Torrelles JB, Azad AK, Schlesinger LS. *Mycobacterium tuberculosis* activates human macrophage peroxisome proliferator-activated receptor gamma linking mannose receptor recognition to regulation of immune responses. *J Immunol* (2010) **185**(2):929–42. doi:10.4049/jimmunol.1000866
40. Ghigo E, Capo C, Raoult D, Mege JL. Interleukin-10 stimulates *Coxiella burnetii* replication in human monocytes through tumor necrosis factor down-modulation: role in microbicidal defect of Q fever. *Infect Immun* (2001) **69**(4):2345–52. doi:10.1128/IAI.69.4.2345-2352.2001
41. Ghigo E, Honstettre A, Capo C, Gorvel JP, Raoult D, Mege JL. Link between impaired maturation of phagosomes and defective *Coxiella burnetii* killing in patients with chronic Q fever. *J Infect Dis* (2004) **190**(10):1767–72. doi:10.1086/425041
42. Benoit M, Ghigo E, Capo C, Raoult D, Mege JL. The uptake of apoptotic cells drives *Coxiella burnetii* replication and macrophage polarization: a model for Q fever endocarditis. *PLoS Pathog* (2008) **4**(5):e1000066. doi:10.1371/journal.ppat.1000066
43. Meghari S, Bechah Y, Capo C, Lepidi H, Raoult D, Murray PJ, et al. Persistent *Coxiella burnetii* infection in mice overexpressing IL-10: an efficient model for chronic Q fever pathogenesis. *PLoS Pathog* (2008) **4**(2):e23. doi:10.1371/journal.ppat.0040023
44. Meghari S, Berruyer C, Lepidi H, Galland F, Naquet P, Mege JL. Vanin-1 controls granuloma formation and macrophage polarization in Coxiella burnetii infection. *Eur J Immunol* (2007) **37**(1):24–32. doi:10.1002/eji.200636054
45. Berry MP, Graham CM, McNab FW, Xu Z, Bloch SA, Oni T, et al. An interferon-inducible neutrophil-driven blood transcriptional signature in human tuberculosis. *Nature* (2010) **466**(7309):973–7. doi:10.1038/nature09247
46. Fletcher HA, Keyser A, Bowmaker M, Sayles PC, Kaplan G, Hussey G, et al. Transcriptional profiling of mycobacterial antigen-induced responses in infants vaccinated with BCG at birth. *BMC Med Genomics* (2009) **2**:10. doi:10.1186/1755-8794-2-10
47. Tang Y, Hua SC, Qin GX, Xu LJ, Jiang YF. Different subsets of macrophages in patients with new onset tuberculous pleural effusion. *PLoS One* (2014) **9**(2):e88343. doi:10.1371/journal.pone.0088343
48. Montoya D, Cruz D, Teles RM, Lee DJ, Ochoa MT, Krutzik SR, et al. Divergence of macrophage phagocytic and antimicrobial programs in leprosy. *Cell Host Microbe* (2009) **6**(4):343–53. doi:10.1016/j.chom.2009.09.002
49. Desnues B, Lepidi H, Raoult D, Mege JL. Whipple disease: intestinal infiltrating cells exhibit a transcriptional pattern of M2/alternatively activated macrophages. *J Infect Dis* (2005) **192**(9):1642–6. doi:10.1086/491745
50. Moos V, Schmidt C, Geelhaar A, Kunkel D, Allers K, Schinnerling K, et al. Impaired immune functions of monocytes and macrophages in Whipple's disease. *Gastroenterology* (2010) **138**(1):210–20. doi:10.1053/j.gastro.2009.07.066
51. Geelhaar-Karsch A, Schinnerling K, Conrad K, Friebel J, Allers K, Schneider T, et al. Evaluation of arginine metabolism for the analysis of M1/M2 macrophage activation in human clinical specimens. *Inflamm Res* (2013) **62**(9):865–9. doi:10.1007/s00011-013-0642-z
52. Al Moussawi K, Ghigo E, Kalinke U, Alexopoulou L, Mege JL, Desnues B. Type I interferon induction is detrimental during infection with the Whipple's disease bacterium, *Tropheryma whipplei*. *PLoS Pathog* (2010) **6**(1):e1000722. doi:10.1371/journal.ppat.1000722
53. Desnues B, Raoult D, Mege JL. IL-16 is critical for Tropheryma whipplei replication in Whipple's disease. *J Immunol* (2005) **175**(7):4575–82. doi:10.4049/jimmunol.175.7.4575
54. Rayamajhi M, Humann J, Kearney S, Hill KK, Lenz LL. Antagonistic crosstalk between type I and II interferons and increased host susceptibility to bacterial infections. *Virulence* (2010) **1**(5):418–22. doi:10.4161/viru.1.5.12787
55. Honstettre A, Imbert G, Ghigo E, Gouriet F, Capo C, Raoult D, et al. Dysregulation of cytokines in acute Q fever: role of interleukin-10 and tumor necrosis factor in chronic evolution of Q fever. *J Infect Dis* (2003) **187**(6):956–62. doi:10.1086/368129

Conflict of Interest Statement: The authors declare that the research was conducted in the absence of any commercial or financial relationships that could be construed as a potential conflict of interest.

Received: 24 July 2014; accepted: 25 September 2014; published online: 10 October 2014.
Citation: Ka MB, Daumas A, Textoris J and Mege J-L (2014) Phenotypic diversity and emerging new tools to study macrophage activation in bacterial infectious diseases. Front. Immunol. 5:500. doi: 10.3389/fimmu.2014.00500
This article was submitted to Inflammation, a section of the journal Frontiers in Immunology.

DISCUSSION et PERSPECTIVES

Nous allons discuter les deux approches auxquelles nous nous sommes intéressés dans cette thèse à savoir la spectrométrie de type MALDI-TOF et la mesure de la formation des granulomes. Ces 2 approches originales apportent une aide dans la prise en charge des patients infectés dont on a rappelé les enjeux et les risques.

1. La spectrométrie de masse de type MALDI-TOF

La spectrométrie de masse de type MALDI-TOF est devenue dans les laboratoires de microbiologie, un outil indispensable à l'identification des germes à partir de cultures liquides ou solides, ou de fluides biologiques infectés [137]. Ses atouts sont nombreux, rapidité et précision d'identification, utilisation aisée et faible coût par échantillon [74]. Certes l'achat et l'entretien de l'appareil est onéreux, mais sur le long terme l'outil semble largement rentabilisé. En effet, une identification rapide faite directement à partir des prélèvements permet une optimisation de la prise en charge du patient en minimisant les coûts (réduction de la prescription d'antibiotiques à large spectre, de l'émergence de résistances notamment). Même si l'identification rapide des bactéries par la technique MALDI-TOF permet d'adapter l'antibiothérapie probabiliste, la détermination de la sensibilité aux antibiotiques est l'analyse qui conditionne le bon traitement anti-infectieux pour le patient. Peu de bactéries sont concernées par des tests rapides de recherche de résistances. De nombreuses études montrent la capacité de la technique pour caractériser les enzymes ou les produits de dégradation dus aux mécanismes de résistance aux antibiotiques [138]. Cependant, aucune de ces méthodes n'est actuellement utilisée en routine.

Au regard de ces nombreux avantages, en utilisant la même approche, nous avons montré qu'il était possible d'identifier des cellules entières sans extraction préalable, en particulier des cellules immunitaires mais aussi des mélanges cellulaires et de distinguer différents états d'activation. Nous avons retrouvé une signature IFN-γ et IL-10 chez tous les patients septiques ainsi qu'une signature CpG ODN indépendamment de la documentation microbiologique suggérant une activation à un pathogène bactérien.

La principale limite de cette étude est cependant de ne pas avoir étudié le profil spectral des PBMCs de patients présentant un SIRS d'origine non infectieuse afin de s'assurer de la spécificité de la signature CpG ODN. A ce jour, aucune étude n'a été retrouvée dans la littérature sur ce sujet. Si cette technique permet d'aider le clinicien dans la décision de débuter un traitement anti-infectieux avant même les résultats des prélèvements infectieux, nous n'avons pas trouvé d'indices pour identifier l'agent infectieux impliqué. En effet, la sensibilité de la technique ne permet pas d'aller à une caractérisation plus précise du stimulus bactérien. Notre travail ne peut donc pas être une alternative à la spectrométrie de masse de type MALDI-TOF pour l'identification des micro-organismes. On peut donc voir cette technique comme un outil d'aide à la prise en charge thérapeutique rapide d'un patient en SIRS mais aussi nous pourrions envisager qu'elle soit une aide pour monitorer la réponse immunitaire à l'infection. Le profil d'activation des PBMCs varie peut-être en fonction du temps ce que nous n'avons pu mettre en évidence compte tenu des critères d'inclusion stricts des patients dans l'étude. Une variation du profil d'activation des PBMCs pourrait permettre de guider au mieux et de personnaliser la prise en charge thérapeutique du patient.

Sur le plan pratique, bien que la technique semble simple et indépendante de l'opérateur, sa principale difficulté concerne le mélange échantillon/matrice et son dépôt sur la plaque - métallique de support. Un excès d'échantillon de même qu'un mauvais dépôt peuvent altérer la qualité du spectre et rendre l'identification difficile. Une certaine précision est également nécessaire afin de ne pas contaminer l'échantillon voisin.

Une des questions qui se pose concerne l'identification précise des protéines spécifiques constituant les signatures obtenues par MALDI-TOF. Bien que cela ne soit pas un prérequis pour l'usage du MALDI-TOF en clinique dans le contexte d'un SIRS, elle présente néanmoins plusieurs intérêts. L'identification des protéines spécifiques permet de réaliser une étape de validation par des méthodes indépendantes de type immunologique (ELISA), et donc d'augmenter la valeur prédictive de la signature spectrale. Par ailleurs, la caractérisation de ces marqueurs potentiels peut permettre d'améliorer la compréhension de la réponse immunitaire. Enfin dans le domaine de la cancérologie, dans certains cas où la caractérisation des marqueurs a été effectuée, les protéines identifiées correspondaient à des protéines majoritaires du sérum comme l'apolipoprotéine A1, la transthyrétine ou l'α-antitrypsine. On peut alors de se demander si ces marqueurs voient leur expression altérée spécifiquement en réponse à la

prolifération tumorale ou de manière non spécifique en réponse à des épiphénomènes tels que l'état général du patient ou des processus inflammatoires ?

C'est ainsi que le SELDI-TOF *(surfaced-enhanced laser desorption/ionization time-of-flight)* présente également de nombreux avantages (simplicité d'utilisation, sensibilité et capacité d'analyse à haut débit des échantillons). Cette technique permet la séparation, la détection et l'analyse de protéines, directement à partir de l'échantillon biologique avec une sensibilité de l'ordre de la femtomole. Elle est toutefois limitée par la gamme de masse protéique analysable, avec une très bonne détection pour les protéines inférieures à 20-30 kDa et une sensibilité moindre pour les protéines de plus hautes masses. Cette technique permet d'obtenir une vue d'ensemble des peptides et des protéines présents dans l'échantillon testé. L'analyse différentielle et statistique de l'ensemble des données fournies par les profils protéiques des groupes témoins et pathologiques repose ensuite sur des algorithmes informatiques permettant d'extraire des spectres de masse la meilleure combinaison de marqueurs capables de discriminer chacun des deux groupes. Cette technologie a permis l'émergence du concept de signature protéique tumorale. Dès 2002, un profil protéique constitué de cinq marqueurs permettait de dépister, à partir d'un simple échantillon sanguin, des cancers de l'ovaire dès le stade I (stade le plus précoce) avec une sensibilité de 100 %, une spécificité de 95 % et une valeur prédictive positive de 94 % [139]. Des résultats similaires ont été obtenus par la suite pour les cancers du sein, de la vessie, du pancréas, du rein ou du foie à partir d'échantillons variés [140,141]. Une méta-analyse réalisée à partir des données issues de cinq publications indépendantes a cependant suggéré un défaut de reproductibilité d'un laboratoire à l'autre [142]. En fait, il est apparu que l'établissement des profils protéiques était très dépendant des algorithmes informatiques utilisés. Ainsi une validation et une standardisation des techniques utilisées sont nécessaires pour les rendre utilisables en clinique.

D'autres approches sont à la disposition des cliniciens pour appréhender la réponse du système immunitaire à un pathogène. Parmi celles-ci, on peut citer la cytométrie de flux qui a permis la mise en évidence d'une multitude de cellules du système immunitaire, de leur rôle physiologique ou en pathologie [143]. L'une des difficultés avec la cytométrie en flux c'est le nombre restreint de fluorochromes et le nombre limité de longueurs d'ondes possibles [144]. De plus, il est nécessaire d'utiliser des longueurs d'ondes d'excitation distinctes pour chaque fluorochrome, ce qui implique d'équiper les instruments de plusieurs lasers fonctionnant simultanément. Par ailleurs, le spectre d'émission de chaque fluorochrome peut être large, ce

qui entraîne des recouvrements dans la détection de la lumière émise lorsque plusieurs marqueurs (et donc plusieurs fluorochromes) sont analysés sur une même cellule. Pour s'affranchir de ces limites, la cytométrie de masse a vu le jour. Les anticorps, ou tout autre ligand utilisé pour marquer la cellule, sont couplés à un métal. Les cellules marquées sont vaporisées et introduites une à une dans une chambre à plasma où elles sont atomisées et ionisées. Chaque cellule génère ainsi un nuage d'ions dont le temps de vol (TOF) est analysé par spectrométrie de masse. Puisque le métal n'est pas un produit naturel de la cellule, la signature de chaque métal est ainsi spécifique du marqueur cellulaire identifié. L'avantage majeur de cette technologie est l'absence de recouvrement des signaux obtenus pour chaque métal dans les différents canaux de détection. En effet, chaque métal produit un signal unique qui est fonction de son poids moléculaire. Près de 60 métaux peuvent ainsi être détectés simultanément [145]. L'utilisation de la spectrométrie de masse permet aussi une quantification directe et absolue, sans traitement nécessaire des données brutes.

A noter également un intérêt croissant pour les techniques de biologie moléculaire. La technologie des microarrays, ou biopuces, permet d'analyser simultanément plusieurs milliers de gènes au sein d'un seul échantillon. Les puces transcriptomiques permettent de savoir, à l'échelle du génome dans un compartiment cellulaire donné, quels gènes sont actifs, et dans quelle proportion ils sont transcrits. Le transcriptome est une photographie « instantanée » de l'expression du génome. Aujourd'hui, l'analyse du transcriptome est également un outil d'analyse de la réponse de l'hôte à l'agression. Les résultats des puces transcriptomiques permettent ainsi de décrire la réponse de l'hôte à diverses agressions notamment à l'infection et ont permis la découverte de biomarqueurs diagnostiques, thérapeutiques ou encore pronostiques. Ainsi à titre d'exemple, la comparaison des profils transcriptomiques leucocytaires sanguins de patients atteints de pneumopathie à ceux de patients admis en réanimation avec une présentation clinique semblable mais sans infection, a permis d'identifier une signature de 78 gènes spécifiques du diagnostic de pneumopathie [57]. Le test SeptiCyte LAB en mesurant simultanément le niveau d'expression de 4 gènes (CAECAM4, LAMP1, PLA2G7 et PLAC8), concurrence notre approche en MALDI-TOF en permettant de distinguer les patients admis en réanimation pour un sepsis des patients admis pour un SIRS d'origine non infectieuse [146]. Des signatures spécifiques ont également été identifiées comme associées à un mauvais pronostic. Ainsi, l'étude des profils transcriptomiques leucocytaires sanguins de patients admis en réanimation pour une pneumopathie a permis d'identifier 2 sous-groupes de patients présentant, malgré des caractéristiques cliniques similaires, des profils d'expression

génomiques particuliers SRS1 and SRS2. Les patients SRS1 présentaient une mortalité significativement plus élevée à J14 que les patients SRS2 [147]. Une des difficultés est cependant l'influence de nombreux facteurs sur les réponses comme le temps (la réponse de l'hôte est variable en fonction du délai écoulé depuis le début de l'infection et celui de la prise en charge), l'hôte et le micro-organisme. Cette technique s'intègre totalement dans l'optique d'une prise en charge personnalisée, adaptée à la situation clinique mais aussi à la réponse spécifique du patient en temps réel bien que non utilisable en routine clinique pour l'instant.

À l'heure actuelle, il est impératif de valider nos résultats sur une plus grande cohorte de patients en SIRS et de comparer les différents systèmes disponibles quant à leurs performances techniques. Enfin, le champ d'investigation des différentes approches de spectrométrie de masse est très largement ouvert permettant d'envisager d'identifier les protéines spécifiques des profils spectraux et de monitorer la réponse aux traitements.

2. Le modèle de formation de granulomes *in vitro*

Le granulome est la résultante d'une coopération intense entre les cellules de la réponse innée et adaptative dans le but d'éliminer un agent pathogène. L'évaluation *in vitro* de sa formation permet ainsi d'explorer la fonctionnalité des différents acteurs du système immunitaire et leurs interactions et de mieux comprendre les complications de son dysfonctionnement en cas de sepsis. Nous avons ainsi étudié la capacité de sujets en sepsis sévère et de sujets âgés infectés à former des granulomes en réponse à des extraits de *Coxiella burnetii* et de BCG par rapport à des sujets sains.

Nous avons retrouvé un défaut de formation de granulomes chez les patients septiques quel que soient leur âge et les extraits bactériens utilisés, aux différents temps d'analyse. Ainsi, la formation *in vitro* de granulomes pourrait servir à évaluer le degré d'immunosuppression et le monitorer en réponse à un traitement voir évaluer le pronostic.

Pour expliquer le défaut de formation de granulomes, les patients en sepsis sévère ne formant pas de granulome présentaient des taux de monocytes significativement plus faibles et/ou une lymphopénie. Chez la personne âgée, une dénutrition était retrouvée chez les patients ne formant pas de granulome. Contrairement à l'étude chez les patients en sepsis, les sujets âgés

incapables de former des granulomes ne présentaient pas de monocytopénie et/ou de lymphopénie.

Le dosage du TNF dans les surnageants a mis en évidence des taux significativement plus faibles chez les patients qui ne forment pas de granulomes sans augmentation de l'IL-10 en parallèle. De plus, ce défaut de formation était associé à un défaut de différenciation des macrophages en cellules épithélioides et en cellules géantes multinucléés (MGCs) et à une down-modulation des gènes impliqués dans la polarisation M1/M2 des macrophages à l'exception de TNFSF10 et à une down-modulation également des gènes du granulome.

Pour confirmer le rôle du TNF dans la formation des granulomes, qui en clinique a du sens (susceptibilité des patients sous anti-TNF aux infections et réactivation de tuberculose latente), Soraya Mezouar dans l'équipe du Pr MEGE a étudié l'impact de l'étanercept et de l'adalimumab, sur la formation du granulome [148]. Ces 2 thérapeutiques actuellement couramment utilisées dans des indications diverses (rhumatismes inflammatoires, psoriasis, maladie de Crohn notamment), se lient au TNF, neutralisant ainsi sa fonction biologique en bloquant son interaction avec ses récepteurs. Leur travail a mis en évidence que l'étanercept retarde la formation de granulome et réduit la génération de cellules géantes multinucléées (MGCs). Sur le plan transcriptomique, une surexpression des gènes de la polarisation M1 est observée mais également une augmentation de la sécrétion d'IL-10 qui participe au défaut de formation de MGCs en inhibant la fusion cellulaire. Leurs résultats montrent que l'adalimumab, lui aussi induit un défaut de formation de MGCs mais indépendamment de l'IL-10 dont la sécrétion n'est pas modifiée. L'adalimumab impacterait la formation des MGCs plutôt en induisant une apoptose des macrophages.

Récemment, Djalma A. Alves da Silva et al. [149], ont quant à eux étudié l'impact de l'infliximab sur la formation *in vitro* du granulome et la production de cytokines (TNF-α, IFN-γ, IL-12p40, IL-10 and IL-17). Comme utilisé au sein du laboratoire, ils ont étudié la formation des granulomes en incubant les PBMCs de patients (32 avec une tuberculose active, 27 guéris et 17 contrôles) avec des billes de sépharose couplées à des extraits de *Mycobacterium bovis*. Leurs résultats montrent une formation significativement plus importante de granulomes chez les patients guéris par rapport aux patients infectés et aux patients sains en l'absence d'anti-TNF. Sous infliximab, la formation des granulomes chez les patients guéris est significativement réduite alors qu'elle n'est pas significativement impactée dans les 2 autres groupes. Ils ne se sont pas intéressés à la formation des MGCs mais à la production de cytokines

qui est significativement diminuée dans les 3 groupes. L'intérêt de cette étude est de montrer que malgré l'impact négatif de l'infliximab sur la production de nombreuses cytokines, la formation des granulomes n'est diminuée que dans le groupe des patients guéris de la tuberculose. Cela suggère l'implication d'autres cytokines ou chimiokines, ainsi que de molécules d'adhésion qui pourraient être directement responsables de l'adhésion intercellulaire dans la formation de granulomes [33–35] et de voies de signalisation en aval de l'action de ces cytokines.

Ces différentes études montrent sur le plan pratique que l'utilisation de ce modèle est facile et reproductible. L'évaluation de la formation des granulomes n'est par contre pas standardisée. Dans l'étude de Djalma A. Alves da Silva et al. [149], il utilise un score allant de 1 « billes nues » à 6 lorsque plusieurs couches de cellules sont mises en évidence avec des MGCs. Dans l'équipe, l'évaluation était plus simple avec la distinction billes nues et granulomes lors que les billes étaient totalement recouvertes de cellules.

Le modèle de formation *in vitro* de granulome est un bon modèle pour mettre en évidence un défaut de la réponse immunitaire quel que soit sa cause et ainsi détecter les patients potentiellement à risque d'évolution défavorable. Deknuydt et al. [122] ont montré une diminution significative de la formation de granulomes chez les traumatisés crâniens par rapport à des sujets sains et parmi les traumatisés crâniens, ceux développant une pneumopathie nosocomiale en formaient significativement moins que ceux non infectés. Une des limites de nos travaux dans nos 2 populations est l'absence d'analyse du devenir des patients par rapport leur capacité à former des granulomes pour savoir si le défaut de formation de granulomes est associé un moins bon pronostic.

Comme nos résultats et ceux de Mezouar et al. [147], Deknuydt et al. [122] ont montré une diminution des MGCs dans les granulomes. La formation des MGCs est ainsi nécessaire au développement des granulomes. Le rôle du TNF semble central mais d'autres mécanismes sont également mis en jeu (défaut de fusion, apoptose macrophagique). Nous avons en effet montré que l'ajout de TNF ne permettait pas de corriger le défaut de formation de granulomes [14].

L'utilisation de ce modèle est difficilement envisageable en routine clinique bien que le recueil des PBMCs soit relativement facile et rapide et que le défaut ou le retard de formation des granulomes s'observe le plus souvent dès le 3^{ième} jour. Il peut par contre être utilisé comme outil d'évaluation de l'impact de nouvelles thérapeutiques sur le système immunitaire. Il serait

ainsi intéressant d'étudier s'il y a un impact de la dose d'anti-TNF sur le défaut de formation des MGCs et sur le pronostic. Dans ce cas, ce modèle pourrait servir à monitorer la réponse immunitaire et à personnaliser le traitement.

CONCLUSION

En conclusion, la réponse de l'hôte à l'infection est complexe. Son exploration nécessite des approches combinées dans le but de permettre une prise en charge optimisée et personnalisée. Notre travail a reposé sur deux approches : la spectrométrie de masse MALDI-TOF et la formation *in vitro* de granulomes.

En spectrométrie de masse MALDI-TOF, nous avons pu identifier différents profils d'activation des cellules de l'immunité et mettre en évidence une signature spectrale spécifique chez les patients septiques apportant ainsi une aide au clinicien pour orienter la prise en charge du patient avant même d'obtenir une éventuelle identification microbiologique. Par l'étude de la formation *in vitro* de granulomes, nous avons mis en évidence un défaut de formation de granulomes chez les patients septiques quel que soient leur âge dont les causes sont multiples.

Notre travail démontre le potentiel de ces 2 outils dans l'évaluation de la réponse de l'hôte à l'infection. Nos résultats ouvrent sur des perspectives cliniques pour la spectrométrie de masse après la validation de la signature spectrale retrouvée dans une plus grande cohorte de patients comprenant des patients en SIRS d'origine non infectieuse. Quant à l'étude de la formation *in vitro* des granulomes, elle pourrait permettre de monitorer l'impact sur la réponse immunitaire de traitements pris au long cours par les patients afin de personnaliser le traitement et diminuer le risque de complications infectieuses.

REFERENCES BIBLIOGRAPHIQUES

[1] Dellinger RP, Levy MM, Rhodes A, Annane D, Gerlach H, Opal SM et al. Surviving sepsis campaign: International guidelines for management of severe sepsis and septic shock, 2012. Crit Care Med. 2013;41:580-637.

[2] Singer M, Deutschman CS, Warren Seymour C, et al. The Third International Consensus Definitions for Sepsis and Septic Shock (Sepsis-3). JAMA. 2016;315:801-10.

[3] Zambon M, Ceola M, Almeida-de-Castro R, Gullo A, Vincent JL. Implementation of the Surviving Sepsis Campaign guidelines for severe sepsis and septic shock: we could go faster. J Crit Care. 2008;23:455-60.

[4] Liu VX, Fielding-Singh V, Greene JD, Baker JM, Iwashyna TJ, Bhattacharya J, Escobar GJ. The Timing of Early Antibiotics and Hospital Mortality in Sepsis. Am J Respir Crit Care Med. 2017;196:856-863.

[5] Wester AL, Dunlop O, Melby KK, Dahle UR, Wyller TB. Age-related differences in symptoms, diagnosis and prognosis of bacteremia. BMC Infect Dis. 2013;13:346.

[6] Seigel TA, Cocchi MN, Salciccioli J, Shapiro NI, Howell M, Tang A, et al. Inadequacy of temperature and white blood cell count in predicting bacteremia in patients with suspected infection. J Emerg Med.2012;42:254-9.

[7] Adrie C, Alberti C, Chaix-Couturier C, Azoulay E, De Lassence A, Cohen Y, et al. Epidemiology and economic evaluation of severe sepsis in France: age, severity, infection site, and place of acquisition (community, hospital, or intensive care unit) as determinants of workload and cost. J Crit Care. 2005;20:46-58.

[8] Faix JD. Biomarkers of sepsis. Crit Rev Clin Lab Sci. 2013;50:23-36.

[9] Hotchkiss RS, Monneret G, Payen D. Sepsis-induced immunosuppression: from cellular dysfunctions to immunotherapy. Nat Rev Immunol. 2013;13:862-74.

[10] Tolsma V, Schwebel C, Azoulay E, Darmon M, Souweine B, Vesin A, et al. Sepsis severe or septic shock: outcome according to immune status and immunodeficiency profile. Chest. 2014;146:1205-1213.

[11] Goronzy JJ, Weyand CM. Understanding immunosenescence to improve responses to vaccines. Nat Immunol. 2013;14:428-36.

[12] Vallet H, Fali T, Sauce D. [Aging of the immune system: From fundamental to clinical data]. Rev Med Interne. 2019;40:105-111.

[13] Hearps AC, Martin GE, Angelovich TA, Cheng W-J, Maisa A, Landay AL, et al. Aging is associated with chronic innate immune activation and dysregulation of monocyte phenotype and function. Aging Cell. 2012;11:867-75.

[14] Sauce D, Dong Y, Campillo-Gimenez L, Casulli S, Bayard C, Autran B, et al. Reduced oxidative burst by primed neutrophils in the elderly individuals is associated with increased levels of the CD16bright/CD62Ldim immunosuppressive subset. J Gerontol A Biol Sci Med Sci. 2017;72:163-72.

[15] Naylor K, Li G, Vallejo AN, Lee W-W, Koetz K, Bryl E, et al. The influence of age on T cell generation and TCR diversity. J Immunol Baltim Md 1950; 2005;174:7446-52.

[16] Johnson SA, Cambier JC. Ageing, autoimmunity and arthritis: senescence of th eB cell compartment – implications for humoral immunity. Arthritis Res Ther. 2004;6:131-9.

[17] Xia S, Zhang X, Zheng S, Khanabdali R, Kalionis B, Wu J, et al. An update on inflamm-aging: mechanisms, prevention, and treatment. J Immunol Res. 2016;2016:8426874.

[18] van Engelen TSR, Wiersinga WJ, Scicluna BP, van der Poll T. Biomarkers in Sepsis. Crit Care Clin. 2018;34:139-152.

[19] Lemarié J, Gibot S. [Combining biomarkers to improve sepsis diagnosis in the intensive care unit]. Réanimation. 2013.22:306-313.

[20] Ouedraogo R, Flaudrops C, Ben Amara A, Capo C, Raoult D, Mege JL. Global analysis of circulating immune cells by matrix-assisted laser desorption ionization time-of-flight mass spectrometry. PLoS One. 2010;5:e13691.

[21] Delaby A, Espinosa L, Lépolard C, Capo C, Mège JL. 3D reconstruction of granulomas from transmitted light images implemented for long-time microscope applications. J Immunol Methods. 2010; 360:10-9.

[22] Delaby A, Gorvel L, Espinosa L, Lépolard C, Raoult D, Ghigo E, et al. Defective monocyte dynamics in Q fever granuloma deficiency. J Infect Dis. 2012; 205:1086-94.

[23] Parkin J, Cohen B. An overview of the immune system. Lancet. 2001;357:1777-89.

[24] Medzhitov R, Janeway CA Jr. Innate immune induction of the adaptive immune response. Cold Spring Harb Symp Quant Biol. 1999;64:429-35.

[25] Leadbetter EA, Rifkin IR, Hohlbaum AM, Beaudette BC, Shlomchik MJ, Marshak- Rothstein A. Chromatin-IgG complexes activate B cells by dual engagement of IgM and Toll-like receptors. Nat Immunol. 2002;416:603-7.

[26] Bach JF. The relation between the decrease of infectious diseases and the increase of auto-immune and allergic diseases. N Engl J Med. 2002;347:911-20.

[27] Sattler S. The Role of the Immune System Beyond the Fight Against Infection. Adv Exp Med Biol. 2017;1003:3-14.

[28] McKenzie AN, Spits H, Eberl G. Innate lymphoid cells in inflammation and immunity. Immunity. 2014;41:366-74.

[29] Eberl G, Di Santo JP, Vivier E. The brave new world of innate lymphoid cells. Nat Immunol.2015;16:1-5.

[30] Rus H, Cudrici C, Niculescu F. The role of the complement system in innate immunity. Immunol Res. 2005;33:103-12.

[31] Garlanda C, Bottazzi B, Bastone A, Mantovani A. Pentraxins at the crossroads between innate immunity, inflammation, matrix deposition, and female fertility. Annu Rev Immunol. 2005;23:337-66.

[32] Peiser L, Mukhopadhyay S, Gordon S. Scavenger receptors in innate immunity. Curr Opin Immunol. 2002;14:123-8.

[33] Cambi A, Figdor CG. Levels of complexity in pathogen recognition by C-type lectins. Curr Opin Immunol. 2005;17:345-51.

[34] Takeda K, Kaisho T, Akira S. Toll-like receptors. Annu Rev Immunol. 2003;21:335-76.

[35] Girardin SE, Boneca IG, Carneiro LA, Antignac A, Jéhanno M, Viala J et al. Nod1 detects a unique muropeptide from gram negative bacterial peptidoglycan. Science. 2003;300:1584-7.

[36] Yoneyama M, Kikuchi M, Matsumoto K, Imaizumi T, Miyagishi M, Taira K et al. Shared and unique functions of the DExD/H-box helicases RIG-I, MDA5, and LGP2 in antiviral innate immunity. J Immunol. 2005;175:2851-8.

[37] Casanova JL, Abel L, Quintana-Murci L. Human TLRs and IL-1Rs in Host Defense : Natural Insights from Evolutionary, Epidemiological, and Clinical Genetics. Annu Rev Immunol. 2011;29:447-491.

[38] Takeda K, Akira S. Toll-like receptors. Curr Protoc Immunol. 2015;109:14.12.1-10.

[39] Lim JJ, Grinstein S, Roth Z. Diversity and Versatility of Phagocytosis: Roles in Innate Immunity, Tissue Remodeling, and Homeostasis. Front Cell Infect Microbiol. 2017;7:191.

[40] Chalifour A, Jeannin P, Gauchat JF, et al. Direct bacterial protein PAMP recognition by human NK cells involves TLRs and triggers alpha-defensin production. Blood. 2004;104:1778-83.

[41] Waisman A, Lukas D, Clausen BE, Yogev N. Dendritic cells as gatekeepers of tolerance. Semin Immunopathol. 2017;39:153-163.

[42] Zygmunt B., Veldhoen M. T helper cell differentiation more than just cytokines. Advances in Immunology. 2011;109:159-196.

[43] Ivanova EA, Orekhov AN. T Helper Lymphocyte Subsets and Plasticity in Autoimmunity and Cancer: An Overview. Biomed Res Int. 2015;2015:327470.

[44] Cui W, Kaech SM. Generation of effector CD8+ T cells and their conversion to memory T cells. Immunol Rev. 2010;236:151-66.

[45] Kumaran Satyanarayanan S, El Kebir D, Soboh S, Butenko S, Sekheri M, Saadi J, et al. IFN-β is a macrophage-derived effector cytokine facilitating the resolution of bacterial inflammation. Nat Commun. 2019;10:3471.

[46] Clark RA. Resident memory T cells in human health and disease. Sci Transl Med. 2015;7:269rv1.

[47] Rhodes A, Evans LE, Alhazzani W, Levy MM, Antonelli M, Ferrer R, et al. Surviving Sepsis Campaign: international guidelines for management of sepsis and septic shock: 2016. Intensive Care Med. 2017;43:304-77.

[48] Silvestre J, Póvoa P, Coelho L, Almeida E, Moreira P, Fernandes A, et al.Is C-reactive protein a good prognostic marker in septic patients? Intensive Care Med. 2009;35:909-13.

[49] Luzzani A, Polati E, Dorizzi R, Rungatscher A, Pavan R, Merlini A. Comparison of procalcitonin and C-reactive protein as markers of sepsis. Crit Care Med. 2003;3:1737-41.

[50] Wacker C, Prkno A, Brunkhorst FM, Schlattmann P. Procalcitonin as a diagnostic marker for sepsis: a systematic review and meta-analysis. Lancet Infect Dis. 2013;13:426-35.

[51] Simon L, Gauvin F, Amre DK, Saint-Louis P, Lacroix J. Serum procalcitonin and C-reactive protein levels as markers of bacterial infection: a systematic review and meta-analysis. Clin Infect Dis. 2004;39:206617.

[52] Sakr Y, Burgett U, Nacul FE, Reinhart K, Brunkhorst F. Lipopolysaccharide binding protein in a surgical intensive care unit: a marker of sepsis? Crit Care Med. 2008;36:2014-22.

[53] Wu Y, Wang F, Fan X, Bao R, Bo L, Li J, Deng X. Accuracy of plasma sTREM-1 for sepsis diagnosis in systemic inflammatory patients: a systematic review and meta-analysis. Crit Care. 2012;16:R229.

[54] Backes Y, van der Sluijs KF, Mackie DP, Tacke F, Koch A, Tenhunen JJ, et al. Usefulness of suPAR as a biological marker in patients with systemic inflammation or infection: a systematic review. Intensive Care Med. 2012;38:1418-28.

[55] Gibot S, Béné MC, Noel R, Massin F, Guy J, Cravoisy A, et al. Combination biomarkers to diagnose sepsis in the critically ill patient. Am J Respir Crit Care Med. 2012;186:65-71.

[56] Kofoed K, Andersen O, Kronborg G, Tvede M, Petersen J, Eugen-Olsen J, et al. Use of plasma C-reactive protein, procalcitonin, neutrophils, macrophage migration inhibitory factor, soluble urokinase-type plasminogen activator receptor, and soluble triggering receptor expressed on myeloid cells-1 in combination to diagnose infections: a prospective study. Crit Care. 2007;11:R38.

[57] Scicluna BP, Klein Klouwenberg PM, van Vught LA, Wiewel MA, Ong DS, Zwinderman AH, et al. A molecular biomarker to diagnose community-acquired pneumonia on intensive care unit admission. Am J Respir Crit Care Med. 2015;192:826-35.

[58] Miller RR, Lopansri BK, Burke JP, Levy M, Opal S, Rothman RE, et al. Validation of a Host Response Assay, SeptiCyte LAB, for Discriminating Sepsis from Systemic Inflammatory Response Syndrome in the ICU. Am J Respir Crit Care Med. 2018;198:903-13.

[59] Ephraim L. Tsalik, Ricardo Henao, Marshall Nichols, Thomas Burke, Emily R. Ko, Micah T, et al. Host gene expression classifiers diagnose acute respiratory illness etiology. Sci Transl Med. 2016;8:322ra11.

[60] Suarez NM, Bunsow E, Falsey AR, et al. Superiority of transcriptional profiling over procalcitonin for distinguishing bacterial from viral lower respiratory tract infections in hospitalized adults. J Infect Dis. 2015;212:213-22.

[61] Parnell GP, McLean AS, Booth DR, Armstrong NJ, Nalos M, Huang SJ, et al. A distinct influenza infection signature in the blood transcriptome of patients with severe community-acquired pneumonia. Crit Care. 2012;16:R157.

[62] Sweeney TE, Wong HR, Khatri P. Robust classification of bacterial and viral infections via integrated host gene expression diagnostics. Sci translational Med. 2016;8:346ra91.

[63] Tang BMP, McLean AS, Dawes IW, Huang SJ, Cowley MJ, Lin RCY: Gene expression profiling of gram-positive and gram-negative sepsis in critically ill patients. Crit. Care Med. 2008.36:1125-28.

[64] Tang BMP, McLean AS, Dawes IW, Huang SJ, Lin RCY: Gene-expression profiling of peripheral blood mononuclear cells in sepsis. Crit. Care Med. 2009;37:882-88.

[65] Ludwig KR, Hummon AB. Mass spectrometry for the discovery of biomarkers of sepsis. Mol Biosystems. 2017;13:648-64.

[66] Schmerler D, Neugebauer S, Ludewig K, Bremer-Streck S, Brunkhorst FM, Kiehntopf M. Targeted metabolomics for discrimination of systemic inflammatory disorders in critically ill patients. J Lipid Res. 2012;53:1369-75.

[67] Oved K, Cohen A, Boico O, Navon R, Friedman T, Etshtein L et al. A novel host-proteome signature for distinguishing between acute bacterial and viral infections. PLoS One. 2015;10:e0120012.

[68] Fenselau C, Demirev PA. Characterization of intact microorganisms by MALDI mass spectrometry. Mass Spectrom Rev. 2001;20:157-71.

[69] Mann M, Hendrickson RC, Pandey A. Analysis of proteins and proteomes by mass spectrometry. Annu Rev Biochem. 2001;70:437-73.

[70] Greco V, Piras C, Pieroni L, Ronci M, Putignani L, Roncada P, Urbani A. Applications of MALDI-TOF mass spectrometry in clinical proteomics. Expert Rev Proteomics. 2018;15:683-696.

[71] Schubert S, Kostrzewa M. MALDI-TOF MS in the Microbiology Laboratory: Current Trends. Curr Issues Mol Biol. 2017;23:17-20.

[72] Clark AE, Kaleta EJ, Arora A, Wolk DM. Matrix-assisted laser desorption ionization-time of flight mass spectrometry: a fundamental shift in the routine practice of clinical microbiology. Clin Microbiol Rev. 2013;26:547-603.

[73] Keys CJ, Dare DJ, Sutton H, Wells G, Lunt M, McKenna T, et al. Compilation of a MALDI-TOF mass spectral database for the rapid screening and characterisation of bacteria implicated in human infectious diseases. Infect Genet Evol. 2004;4:221-42.

[74] Bright JJ, Claydon MA, Soufian M, Gordon DB. Rapid typing of bacteria using matrix-assisted laser desorption ionisation Time of flight mass spectrometry and pattern recognition software. J Microbiol Methods. 2002;48:127-38.

[75] Wolk DM, Clark AE. Matrix-Assisted Laser Desorption Time of Flight Mass Spectrometry. Clin Lab Med. 2018;38:471-86.

[76] Ryzhov V, Fenselau C. Characterization of the protein subset desorbed by MALDI from whole bacterial cells. Anal Chem. 2001;73:746-50.

[77] Holland RD, Duffy CR, Rafii F, Sutherland JB, Heinze TM, Holder CL, et al. Identification of bacterial proteins observed in MALDI-TOF mass spectra from whole cells. Anal Chem. 1999;71:3226-30.

[78] Seng P, Drancourt M, Gouriet F, La Scola B, Fournier PE, Rolain JM, et al. Ongoing revolution in bacteriology: routine identification of bacteria by matrix-assisted laser desorption ionization Time of flight mass spectrometry. Clin Infect Dis. 2009;49:543-51.

[79] Normand AC, Becker P, Gabriel F, Cassagne C, Accoceberry I, Gari-Toussaint M, et al. Validation of a New Web Application for Identification of Fungi by Use of Matrix-Assisted Laser Desorption Ionization–Time of Flight Mass Spectrometry. J Clin Microbiol. 2017;55:2661-70.

[80] Neelja Singhal, Manish Kumar, Pawan K. Kanaujia, Jugsharan S. Virdi. MALDI-TOF mass spectrometry: an emerging technology for microbial identification and diagnosis. Front Microbiol. 2015;6:791.

[81] Barbara A. Body, Melodie A. Beard, E. Susan Slechta, Kimberly E. Hanson, Adam P. Barker, N. Esther Babady, et al. Evaluation of the Vitek MS v3.0 Matrix-Assisted Laser Desorption Ionization–Time of Flight Mass Spectrometry System for Identification of Mycobacterium and Nocardia Species J Clin Microbiol. 2018;56: e00237-18.

[82] Gautier M, Ranque S, Normand AC, Becker P, Packeu A, Cassagne C, et al. Matrix-assisted laser desorption ionization time-of-flight mass spectrometry: revolutionizing clinical laboratory diagnosis of mould infections. Clin Microbiol Infect. 2014;20:1366-71.

[83] Jamal W, Saleem R, Rotimi VO. Rapid identification of pathogens directly from blood culture bottles by Bruker matrix-assisted laser desorption laser ionization time of flight mass spectrometry versus routine methods. Diagn Microbiol Infect Dis. 2013;76:404-8.

[84] Clerc O, Prod'hom G, Vogne C, Bizzini A, Calandra T, Greub G. Impact of matrix-assisted laser desorption ionization time-of-flight mass spectrometry on the clinical management of patients with Gram-negative bacteremia: a prospective observational study. Clin Infect Dis. 2013;:1101-7.

[85] Ferreira L, Sanchez-Juanes F, Gonzalez-Avila M, Cembrero-Fucinos D, Herrero- Hernandez A, Gonzalez-Buitrago JM, et al. Direct identification of urinary tract pathogens from urine samples by matrix-assisted laser desorption ionization time of flight mass spectrometry. J Clin Microbiol. 2010;48:2110-5.

[86] Sánchez-Juanes F, Siller Ruiz M, Moreno Obregón F, Criado González M, Hernández Egido S, de Frutos Serna M, et al. Pretreatment of urine samples with SDS improves direct identification of urinary tract pathogens with matrix-assisted laser desorption ionization-time of flight mass spectrometry. J Clin Microbiol. 2014;52:335-8.

[87] Sparbier K, Schubert S, Weller U, Boogen C, Kostrzewa M. Matrix-assisted laser desorption ionization time of flight mass spectrometry-based functional assay for rapid detection of resistance against beta-lactam antibiotics. J Clin Microbiol. 2012;50:927-37.

[88] Hrabak J, Chudackova E, Walkova R. Matrix-assisted laser desorption ionization time of flight (maldi-tof) mass spectrometry for detection of antibiotic resistance mechanisms: from research to routine diagnosis. Clin Microbiol Rev. 2013;26:103-14.

[89] Alvarez-Buylla A, Picazo JJ, Culebras E. Optimized method for Acinetobacter species carbapenemase detection and identification by matrix-assisted laser desorption ionization time of flight mass spectrometry. J Clin Microbiol. 2013;51:1589-92.

[90] Griffin PM, Price GR, Schooneveldt JM, Schlebusch S, Tilse MH, Urbanski T, et al. Use of matrix-assisted laser desorption ionization time of flight mass spectrometry to identify vancomycin-resistant enterococci and investigate the epidemiology of an outbreak. J Clin Microbiol. 2012;50:2918-31.

[91] Florio W, Tavanti A, Barnini S, Ghelardi E, Lupetti A. Recent Advances and Ongoing Challenges in the Diagnosis of Microbial Infections by MALDI-TOF Mass Spectrometry. J Biotechnol. 2014;184:84-93.

[92] Munteanu B, von Reitzenstein C, Hänsch GM, Meyer B, Hopf C. Sensitive, robust and automated protein analysis of cell differentiation and of primary human blood cells by intact cell MALDI mass spectrometry biotyping. Anal Bioanal Chem. 2012;404:2277-86.

[93] Povey JF, O'Malley CJ, Root T, Martin EB, Montague GA, Feary M, et al Hanrieder. Rapid high-throughput characterisation, classification and selection of recombinant mammalian cell line phenotypes using intact cell MALDI-ToF mass spectrometry fingerprinting and PLS-DA modelling. J Biotechnol. 2014;184:84-93.

[94] Hanrieder J, Wicher G, Bergquist J, Andersson M, Fex-Svenningsen A. MALDI mass spectrometry based molecular phenotyping of CNS glial cells for prediction in mammalian brain tissue. Anal Bioanal Chem. 2011;401:135-47.

[95] Karger A, Bettin B, Lenk M, Mettenleiter TC. Rapid characterisation of cell cultures by matrix-assisted laser desorption/ionisation mass spectrometric typing. J Virol Methods. 2010;164:116-21.

[96] Labas V, Teixeira-Gomes AP, Bouguereau L, Gargaros A, Spina L, Marestaing A, et al. Intact cell MALDI-TOF mass spectrometry on single bovine oocyte and follicular cells combined with top-down proteomics: A novel approach to characterise markers of oocyte maturation. J Proteomics. 2018;175:56-74.

[97] Schwamb S, Munteanu B, Meyer B, Hopf C, Hafner M, Wiedemann P. Monitoring CHO cell cultures: cell stress and early apoptosis assessment by mass spectrometry. J Biotechnol. 2013;168:452-61.

[98] Maurer K, Eschrich K, Schellenberger W, Bertolini J, Rupf S, Remmerbach TW. Oral brush biopsy analysis by MALDI-ToF Mass Spectrometry for early cancer diagnosis. Oral Oncol. 2013;49:152-6.

[99] Amann JM, Chaurand P, Gonzalez A, Mobley JA, Massion PP, Carbone DP, et al. Selective profiling of proteins in lung cancer cells from fine-needle aspirates by matrix-assisted laser desorption ionization time-of-flight mass spectrometry. Clin Cancer Res. 2006;12:5142-50.

[100] Dong H, Shen W, Cheung MT, Liang Y, Cheung HY, Allmaier G, Kin-Chung Au O, Lam YW. Rapid detection of apoptosis in mammalian cells by using intact cell MALDI mass spectrometry. Analyst. 2011;136:5181-9.

[101] Kober SL, Meyer-Alert H, Grienitz D, Hollert H, Frohme M. Intact cell mass spectrometry as a rapid and specific tool for the differentiation of toxic effects in cell-based ecotoxicological test systems. Anal Bioanal Chem. 2015;407:7721-31.

[102] Chiu NH, Jia Z, Diaz R, Wright P. Rapid differentiation of in vitro cellular responses to toxic chemicals by using matrix-assisted laser desorption/ionization time-of-flight mass spectrometry. Environ Toxicol Chem. 2015;34:161-6.

[103] Munteanu B, Meyer B, von Reitzenstein C, Burgermeister E, Bog S, Pahl A, et al. Label-free in situ monitoring of histone deacetylase drug target engagement by matrix-assisted laser desorption ionization-mass spectrometry biotyping and imaging. Anal Chem. 2014;86:4642-7.

[104] Feng HT, Wong NS, Sim LC, Wati L, Ho Y, Lee MM. Rapid characterization of high/low producer CHO cells using matrix-assisted laser desorption/ionization time-of-flight. Rapid Commun Mass Spectrom. 2010;24:1226-30.

[105] Feng HT, Sim LC, Wan C, Wong NS, Yang Y. Rapid characterization of protein productivity and production stability of CHO cells by matrix-assisted laser desorption/ionization time-of-flight mass spectrometry.Rapid Commun Mass Spectrom. 2011;25:1407-12.

[106] Pagán AJ, Ramakrishnan L. The Formation and Function of Granulomas. Annu Rev Immunol. 2018;36:639-65.

[107] Peyron P, Vaubourgeix J, Poquet Y, Levillain F, Botanch C, Bardou F, et al. Foamy macrophages from tuberculous patients' granulomas constitute a nutrient-rich reservoir for M. tuberculosis persistence. PLoS Pathog. 2008;4:e1000204.

[108] Crawford CL, Hardwicke PM. Experimental leprosy: a model of epithelioid cell granuloma. Int J Dermatol. 2011;50:255-61.

[109] Helming L, Gordon S. Molecular mediators of macrophage fusion. Trends Cell Biol. 2009;19:514-22.

[110] Puissegur MP, Lay G, Gilleron M, Botella L, Nigou J, Marrakchi H, et al. Mycobacterial lipomannan induces granuloma macrophage fusion via a TLR2-dependent, ADAM9- and beta1 integrin-mediated pathway. J Immunol. 2007;178:3161-9.

[111] Lay G, Poquet Y, Salek-Peyron P, Puissegur MP, Botanch C, Bon H, et al. Langhans giant cells from M. tuberculosis-induced human granulomas cannot mediate mycobacterial uptake. J Pathol. 2007;211:76-85.

[112] Milde R, Ritter J, Tennent GA, et al. Multinucleated giant cells are specialized for complement-mediated phagocytosis and large target destruction. Cell Rep. 2015;13:19376-8.

[113] Ordway D, Higgins DM, Sanchez-Campillo J, Spencer JS, Henao-Tamayo M, Harton M, et al. XCL1 (lymphotactin) chemokine produced by activated CD8 T cells during the chronic stage of infection with Mycobacterium tuberculosis negatively affects production of IFN-gamma by CD4 T cells and participates in granuloma stability. J Leukoc Biol. 2007;82:1221-9.

[114] Yap G, Cheever A, Caspar P, Jankovic D, Sher A. Unimpaired down-modulation of the hepatic granulomatous response in CD8 T-cell- and gamma interferon-deficient mice chronically infected with Schistosoma mansoni. Infect Immun. 1997;65:2583-6.

[115] Co DO, Hogan LH, Il-Kim S, Sandor M. T cell contributions to the different phases of granuloma formation. Immunol Lett. 2004;92:135-42.

[116] Saunders BM, Frank AA, Orme IM, Cooper AM. CD4 is required for the development of a protective granulomatous response to pulmonary tuberculosis. Cell Immunol. 2002;216:65-72.

[117] Grencis RK. Immunity to helminths: resistance, regulation, and susceptibility to gastrointestinal nematodes. Annu Rev Immunol. 2015;33:201-25.

[118] Tubo NJ, Jenkins MK. CD4+ T Cells: guardians of the phagosome. Clin Microbiol Rev. 2014;27:200-13.

[119] Silva DAAD, Silva MVD, Barros CCO, Alexandre PBD, Timóteo RP, Catarino JS, et al. TNF-α blockade impairs in vitro tuberculous granuloma formation and down modulate Th1, Th17 and Treg cytokines. PLoS One. 2018;13:e0194430.

[120] Saunders BM, Britton WJ. Life and death in the granuloma: immunopathology of tuberculosis. Immunol Cell Biol. 2007;85:103-11.

[121] Lammas DA, De Heer E, Edgar JD, Novelli V, Ben-Smith A, Baretto R, et al. Heterogeneity in the granulomatous response to mycobacterial infection in patients with defined genetic mutations in the interleukin 12-dependent interferon-gamma production pathway. Int J Exp Pathol. 2002;83:1-20.

[122] Deknuydt F, Roquilly A, Cinotti R, Altare F, Asehnoune K. An in vitro model of mycobacterial granuloma to investigate the immune response in brain-injured patients. Crit Care Med. 2013 Jan;41(1):245-54.

[123] Mège JL, Mehraj V, Capo C. Macrophage polarization and bacterial infections. Curr Opin Infect Dis. 2011;24:230-4.

[124] Portevin D, Pflüger V, Otieno P, Brunisholz R, Vogel G, Daubenberger C. Quantitative whole-cell MALDI-TOF MS fingerprints distinguishes human monocyte sub-populations activated by distinct microbial ligands. BMC Biotechnol. 2015;15:24.

[125] Million M, Lepidi H, Raoult D. Q fever: current diagnosis and treatment options. Med Mal Infect. 2009;39:82-94

[126] Raoult D, Marrie T, Mege J. Natural history and pathophysiology of Q fever. Lancet Infect Dis. 2005;5:219-26

[127] Fournier PE, Marrie TJ, Raoult D. Diagnosis of Q fever. J Clin Microbiol. 1998;36:1823-34.

[128] Fenollar F, Fournier PE, Carrieri MP, Habib G, Messana T, Raoult D. Risks factors and prevention of Q fever endocarditis. Clin Infect Dis. 2001;33:312-6.

[129] Salgame P, Geadas C, Collins L, Jones-López E, Ellner JJ. Latent tuberculosis infection--Revisiting and revising concepts. Tuberculosis (Edinb). 2015;95:373-84.

[130] Annane D, Bellissant E, Cavaillon JM. Septic shock. Lancet. 2005;365:63-78.

[131] Hotchkiss RS, Coopersmith CM, McDunn JE, Ferguson TA. The sepsis seesaw: tilting toward immunosuppression. Nat Med. 2009;15:496-7.

[132] Zeni F, Freeman B, Natanson C. Anti-inflammatory therapies to treat sepsis and septic shock: a reassessment. Crit Care Med. 1997;25:1095-100.

[133] Monneret G, Venet F, Pachot A, et al. Monitoring immune dysfunctions in the septic patient: a new skin for the old ceremony. Mol Med. 2008;14:64-78.

[134] Pawelec G, Gupta S. Editorial: Immunology of Aging. Front Immunol. 2019;10:1614.

[135] Martin GS, Mannino DM, Moss M. The effect of age on the development and outcome of adult sepsis. Crit Care Med. 2006;34:15-21.

[136] Delano MJ, Ward PA. The immune system's role in sepsis progression, resolution, and long-term outcome. Immunol Rev. 2016;274:330-53.

[137] Luethy PM, Johnson JK. The Use of Matrix-Assisted Laser Desorption/Ionization Time-of-Flight Mass Spectrometry (MALDI-TOF MS) for the Identification of Pathogens Causing Sepsis. J Appl Lab Med. 2019;3:675-85.

[138] Oviaño M, Bou G. Matrix-Assisted Laser Desorption Ionization-Time of Flight Mass Spectrometry for the Rapid Detection of Antimicrobial Resistance Mechanisms and Beyond. Clin Microbiol Rev. 2018;32.

[139] Petricoin EF, Ardekani AM, Hitt BA, Levine PJ, Fusaro VA, Steinberg SM et al. Use of proteomic patterns in serum to identify ovarian cancer. Lancet 2002 ; 359 : 572-7.

[140] Koopmann J, Zhang Z, White N, Rosenzweig J, Fedarko N, Jagannath S et al. Serum diagnosis of pancreatic adenocarcinoma using surface-enhanced laser desorption and ionization mass spectrometry.Clin Cancer Res 2004 ; 10 : 860-8.

[141] Vlahou A, Laronga C, Wilson L, Gregory B, Fournier K, McGaughey D et al. A novel approach toward development of a rapid blood test for breast cancer.Clin Breast Cancer 2003 ; 4 : 203-9.

[142] Diamandis EP. Mass spectrometry as a diagnostic and a cancer biomarker discovery tool : opportunities and potential limitations.Mol Cell Proteomics 2004 ; 3 : 367-78.

[143] De Rosa SC, Roederer M. Eleven-color flow cytometry. A powerful tool for elucidation of the complex immune system. Clin Lab Med. 2001;21:697-712.

[144] Lawrence WG, Varadi G, Entine G, Podniesinski E, Wallace PK. Enhanced red and near infrared detection in flow cytometry using avalanche photodiodes. Cytometry A. 2008;73:767-76.

[145] Bandura DR, Baranov VI, Ornatsky OI, et al. Mass cytometry: technique for real time single cell multitarget immunoassay based on inductively coupled plasma time-of-flight mass spectrometry. Anal Chem 2009 ; 81 : 6813–6822.

[146] McHugh L, Seldon TA, Brandon RA, Kirk JT, Rapisarda A, Sutherland AJ, et al. A Molecular Host Response Assay to Discriminate Between Sepsis and Infection-Negative Systemic Inflammation in Critically Ill Patients: Discovery and Validation in Independent Cohorts. PLoS Med. 2015;12:e1001916.

[147] Davenport EE, Burnham KL, Radhakrishnan J, Humburg P, Hutton P, Mills TC et al. Genomic landscape of the individual host response and outcomes in sepsis: a prospective cohort study. Lancet Respir Med. 2016;4:259-71.

[148] Mezouar S, Diarra I, Roudier J, Desnues B, Mege JL. Tumor Necrosis Factor-Alpha Antagonist Interferes with the Formation of Granulomatous Multinucleated Giant Cells: New Insights Into Mycobacterium tuberculosis Infection. Front Immunol. 2019;10:1947.

[149] Silva DAAD, Silva MVD, Barros CCO, Alexandre PBD, Timóteo RP, Catarino JS et al.TNF-α blockade impairs in vitro tuberculous granuloma formation and down modulate Th1, Th17 and Treg cytokines. PLoS One. 2018;13:e0194430.

Annexes

Identification de différents états d'activation des cellules mononuclées du sang par spectrométrie de masse de type MALDI-TOF

A. DAUMAS[a,b], J. TEXTORIS[b], R. OUEDRAOGO[b], C. CAPO[b], P. VILLANI[a], J-L. MEGE[b]
[a]Service de médecine interne, post-urgences et thérapeutique Hôpital de la TIMONE, MARSEILLE
[b]CNRS UMR 7278, INSERM U1095, Faculté de médecine TIMONE, AIX-MARSEILLE Université

INTRODUCTION

Une technique innovante, la spectrométrie de masse (SM) MALDI-TOF couplant une source d'ionisation laser assistée par une matrice (MALDI pour *Matrix-Assisted Laser Desorption/Ionisation*) et un analyseur à temps de vol (TOF pour *time-of-flight*), s'est imposée récemment pour l'identification des bactéries.
Nous avons montré que la SM MALDI-TOF distingue différents types de cellules eucaryotes et divers états d'activation d'une même cellule immunitaire: des profils caractéristiques ont été obtenues en stimulant des macrophages par de l'IFN-γ ou de l'IL-4 (macrophages dits M1 ou M2).
Nous montrons ici l'application clinique de cette technique aux cellules mononuclées du sang (PBMCs).

PATIENTS ET METHODES

Les PBMCs de sujets sains et de patients en sepsis ont été isolées par gradient de Ficoll. Les PBMCs de sujets sains ont été mises en culture (10^6 cellules) et stimulées ex vivo pendant 18 heures par 20ng/ml de cytokines inflammatoires (IFN-γ) ou immunorégulatrices (IL-4, IL-10), du LPS de E. coli, ligand de TLR4 (1µg/ml), du PGN de Bacillus subtilis, ligand de TLR2 (10µg/ml), des oligo *CpG*, ligand de TLR9 (2µg/ml) et du Poly(I/C), ligand de TLR3 (25µg/ml). Elles ont également été stimulées par des bactéries inactivées (10 bactéries par cellule: Staphylococcus aureus, Streptococcus agalactiae du groupe B, Escherichia coli et Pseudomonas aeruginosa). Les échantillons ont été analysés en MALDI-TOF (AutoflexII, Bruker Daltonics) (Figure 1). Les spectres des PBMCs des patients en sepsis ont été comparés aux spectres des PBMCs stimulées in vitro à l'aide des logiciels FlexControl, FlexAnalysis 2.4 et MALDI Biotyper 3.

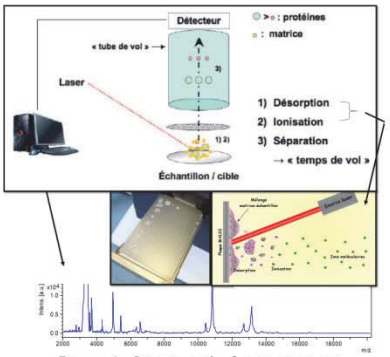

Figure 1: Principes de fonctionnement d'un SM MALDI-TOF

RESULTATS

- Les spectres obtenus sont composés d'un ensemble de pics (m/z compris entre 2000 et 14000 Da), dont un pic majeur à 4964 Da (Figure 1).
- Comparés à des spectres de référence, les spectres des PBMCs se classent parmi les leucocytes circulants (lymphocytes, monocytes et PMN) (Figure 2). La comparaison des spectres MALDI-TOF permet de distinguer patients sains et septiques (Figure 3).
- La comparaison des spectres des patients septiques aux spectres des PBMCs stimulées in vitro met en évidence une composante inflammatoire (IFN-γ) et une composante immunorégulatrice (IL-10) en accord avec l'histoire naturelle du sepsis. A noter également un appariement avec le spectre des PBMCs stimulées par *CpG* ODN en faveur d'une origine bactérienne du sepsis (Figure 4).
- L'analyse en SM MALDI-TOF des patients septiques n'a cependant pas permis de mieux caractériser l'infection in vivo par l'identification d'une « signature LPS » pour les infections par des bactéries à Gram négatif ou d'une « signature PGN » pour les infections par des bactéries à Gram positif. L'analyse n'a également pas permis d'identifier le pathogène en cause in vivo par un appariement significatif aux spectres générés ex vivo par stimulation par des bactéries (Figure 4).

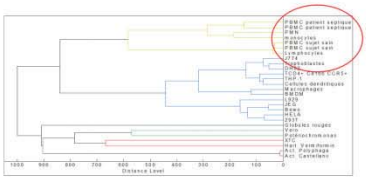

Figure 2: Représentation en dendrogramme des spectres des PBMCs parmi les spectres de 23 types cellulaires

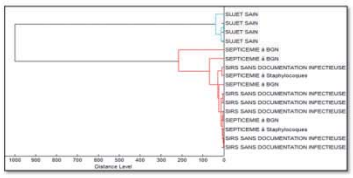

Figure 3: Dendrogramme des spectres des sujets sains et patients septiques

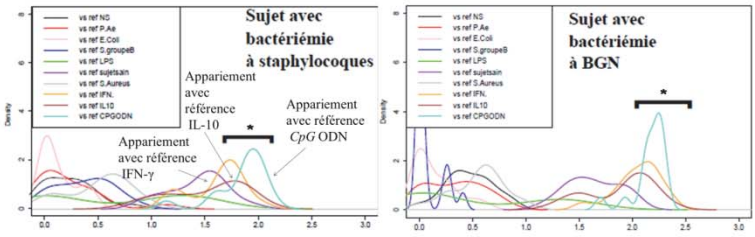

Figure 4: Comparaison des spectres des patients avec les spectres des PBMCs stimulés in vitro

CONCLUSION

Cette première étude analysant par SM MALDI-TOF des PBMC de patients montre comment différents états d'activation des PBMCs in vivo peuvent être identifiés à partir d'une simple prise de sang. Elle ouvre la voie à de nombreuses applications en pathologie humaine notamment pour distinguer inflammation et infection.

REFERENCES: [1] Ouedraogo et al PLoS One 2010;5:e13691 [2] Ouedraogo et al. J Proteomics 2012;75:5523-32 [3] Drancourt M. Clin Microbiol Infect 2010;16:1620-5

Abstract Preview - Step 3/4

- print version -

Topic: Pathophysiology

Title: IDENTIFICATION OF VARIOUS ACTIVATION STATES OF MACROPHAGES BY MALDI-TOF MASS SPECTROMETRY

Author(s): **J. Textoris**[1,2], R. Ouedraogo[1], A. Daumas[1], E. Ghigo[1], C. Capo[1], M. Leone[1,2], J.-L. Mège[1]

Institute(s): [1]*Aix-Marseille Univ, URMITE, CNRS U7278, INSERM U1095, Marseille cedex, France,* [2]*Assistance Publique Hôpitaux de Marseille, Service d'anesthésie et de réanimation, hôpital Nord, Marseille cedex, France*

Text: **INTRODUCTION.** Matrix-Assisted Laser Desorption/Ionisation, Time-Of-Flight Mass Spectrometry (MALDI-TOF MS) was applied for the analysis of microorganisms for their taxonomic characterization. This approach has been developed as a diagnostic tool readily available for routine: high-hroughput analysis of microbial isolates from clinical specimens by whole-cell mass spectrometry, *i.e.* the direct analysis of whole bacterial cell without a preceding fractionation or separation by chromatography or electrophoresis. We have previously shown that this technology can also discriminate various eukaryote cells, particularly immune blood cells (1).

OBJECTIVES. The purpose of this study is to assess the ability and accuracy of whole-cell MALDI-TOF MS to discriminate various activation states of a single cell type. Due to its known plasticity in response to its environment, we decided to study macrophages.

METHODS. Human Peripheral Blood Mononuclear Cells were isolated from blood samples after sedimentation through a Ficoll density cushion, and monocytes were purified by CD14+ magnetic cell sorting. Monocytes were differentiated into macrophages by incubation in RPMI 1640 with 20 mM HEPES, 10% human serum AB+, 2 mM L-glutamine, 100 IU/ml penicillin and 100 µg/ml streptomycin for 3 days, after which fetal calf serum was substituted for the human serum for 4 additional days. Macrophages were stimulated for 18 hours with 20 ng/ml recombinant human cytokines (IFN-γ, TNF, IL-4, IL-10, TGF-β) or LPS (1µg/mL) or heat inactivated bacteria (group B *Streptococci, Staphylococcus aureus, Coxiella burnetii, Orientia tsutsugamushi*, or bacille de Calmette et Guerin (BCG); 50 bacteria per cell). Stimulated or control cells were analyzed by MALDI-TOF MS (AutoFlex II/Bruker Daltonics). Raw data were normalized and analyzed with the R statistical software, the *MALDIquant* library and specific algorithms.

RESULTS. MALDI-TOF spectra from various samples were composed by a series of peaks from 2 to 16 kDa. The comparison of various spectra (based on common and specific peaks, and intensity variation of common peaks) discriminated M1 (IFN-γ stimulated) polarized macrophages from M2 (IL-4 stimulated) polarized macrophages. Moreover, the accuracy of whole-cell MALDI-TOF MS could discriminate cells stimulated with various M1 (IFN-γ, TNF, LPS) or M2 (IL-4, IL-10, TGF-β) agonists. Finally, specific fingerprints separated the bacterial-activated macrophages.

CONCLUSIONS. we showed for the first time that whole-cell MALDI-TOF MS identifies in a fast, easy and unexpensive manner, various activation states of a single cell type. The specific fingerprints we found may be useful for studying the activation of macrophages under pathological conditions. It opens the way to a new investigation tool to study inflammation at the bedside.

REFERENCE(S). Ouedraogo R *et al.* PLoS ONE 2010. 5: e13691.

Keywords: 1. Biomarkers
2. Immunology - Innate immunity
3. Research

Impaired in vitro granuloma formation by PBMC from severe septic patients: a new tool to decipher the host response to sepsis ?

Julien Textoris, Julie Alingrin, Aurélie Daumas, Laurent Gorvel, Eric Ghigo, Jean-Louis Mège
Aix-Marseille Université. URMITE, CNRS UMR 7278, INSERM U1095, Faculté de médecine de Marseille
Assistance Publique - Hôpitaux de Marseille

Introduction

Despite improvement in its management in intensive care, sepsis remains a major cause of morbidity and mortality worldwide. The host response to sepsis implies both an overwhelming inflammatory response leading to organ failure and an immunoregulatory response favoring nosocomial infections and viral reactivations (Fig. 1). However, the pathophysiology is complex and still poorly understood. We developed an in vitro model of granuloma formation to assess an integrated immune response and compared the ability of PBMC from severe septic patients and healthy volunteers to form complete granuloma.

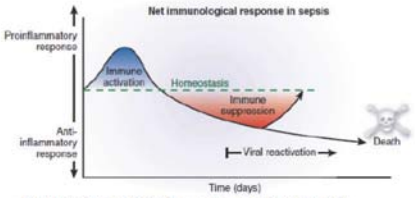

Figure 1: Immunological response over time in sepsis.
(From Hotchkiss R *et al.* Nat Med. (2009) 15(5):496-7)

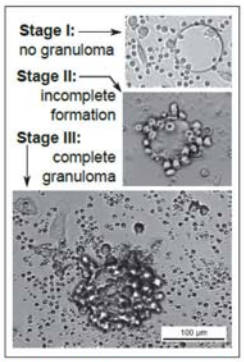

Figure 2: In vitro granuloma formation

Material and Methods

We collected PBMC from 19 severe septic patients at the time of sepsis diagnosis. Nine healthy volunteers and 9 patients with cured chronic Q fever were also included as controls. In vitro granuloma formation was assessed in 96-well culture dish at day 3, 6 and 9 after incubation of 2.5×10^5 PBMCs with 100 sepharose beads coated with either *Coxiella burnetii* or Bacille Calmette et Guérin (*Mycobacterium bovis*) extracts. Granuloma formation was assessed as the percentage of complete granuloma over the total beads number (Fig. 2 and 3).

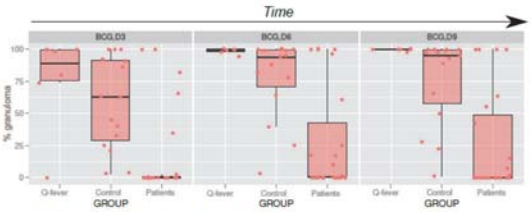

Figure 3: granuloma formation over time

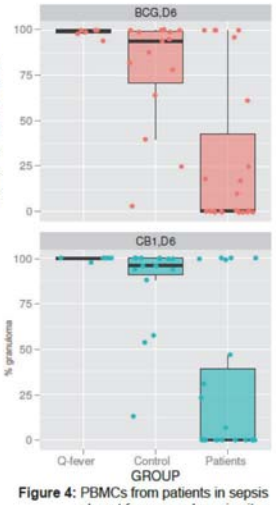

Figure 4: PBMCs from patients in sepsis do not form granuloma in vitro

Results

PBMCs from healthy volunteers and cured Q fever patients were able to form complete granulomas in 6 days (Fig. 4). There was no difference between the use of *C. burnetii* or *M. bovis* coating. Most of the septic patients (n=14) were unable to form granuloma. Three remaining patients form only partial granulomas at day 6 and day 9. We found that a quantitative defect – the presence of either lymphopenia (<1.5 10^9/L) or monocytopenia (< 0.2 10^9/L, Fig. 5) – or a qualitative defect – a lower TNF/IL10 ratio (Fig. 6) – were associated with impaired granuloma formation.

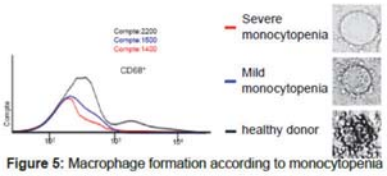

Figure 5: Macrophage formation according to monocytopenia

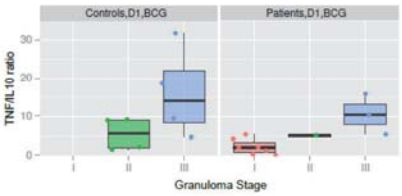

Figure 6:
TNF/IL10 ratio

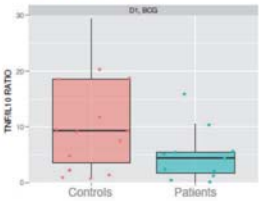

Conclusions

PBMCs from septic patient are unable to form granuloma in vitro in response to bacterial extracts. In vitro granuloma formation is thus able to assess the host response, as it was also demonstrated Ashenoune et al in a different model (brain trauma). This model may help us to decipher some aspects of the host response to sepsis in order to design new biomarkers or therapeutic targets.

Population characteristics (n=19).

Age:	57 [50-67] y.
Sex:	17 men
SAPS II:	40 [30-49]
SOFA :	7.5 [6-10]
ICU length of stay:	12 [9-17] d.
Ventilation duration:	9 [6-13] d.
Shock duration:	3 [2-5] d.
Mortality:	5 (26%)

Assistance Publique Hôpitaux de Marseille

Aix*Marseille université

R267

Évaluation de la réponse immune de patients en sepsis grave : un modèle de formation de granulomes in vitro

J. Alingrin [1,*], A. Daumas [1], M. Leone [2], J.-L. Mege [1], J. Textoris [2]
[1] *Aix-Marseille Université, URMITE, CNRS UMR 7278, INSERM U1095, Faculté de médecine Timone, 27, boulevard Jean Moulin, 13385 Marseille, France*
[2] *Assistance Publique Hôpitaux de Marseille, Service d'anesthésie et de réanimation, hôpital Nord, chemin des Bourelly, 13915 Marseille, France, Marseille, France*
* *Auteur correspondant.*

Introduction Malgré les progrès de la médecine, le sepsis demeure une cause majeure de décès en réanimation. Cependant, la physiopathologie du sepsis est encore mal comprise. Au cours du temps, le sepsis met en jeu à la fois une réponse inflammatoire responsable des défaillances d'organe, et une réponse immunorégulatrice qui favorise l'apparition d'infections nosocomiales et augmentent la mortalité. Pour étudier cette immunosuppression des patients en sepsis, nous proposons un modèle de formation de granulomes in vitro.
Matériel et méthodes Nous avons évalué la capacité des cellules mononuclées du sang de 19 patients septiques admis en réanimation, à former des granulomes in vitro, comparativement à deux groupes contrôles : volontaires sains ($n=9$) et fièvre Q guéries ($n=9$). Ce modèle utilise des billes de sépharose couplées aux extraits bactériens de Coxiella burnetii ou Mycobacterium bovis, incubées avec les cellules.
Résultats Il existe un défaut de formation de granulome chez les patients en sepsis. En effet, contrairement aux 18 volontaires sains, 14 patients n'ont pas formé de granulome ($p < 0,05$). La numération anormale des patients en sepsis explique partiellement ce résultat. En effet certains patients sont lymphopéniques ou monocytopéniques. Ces résultats ont été confirmés par cytométrie en flux. Par ailleurs, le rôle des cytokines, et notamment du *Tumor Necrosis Factor*, est prépondérant dans la formation de granulome puisque le défaut de formation de granulome est associé à un déficit de production de *Tumor Necrosis Factor*. Ce déficit qualitatif est une autre hypothèse pour l'absence de formation des granulomes (Fig. 1)
Discussion Les cellules mononuclées de patients de réanimation en sepsis grave, connus pour présenter une immunodépression, sont incapables de former des granulomes in vitro. Ce modèle permet donc d'étudier la réponse de l'hôte de manière intégrée, in vitro au laboratoire. L'utilisation de ce nouvel outil permettra d'identifier de nouveaux biomarqueurs et de tester de nouvelles stratégies thérapeutiques.

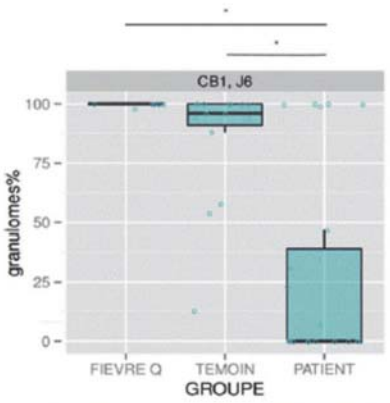

Pourcentage de granulomes formés pour la condition de billes couplées aux extraits de CB, au 6ème jour. Il existe une différence significative entre le nombre de granulomes formés par les PBMC des témoins (fièvre Q guéris, et témoins sains) et le groupe sepsis. (*p<0,05)

Les patients en sepsis ne sont pas capables de former des granulomes

Fig. 1

Déclaration d'intérêts Les auteurs n'ont pas transmis de déclaration de conflits d'intérêts.
Pour en savoir plus
Crit Care Med 2013;41(1):245–254.
http://dx.doi.org/10.1016/j.annfar.2014.07.297

CO035

Rôle des inhibiteurs du TNF sur la formation in vitro de granulome

P. Belenotti[1,*], A. Daumas[2], B. Coiffard[3], C. Capo[3], E. Ghigo[3], J. Serratrice[1], P.J. Weiller[4], J. Roudier[5], J.L. Mege[3]

[1] *Médecine interne, hôpital de la Timone, Marseille*

[2] *Médecine interne, gériatrie et thérapeutique, hôpital de la Timone, Marseille*

[3] *CNRS-UMR 7278 Inserm U1095, faculté de médecine secteur Timone (Aix-Marseille université), Marseille*

[4] *Médecine interne, hôpital de la Conception (AP–HM), Marseille*

[5] *Rhumatologie, hôpital Sainte-Marguerite, Marseille*

* *Auteur correspondant.*

Adresse e-mail : elbe.belenotti@gmail.com (P. Belenotti)

Introduction Les inhibiteurs du TNF, tels que les anticorps monoclonaux (mAb) anti-TNF ou les récepteurs solubles du TNF (sTNFR2), ont révolutionné le pronostic de certaines maladies inflammatoires, au prix de complications infectieuses, dont des réactivations de tuberculose particulièrement disséminées. Leur impact sur la formation in vitro du granulome n'a jamais été étudié à ce jour.

Matériels et méthodes La capacité des cellules mononucléées du sang périphérique (PBMCs) de 7 volontaires sains à former des granulomes in vitro en présence de billes Sepharose recouvertes d'extraits de *Mycobacterium bovis* en présence de mAb anti-TNF ou de sTNFR2 a été testée.

Résultats Les mAb anti-TNF et sTNFR2 n'inhibent pas la formation in vitro des granulomes dirigés contre *M. bovis*. Ils affectent en revanche la composition des cellules composant le granulome, qui en condition contrôle comporte 60 % de macrophages et 40 % de lymphocytes, alors que ceux formés en présence de mAb comportent surtout de lymphocytes majoritairement CD4+. Alors que les granulomes contrôles contiennent des cellules géantes multinucléées, celles-ci sont totalement absentes en présence des deux drogues, alors que ces cellules géantes multinucléées sont d'origine macrophagique vue qu'elles expriment le marquer CD68. La production de TNF et d'IL-10 est différente en présence des inhibiteurs du TNF, notamment du mAb anti-TNF avec un rapport TNF/IL-10 effondré alors qu'il est élevé en condition contrôle. Cette modification cytokinique pourrait expliquer la prédominance de lymphocytes TCD4+ immunorégulateurs au détriment des cellules géantes multinucléées en présence du mAb anti-TNF.

Conclusion Les inhibiteurs du TNF n'affectent pas la formation in vitro des granulomes dirigés contre M. bovis mais inhibent la maturation en cellules multinucléées des PBMCs. On peut supposer que ce défaut de maturation affecte les fonctions des granulomes et expliquerait le caractère disséminé des tuberculoses chez les patients traités par inhibiteurs du TNF.

Déclaration d'intérêts Les auteurs déclarent ne pas avoir de conflits d'intérêts en relation avec cet article.

http://dx.doi.org/10.1016/j.revmed.2014.10.052

La formation de granulomes in vitro : outil d'évaluation de la réponse immune chez la personne âgée

A. Daumas (1) ; C. Chartier (2) ; J. Alingrin (3) ; P. Belenotti (4) ; C. Lepolard (2) ; E. Ghigo (2) ; C. Capo (2) ; P. Villani (1) ; JL. Mege (2)
(1) Médecine interne, Gériatrie et Thérapeutique, Hôpital de la Timone, Marseille; (2) Cnrs-umr 7278 inserm u 1095, Faculté de Médecine secteur Timone (Aix-Marseille Université), Marseille; (3) Service d'anesthésie et de réanimation, Hôpital Nord, Marseille; (4) Médecine interne, Hôpital de la Timone, Marseille

Numéro : **000692**
Orateur : **A. Daumas**
Structure : **Structure 1**
Thème : **Communications libres**
Mode de présentation : **Poster**
Liste des mots clés :
- Infections
- Sujet âgé

Conflit d'intérêts : **non**
Recherche fondamentale : **Oui**
☑ Engagement de cession de droits
Mis à jour le : **lundi 23 février 2015 23:34**

Introduction
La susceptibilité infectieuses des sujets âgés est complexe, non seulement liée à l'immunosénescence mais aussi à des altérations physiologiques et pathologiques des barrières protectrices et à l'interaction des pathologies associées en première ligne desquelles la maltritution. Cependant ce déclin n'est pas homogène. Le granulome est une formation anatomopathologique incluant l'ensemble des cellules de la réponse immune ayant pour but de limiter la dissémination des agents infectieux et de favoriser leur élimination par les cellules immunitaires. Afin d'étudier réponse immunitaire des sujets âgés, nous avons comparé la formation de granulomes par les cellules mononuclées du sang périphérique (PBMCs) de patients âgés en sepsis par rapport à des sujets âgés non septiques.

Patients et méthodes
Nous avons évalué la capacité au cours du temps de 22 patients âgés septiques hospitalisés, à former des granulomes in vitro, comparativement à 22 patients âgés non septiques. Nous avons pour cela utilisé des billes de sépharose couplées aux extraits bactériens de *Coxiella burnetii* ou *Mycobacterium bovis*, incubées avec les cellules. Les cellules des granulomes ont été analysées à J0, J3, J6 et J9, par coloration de May-Grumwald-Giemsa après récupération des cellules par centrifugation (Cytospin®). Ces résultats ont été corrélés à ceux obtenus par cytométrie en flux. Une étude de la cinétique de la sécrétion des cytokines (TNFα et IL-10) au cours de la granulogénèse a été réalisée sur les surnageants de cultures.

Résultats
Il existe un défaut de formation de granulomes chez les patients âgés en sepsis. Quel que soit le temps de formation, il y a une différence significative entre le pourcentage de granulomes formés à partir des PBMC de sujets âgés non septiques et des PBMC de patients en sepsis. L'absence de formation de granulomes est associée à un taux de globules blancs et de monocytes circulants plus bas. La cellularité des granulomes est par contre comparable entre les patients septiques et les patients non septiques. On note l'apparition de macrophages activés et de cellules géantes multinuclées au cours du temps et une augmentation du taux de lymphocytes CD4+. La sécrétion de TNFα est plus faible que la sécrétion d'IL-10 et leurs taux diminuent au cours du temps. Le ratio TNFα/IL-10 est plus élevé chez les patients septiques qui forment par rapport aux sujets non septiques. Par contre, on note un déficit en TNFα chez les sujets âgés septiques ne formant pas de granulomes. Ces résultats sont communs pour les 2 conditions:d'étude (*Coxiella burnetii* et *Mycobacterium bovis*).

Conclusion
Le sepsis induit un état d'immunodépression qui favorise la survenue de surinfections et alourdit le pronostic des patients âgés. Ce modèle permet donc d'étudier la réponse de l'hôte de manière intégrée, in vitro au laboratoire. L'utilisation de ce nouvel outil pourrait permettre de tester de nouvelles hypothèses thérapeutiques.

Références bibliographiques principales

- Deknuydt F, Roquilly A, Cinotti R, Altare F, Asehnoune K. An in vitro model of mycobacterial granuloma to investigate the immune response in brain-injured patients. Crit Care Med. 2013;4:245-54.

Résumé

Introduction : Le sepsis constitue une des principales causes de mortalité tant en médecine ambulatoire qu'en milieu hospitalier notamment dans la population gériatrique. Un diagnostic précoce ainsi que l'identification de la gravité du tableau sont les 2 principaux éléments nécessaires pour une prise en charge rapide, optimale, synonyme d'amélioration du pronostic. La réalité clinique est qu'il est souvent difficile d'affirmer le caractère infectieux de la réaction inflammatoire systémique observée et que malgré l'amélioration des techniques microbiologiques, jusqu'à 40% des infections ne sont pas documentées.

Patients et méthodes : Nous avons utilisé la spectrométrie de masse MALDI-TOF, outil de routine pour l'identification des micro-organismes pour identifier un profil de réponse spécifique des PBMCs à une agression infectieuse. Cette approche pourrait ainsi apporter une aide au clinicien pour orienter la prise en charge du patient avant même l'identification microbiologique. Nous nous sommes également intéressés à la formation *in vitro* de granulomes, structures organisées de la réponse immunitaire, comme moyen d'exploration de l'immunodépression du patient en sepsis sévère et de la personne âgée infectée, à risque d'infections nosocomiales.

Résultats : Nous avons identifié des signatures spécifiques chez les cellules mononucléées stimulées *in vitro* par des agonistes M1, des cytokines M2 ou différentes bactéries. La comparaison de spectres de patients en sepsis sévère avec ou sans documentation microbiologique avec les spectres des PBMCs stimulés *in vitro* a ensuite mis en évidence chez tous les patients une signature spectrale de type Interleukine IL-10 et Interféron IFN-γ ainsi qu'une signature spectrale oligodésoxynucléotides CPG (CpG ODN) suggérant une étiologie bactérienne. L'évaluation *in vitro* de la formation de granulomes a permis de mettre en évidence un défaut de formation de granulomes chez les patients septiques quel que soient leur âge. Pour expliquer ce défaut, les patients en sepsis sévère ne formant pas de granulome présentaient des numérations de monocytes et de lymphocytes diminuées. Chez la personne âgée, une dénutrition était retrouvée chez les patients ne formant pas de granulome. Un déficit en TNF sans augmentation de l'IL-10 associé à un défaut de différenciation des macrophages en cellules épithélioides et en cellules géantes multinucléées sont retrouvés en cas de défaut de formation de granulomes.

Discussion

La spectrométrie de masse MALDI-TOF par son approche de caractérisation cellulaire par « profiling » à partir de l'analyse directe des cellules entières présente de nombreux avantages car elle requiert très peu de préparation des échantillons cellulaires et aucune extraction ou séparation préalable des biomolécules. Elle est extrêmement sensible et reproductible. Malgré les limites de nos travaux, la spectrométrie de masse pourrait permettre de distinguer un SIRS en lien avec une pathologie inflammatoire ou infectieuse ou encore d'aider le clinicien dans un contexte de SIRS non infectieux à dépister l'apparition d'une complication infectieuse avant même la clinique et l'identification d'un micro-organisme sur des prélèvements. La mesure de la formation *in vitro* de granulomes pourrait quant à elle permettre d'évaluer le degré d'immunosuppression et servir à monitorer la réponse immune en réponse à un traitement. D'autres études sont nécessaires pour comprendre les différents mécanismes impliqués dans le défaut de formation des cellules géantes multinucléées.

Conclusion : La réponse de l'hôte à l'infection est complexe. Son exploration nécessite des approches combinées afin de permettre une personnalisation des thérapeutiques dans le cadre du suivi des patients.

Summary

Introduction: Sepsis is a major cause of mortality in both outpatient medicine and hospitals, especially in the geriatric population. Early diagnosis and identification of the severity of the picture are crucial to ensuring swift and optimal management, which is synonymous with a better prognosis. However, the clinical reality is that it is often hard to confirm the infectious nature of the systemic inflammatory response syndrome observed and that, despite advances in microbiological techniques, up to 40% of infections are not documented.

Patients and methods: We used MALDI-TOF mass spectrometry, a routine method for the identification of microorganisms, to identify a specific response profile of PBMCs to infectious aggression. This approach could be used to help clinicians determine patient treatment even before microbiological identification. We also investigated the *in vitro* formation of granulomas–organized structures formed as an immune response–to explore immunodepression in patients with severe sepsis and infected elderly subjects susceptible to nosocomial infections.

Results: We identified specific signatures in monocytes stimulated *in vitro* by M1 agonists, M2 cytokines or various bacteria. The comparison of the spectra of patients with severe sepsis (with or without microbiological evaluation) with the spectra of PBMCs stimulated *in vitro* highlighted an Interleukin IL-10 and Interferon IFN-γ-type spectral signature in all the patients as well as a CpG oligodeoxyribonucleotide (CpG-ODN) spectral signature, thus indicating a bacterial etiology. The assessment of granuloma formation *in vitro* highlighted the absence of granuloma formation in patients with sepsis regardless of their age. The lower monocyte and leukocyte counts in patients with severe sepsis not forming granulomas could explain this defect. In elderly subjects, malnutrition was observed in patients not forming granulomas. A TNF deficiency without an increase in IL-10 associated with defective differentiation of macrophages into epithelioid cells and multinuclear giant cells was observed in cases of defective granuloma formation.

Discussion

The direct analysis of whole cells using MALDI-TOF mass spectrometry profiling offers numerous advantages as it requires very little sample preparation and no prior extraction or separation of the biomolecules. Furthermore, this technique is extremely sensitive and reproducible. Despite the limitations of our research, mass spectrometry could help distinguish SIRS associated with an inflammatory or infectious condition or even help the clinician in cases of non-infectious SIRS to detect the onset of an infectious complication even before the appearance of any clinical signs or the identification of the microorganism. The assessment of granuloma formation *in vitro* could be used to determine the degree of immunosuppression and to monitor the immune response to therapy. Further studies are necessary to understand the different mechanisms involved in the defective formation of multinuclear giant cells.

Conclusion: The host response to infection is complex and its exploration requires the use of combined methods to personalize therapy within the context of patient follow-up.

Résumé

Introduction : Le sepsis constitue une des principales causes de mortalité tant en médecine ambulatoire qu'en milieu hospitalier notamment dans la population gériatrique. Un diagnostic précoce ainsi que l'identification de la gravité du tableau sont les 2 principaux éléments nécessaires pour une prise en charge rapide, optimale, synonyme d'amélioration du pronostic. La réalité clinique est qu'il est souvent difficile d'affirmer le caractère infectieux de la réaction inflammatoire systémique observée et que malgré l'amélioration des techniques microbiologiques, jusqu'à 40% des infections ne sont pas documentées.

Patients et méthodes : Nous avons utilisé la spectrométrie de masse MALDI-TOF, outil de routine pour l'identification des micro-organismes pour identifier un profil de réponse spécifique des PBMCs à une agression infectieuse. Cette approche pourrait ainsi apporter une aide au clinicien pour orienter la prise en charge du patient avant même l'identification microbiologique. Nous nous sommes également intéressés à la formation *in vitro* de granulomes, structures organisées de la réponse immunitaire, comme moyen d'exploration de l'immunodépression du patient en sepsis sévère et de la personne âgée infectée, à risque d'infections nosocomiales.

Résultats : Nous avons identifié des signatures spécifiques chez les cellules mononucléées stimulées *in vitro* par des agonistes M1, des cytokines M2 ou différentes bactéries. La comparaison de spectres de patients en sepsis sévère avec ou sans documentation microbiologique avec les spectres des PBMCs stimulés *in vitro* a ensuite mis en évidence chez tous les patients une signature spectrale de type Interleukine IL-10 et Interféron IFN-γ ainsi qu'une signature spectrale oligodésoxynucléotides CPG (CpG ODN) suggérant une étiologie bactérienne. L'évaluation *in vitro* de la formation de granulomes a permis de mettre en évidence un défaut de formation de granulomes chez les patients septiques quel que soient leur âge. Pour expliquer ce défaut, les patients en sepsis sévère ne formant pas de granulome présentaient des numérations de monocytes et de lymphocytes diminuées. Chez la personne âgée, une dénutrition était retrouvée chez les patients ne formant pas de granulome. Un déficit en TNF sans augmentation de l'IL-10 associé à un défaut de différenciation des macrophages en cellules épithélioides et en cellules géantes multinucléées sont retrouvés en cas de défaut de formation de granulomes.

Discussion

La spectrométrie de masse MALDI-TOF par son approche de caractérisation cellulaire par « profiling » à partir de l'analyse directe des cellules entières présente de nombreux avantages car elle requiert très peu de préparation des échantillons cellulaires et aucune extraction ou séparation préalable des biomolécules. Elle est extrêmement sensible et reproductible. Malgré les limites de nos travaux, la spectrométrie de masse pourrait permettre de distinguer un SIRS en lien avec une pathologie inflammatoire ou infectieuse ou encore d'aider le clinicien dans un contexte de SIRS non infectieux à dépister l'apparition d'une complication infectieuse avant même la clinique et l'identification d'un micro-organisme sur des prélèvements. La mesure de la formation *in vitro* de granulomes pourrait quant à elle permettre d'évaluer le degré d'immunosuppression et servir à monitorer la réponse immune en réponse à un traitement. D'autres études sont nécessaires pour comprendre les différents mécanismes impliqués dans le défaut de formation des cellules géantes multinucléées.

Conclusion : La réponse de l'hôte à l'infection est complexe. Son exploration nécessite des approches combinées afin de permettre une personnalisation des thérapeutiques dans le cadre du suivi des patients.

Summary

Introduction: Sepsis is a major cause of mortality in both outpatient medicine and hospitals, especially in the geriatric population. Early diagnosis and identification of the severity of the picture are crucial to ensuring swift and optimal management, which is synonymous with a better prognosis. However, the clinical reality is that it is often hard to confirm the infectious nature of the systemic inflammatory response syndrome observed and that, despite advances in microbiological techniques, up to 40% of infections are not documented.

Patients and methods: We used MALDI-TOF mass spectrometry, a routine method for the identification of microorganisms, to identify a specific response profile of PBMCs to infectious aggression. This approach could be used to help clinicians determine patient treatment even before microbiological identification. We also investigated the *in vitro* formation of granulomas–organized structures formed as an immune response–to explore immunodepression in patients with severe sepsis and infected elderly subjects susceptible to nosocomial infections.

Results: We identified specific signatures in monocytes stimulated *in vitro* by M1 agonists, M2 cytokines or various bacteria. The comparison of the spectra of patients with severe sepsis (with or without microbiological evaluation) with the spectra of PBMCs stimulated *in vitro* highlighted an Interleukin IL-10 and Interferon IFN-γ-type spectral signature in all the patients as well as a CpG oligodeoxyribonucleotide (CpG-ODN) spectral signature, thus indicating a bacterial etiology. The assessment of granuloma formation *in vitro* highlighted the absence of granuloma formation in patients with sepsis regardless of their age. The lower monocyte and leukocyte counts in patients with severe sepsis not forming granulomas could explain this defect. In elderly subjects, malnutrition was observed in patients not forming granulomas. A TNF deficiency without an increase in IL-10 associated with defective differentiation of macrophages into epithelioid cells and multinuclear giant cells was observed in cases of defective granuloma formation.

Discussion

The direct analysis of whole cells using MALDI-TOF mass spectrometry profiling offers numerous advantages as it requires very little sample preparation and no prior extraction or separation of the biomolecules. Furthermore, this technique is extremely sensitive and reproducible. Despite the limitations of our research, mass spectrometry could help distinguish SIRS associated with an inflammatory or infectious condition or even help the clinician in cases of non-infectious SIRS to detect the onset of an infectious complication even before the appearance of any clinical signs or the identification of the microorganism. The assessment of granuloma formation *in vitro* could be used to determine the degree of immunosuppression and to monitor the immune response to therapy. Further studies are necessary to understand the different mechanisms involved in the defective formation of multinuclear giant cells.

Conclusion: The host response to infection is complex and its exploration requires the use of combined methods to personalize therapy within the context of patient follow-up.